Bioengineering the Human Muscle Stem-Cell Niche for Therapeutic Applications

Thèse N° 7225

Présentée le 30 août 2019

à la Faculté des sciences de la vie
Programme doctoral en biotechnologie et génie biologique

pour l'obtention du grade de Docteur ès Sciences

par

Omid MASHINCHIAN

Acceptée sur proposition du jury

Prof. D. Pioletti, président du jury
Dr. J. Feige, Prof. M. Lütolf, directeurs de thèse
Prof. S. Tajbakhsh, rapporteur
Prof. A. Ocampo, rapporteur
Prof. O. Bar-Nur, rapporteur

2019

ÉCOLE POLYTECHNIQUE
FÉDÉRALE DE LAUSANNE

A **winner** is a **dreamer**

who **never** gives up.

- Nelson Mandela

Acknowledgements

Foremost, I would like to express my sincere gratitude to my tremendous advisor, Dr. **Jérome Feige** for the continuous support of my Ph.D study and research, for his patience, motivation, enthusiasm, and immense-knowledge. I could not have imagined having a better advisor and mentor for my Ph.D-life. His advice on both research as well as on my career have been priceless. **Jerome** is someone you will instantly love and never forget once you meet him. He's the funniest advisor and one of the smartest people I know. I wish that I could be as lively, enthusiastic, and energetic as **Jerome**, in future. **Jerome** has been supportive and has given me the freedom to manage various projects without objection by providing me daily-insightful discussions. Apart from academic-life and science, he is one of my best friends. I am always calling him, "my 2nd father", as his invaluable advises and supports not only impacted my scientific-future but also directed and shaped my personal life as well. I would wish to reciprocate only part of his enormous favors during my life. Thanks dear **Jerome** for your effort in guiding me, motivating me and most importantly for making me exactly what I am today.

My sincere thanks also goes to Dr. **Florian Bentzinger**. He was my first and still my "best teacher" during my academic studies. **Florian** taught me how to design, manage and operate a scientific project. He supervised me in a daily basis and for me it would not have been possible to do the PhD without the support and guidance of him. I am always deeply grateful to **Florian**, who believed enough in what I am doing on science and to accept becoming my supervisor in a beginning of my PhD journey. Thank you as well for guiding me, often with big doses of patience. To me, **Florian**, is the smartest and greatest mentor and indeed, I would wish to be like him on my future career. He is my scientific "role-model", forever. Thanks again dear **Florian** for all the supports, motivation and teachings. I am standing in this position, all because of you.

My deep appreciation goes out to my co-advisor, Professor **Matthias Lütolf**. He has always provided insightful discussions about my research. He was the best cutting-edge scientific resource for getting my science questions answered and was instrumental in helping me crank out this thesis. **Matthias** has provided me a very inspiring and fascinating environment in what concerns the extraordinary quality of his academic staff, and that experience will leave marks beyond this PhD-thesis. Thanks again dear **Matthias** for all the great opportunities you have provided to me.

Besides my advisor, I would like to thank the rest of my thesis committee; Professor **Shahragim Tajbakhsh** (Institut Pasteur, FRANCE), Professor **Ori Bar-Nur** (ETH Zürich, SWITZERLAND), Professor **Alejandro Ocampo** (UNIL, SWITZERLAND) & Professor **Dominique Pioletti** (EPFL Lausanne, SWITZERLAND) for agreeing to serve on the committee on short notice. I earnestly hope to have the chance to more contribute to regenerative medicine field in the future through active collaborations with them.

I will forever be thankful to my great mentor and advisor, Dr. **Filippo De Franceschi**, for his fabulous support and encouragement during the past years on optimizing of many technical problem. His enthusiasm and love for teaching is contagious. Without his guidance and constant feedback this PhD would not have been achievable. **Filippo** is a lovely friend and best mentor. Thanks for everything brother.

I thank my fellow-labmates in the Nestlé Institute of Health Sciences: Mr. **Nagabhooshan Hegde**, Mr. **Joris Michaud**, Ms. **Sonia Karaz**, Dr. **Eugenia Migliavacca**, Dr. **Federico Sizzano**, Mr. **Alessio Palini**, Ms. **Sylviane Metairon**, Dr. **Frederic Raymond**, Dr. **Patrick Descombes**, Mr. **Jose Luis Sanchez Garcia**, Dr. **Marine Kraus**, Ms. **Corinne Haller**, Ms. **Umji Lee**, Dr. **Maria Marques de Lima** and Dr. **Pascal Steiner**, for their invaluable advices and feedbacks on my research and for always being so supportive of my work and, especially for the stimulating discussions, for the sleepless nights we were working together before many deadlines, and for all the fun we have had in the last four years. Also, I deeply appreciate my fellows at LSCB – Laboratory of Stem Cell Bioengineering – EPFL and SUN-Bioscience company; Dr. **Sylke Hoehnel** and Dr. **Nathalie Brandenberg** whom constantly supported and helpful throughout my Ph.D.

In particular, my special appreciation goes to my very-lovely friends; to my brothers: Dr. **Gabriele Civiletto**, Mr. **Gabriele Dammone**, Mr. **Philipp Rhein** & Dr. **Benjamin Weger**; to my lovely sisters: Ms. **Sara Ancel**, Ms. **Tanja Sonntag**, Dr. **Caterina Collodet** & Dr. **Isabelle Chareyron**, for all the support and encouragements. You guys were always real pals and part of my family, always, forever! I am also grateful to the Nestlé Research community for fruitful discussion and support, in particular the Musculo-Skeletal Health group, and Dr. **Eric Rolland** & Dr. **Ed Baetge**.

I also thank my supervisors during undergraduate studies, Professor **Morteza Mahmoudi** (Brigham and Women's Hospital, Harvard Medical School) & Professor **Yadollah Omidi** (RCPN, Tabriz University of Medical Sciences). I honestly owe my scientific-foundation to you.

Last but not the least, most importantly, none of this would have been possible without the love and patience of my family. I would like to thank my beautiful Mother; Ms. **Shamsi Tafrishi** and my Brother; Dr. **Milad Mashinchian**. Dear Mom; thank you for all you do for me and our family. Thank you for believing in me, encouraging me to do my best and to try new things. Again thanks for all the support you have given throughout the years. My mother: "*you are the reason of my life*".

In memory of my Father

Houshang (Amir) Mashinchian

Abstract

In spite of decades of research, no feasible method for obtaining sufficient numbers of uncommitted muscle stem cells (MuSCs) for therapy of degenerative muscle diseases exists. One of the most fundamental problems associated with stem cell therapy of muscle is that removal of MuSCs from their tissue microenvironment and expansion in conventional culture induces their terminal commitment to myogenic differentiation. This *in-vitro* loss of stemness impairs the long-term engraftment potential of MuSCs and renders them unsuitable for stem cell therapy. In another disease relevant context, aging, dramatic changes in the functionality of MuSCs have been shown to depend on an altered composition of their microenvironment. Thus, muscle progenitors are fundamentally dependent on their local environment, commonly known as the “stem cell niche", and a better understanding of its role in guiding stem cell function is highly relevant for the development of therapies for aging and muscle diseases.

The muscle stem cell niche is composed of diverse cellular and acellular elements, including different supportive cell types, growth factors and extracellular matrix, and as outlined above, is critical for maintaining healthy stem cell characteristics such as the capacity for self-renewal, commitment, and differentiation. Using molecular biology approaches, we decided to interrogate (I) the role of the cellular environment on stem cell commitment, (II) to test whether, in a physiological context, the systemic circulation has niche-independent effects on MuSC stemness, and (III) to study a population of MuSC-supportive cells that is affected by the aging process.

In the first study of this thesis, we have successfully developed an organoid-like-approach for the scalable derivation of uncommitted MuSCs from human induced pluripotent stem cells (iPSCs) in a biologically faithful cellular 3D-environment in suspension embryoids. To this end, we employed human iPSCs and a spectrum of immortalized cell lines to screen for 3D-aggregation conditions promoting mesoderm formation and subsequent specification to the myogenic lineage without the parallel upregulation of myogenic commitment markers. Compared to myogenic cells derived from adult human skeletal muscle, this niche-mimetic embryoid derived progenitors display significantly enhanced engraftment into the muscle stem cell position peripheral to muscle fibers, and restoration of dystrophin expression when transplanted into muscles of a mouse model of Duchenne muscular dystrophy.

In a second study, we present a novel method for encapsulation of human muscle progenitors in highly diffusible polyethersulfone hollow fiber capsules to identify highly specific “transcriptional-signature” induced by systemic aging *in-vivo*. This technique allows to study the systemic circulation in health, disease and aging at an unprecedented level in human cell types of choice.

Finally, in our third study, we investigated the cellular cross-talk between muscle stem cells and non-myogenic niche-based cell type, called fibro/adipogenic progenitors (FAPs). Interestingly, the

support-function and the cross-talk with stem cells are dramatically impaired in aged FAPs. We demonstrate that this mechanism can be targeted to rejuvenate myogenesis.

Taken together, “mimicking” the physicochemical-interactions of MuSCs with their niche-resident cell types, represents a powerful opportunity to manipulate MuSC function in aging and disease.

Key-words:

Stem cell therapy, Skeletal muscle, Muscle stem cells, iPSCs, Mesoderm, Organoid, Niche, Embryoid, Dystrophin, FAPs, Aging, Disease modeling, Cell therapy

Résumé

En dépit des décennies de recherche, il n'existe à ce jour aucune méthode permettant d'obtenir des cellules souches musculaires (MuSCs) en quantité suffisante en vue d'une utilisation à des fins thérapeutiques, notamment dans l'éventualité d'un traitement contre les myopathies. L'un des problèmes fondamentaux associé à la thérapie par cellules souches du muscle relève du fait que l'extraction des cellules souches musculaires de leur environnement tissulaire, ainsi que leur expansion dans un contexte de culture conventionnelle, induit leur engagement définitif dans la différentiation myogénique. La perte de leur caractère souche *in-vitro* compromet le potentiel de greffe à long terme des cellules souches de muscle et rend leur utilisation impropre pour la thérapie cellulaire. Dans un autre contexte pertinent à la maladie, celui du vieillissement, il a été démontré que les changements spectaculaires impactant la fonctionnalité des MuSCs résultent d'une modification de la composition de leur microenvironnement. Ainsi, les précurseurs musculaires dépendent en grande partie de leur environnement local, communément appelé niche, et une meilleure compréhension de son rôle est nécessaire afin de promouvoir le développement de thérapies contre le vieillissement et les maladies musculaires.

La niche dans laquelle résident les cellules souches du muscle est composée de divers éléments cellulaires et acellulaires, à l'instar de divers types de cellules de soutien, de facteurs de croissance et de matrice extracellulaire. De plus, la niche se révèle essentielle au maintien des caractéristiques des cellules souches saines, notamment de leur capacité à se renouveler, à s'engager et à se différentier. En utilisant des approches de biologie moléculaire, nous nous sommes intéressés (I) au rôle de l'environnement cellulaire sur l'engagement des cellules souches, (II) à savoir si, dans un contexte physiologique, la circulation systémique peut avoir un impact sur le caractère souche des cellules souches musculaires qui soit indépendant de la niche et (III) à l'impact du processus de vieillissement sur une population de cellules agissant en tant que soutien pour les MuSCs.

Dans la première étude de cette thèse, nous avons mis au point avec succès une méthode de différentiation de cellules souches musculaires dans des organoïdes tridimensionnels qui permet la dérivation de progéniteurs musculaires humains dans un état souche à partir de cellules pluripotentes induites (IPS). Pour ce faire, nous avons combiné des cellules IPS humaines à des lignées cellulaires immortalisées permettant ainsi de cribler différentes conditions d'agrégation tridimensionnelle favorisant la formation du mésoderme et sa spécification ultérieure en une lignée myogénique sans pour autant sur-exprimer de marqueurs d'engagement myogénique. Comparés aux cellules myogéniques dérivées du muscle squelettique humain adulte, ces précurseurs dérivés d'embryoïdes mimétiques de la niche présentent une augmentation significative de leur capacité à se greffer en position satellite des fibres musculaires comme les cellules souches musculaires

endogènes. Par ailleurs, leur transplantation dans les muscles d'un modèle murin de la myopathie de Duchenne permet la restauration de l'expression de la dystrophine.

Dans une deuxième étude, nous proposons une nouvelle méthode d'encapsulation des précurseurs musculaires humains à l'intérieur de capsules hautement diffusibles en fibre de polyethersulfone dans le but d'identifier une signature transcriptionnelle *in-vivo* induite spécifiquement par le vieillissement systémique. Cette technique permet d'étudier l'influence de la circulation systémique au cours du vieillissement et des pathologies musculaires, et ce, dans un modèle de cellules humaines qui confère une relevance thérapeutique de premier plan.

Enfin, dans le cadre de notre troisième étude, nous nous sommes intéressés à la communication cellulaire entre les cellules souches du muscle et des cellules non-myogéniques trouvées dans la niche, les précurseurs fibro-adipogéniques (FAPs). Il est intéressant de noter que la fonction de soutien, ainsi que la communication avec les cellules souches, est considérablement altérée dans les FAPs âgés. Nous démontrons que ce mécanisme peut être ciblé afin de restaurer la myogenèse.

En définitive, imiter les interactions physico-chimiques des MuSCs avec d'autres types cellulaires résidant dans la niche représente une opportunité inouïe de manipuler la fonction des cellules souches du muscle dans le contexte du vieillissement et de la maladie.

Mots-clés:

Thérapie par cellules souches, muscle squelettique, cellules souches musculaires, iPSCs, mésoderme, organoïde, niche, embryoïde, dystrophine, FAPs, vieillissement, modélisation des maladies, thérapie cellulaire

TABLE OF CONTENTS

Chapter 1:

Introduction

Background & Rationale:

Complex higher-order regulatory interrelationships with the tissue and factors in the systemic circulation are integrated and propagated to the stem cells through their “niche”. The stem cell niche in skeletal muscle tissue is both, a paradigm for a structurally and functionally relatively static niche that maintains stem cell “quiescence” during tissue homeostasis and a highly dynamic regenerative niche that is subject to extensive structural remodeling and a flux of different support cell populations. Conditions ranging from aging to chronically degenerative skeletal muscle diseases affect the composition of the niche and thereby impair the regenerative potential of muscle stem cells (MuSCs).

The MuSC niche is significantly altered during aging and directly affects the maintenance and regenerative capacity of skeletal muscle tissue. A holistic and integrative understanding of the extrinsic mechanisms regulating MuSCs in a broad physiological context will be imperative for the identification of regulatory hubs in the niche interactome that can be targeted to maintain, restore, or enhance the regenerative capacity of muscle tissue. Furthermore, diverse pathologic changes in the MuSC-niche during muscle diseases can both stimulate fibrosis and inhibit myogenesis.

In order to develop new opportunities to ameliorate muscle repair and regeneration, it is required to better understand the microenvironmental regulation of MuSCs and how the stem cell niche dysfunction can contribute to disease. In this context, we summarized in this chapter the function of muscle stem cells during the process of skeletal muscle regeneration and also discussed emerging therapeutic applications.

Author-list & contribution:

Omid Mashinchian, Addolorata Pisconti, Emmeran Le Moal & C. Florian Bentzinger

Publication*:

The Muscle Stem Cell Niche in Health and Disease. **Curr Top Dev Biol**. 126: 23-65; 2018

DOI: 10.1016/bs.ctdb.2017.08.003. PMID: 29305000.

Reprinted with permission from © Elsevier (Appendix 1.)

Highlight:

C.F. Bentzinger. Best Supporting Actors. **Science**. 643: 1051; 2019

DOI: 10.1126/science.aaw3613. PMID: 30846594.

Reprinted with permission from © Science/AAAS (Appendix 2.)

*__Curr Top Dev Biol__. 126, 2018. Reprinted with permission from © Elsevier.

1. Introduction

Skeletal muscle is the most abundant tissue of the human body [1, 2]. Its contractile properties are essential for vital functions such as locomotion, postural support and breathing. In addition, skeletal muscle has important endocrine and paracrine functions, and regulates thermogenesis and systemic metabolism [3]. Apart from plastic adaptations to exercise or disuse, skeletal muscle function and mass remains relatively stable until the third or fourth decade of life [4, 5]. In aged individuals, skeletal muscle becomes naturally smaller and weaker, and its metabolic activity decreases [6]. However, an active healthy lifestyle and balanced nutritional intake can help to preserve muscle mass and quality to some extent into old age [7].

As a consequence of contractile activity and stretch, the skeletal muscle fiber sarcolemma and T-tubule system can be affected by micro-lesions. Skeletal muscle injuries at a larger scale, such as strains, contusions and lacerations, can occur due to accidents or surgery. While micro-lesions in the muscle fiber membrane are immediately sealed through a repair-patch containing specialized lipids and proteins, muscle fibers undergoing necrosis are rebuilt through cell-cell fusion of myoblasts [8, 9]. In addition, myoblasts might contribute to tissue repair by fusing to non-lethally damaged muscle fibers [10].

Myoblasts are generated by tissue resident stem cells termed "satellite cells" or muscle stem cells (MuSCs) [11, 12]. Following injury, the MuSC pool expands and gives rise to a subpopulation of transiently expanding cells that are committed to differentiation [9]. Committed MuSC subsequently become myoblasts. Myoblasts can still proliferate but will ultimately differentiate into post-mitotic myocytes that fuse to existing fibers or to each other. Due to self-renewal mechanisms, such as asymmetric division, stochastic expansion and differentiation, the MuSC pool remains at constant size following bouts of regeneration [13].

Owing to the MuSCs, skeletal muscle tissue has an outstanding ability to recover from damage and can undergo multiple cycles of de- and regeneration without any loss of functionality or major consequences on tissue architecture [14]. However, a range of conditions such as aging, muscular dystrophy, cancer cachexia, and diabetes affect the composition of muscle tissue and can impair the function of MuSCs [15]. These pathologies can lead to a vicious cycle of impaired muscle functionality and regenerative failure. For instance, in aging, hip arthritis or osteoporotic fractures, can require invasive surgery that causes significant muscle damage [16]. Due to the age-associated reduction in MuSC function, recovery from such muscle damage is slow. Prolonged immobilization during the healing process may in turn accelerate disuse atrophy, weaken the patients further and increase the risk for falls that will necessitate additional surgical interventions. Muscular dystrophy, is another example of a condition in which regenerative failure is a contributor to pathology. This group of diseases is largely caused by mutations that lead to an instability of muscle fibers inducing chronic de- and regeneration of the muscle tissue. At a certain point, MuSCs in dystrophic muscles become

*__Curr Top Dev Biol__. 126, 2018. Reprinted with permission from © Elsevier.

incapable to compensate for fiber degeneration and the tissue deteriorates progressively [17]. Thus, strategies to improve the function of MuSCs hold great therapeutic promise and may help to maintain or restore functional skeletal muscle mass in aging and disease.

MuSC function is regulated at two levels. Firstly, through intrinsic pre-programmed mechanisms and, secondly, through extrinsic regulation imposed by the stem cell microenvironment, the so called "stem cell niche" (**Figure 1**). The stem cell niche concept was first proposed by Raymond Schofield based on the observation that hematopoietic stem cells require the association with support cells to maintain their stem cell character [18]. The stem cell niche has subsequently been defined as a specific anatomic location that regulates how stem cells participate in tissue generation, maintenance and repair [19]. The niche maintains adult stem cells throughout life and instructs fundamental stem cell behaviors such as quiescence, self-renewal, lineage progression and differentiation. In skeletal muscle, the niche is relatively static under homeostatic conditions, but becomes dynamically remodeled following injury. During the regenerative response, MuSC function is controlled by a spatiotemporally tightly coordinated flux of different cell types. Regulatory signals originating from these cells involve the remodeling and deposition of extracellular matrix (ECM), the release of growth factors, and direct cellular interactions.

In this article, we will review the composition and the regulatory function of the MuSC niche. In addition, we summarize how aging and disease affect the niche, and discuss how these processes can be targeted for the development of stem cell based therapeutic approaches.

*__Curr Top Dev Biol__. 126, 2018. Reprinted with permission from © Elsevier.

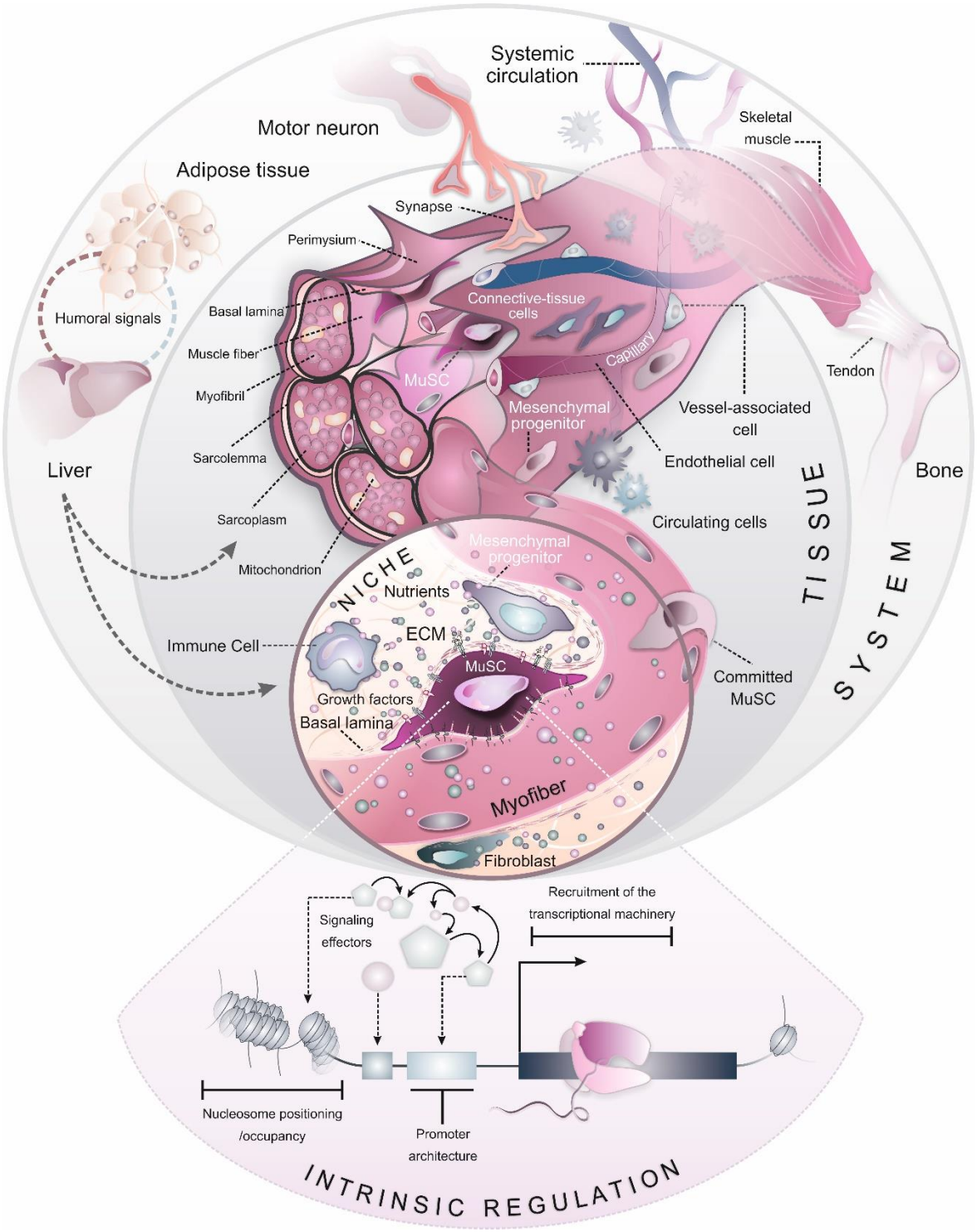

Figure 1. Intrinsic and extrinsic regulation of MuSCs. The niche microenvironment is composed of structural elements, locally bound and secreted signaling molecules, and cell-cell interactions. Systemic signals such as nutrients, hormones and circulating growth factors can regulate MuSC function directly, or influence them through effects mediated on the tissue level or imposed by support cells. Intrinsic mechanisms such as epigenetic adaptations, telomerase activity and constitutively activated or repressed signaling loops that act in concert with extrinsic mechanisms to regulate MuSC function.

***Curr Top Dev Biol**. 126, 2018. Reprinted with permission from © Elsevier.

2. The Perinatal Muscle Stem Cell Niche

Perinatally, skeletal muscles go through a phase of intense growth [20]. At this stage MuSCs are highly proliferative and account for about 30% of sublaminal nuclei [21, 22]. Thus, active MuSCs comprise a major cell population in growing postnatal muscle. Auto-regulatory deposition of ECM components by MuSCs has emerged as an important mechanism shaping the niche in this period [23]. Fetal and postnatal MuSCs express high levels of certain ECM molecules some of which are differentially regulated when compared to quiescent or active adult MuSCs. For instance, both, fetal and quiescent adult MuSCs synthesize high levels of the ECM protein collagen VI, while activated adult MuSCs do not deposit this factor into their niche [23, 24]. Collagen VI has been shown to be involved in bridging ECM components and likely serves as a modulator of biomechanical properties of the perinatal and quiescent MuSC niche. As opposed to collagen VI, the high-molecular weight ECM glycoprotein fibronectin is expressed in the fetal stage as well as in activated adult MuSCs, but displays very low expression in quiescent adult cells [23, 25]. Fibronectin is a ligand for integrin and syndecan receptors that are expressed at high levels by MuSCs and has been shown to be a critical factor mediating the adhesion of proliferating cells to the niche ECM [26-30]. Interestingly, only fetal MuSCs appear to secrete tenascin-C into their niche [23]. Loss of this factor reduces the proliferation and differentiation potential of fetal but not of adult MuSCs. While its molecular function in the perinatal MuSC niche remains to be further investigated, in other tissue niches, tenascin-C is required for modulation of growth factor signals and controls stem cell proliferation and differentiation [31, 32]. Globally, the ECM in developing muscle tissue progresses from an embryonic state that is rich in large chondroitin sulfate proteoglycans implicated in cell adhesion, migration, and proliferation, to a mixture of growth-factor-regulating dermatan sulfate, chondroitin sulfate and heparan sulfate glycosaminoglycans in the perinatal period [33].

Next to regulatory structural elements, the perinatal MuSC niche contains several different cell populations that modulate MuSC function. For instance, a sub-population of PW1+ interstitial cells (PICs) expressing the marker Sca1 at intermediate levels is present in early postnatal muscle [34]. PICs secrete follistatin and insulin-like growth factor-1 (IGF1), which promote proliferation and differentiation of MuSCs [35]. Vice versa, Pax7 knockout mice that are devoid of MuSCs after puberty, display a marked increase in PIC numbers [36]. Thus, MuSCs appear to restrict the number of PICs in postnatal muscle through yet to be identified signals. Apart from PICs, connective tissue fibroblasts are highly abundant in perinatal muscle where they promote the differentiation of MuSCs and the maturation of muscle fiber types [37]. Cells constituting blood vessels, such as endothelial cells, smooth muscle cells and pericytes, represent another important component of the perinatal MuSC niche that is differentially regulated when compared to the adult situation. The microcirculation in perinatal muscle is characterized by small intercapillary distances, short capillary lengths and a

*Curr Top Dev Biol. 126, 2018. Reprinted with permission from © Elsevier.

tortuous network geometry [38]. Endothelial cells have been shown to secrete several different growth factors that promote MuSC proliferation [39, 40]. Postnatally, MuSCs become increasingly associated with pericytes lining the vessel walls. These cells secrete IGF1 and angiopoietin-1, which promotes the progressive withdrawal of MuSCs from the cell cycle and their transition into the quiescent state [40, 41]. Another notable difference between the perinatal and adult niche may originate from neuromuscular signals. Recent work has revealed that neuromuscular junction (NMJ) remodeling can induce regionalized fusion of MuSCs [42]. In contrast to adult muscle fibers that generally contain only one NMJ, muscle fibers in newborn animals are polyinnervated [43]. Therefore, augmented synaptic signals may contribute to the differential regulation of perinatal MuSCs.

Ephrin receptor (Eph) tyrosine kinases, which are involved in cell contact-dependent signaling of MuSCs with muscle fibers, show a highly dynamic expression during development [44, 45]. During the fetal to postnatal transition, MuSCs induce the expression of EphA2 and EphB1. Moreover, the ephrin ligands EfnA1 and EfnB2 are up-regulated at this stage. Next to Eph/ephrin signaling, notch receptors and their ligands, for instance delta-like 1, delta-like 4, jagged 1, and jagged 2, have emerged as signals regulating MuSC function perinatally [46, 47]. During embryonic development, a major source of delta-like1 appears to originate from proliferating committed myogenic progenitors [48-50]. Reduced levels of delta-like 1 or loss of the notch downstream effector RBP-J in fetal muscle progenitors lead to muscle hypotrophy and MuSC exhaustion [50, 51]. Conversely, constitutive notch signaling blocks differentiation and arrests lineage progression [52]. Thus, notch signaling is required for the temporal specification of MuSCs during embryonic development and in the perinatal period. Interestingly, notch signaling in perinatal MuSCs also appears to stimulate them to adhere to developing myofibers and to secrete basal lamina ECM components [53].

Taken together, the secretion and signaling cues of ECM crosstalk with the myogenic lineage and constitute critical regulatory signals in the perinatal MuSC niche.

*__Curr Top Dev Biol__. 126, 2018. Reprinted with permission from © Elsevier.

3. The Quiescent Muscle Stem Cell Niche

During puberty, postnatal muscle growth ceases and the MuSC pool completes the transition into quiescence [54, 55]. In 1961, two pioneering studies have employed electron microscopy to provide the first description of adult quiescent MuSCs adopting a "satellite cell position" in the periphery of muscle fibers in rat and frog muscles [11, 56]. The quiescent state is characterized by a very low cytoplasmic to nuclear volume ratio, a low metabolic activity and mitotic inactivity [57]. Quiescent MuSCs are wedged in-between the plasma membrane of their associated host fiber and the ECM of the basal lamina (**Figure 2**). Thus, their niche is highly polarized and characterized by ECM interactions on their apical pole and cell-cell interactions with the muscle fiber on the basal pole.

The basal lamina ECM is rich in members of the collagen and laminin family, in particular in laminin containing α2, β1 and γ1 subunits (also called laminin-2) and collagen IV [58]. The polymerized collagen and laminin networks in the basal lamina are structurally linked through the glycoprotein nidogen [59, 60]. Heparan sulfate is the glycosaminoglycan component of several heparan sulfate proteoglycans present in the basal lamina and on the surface of cells, including MuSCs and muscle fibers [61]. Heparan sulfates are linear polysaccharides composed of repeated disaccharide units of N-acetylglucosamine and uronic acid which can be variably sulfated in several different positions. Perlecan, which can also bind to laminin and collagen, is an example of an abundant heparan sulfate component of the basal lamina that plays important roles in the local sequestration of growth factors [62].

The linkage of quiescent MuSCs to the basal lamina is established through the apically localized membrane receptors α7β1 integrin and dystroglycan [30, 63-65]. MuSC specific loss of integrin β1 in adult mice leads to a break in quiescence and aberrant cell cycle entry [30]. On the other hand, loss of laminin α2 in mice reduces the number of myogenic progenitors generated during development and the MuSC pool in perinatal muscle fails to undergo the normal progressive reduction in cell number relative to fetal muscles [66]. Together, with the observation that postnatally, laminin α2 deficiency also leads to increased expression of the differentiation marker myogenin, this supports the idea that impaired basal lamina interactions prevent or disrupt MuSC quiescence. Interestingly, laminin α2 deficiency induces a secondary loss of the α7β1 integrin and, vice-versa, integrin α7 knockout mice display reduced levels of laminin α2 [67, 68].

Gene expression studies revealed that quiescent MuSCs contribute to the ECM in their own microenvironment [25, 69]. Candidate auto-regulatory ECM components include vitronectin, laminins, perlecan, decorin, nidogen, biglycan and collagen VI. Quiescent MuSCs also express the transmembrane proteoglycans syndecan-3 and -4, which carry extracellular heparan sulfate and chondroitin sulfate chains allowing for binding of several growth factors such as fibroblast growth

*__Curr Top Dev Biol__. 126, 2018. Reprinted with permission from © Elsevier.

factors (FGFs), hepatocyte growth factor (HGF), vascular endothelial growth factor (VEGF) and transforming growth factor beta 1 (TGFβ1) [28, 70, 71]. In addition, syndecans can serve as co-receptors for integrins. Loss of syndecan-3 leads to spontaneous MuSC activation in adult muscles, while deletion of syndecan-4 has no effect on the base-line stem cell pool [72, 73]. Since syndecan-3 knockout cells exhibit increased ERK map kinase phosphorylation following stimulation with FGF-2 or HGF, it has been suggested that they are missing an inhibitory signal rendering them overly sensitive to growth factors. Apart from syndecan-3, MuSCs employ multiple other strategies to limit the impact of growth factor signals in their niche. These include the attenuation of FGF mediated ERK signaling by the receptor tyrosine kinase inhibitor sprouty 1, as well as the expression of the insulin-like growth factor-2 (IGF2) inhibitor insulin-like growth factor-binding protein 6 [74, 75]. Notably, the importance of restricted growth factor signaling in maintaining the quiescent stem cell state is underlined by the observation that a culture medium containing FGF and HGF receptor inhibitors promotes MuSC in quiescence *in-vitro* [76].

Apart from the basal lamina, the muscle fiber membrane represents another major compartment of the quiescent MuSC niche. Quiescent MuSCs and muscle fibers interact through the sialomucin CD34 and m-cadherin [77-79]. Interestingly, m-cadherin knockout mice display no overt muscle phenotype and it has been postulated that this could be due to compensation by other cadherins, in particular n-cadherin [80, 81]. Furthermore, n-cadherin and m-cadherin have been introduced as components of the quiescence-promoting MuSC-niche which could be utilized as potential targets in therapeutic strategies [82].

Quiescent MuSC also express the calcitonin receptor suggesting that electrical signals from innervated myofibers are involved in the regulation of the quiescent state [69]. Loss of the calcitonin receptor specifically from MuSCs leads to a break in quiescence, cell cycle entry and extravasation into the interstitial space [83]. Furthermore, notch ligands present at the surface of myofibers can likely bind to receptors at the surface of MuSC to promote the maintenance of quiescence. Genetic ablation of the notch effector RBP-J in MuSCs results in spontaneous activation and terminal differentiation [52, 84]. Conversely, constitutive expression of the notch intracellular domain in myoblasts inhibits s-phase entry and Ki67 expression, and stimulates expression of the self-renewal marker Pax7 [85]. In addition, syndecan-3 interacts with notch receptors and is required for notch processing and signal transduction [86]. Recently, it has been shown that myofibers express an E3 ubiquitin ligase family member called mind bomb 1 that allows the activation of notch signalling to prime MuSC towards quiescence [87]. Notably, mind bomb 1 is induced by sex hormones, which connects alterations in the quiescent stem cell niche to the systemic circulation. Moreover, a recent study using chromatin immunoprecipitation followed by sequencing revealed that Notch–Collagen V (COLV)–Calcitonin receptor signalling cascade is required to maintain the MuSC in a quiescent state in a cell-autonomous manner [88].

*__Curr Top Dev Biol__. 126, 2018. Reprinted with permission from © Elsevier.

In addition to the myofiber, blood vessels have been implicated in the maintenance of the quiescent MuSC state. Histological observations have revealed a close proximity between MuSCs and endothelial cells, and a linear relationship between MuSC numbers and capillarization has been demonstrated [39]. Vessel associated smooth muscle cells and pericytes have been shown to exert paracrine secretion of angiopoietin 1 that binds to Tie2 receptors on the surface of MuSCs and thereby promotes their quiescence [40, 89].

Traditionally, the study of quiescence has been hindered by the fact that MuSCs become activated within a very short time window after isolation, making it difficult to examine them in a true quiescent state *in-vitro*. Notably, the Rando group has recently described a culture model for the maintenance of isolated quiescent MuSCs [76]. The authors developed collagen based artificial myofibers with an elasticity around 1,3 kPa that were functionalized with the vascular cell adhesion protein 1 ligand α4β1 integrin and that were coated with a layer of laminin. In combination with a specialized medium, this engineered microenvironment allowed for the prolonged *in-vitro* maintenance of mouse and human MuSCs that display key characteristics of quiescent cells.

Overall, a wide range of niche mediated mechanisms regulate MuSC quiescence. In particular, attachment sites in the basal lamina, cell-cell receptors presented by muscle fibers, and ECM that sequesters growth factors are critical characteristics of the quiescent MuSC niche.

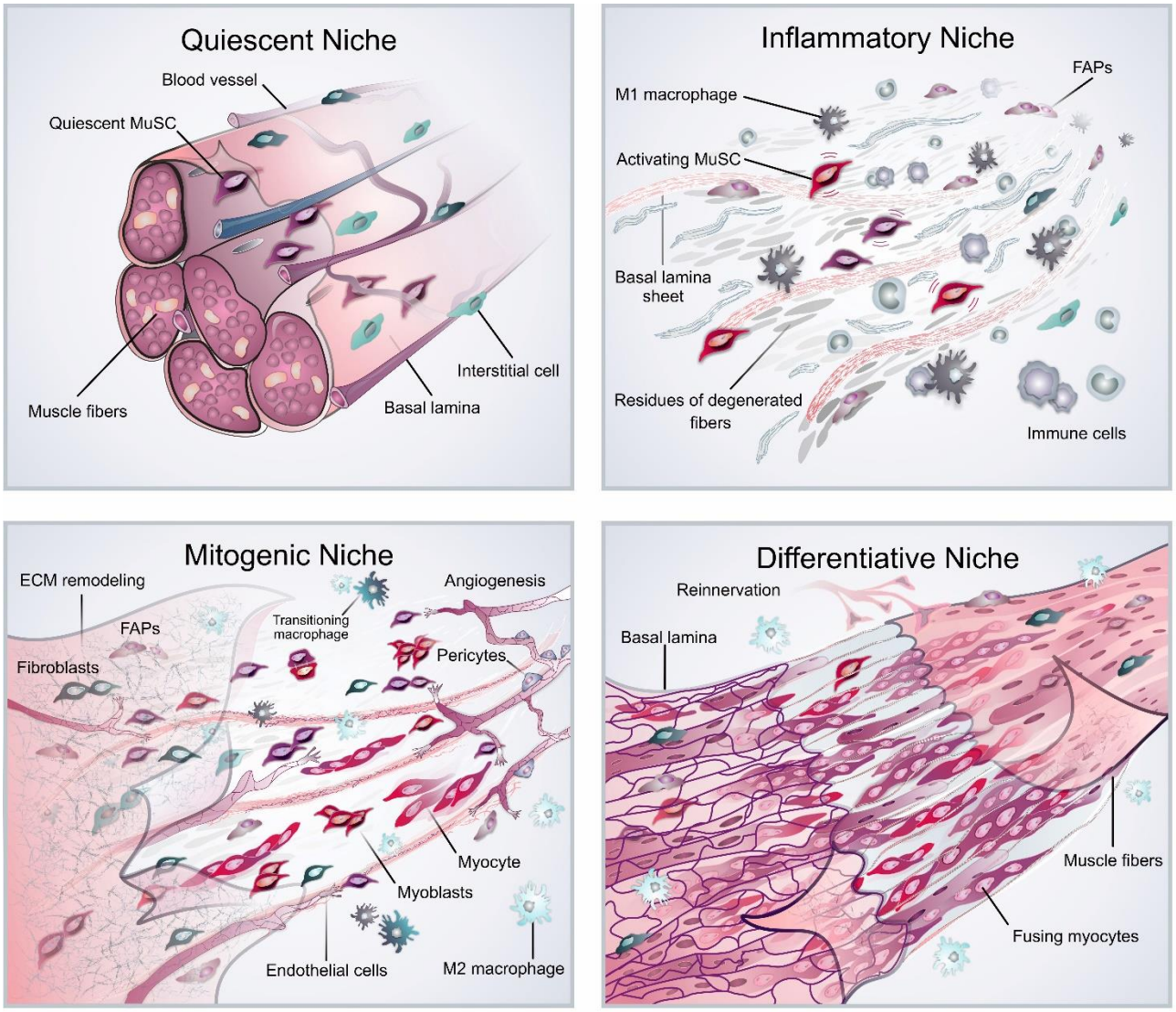

Figure 2. The adult MuSC niche in homeostasis and regeneration. The stem cell niche that maintains MuSCs in their quiescent state in the absence of muscle injury contains a relatively well defined number of macroscopic elements, namely the interface with the muscle fibers and the basement membrane, as well as nearby capillaries. In the immediate phase following injury, the niche contains debris of degenerated muscle fibers and a high abundance of pro-inflammatory immune cells. Subsequently, the niche changes into a milieu that promotes the proliferation of MuSCs and that is characterized by extensive ECM synthesis by fibroblastic cells and angiogenesis. In the differentiative phase, anti-inflammatory macrophage subtypes become dominant and MuSC derived myoblasts fuse into young muscle fibers that are reinnervated, and basement membranes mature.

*

4. The Regenerative Muscle Stem Cell Niche

Much of our knowledge about muscle regeneration and MuSC function originates from experimental injury models in rodents. Multiple protocols including freeze injury, intramuscular injection of barium chloride, glycerol, or the snake venoms notexin and cardiotoxin, have been well established in the research community. Depending on the injury paradigm considerable variation in the kinetics of the MuSC response, the engagement of support cells and re-vascularization dynamics need to be taken in to consideration [90, 91]. The regenerative response that follows all types of muscle injury can be broadly divided into three distinct phases (**Figure 2**). An initial inflammatory phase during which the tissue is cleared of necrotic muscle fibers, a mitogenic period characterized by extensive muscle progenitor and support cell proliferation, and a differentiative period during which new muscle fibers are generated through myoblast fusion. In the following paragraphs, we discuss how the cellular and acellular microenvironment regulates MuSCs during these different phases of muscle regeneration.

4.1. The Inflammatory Niche

At early timepoints following muscle injury necrotic muscle fibers hypercontract within their basal lamina sheet [92]. The remaining basal laminae, that have been termed “ghost fibers”, serve as a template for the subsequent de-novo formation of muscle fibers during regenerative myogenesis and guide motor neuron growth cones for reinnervation at original synaptic sites [93-98]. Destruction of the basal lamina tubes during muscle injury using trypsin leads to a disorientation of myoblasts and transiently irregular myofiber pattern [93]. Moreover, activated MuSCs that happen to migrate away from the basal lamina ghost and start to divide in the interstitial space form branched disorganized myotubes [97]. Migration of MuSCs on the basal lamina has been shown to depend on the laminin receptor integrin α7β1 [99]. Transcriptional profiling of regenerating muscles revealed that early after muscle injury remnant basal lamina is modified by matrix remodeling enzymes that contribute to the liberation of growth factors and cytokines from it, while in later stages of regeneration extensive *de-novo* synthesis of ECM components is induced [100, 101].

Immediately after muscle injury circulating fibrin, is deposited at the injury site where it stabilizes the tissue and provides a scaffold for the engagement of infiltrating immune cells [102]. Necrosis of damaged muscle fibres leads to leakage of normally muscle-compartmentalized factors into the surrounding tissue and the circulation [103, 104]. These damage-associated molecular patterns (DAMPs), which include DNA, heat shock proteins, and the redox-sensitive high-mobility group box 1, collectively contribute to immune cell recruitment mediated by toll-like receptors [105]. In a zebrafish model, a tissue-scale gradient of hydrogen peroxide observed in the first minutes after muscle injury has been linked to leukocyte recruitment at the damaged site [106]. This observation suggests that a

*__Curr Top Dev Biol__. 126, 2018. Reprinted with permission from © Elsevier.

cascade of both chemical and biological molecules orchestrates the earliest events of the immune response.

Muscle resident mastocytes and macrophages sense DAMPs and recruit neutrophils by releasing pro-inflammatory cytokines, including the chemoattractants CXC-chemokine ligand 1 and CC-chemokine ligand 2 (CCL2) [107]. Cytotoxic lymphocytes have recently also been described to contribute to CCL2 production early after muscle damage [108]. CCL2 signaling is critical for the early immune response as genetic ablation of its receptor CC-chemokine receptor 2 reduces subsequent macrophage recruitment and impairs regeneration [109]. Neutrophils peak their number early after the induction of injury and initiate the phagocytic clearance of muscle fiber debris [104, 110]. Eosinophils become abundant in the injured area after about one day and secrete interleukin (IL) 4, which promotes the proliferation of fibro-adipogenic progenitors (FAPs) and stimulates them to contribute to tissue clearance [111]. Following the onset of neutrophil infiltration, circulating blood monocytes, also referred to as patrolling monocytes, extravasate and enter the regenerating muscles [112]. These cells are then primed towards a pro-inflammatory M1 macrophage phenotype by T helper 1 cytokines [113]. M1 macrophages further support phagocytosis of cellular debris and release cytokines and nitric oxide-related molecules that generate a proinflammatory and nitrosative environment [114, 115]. Both Neutrophils and macrophages release the cytokine tumor necrosis factor (TNF) α which curbs the high expression of Pax7 and notch in quiescent cells to levels permissive for myogenesis [116, 117].

Early studies have reported that HGF expression is steeply upregulated in injured muscles [118]. Subsequently, it was shown that quiescent MuSCs express the HGF receptor c-Met and enter the cell cycle upon HGF stimulation [119, 120]. HGF is deposited in the basal lamina and liberated due to matrix metalloproteinase (MMP) 2 activation, which is mediated by nitric oxide derived from infiltrating cells [121, 122]. The earliest stage of MuSC activation has been shown to involve a HGF-induced transition from the quiescent state to a poised alert state [123]. Interestingly, a transition into the alert state also occurs in muscles distant from the injury site due to proteolytic activation of HGF by systemic hepatocyte growth factor activator (HGFA) [124]. Next to HGF, FGF2 has also been shown to be involved in MuSC activation. The ability of both HGF and FGF2 to induce MAP kinase signaling in MuSCs, depends on syndecan-4 [72]. Syndecan-4 knockout MuSCs display delayed entry into the cell cycle and an impaired upregulation of the myogenic commitment marker MyoD. An additional mechanism involved in the activation of MuSCs involves the quiescence marker CD34 that, under homeostatic conditions, interfaces with the muscle fiber [79]. MuSCs in CD34 knockout mice show impaired entry into proliferation and delayed myogenic progression [125]. Thus, CD34 is required for the activation of MuSCs in early stages after injury, possibly by sensing the altered membrane properties of necrotic fibers.

*__Curr Top Dev Biol__. 126, 2018. Reprinted with permission from © Elsevier.

4.2. The Mitogenic Niche

Following the inflammatory response that characterizes the early stages of muscle regeneration, the MuSC niche becomes permissive to proliferation. During this period the MuSC pool expands and a large number of transiently amplifying myoblasts committed to differentiation are generated. The fibrinolytic proteases uPA and plasmin are critical for resolving the transient pro-inflammatory fibrin rich matrix that formed at the site of muscle injury [126, 127]. The importance of this process is illustrated by the persistent accumulation of fibrin, and the occurrence of chronic inflammation and fibrosis in transgenic mice lacking uPA and plasmin. MMPs are an additional class of proteolytic enzymes involved in remodelling of the ECM during the expansion of the MuSC pool [128]. For instance, MMP10 released from vascular cells and MuSCs is induced in early stages of muscle regeneration [129]. This protease degrades a variety of ECM components and can activate other MMPs [130, 131]. MMP10 knockout mice display impaired MuSC proliferation and differentiation, and contain fewer arterioles. Paradoxically, regenerating muscle tissue of MMP10 knockout mice contains lower levels of collagen, laminin and fibronectin, which is likely due to the compensatory upregulation and activation of other MMPs [129].

Apart from proteolytic modifications, the structural composition of the niche during the proliferative response of MuSCs and their support cells, is dramatically modified through the *de-novo* deposition of several ECM components. One of the most strongly induced components of this regenerative matrix is the glycoprotein fibronectin [29]. In activated MuSCs, fibronectin binds to integrins containing β1 subunits and to the Frizzled-7/Syndecan-4 (Fzd7/Sdc4) co-receptor complex [25, 30]. Fibronectin is produced by a range of cells in muscle tissue including fibroblasts, FAPs, cells of the hematopoietic fibrogenic lineage, as well as MuSCs themselves [29, 132]. Adhesion to fibronectin is required to prevent anchorage-dependent cell death and regulates asymmetric division and strand segregation of MuSCs [25, 133]. Linking niche adhesion of MuSCs to growth factor signaling, integrin β1 has been shown to cooperate with FGF2, while the Fzd7/Sdc4 co-receptor complex potentiates Wnt7a signaling [25, 30]. Both, the FGF receptor 1 and the Fzd7/Sdc4 complex have been demonstrated to be critical for self-renewal mechanisms regulating the MuSC pool during regenerative myogenesis [25, 134, 135]. Collagen VI, released from fibroblasts, represents another ECM protein that is upregulated during the peak of MuSC proliferation [24]. Deposition of collagen VI in the MuSC niche is critical for the regulation of its mechanical properties. Collagen VI knockout mice show impaired MuSC function and muscle regeneration that is due to tissue elasticity diverging from the optimal 12 kPa of normal muscle to around 7 kPa [136].

Several growth factors released from the niche ECM or originating directly from cellular sources, have been implicated in the regulation of the MuSC pool during the regenerative response [137]. For instance, basal lamina bound FGF2 that is derived from MuSCs, myofibers and fibroblasts, promotes

expansion and maintenance of the MuSCs by repressing terminal myogenic differentiation [134, 138-144]. IGF1 originating from the systemic circulation or locally produced in muscle tissue, represents another factor that has been shown to promote an expansion of the MuSC pool [145-147]. IGF1 downregulates expression of the cell-cycle inhibitor p27kip and thereby increases MuSC proliferation [147, 148].

The mitogenic response of MuSCs is coordinated by a range of resident and infiltrating cells. In particular, immune cells have emerged as pivotal regulators of the MuSCs in this phase. Activated MuSCs attract monocytes that eventually differentiate into macrophages and mediate cell-cell contact induced inhibition of apoptosis [149]. M1 macrophages that are still present in the niche during the proliferative MuSC response, release TNFα, IL-6, IL-1β and VEGF to stimulate MuSC proliferation and limit early differentiation [112, 114]. Secretion of interferon (IFN) γ by M1 macrophages, lymphocytes, and natural killer cells, correlates with MuSC expansion [150]. IFNγ induces the myogenic differentiation repressor MHC Class II transactivator that prevents myogenic differentiation [151]. In the recent years, a role for muscle regulatory T (Treg) cells within the mitogenic MuSC niche has emerged [152]. These resident cells, with high clonogenic potential, accumulate in injured skeletal muscle around the time when MuSC proliferation is maximal, and their genetic ablation impairs muscle regeneration and increases collagen deposition. This might be due to altered transition of M1 to M2 macrophages, as well as to a loss of direct supportive signals for MuSCs. Illustrating the complexity of cellular crosstalk in the niche, IL-33 expressed from FAPs has been shown to be required for the recruitment of Treg cells to injured muscle [153].

At more advanced timepoints during the proliferative expansion of the MuSC pool, when the first myoblasts begin to differentiate, M2 macrophages become dominant over M1 macrophages in the regenerating tissue [154]. M1 deactivation is required for sequential steps of macrophage activation [155]. IGF1 has been shown to be essential for this process [156]. Its genetic loss from myeloid cells impairs M1 to M2 skewing, dysregulates tissue cytokine levels and impairs muscle repair. Similarly, a null mutation of IL-10 amplifies M1 on the expense of M2 macrophages due to blunted skewing, and leads to premature differentiation of MuSCs [157]. Supporting these observations, diphtheria toxin mediated ablation of intramuscular macrophages during the transitional period leads to defective regeneration [112]. Thus, efficient skewing of macrophage phenotypes is critical for the regulation of the MuSC pool. Transcriptomic profiling of muscle macrophage subsets from regenerating muscles revealed that M2 macrophages express a large set of ECM-related genes such as thrombospondin-4, microfibrillar-associated protein 5, lumicam and dermatopontin, and thereby significantly contribute to structural remodeling of the niche [113].

Next to immune cells, the expansion of the MuSC pool is supported by fibroblasts that display comparable proliferation kinetics [158]. Partial ablation of fibroblasts during muscle regeneration

*__Curr Top Dev Biol__. 126, 2018. Reprinted with permission from © Elsevier.

reduces the number of MuSCs, leads to premature differentiation and reduces the size of myofibers formed in late myogenic stages. Since fibroblasts are major producers of ECM, these effects are likely due to a deregulation of the niche architecture. FAPs represent another rapidly expanding niche cell type that supports MuSCs in response to injury [159, 160]. FAPs regulate MuSCs through the secretion of promyogenic cytokines and ECM. Inhibition of FAP-induced transient collagen deposition using the pharmacological tyrosine kinase inhibitor Nilotinib impairs MuSC expansion and results in defective muscle regeneration [161].

Angiogenesis and myogenesis have been reported to proceed in parallel after skeletal muscle injury [162, 163]. Pro-angiogenic factors as such as VEGF, angiopoietin-1 and -2 increase markedly in regenerating muscle tissue [164]. Cycling MuSCs are largely co-localized with endothelial cells and release VEGF to stimulate microvascular sprout frequency and enlargement [39, 165]. Reciprocally, endothelial cells appear to promote MuSC proliferation through the release of several growth factors including IGF1 and FGF2.

4.3. The Differentiative Niche

After the proliferative phase, myoblasts will extensively fuse to generate multinucleated muscle fibers and MuSCs that resisted myogenic commitment, will begin to transition back into the quiescent state. During this period the vasculature enlacing the basal lamina tubes of the newly generated muscle fibers becomes denser and more organized, and pericytes and smooth muscle cells are recruited to stabilize its structure [91, 163, 166]. Analogous to the mechanism that promotes the acquisition of quiescence during postnatal development, the activation of the Tie-2 receptor in MuSCs by pericyte-derived angiotensin 1 progressively promotes their withdrawal from the cell cycle [40, 41]. This process is essential to guarantee the availability of sufficient quiescent MuSCs that can be activated for subsequent rounds of regeneration.

During myoblast fusion, changes in the heparan sulfate content of the niche ECM lead to an increased retention of pro-proliferative anti-differentiative growth factors [61]. For instance, differentiating myoblasts sequester FGF2 through the lipid raft associated proteoglycan glypican-1 and, at the same time, downregulate the expression of syndecans, FGF and HGF receptors [167, 168]. Certain growth factors such as IGF2 also promote differentiation directly. IGF2 induces the expression of the cyclin-dependent kinase inhibitor p21 to promote cell cycle exit and cell fusion [169-171].

During the differentiation phase, immune cells are mainly primed to limit inflammatory responses and to promote tissue repair through the release of anti-inflammatory cytokines such as IL-10 [157]. In macrophages, the lipid activated peroxisome proliferator activated receptor gamma (PPARγ), has been shown to be required for the transcription of growth differentiation factor 3, which decreases myoblast proliferation and promotes fusion [172]. FAPs have also been suggested to promote

*__Curr Top Dev Biol__. 126, 2018. Reprinted with permission from © Elsevier.

myogenic differentiation through the secretion of IL-6 [159]. As myogenesis progresses and muscle fibers become more mature FAP numbers are reduced through apoptosis induced by macrophage derived TNFα [173].

Interestingly, pericytes themselves as well as PDGF receptor negative PICs have been shown to participate in muscle fiber formation during the differentiative stage of regeneration [34, 36, 174-176]. The niche signals required for fate decisions and recruitment of these interstitial cell types to myogenesis remain to be elucidated, and appear to involve a complex interplay with other regenerative processes such as reinnervation, angiogenesis, fibrosis and adipogenesis [166, 177].

Altogether, the MuSC niche instructs all stages of regenerative myogenesis through the timed availability of signals originating from supportive cell types and from the ECM. The different cell types involved in these processes communicate extensively and coordinate their function to create the transitory environmental conditions that control MuSC activation, proliferation, self-renewal, differentiation and return to quiescence. As outlined in the subsequent paragraphs these processes are highly susceptive to perturbation and their deregulation in aging and disease can have profound consequences on muscle regeneration.

*__Curr Top Dev Biol__. 126, 2018. Reprinted with permission from © Elsevier.

5. The Muscle Stem Cell Niche in Aging

Virtually every tissue of the body undergoes a decline as an organism ages. The molecular mechanisms of aging are complex and for many tissues have been shown to involve a failure of stem cells to maintain tissue integrity and function over time [178, 179] (**Figure 3**). In case of human skeletal muscle, one of the most prominent features of aging is the loss of muscle mass and strength, also known as sarcopenia, which is accompanied by an impaired regenerative capacity and a pathological increase in baseline ECM levels [180].

The implications of MuSCs in muscle aging are subject to a long-lasting debate. One hypothesis, the numerical stem cell aging theory, is that MuSCs become less abundant with aging thus can contribute less to muscle maintenance and regeneration. Indeed, several studies have provided evidence that a decline in MuSC numbers occurs with aging both in humans and rodents [181-187]. However, recent results suggest that ablation of a large fraction of MuSCs does not accelerate nor exacerbate sarcopenia [188]. It is important to consider that some MuSCs where surviving the ablation procedure employed in this study and it is not yet known “how few is too few MuSCs” for maintenance of muscle tissue throughout life [189]. Notably, transplantation of just a few myofibers carrying no more than a few dozens of associated MuSCs into regenerating host muscles has been shown to contribute to large portions of the recipient tissue [190, 191]. It has also been described that next to a complete loss of regenerative capacity following injury, fibrosis was increased in old mice that had had their MuSC pool depleted earlier in life [188]. This phenomenon has been recently mechanistically explained by the same group with a loss of MuSC-mediated inhibition of fibroblast activity via exosomes secreted by MuSCs [192].

A second hypothesis on muscle aging, the functional stem cell aging theory, argues that old MuSCs become exhausted and fail to maintain the tissue due to environmental changes and cell-intrinsic mechanisms. Strong evidence has been provided in the last two decades in support of this theory and important links with the numeric stem cell aging hypothesis have emerged [193]. Compared to organs such as the gut or the skin, most skeletal muscles have a relatively low cellular turnover and MuSCs persist in a quiescent state with low metabolic activity over prolonged periods of life [194-196]. Therefore, an intrinsic mechanism that limits number of divisions or the function of the cells through a combination of telomere attrition, DNA and oxidative damage, misfolded proteins, or mitochondrial dysfunction, would appear to be less dominant in contributing to MuSC aging than altered environmental signals in the surrounding tissue. Interestingly, recent work has shown that even aspects of aging that have traditionally been considered intrinsic can be influenced by environmental stimuli. For instance, telomere length is conserved in MuSCs from healthy and physically active individuals [197]. This observation suggests that the control of telomere length is a dynamic process that can be affected by environmental stimuli and therefore may not be exclusively intrinsically

*__Curr Top Dev Biol__. 126, 2018. Reprinted with permission from © Elsevier.

regulated. Similarly, epigenetic adaptations occurring with age can be modulated by environmental signals. A recent study by the Conboy group has shown that the loci of cyclin/cyclin-dependent kinase inhibitors p21 and p16 are less epigenetically silenced in MuSCs from old mice than in MuSCs from young mice [198]. FGF-2 signaling can silence the p21 locus in old MuSCs and thereby restores cell proliferation. Lastly, several signaling pathways have been shown to be rewired in a sustained fashion in aged MuSCs contributing to impaired proliferation or function [134, 140, 199-201]. Depending on definitions, this phenomenon may be considered an intrinsic or "cell-autonomous" property since it persists to some degree in isolated cells. However, recent studies indicate that disrupted environmental signals originating from the stem cell niche ECM may be upstream mechanisms leading to some of these long-lasting changes [29, 30].

First evidence that the aged environment plays a critical role in regulating muscle regenerative capacity was provided by transplantation experiments in which extensor digitorum longus muscles were grafted between young or old donor rats [202]. The results showed that when the recipient was young, no difference in the regenerative capacity of either young or old donor grafts was observed. In contrast, when the recipient was old, both young and old donor grafts failed to regenerate efficiently. These results clearly suggested that the old environment prevents regeneration. Subsequently, Conboy et al. showed that replacing the systemic environment of old mice with that of young mice via heterochronic parabiosis was able to improve the regenerative potential of old mice [203]. This observation supports the idea that age affected systemic signals can either influence MuSCs directly or promote the function of supportive cells in the niche. Furthermore, several groups have shown that MuSCs explanted from both old and young mice show similar replicative and differentiative potential in culture [204]. In contrast, if MuSCs are explanted along with their accompanying myofiber and basement membrane ECM, which constitute a portion of the stem cell niche, old cells show an impaired proliferative capacity [134, 204]. Thus, under conditions where the native aged environment is partially present, the regenerative potential of old MuSCs is impaired, while in isolation, the regenerative potential of old and young MuSCs becomes equalized. However, this aspect remains controversial for human cells for which some groups observed no difference in culture when MuSCs where obtained from either young or old donors, while others reported a dramatic reduction in proliferative potential and accelerated senescence of aged cells [205, 206].

In the course of the heterochronic parabiosis experiments outlined above, notch signalling was identified to be involved in mediating the positive effects of a youthful systemic environment on MuSCs. Inhibition of notch impairs regeneration in young muscle while forced expression of notch restores regeneration of old muscle [204]. The notch pathway has also been studied in the context of cross-talk with other aging mechanisms, especially with TGFβ signals. In aged MuSCs, forced activation of notch blocks TGFβ-induced expression of several cyclin-dependent kinase inhibitors, namely p15, p15, p21 and p27 via Smad3 [207]. Notably, the effect of TGFβ on myoblast proliferation

*__Curr Top Dev Biol__. 126, 2018. Reprinted with permission from © Elsevier.

is dose-dependent with small amounts promoting MuSC proliferation and higher concentrations having inhibitory effects [208]. Importantly, blood levels of TGFβ1 increase with age, both in humans and in mice, possibly reaching concentrations that exceed the threshold for negative effects on MuSCs. Similarly, growth differentiation factor 11 (GDF11), another member of the TGFβ superfamily, is found in increased levels in the aged systemic circulation and inhibits MuSC function [209]. Correspondingly, a recent study by Hinken et al., indicated no positive-effect of GDF11 on MuSCs expansion *in-vitro* [210]. But, some controversies exist regarding the role of GDF11 as a therapeutic agent in muscle growth and regenerative processes as initial studies exploiting heterochronic-parabiosis, demonstrated GDF11 as a protein capable of the rejuvenative influence on reversing the skeletal muscle dysfunction [211]. Nevertheless, one possible reason for the current controversy surrounding GDF11 and some skepticism related to the results is that these studies rely on serum or plasma levels of GDF 11 and the performed analyses are associated with the different methods of processing of blood samples which could cause an increase in GDF11 levels in either plasma/serum [212, 213].

Heparan sulfates are a major binder of growth factors in the ECM [214]. In aged mouse muscles, the heparan sulfate composition changes and its binding capacity for growth factors becomes altered. Heparan sulfate extracted from young muscle can, for instance, inhibit the mitotic activity of FGF2, while extracts from old muscle have inverse effects [61]. Thus, heparan sulfate from aged muscle fails to efficiently sequester growth factors, which may lead to a break in MuSC quiescence [140]. Interestingly, the higher availability of FGF2 in the aged niche is paralleled by decreased sensitivity of the FGF receptor 1 [30, 134]. Next to FGF2, heparan sulfate also binds signalling molecules of the Wnt family, which display increased activity in aged muscle [215]. These age-associated increases in Wnt signalling have been connected to an activation of β-catenin mediated canonical signaling in myoblasts that trigger an increased conversion into fibroblasts. Fibroblasts are able so secrete copious amounts of certain ECM components and further exacerbate fibrosis of old muscles. Since MuSCs seeded on decellularized ECM derived from old muscles express fibrogenic markers and are less myogenic than cells seeded on ECM from young muscle, the altered aged structural environment appears to also directly contribute to fibrogenic conversion [216]. FAPs are another fibrogenic cell type closely related to fibroblasts that is resident in skeletal muscles and that appears to contribute to tissue fibrosis. Recent work has revealed that limiting the proliferation of FAPs through facilitating the expression of a truncated intronic variant of PDGFRα that acts as a decoy that limits PDGF signalling, can reduce fibrosis in aged muscles [217]. In contrast to the age-associated increase in collagen-rich ECM in homeostatic muscles, the transient regenerative matrix that instructs MuSCs following injury is reduced in aged muscles [29]. For instance, reduced upregulation of fibronectin leads to insufficient activation of integrin receptors, reduced sensitivity to FGF2 signaling and to increased anchorage dependent cell death of MuSCs [29, 30]. Reactivation of integrin

*__Curr Top Dev Biol__. 126, 2018. Reprinted with permission from © Elsevier.

or restoration of youthful levels fibronectin in old regenerating muscles rescues MuSC function and improves the regenerative potential of aged muscles.

Next to changes that manifest at the level of the ECM, aged skeletal muscle tissue is also characterized by altered microvascular structure and function, mild chronic inflammation and increased production of reactive oxygen species [218, 219]. These phenomena appear to be closely interconnected. For instance, higher numbers of immune cells in the aged niche increase reactive oxygen species levels, which in turn might affect nitric oxide signaling and thereby lead to altered vascular function [218, 220]. The chronic inflammatory state that characterizes aged muscle is also present in other tissues and has been termed as "inflammaging" [221]. In skeletal muscle this phenomenon is associated with altered levels of several cytokines [222-226]. TNFα appears to decrease myoblast differentiation in aged muscles and thereby impairs regeneration. IL-6, which is similarly increased with aging, might also perturb MuSC function [200, 227]. Jack/STAT signalling, which is downstream of IL-6, is increased in aged MuSCs, and its inhibition restores self-renewal and myogenic potential [199, 200]. Yet another inflammation-related factor that increases with aging and might directly affect MuSC function is osteopontin secreted by aged CD11+ macrophages. Neutralization of osteopontin promotes MuSC differentiation and improves the regenerative capacity of old muscles [228].

In conclusion, extensive evidence supports the notion that the MuSC niche is significantly altered with aging and that such changes inevitably affect the maintenance and regenerative capacity of skeletal muscle tissue. The development of interventions that holistically stall the aging process or even rejuvenate muscle, will be facilitated by the identification of the physiological upstream triggers leading to the deterioration of the stem cell niche with old age.

*__Curr Top Dev Biol__. 126, 2018. Reprinted with permission from © Elsevier.

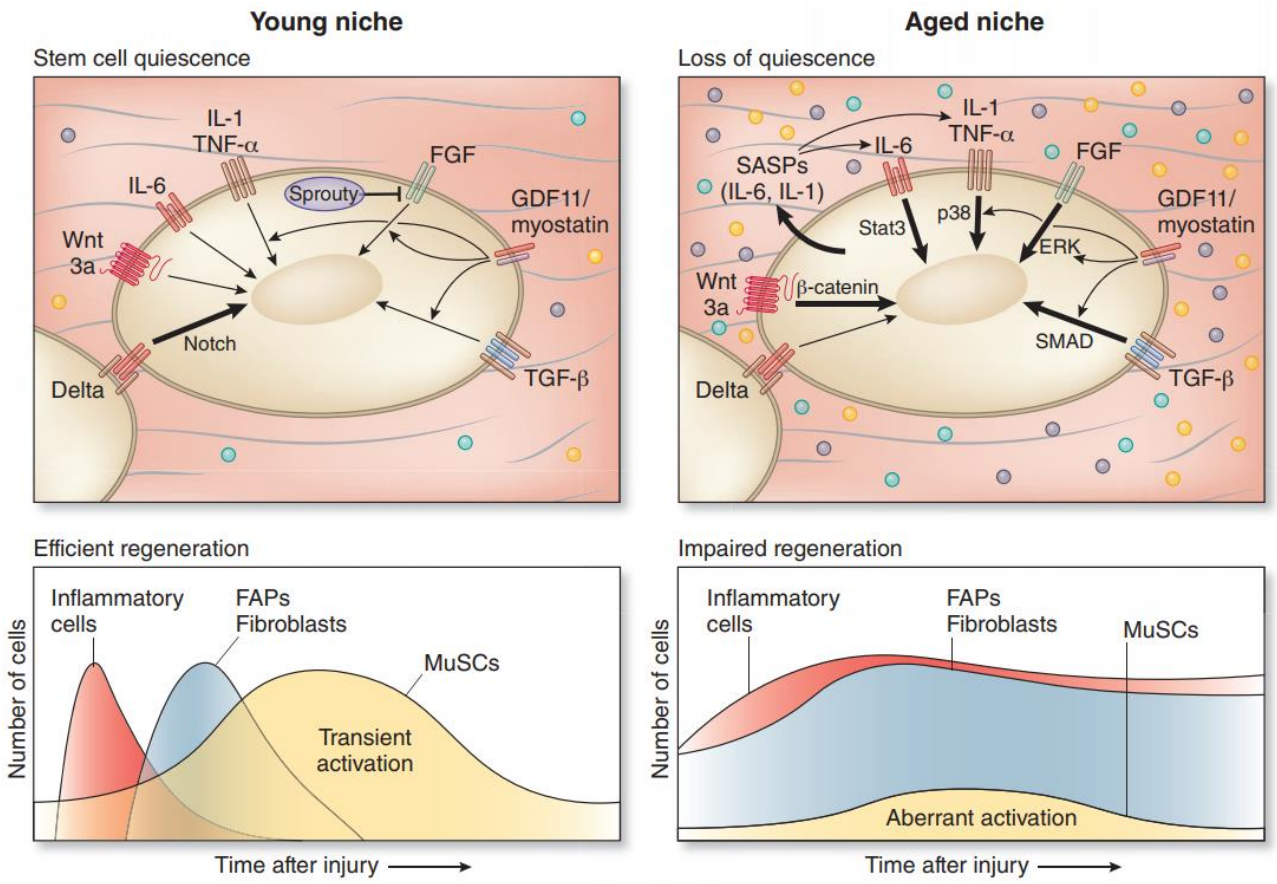

Figure 3. Intrinsic and extrinsic regulators influence age-related changes in MuSC function. MuSCs are transiently activated in young muscles by stimulating regulatory pathways (e.g., Delta–Notch) through released inflammatory cytokines and diverse growth factor signaling leaded by immune cells, fibroblasts and fibro/adipogenic progenitors (FAPs) [13, 229]. However, self-renewal signals (e.g., Delta [230]) in aged muscles are dramatically diminishing and concurrently inflammatory and fibrogenic signals are amplifying, causing in aberrant stem cell activation and subsequently loss of quiescence in MuSCs [231-235]. In the schematic illustration, the thickness of the arrow shows the strength of activation of the different pathway in young and aged MuSCs. Reprinted with permission from [179] © Springer Nature (2015) (Appendix 3.).

*__Curr Top Dev Biol__. 126, 2018. Reprinted with permission from © Elsevier.

6. The Pathologic Muscle Stem Cell Niche

Several diseases, including primary myopathies, neuromuscular, metabolic and inflammatory disorders, are associated with changes in the MuSC niche. The best studied group of primary myopathies in the context of pathologic changes in the MuSC niche, are the muscular dystrophies. In the majority of muscular dystrophies described so far, muscle fibers are structurally more fragile and tend to rupture under the mechanical stress of contraction [236]. This causes protein leakage which attracts inflammatory cells such as neutrophils, macrophages, natural killer cells and lymphocytes [237]. The presence of several foci of injury in dystrophic muscle, which develop asynchronously and continuously, trigger an inflammatory response that is different from the one caused by acute trauma-induced injury [238]. In muscular dystrophy, inflammation becomes chronic and the continuous presence of inflammatory cells dramatically alters the MuSC niche through thickening and stiffening of the extracellular matrix and the accumulation of ectopic adipose tissue [17]. In the long run, these sustained changes in the extracellular milieu impair MuSC function up to the point where they can no longer compensate for the dystrophic muscle fiber degeneration. This state of regenerative failure leads to a deterioration of the tissue and progressively impairs muscle functionality.

Early studies using traditional biochemical and histological approaches to characterize the extracellular environment, have identified an accumulation of collagen type I, III, IV and V in human dystrophic muscles [239, 240]. *In-vitro* studies carried out with isolated myogenic cells obtained from dystrophic patients suggested that the increase in collagen deposition in these conditions was due to augmented cell autonomous secretion [241]. However, this simplified view has been revised and it is now clear that dystrophic muscle fibrosis is the result of highly complex processes involving several cell types that act in concert with myogenic cells, namely FAPs, macrophages, pericytes and other cells of mesenchymal or hematopoietic origin [17].

Next to collagens, various heparan sulfate proteoglycans are increased in the ECM in dystrophic muscle compared to healthy muscle [242, 243]. These molecules include perlecan, syndecan 3 and glypican 1 in muscle of Duchenne muscular dystrophy patients and decorin in a mouse model of this disease. Moreover, the expression and levels of ECM modifiers, such as MMPs and their endogenous inhibitors, the tissue inhibitors of metalloproteinases (TIMPs), are also affected in muscular dystrophy [128, 244-246]. These observations suggest that not only the abundance of ECM molecules, but also their structural arrangement becomes altered as a consequence of the disease.

In addition to MMPs and TIMPs, several serine proteases and their endogenous serine protease inhibitors (Serpins) are differentially regulated in muscular dystrophy. These include members of the coagulation cascade, such as the PAI-1/uPA system and those produced by neutrophils, such as neutrophil elastase and its inhibitor serpinb1a and the latent TGFβ-binding protein 4 [247-250]. The

*__Curr Top Dev Biol__. 126, 2018. Reprinted with permission from © Elsevier.

imbalance described for several proteolytic systems in the dystrophic MuSC niche can affect MuSCs in diverse ways. Firstly, it affects the structure of the ECM and therefore adhesion signaling, which is critical for MuSC function [29, 30]. Secondly, it affects the bioavailability and activation status of growth factors, cytokines and other signaling molecules such as TGFβ, CTGF, IL-1, IL-6 and Ang2 that can simultaneously promote fibrosis and inhibit myogenesis [17, 251-255]. Thirdly, it might affect MuSCs directly through protease-activated receptor (PAR) 1 and 2 [256, 257].

Matricellular proteins are ECM bound non-structural proteins that interact with various integrins, growth factor receptors and growth factors to modulate their function and activity [258]. Proteomics-based profiling of dystrophic muscle has revealed an upregulation of several matricellular proteins such as dermatopontin, decorin, asporin, prolargin, periostin, lumican and fibrinogen, while levels of nidogen and fibrillin were found to be decreased [248, 259-261]. The TGFβ inducible protein periostin that can bind to collagen, fibronectin, tenascin-C, bone morphogenetic protein (BMP) 1, and notch 1, was found to play a critical role in the pathogenesis of muscular dystrophy [262]. Genetic deletion of periostin in δ-sarcoglycan null mice, which display a severe form of muscular dystrophy phenotypically similar to Duchenne muscular dystrophy, promotes regeneration and reduces fibrogenesis through inhibition of TGFβ signaling. Likewise, decorin that is upregulated in dystrophic muscles, modulates members of the TGFβ superfamily, especially TGFβ1, TGFβ2, myostatin, BMP2 and connective tissue growth factor signaling, and may thereby contribute to MuSC deregulation [263-268]. Lastly, the chronic matricellular deposition of fibrinogen in dystrophic muscles favors inflammation through sustained leukocyte activation [269]. Inhibition of fibrinogen binding to the αMβ2 integrin receptor limits macrophage activation and ameliorates disease progression in a mouse model of Duchenne muscular dystrophy.

As a consequence of chronic inflammation and the infiltration of CD4+ and CD8+ T cells, macrophages, eosinophils and natural killer T cells, the MuSC niche in dystrophic muscle is highly enriched in signaling molecules such as prostaglandins, cytokines, and chemokines [270]. These molecules can influence the proliferation, differentiation, migration, fusion and survival of myoblasts, and their pathologic deregulation will ultimately affect normal MuSC function and thereby contribute to regenerative failure of dystrophic muscle [104]. Increased prostaglandin levels have been described in muscles of mice and humans with muscular dystrophy [271-273]. Similarly, several cytokines and chemokines, including TNFα, IL-1β, IL-4, IL-6 and IFNγ, are present in higher levels in dystrophic muscles [274-278]. Pharmacologic normalization of IKK/NF-κB mediated cytokine signaling, neutralization of TNFα or genetic ablation of IFNγ, all decrease inflammation and promote regeneration in mouse models of muscular dystrophy [279-281]. Supporting the assumption that these molecules are largely derived from immune cells, experimental depletion of either myeloid or lymphocyte populations greatly reduces dystrophic pathology [282-284]. Moreover, immunosuppressive

*__Curr Top Dev Biol__. 126, 2018. Reprinted with permission from © Elsevier.

therapy with glucocorticoids, can improve muscle strength in patients and in animal models of muscular dystrophy [285-287].

Diseases other than muscular dystrophy can affect the niche and thereby the regenerative capacity of MuSCs. Diabetes mellitus (DM) is defined as a group of metabolic disorders characterized by hyperglycemia due to lack of insulin production or function. As the largest site for glucose uptake in the body and a main regulator of glycemia, skeletal muscle contributes significantly to the pathogenesis of DM. Although much is known about DM-associated changes in skeletal muscle composition and health, it remains subject to ongoing research how the diabetic environment affects MuSCs [288]. Correlating with the general impairment in wound healing capacity in diabetic individuals, it has been shown that muscle regeneration is affected in type 1 and 2 DM [289-295]. Hyperglycemia has been shown to increase free radical species and reducing antioxidant levels in diabetic rats [293, 296]. This phenomenon may involve nitric oxide synthase in endothelial cells that produces more reactive oxygen and nitrogen species when exposed to increased glucose levels [297]. Administration of antioxidative compounds in these animals counteracts muscle fiber proteolysis and improves markers of muscle regeneration [293, 296]. Muscles in obese or diabetic mice and humans also present an increased infiltration of M1 macrophages leading to fibrotic deposition of collagen and abnormal levels of TGFβ, interleukins and TNFα, which may collectively impair normal MuSC function [298-301]. Lastly, the accumulation of proteins or lipids that become glycated as a result of continuous exposure to sugars, exert negative effects on both human and mouse myoblasts [302].

Cachexia is a dramatic loss of skeletal muscle mass that can occur as a consequence of several conditions, including cancer, acquired immunodeficiency syndrome (AIDS), chronic obstructive pulmonary disease (COPD), and heart failure [303]. It is plausible that such dramatic and rapid loss of muscle mass also alters the MuSC niche and affects MuSC function. Indeed, the onset of muscle atrophy usually triggers MuSC activation, while later stages appear to be characterized by reduced MuSC numbers [304-307]. In contrast to dystrophic or diabetic skeletal muscles, muscles from cachectic patients or tumor-bearing mice show no signs of infiltrating immune cells, but exhibit abnormalities in the structure of the basal lamina and the muscle fiber membrane [308, 309]. This altered niche, in combination with changes in circulating serum factors, leads to hyperactivation of both MuSCs and other muscle resident cell populations such as PICs and pericytes. Interestingly, under these conditions MuSCs display sustained expression of the self-renewal factor Pax7 leading to a suppression of the differentiation program and compromised muscle repair. Other adaptations in the cachectic muscles include altered levels of (I) TNFα, which was originally called “cachectin” because of its strong association with cachexia, (II) angiotensin 2, (III) myostatin, (IV) oxidative stress, and (V) corticosteroids [310-316].

*__Curr Top Dev Biol__. 126, 2018. Reprinted with permission from © Elsevier.

Taken together, changes in structural and soluble signals in the MuSC niche contribute to the pathology of several types of muscle disease. Altered dynamics of inflammatory cells appear to be an important upstream trigger involved in most of these adaptations. Thus, further investigation of the intricate interplay of immune cells, MuSCs and other supportive niche cells, will provide us with a much-needed improved understanding of the pathological adaptations in diseased muscle, and will help to device novel therapeutic strategies to maintain, normalize, or restore the endogenous repair potential of MuSCs.

*__Curr Top Dev Biol__. 126, 2018. Reprinted with permission from © Elsevier.

7. Targeting the Niche for Therapy

Several strategies that promote youthful MuSC function and that maintain the regenerative capacity of skeletal muscle into old age, have been trialed both in humans and animal models. Arguably the most successful anti-aging intervention amongst those tested so far, is a moderate but constant level of exercise, which supports MuSCs through a spectrum of adaptations in the niche. Exercise has been shown to promote vascular function and angiogenesis, which are systemically compromised in aging, leaving the MuSC niche depleted of nutrients, oxygen and endothelial cell-mediated support [317-319]. An important mechanism by which physical activity exerts positive effects on the vasculature appears to involve the release of nitric oxide, a regulator of vessel cell proliferation, vascular tone and leukocyte–endothelial cell adhesion [320-323]. Exercise also promotes the release of pro-angiogenic factors such as VEGF that are known to modulate MuSC function directly [39, 324]. Chronic inflammation and oxidative stress have emerged as additional age-associated processes that can be influenced through exercise. Physical activity has been shown to correlate with reduced levels of pro-inflammatory markers in elderly individuals and stabilizes the muscle redox system [325-327]. The positive effects of exercise on the MuSC niche are not limited to better vascular health, reduced inflammation and oxidative stress, but appear to also involve ECM remodeling. Although the response to exercise is globally blunted in older individuals, it still leads to rapid expression of ECM proteins and certain matrix remodeling enzymes, especially various collagens, MMP2 and MMP9 [328-332]. Niche elasticity critically influences MuSC function and aging is generally associated with stiffer muscles [136, 333, 334]. Notably, muscles of aged trained individuals are characterized by reduced collagen cross-linking and therefore display an improved elasticity that may promote MuSC function [335]. Taken together, a moderate but constant training regime is associated with the reversal of a wide spectrum of age-associated changes in the MuSC niche. An important additional benefit of physical activity is that it will contribute to reducing adipose mass and counteract the development or progression of age-related diabetes, which can also affect MuSC function.

As outlined above, the excessive fibrotic deposition of certain ECM molecules that characterizes aging and degenerative muscle diseases, can impair MuSC function through a broad spectrum of mechanisms. Moreover, secreted pro-fibrotic signaling factors often also inhibit MuSCs directly. The TGFβ pathway represents an obvious target for the therapeutic reduction pro-fibrotic signaling in the pathologic niche. Inhibition of TGFβ using neutralizing antibodies or pharmacologic inhibition of its downstream effectors reduces fibrosis and improves MuSC function [336-340]. The peptide hormone angiotensin 2 promotes TGFβ signaling at several levels in the TGFβ signaling pathway [341]. Losartan is an angiotensin 2 receptor antagonist drug approved for the treatment of high blood pressure, which has been shown to reduce skeletal muscle fibrosis in mouse models of both Duchenne and

*__Curr Top Dev Biol__. 126, 2018. Reprinted with permission from © Elsevier.

congenital muscular dystrophy [342-346]. Similarly, the angiotensin-converting enzyme inhibitor Lisinopril has been shown to efficiently reduce fibrosis in dystrophic muscle [347].

Chronic inflammation is a major contributor to pathologic changes in the MuSC niche in aging and muscle disease, and can both promote fibrosis and inhibit myogenesis. Anti-inflammatory treatment with glucocorticoids represents the current standard of care for Duchenne muscular dystrophy. Muscles of prednisone-treated Duchenne muscular dystrophy patients become stronger and contain lower numbers of mononuclear inflammatory cells [286, 287]. Unfortunately, anti-inflammatory treatments can only delay loss of ambulation by a few years and side effects, such as weight gain and reduced bone mineral density, are often quite significant [348]. In support of the idea that reducing inflammation ameliorates pathology in muscular dystrophy by rendering the niche more permissive to MuSC function, the glucocorticoid Deflazacort increases muscle strength and stimulates myogenic differentiation in dystrophic mice [349]. Other anti-inflammatory strategies under investigation for the treatment of muscle diseases involve biologics targeting cytokines, chemokines or other pro-inflammatory signaling. Examples include biologics with anti-TNFα activity, which have proven to ameliorate fibrosis, but may negatively impact cardiac function [350, 351]. A more direct way to reduce chronic inflammation and to reduce peripheral side effects, is to directly target specific pro-inflammatory cell types. For instance, neutrophil depletion via a cytotoxic anti-mouse granulocyte antibody has been shown to reduce muscle necrosis in dystrophic mice [351].

Deregulation of redox control is another hallmark of several muscle disorders and muscle aging. A number of natural and synthetic antioxidant compounds have been trialed for improving muscle health and regeneration. In the context of aging, the green tea component epigallocatechin gallate, vitamin C, vitamin E, beta-carotene, retinol and melatonin have described to be beneficial [352-354]. Epigallocatechin gallate, vitamin C and melatonin have also been demonstrated to improve pathologic features in mouse models of Duchenne muscular dystrophy, while several antioxidative vitamins, zinc, and selenium supplementation have shown efficacy in patients with facioscapulohumeral muscular dystrophy [355-359]. Mitochondrial dysfunction appears to be a critical downstream effect of oxidative stress in muscle pathology [360]. Importantly, damaged mitochondria themselves contribute to the overproduction of reactive oxygen and nitrogen species and thereby exacerbate oxidative damage. Idebenone is a synthetic analogue of coenzyme Q10 and as such has a protective effect on mitochondria. Clinical trials on patients affected by Duchenne muscular dystrophy have shown efficacy of Idebenone based on respiratory function outcomes [361].

In conclusion, aging and degenerative muscle diseases are highly complex processes leading to multifactorial defects in the MuSC niche. Tackling specific aspects of the pathology has proven to ameliorate MuSC dysfunction and future integrative strategies combining treatments that keep immune cells, fibrosis and oxidative stress in check hold great promise. Moreover, the raise of

*__Curr Top Dev Biol__. 126, 2018. Reprinted with permission from © Elsevier.

exercise mimetics may open entirely new avenues for the reversal or prevention of pathologic changes in the MuSC niche [362].

8. Concluding Remarks

Experimental models allowing to genetically tag, modify or ablate cellular components of the MuSC niche have provided important insights into the enormous complexity and interconnectivity of niche elements, as well as their susceptibility to signals arising on the tissue or systemic level. With the emergence of transformative new technologies such as mass cytometry, single cell sequencing and super resolution imaging, the field is poised to leap forward towards a comprehensive road map of the niche regulation of MuSCs in quiescence and during regenerative myogenesis. In the long run, these advancements will provide us with the toolkit and the molecular targets to develop strategies to efficiently boost stem cell function and thereby promote the endogenous regenerative capacity of healthy and diseased muscle. The clinical development of personalized therapies is very slow and faces significant challenges, in particular in the case of rare muscle diseases [363-365]. Thus, therapeutic approaches such as the stimulation of endogenous repair, which may be applicable over a spectrum of muscle diseases and conditions, represent an important complementary path.

*__Curr Top Dev Biol__. 126, 2018. Reprinted with permission from © Elsevier.

Chapter 2:

Aim & Scope of the Thesis

2. Background of My Main Project

The genetics and the pathophysiology of muscle wasting are poorly understood and there is a crucial need for effective treatments to counteract these conditions [366, 367]. Several studies have demonstrated the potential of induced pluripotent stem cells (iPSCs) derived myogenic progenitors for the treatment of muscular dystrophy [368-370]. In **section 2.3** we will review that iPSCs were successfully used to produce multinucleated muscle fibers with organized myofibrils to model the development of the muscle lineage *in-vitro* [369, 370]. These iPSC derived cells are able to reconstitute muscle fibers when grafted into the muscle of dystrophic mdx mice. However, up to date it has not been explored whether it is possible to differentiate iPSCs towards the muscle lineage and stop differentiation at an early stem-cell stage when the cells are not yet committed to fuse into fibers. The availability of such an “uncommitted” cell-type would tremendously advance the options for cell therapy of muscular dystrophy since it would allow for sustained engraftment into the stem cell compartment and life-long genetic correction. However, muscle progenitors are highly dependent on their environment and such a derivation protocol for uncommitted muscle stem cells (MuSCs) would have to take the native environment of the stem cells, the so called “stem cell niche”, into account.

2.1. The Muscle Stem Cell Niche

In **chapter 1**, we discussed the remarkable capacity of MuSCs to self-renew and their role in skeletal muscle growth and repair. In response to damage of muscle tissue, MuSCs become activated, proliferate and a fraction of cells become committed and fuse to repair myofibers. Once tissue repair is complete, the MuSC pool will return to quiescence. Their self-renewal capacity enables MuSCs to maintain the pool of uncommitted cells during muscle repair, while supplying progeny for differentiation. Behavior and fate of tissue-specific stem cells are strongly influenced by structural and biochemical cues emanating from their surrounding microenvironment [371]. MuSCs also reside in a highly specialized environment, which consists of the extracellular matrix (ECM) [372], different types of surrounding cells [373], vascular and neural networks [374], and numerous diffusible molecules (*e.g.,* Wnt, IGF, and FGF) [375]. The dynamic interactions between MuSCs and their niche specifically regulate quiescence, self-renewal, proliferation, and differentiation.

A number of cell types, such as immune cells, endothelial and vessel associated cells, and fibroblasts, are particularly critical mediators of MuSC regulatory niche-signals. For instance, it has been shown that periendothelial cells such as smooth muscle cells and endomysial fibroblasts promote a subset of MuSCs to return to the quiescent state [376]. It was also demonstrated that endothelial cells promote myoblast proliferation in co-culture systems by secreting a large panel of growth factors (*e.g.,* IGF-I, FGF and VEGF) [376]. Moreover, ablation of fibroblasts in muscle

connective tissue altered the regenerative dynamics of MuSCs, leading to premature differentiation and consequently depletion of the stem cell pool [377].

2.2. Myoblasts & Cell Therapy

The first evidence of utilizing “exogenous-myoblasts” in cell therapy was reported by the laboratory of T.A. Partridge in 1989 [378] in innately dystrophin-deficient mdx muscle fibres. The authors successfully reported to induce the conversion of dystrophic-mdx myofibers from negative to dystrophic-positive by intramuscular injection of normal muscle precursor cells [378]. During the following years, myoblast transplantation was successfully achieved into nonhuman-primates which led to optimization of conditions for further clinical applications in humans [379, 380]. These studies represent a critical step towards a better designing of myoblast transplantation strategies in humans, such as types and dosages of immunosuppression [379-381]. Numerous clinical trials in the 1990s tested myoblast transplantation in dystrophic patients [382]. While their results have been announced to the community very positively in the beginning, deep analysis of patient biopsies revealed the existence of dystrophin-positive fibers that were spontaneously “revertant fibers” [383].

All subsequent clinical trials using MuSC derived cells that were amplified *in-vitro*, so called myoblasts, had poor success due to inefficient engraftment [384-386]. As a consequence of their adaptation to the niche of muscle tissue, MuSCs degenerate into committed myoblasts if they are expanded for multiple passages in conventional 2D culture. Myoblasts can proliferate extensively *in-vitro*, but cannot self-renew and are predetermined to differentiate. Consequently, when myoblasts are transplanted the cells are not able to engraft as stem cells and most of them will differentiate and fuse into muscle fibers. In dystrophic tissue that is highly proinflammatory and has a relatively high cellular turnover, these donor derived fibers are then quickly eliminated and the therapeutic effect is lost [385].

Previous works have conclusively revealed loss of MuSC-stemness when grown in-2D based-condition [136, 229, 369]. For instance, niche elasticity significantly influences MuSCs function and their stemness [136]. Thus, common *in-vitro* culture leads to a degeneration of MuSCs because it does not take the niche into account. It is critical to consider this problem when developing protocols for the derivation of muscle progenitors from iPSCs because all current protocols are based on 2D-culture.

2.3. Current Protocols for the Derivation of Myogenic Cells from iPSCs or ES Cells

Pluripotent stem cells (PSCs) exhibit unlimited proliferative potential and possess a strong regenerative potential while maintaining the ability to differentiate into any cell type including skeletal

muscle cells [387, 388] (**Figure 4**). PSCs such as human embryonic stem cells (ESCs) and iPSCs hold great promise as a source of cell replacement therapy for muscular dystrophy. Apart from approaches overexpressing Pax3 or Pax7 [389, 390] in iPSCs and ESCs for myogenic induction, a number of different protocols have been developed over the past years in order to obtain myogenic cells from PSCs without transgenes. Xu et al showed that muscle differentiation in iPSCs could be induced by a simple cocktail of defined chemicals including bFGF, forskolin, and the GSK3β inhibitor BIO [391].

Borchin and colleagues developed a transgene-free protocol for stringent FACS-based purification of IPSC derived PAX3+/PAX7+ muscle precursors that are demonstrated to differentiate in postsort cultures into the mature myocytes [392]. An alternative protocol for the hESCs was introduced by Shelton and colleagues with 90% of skeletal myogenic cells using the GSK3 inhibitor CHIR99021 followed by FGF2. They showed that 47% of treated cells were myosin heavy chain (MYH) positive myocytes/myotubes surrounded by a 43% population of PAX7+ myogenic progenitor cells by 7 weeks [393]. A more recent study reports that after the presomitic mesoderm (PSM) induction by WNT activation, BMP inhibitor was subsequently added and then several growth factors, including FGF2, IGF and HGF, were utilized to induce the final maturation of muscle fibers without the introduction of transgenes or cell sorting [369].

The fact that the respective derivation protocols make use of 2D-culture systems, without paracrine and mechanical signals from the niche, likely leads to commitment and degeneration of PSC derived MuSC and significantly impairs their therapeutic value. In addition, due to their length (>5 weeks) and varied efficiency these protocols remain challenging. In addition, present biochemical differentiation protocols do not take into consideration that in the developing embryo, myogenic fate decisions are not solely controlled by the activation of a few pathways but are directed by a plethora of microenvironmental interactions in a three-dimensional niche, including locally deposited extracellular matrices, heterogeneous cell-cell contacts, and paracrine growth factors. Interestingly, a recent study has been shown that multilineage hPSC-derived artificial skeletal muscle containing vascular endothelial cells, pericytes, and motor neurons could provide deeper insights into human muscle regeneration dynamics [394].

Thus, we hypothesized that mimicking this developmental complexity could increase the efficiency of hiPSC to muscle progenitors (MP) differentiation and maintain myogenic progenitors in a more favorable state of stemness for cell therapy. In this context, we developed a novel derivation system for MuSCs from iPSCs that allows arresting myogenic lineage determination at an uncommitted state by mimicking critical niche signals. We then systematically compared our derivation system to current protocols *in-vitro* and, to primary myoblasts by assessing the engraftment efficiency into the muscle stem cell compartment *in-vivo* (**Chapter 3**).

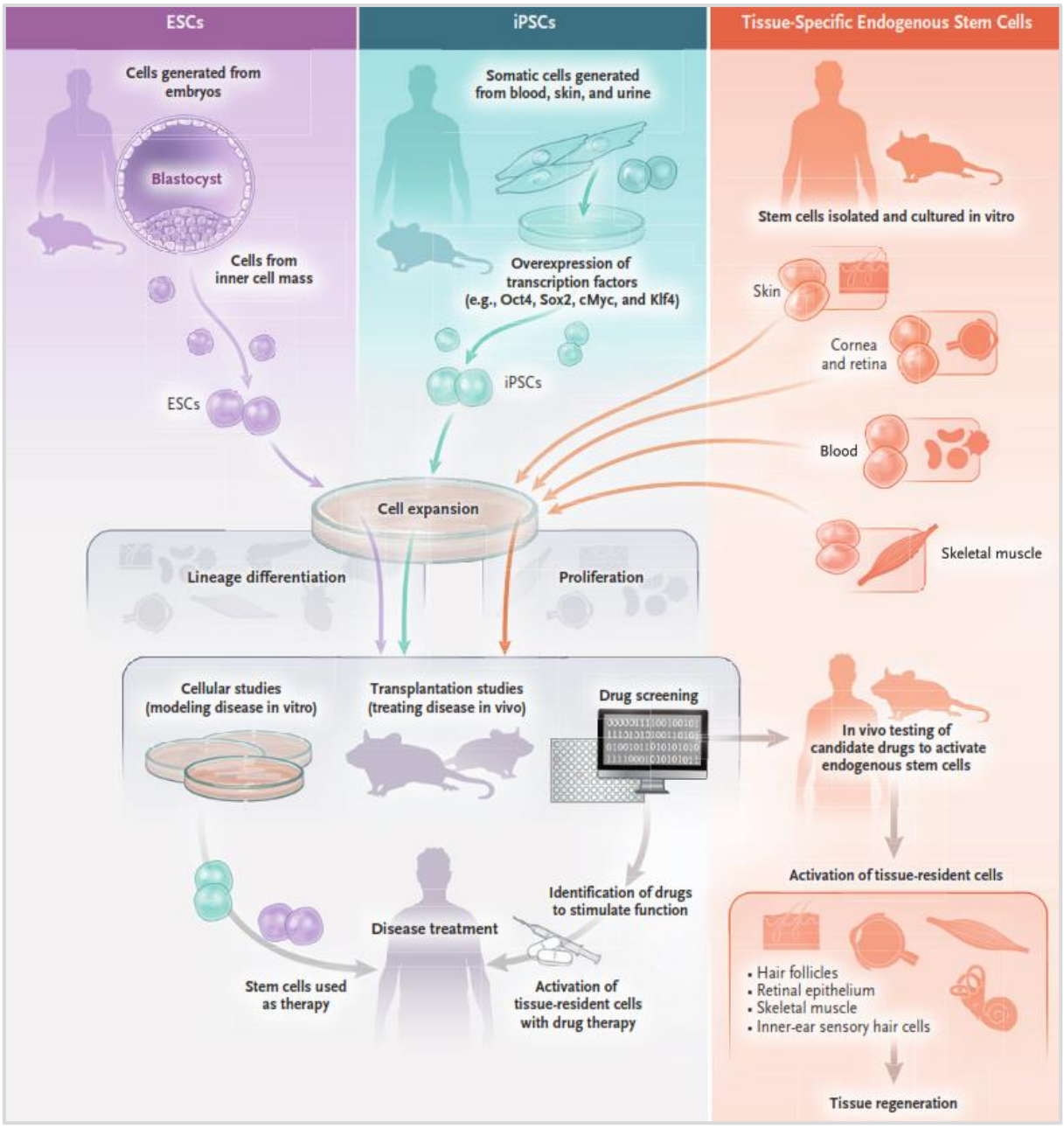

Figure 4. Different source of stem cells and their applications. Tissue-specific endogenous stem cells (adult) are capable of both self-renewal and tissue-restoration in certain tissues (e.g., epidermis, skeletal muscle and blood). Pluripotent stem cells (PSCs) comprising embryonic stem cells (ESCs) which are derived from undifferentiated inner mass cells of blastocyst-stage embryos and human induced pluripotent stem cells (iPSCs) that are generated from adult somatic cells (e.g., blood, skin, or urine) through the overexpression of four transcription factors (OSKM) (Oct4, Sox2, klf4 and c-Myc) [395] *in-vitro*. Patient-specific human iPSCs offer a unique opportunity to model human disease *in-vitro,* screen for drugs and eventually utilizing in clinical-settings. They can be extensively propagated in culture and are able to differentiate toward diverse cell states, such as skeletal muscles and neurons. Reproduced with permission from [387], © Copyright Massachusetts Medical Society (2019) (Appendix 4.).

2.4. Background of the Project 2 & 3

Age-related changes within the stem cell niche contribute directly to the decline the stem cell quiescence and function [235, 396, 397]. Deterioration in the ability of niche-resident stem cells in individual tissues have been proposed to play a role in the observed impairment in tissue homeostasis, repair, and regeneration with “age” [235].

To decipher the procedures that contribute to the decline of the function of the niche with age, it would be required to systematically recognize the diverse factors that directly/indirectly influence stem cell activity. Most importantly, niche-resident cells have to be investigated with the understanding that stem cell identity is governed by “combinatorial” factors involving cell-extrinsic and cell-intrinsic mechanisms in the niche.

A better understanding of the age-related changes in components of the microenvironment and their influence on stem cell fate decisions will facilitate the development of novel therapeutic interventions in order to improve the MuSC activity and skeletal muscle plasticity in aged individuals.

2.5. A “Niche-Mimetic” Approach for Systemic Profiling of Aging

In our second study, introduced as **chapter 4** in the thesis, we developed a novel method to encapsulate human stem cells in highly diffusible polyethersulfone hollow fiber capsules in mice to study systemic-effects on MuSCs and myogenesis independent of local signals from niche. These engineered-fibers can be implanted subcutaneously into mice with different genotype or pathology, and become vascularized over a time-course of ten days. Using aging as a proof of principle, we were able to identify highly specific transcriptional signature induced by systemic aging that covers a wide range of novel age affected factors, as well as pathways previously characterized to be deregulated during aging including Akt/mTOR and cytokine signaling.

This protocol represents an incremental step forward in the field of experimental research into systemic metabolism and the aging process. For the first time, we are able to read out isolated systemic molecular signatures in human cell types of choice. Importantly, the implications of our novel protocol are not limited to preparations of single cell-types. Consequently, human iPSC derived miniature organs and also myogenic progenitors from **chapter 3** could strongly synergize with this method. Future studies employing encapsulated human iPSC derived human tissues will allow to study the systemic circulation in health, disease and aging at an unprecedented level. In addition, our method is (I) feasible to implement in a standard molecular biology laboratory that has a 3D printer at its disposal, (II) can partially replace complicated and ethically challenging parabiosis experiments, and (III) is not limited by species barriers.

2.6. “Supporting Cells” Ameliorate the Regenerative Niche for Muscle Repair

Lastly, as we discussed in the previous chapters, during adult myogenesis, MuSC function is under the control of a wide range of paracrine signals originating from different cell types in the stem cell niche. In the last study (**chapter 5**), we demonstrated that aged mesenchymal fibro/adipogenic progenitors (FAPs) fail to support MuSCs due to reduced secretion of the matricellular protein WNT Inducible Signaling Pathway Protein 1 (WISP1). Our study showed that loss of WISP1 from FAPs contributes to MuSC dysfunction in aged skeletal muscles and demonstrate that this mechanism can be efficiently targeted to rejuvenate regenerative myogenesis.

In conclusion, the chapters presented in this thesis provide new innovative tools and models to study human muscle stem cells, increase our understanding of the muscle stem cell niche and provide an important step-forward in the field of regenerative medicine by creating new opportunities for cell therapy of muscle dystrophy and the treatment of age-associated stem cell dysfunction.

Chapter 3:

An Engineered Multicellular Stem Cell Niche for the 3D Derivation of Human Myogenic Progenitors from iPSCs

Background & Rationale:

One of the most fundamental problems associated with stem cell therapy of skeletal muscle is the limited availably of progenitor cells (uncommitted cells) that can robustly engraft into the stem cell compartment. It has extensively been attempted to isolate adult MuSCs and expand them in 2D-culture to obtain sufficient cell numbers for such treatments. The challenge associated with this approach is that, once isolated from their native-niche and maintained in conventional culture, MuSCs become terminally committed to myogenic differentiation and show a dramatically reduced engraftment potential *in-vivo*.

In this chapter, we presented a novel 3D-method or the derivation of uncommitted MuSCs from human iPSCs. In contrast to all other current 2D-based protocols for the generation of myogenic cells from pluripotent cells, we have focused on conditions that allow for the generation of uncommitted population that maintain the expression of stem cell markers (stemness) but remain negative for commitment factors. We aimed to mimic the niche-microenvironment by using bioengineering approaches for 3D-nurturing the muscle progenitors, as stem cell fate decisions in the embryo are controlled by a plethora of microenvironmental interactions in a three-dimensional niche[398]. To investigate whether recreating aspects of this microenvironmental complexity improves the efficiency of myogenic human iPSC differentiation, we screened cell types present in the developmental or adult stem cell niche in heterotypic “embryoids”.

Briefly, we identify embryonic fibroblasts combined with endothelial cells as the most permissive microenvironmental components for mesoderm induction and myogenic specification of hiPSCs. Embryoid derived progenitors display markedly enhanced engraftment into the satellite cell position, and restoration of dystrophin expression when transplanted into muscles of a mouse model of Duchenne muscular dystrophy.

Altogether, by combining niche-engineering and biochemical pathway targeting, we establish a powerful method for 3D-myogenic hiPSC differentiation with unique disease modeling and cell therapy applications.

Personal contribution:

Lead the project by designing and performing all the experiments, interpreting the results and writing the manuscript.

Current status of the project*:

Manuscript under revision (since May 2019)

*Manuscript under revision (May 2019)

An Engineered Multicellular Stem Cell Niche for the 3D Derivation of Human Myogenic Progenitors from iPSCs

Omid Mashinchian[1,2], Filippo De Franceschi[1], Joris Michaud[1], Sonia Karaz[1], Pascal Stuelsatz[1], Nagabhooshan Hegde[1], Gabriele Dammone[1], Matthias P. Lutolf[3,4], Jerome N. Feige[1,2,#], C. Florian Bentzinger[1,5,#]

1. Nestlé Research
   Ecole Polytechnique Federale de Lausanne (EPFL) Innovation Park
   1015 Lausanne, Switzerland

2. School of Life Sciences
   Ecole Polytechnique Federale de Lausanne (EPFL)
   1015 Lausanne, Switzerland

3. Laboratory of Stem Cell Bioengineering
   Institute of Bioengineering
   School of Life Sciences and School of Engineering
   École Polytechnique Fédérale de Lausanne (EPFL)
   Lausanne, Switzerland

4. Institute of Chemical Sciences and Engineering
   School of Basic Science
   École Polytechnique Fédérale de Lausanne (EPFL)
   Lausanne, Switzerland

5. Département de pharmacologie et physiologie
   Faculté de médecine et des sciences de la santé
   Université de Sherbrooke, Qc, Canada

#: Equal contribution

Corresponding authors: C. Florian Bentzinger, *cf.bentzinger@usherbrooke.ca*
Jerome N. Feige, *Jerome.Feige@rd.nestle.com*

*Manuscript under revision (May 2019)

Main

Myogenic progenitors (MPs) are promising candidates for cell-therapy of skeletal muscle diseases[399, 400]. Human pluripotent stem cells (hPSCs) represent an abundant source for the generation of therapeutic MPs[401-404]. Myogenic hPSC differentiation can be induced by ectopic expression of transcription factors[401, 403, 405-407], or using small molecules and growth factors that modulate pathways involved in mesoderm specification and commitment to the skeletal muscle lineage[404, 408-412]. Protocols for myogenic hPSC differentiation are commonly adapted to two-dimensional culture environments. In contrast, myogenic fate decisions in the embryo are controlled by complex microenvironmental interactions mediated by diverse cell types that deposit extracellular matrices, present heterogeneous cell-cell contacts, and secrete paracrine growth factors[398]. Collectively these niche-elements modulate batteries of intertwined pathways specific to each developmental stage. We hypothesized that recreating aspects of this microenvironmental complexity could improve the efficiency of myogenic hPSC specification and preserve embryonic stem cell characteristics that are favorable for cell-therapy outcomes.

To identify cell types with permissive effects on mesoderm induction and commitment to the myogenic lineage we screened embryonic fibroblasts, mesenchymal stem cells, endothelial cells, as well as adult smooth muscle cells, myoblasts and fibroblasts in combination with human induced pluripotent stem cell (hiPSCs) in suspension embryoids[413] (**Fig. 1a and Supplementary Fig. 1a**). As a readout for this assay we quantified the expression of the conserved myogenic marker Pax7[14, 414]. Embryonic or adult fibroblasts and embryonic mesenchymal stem cells did not increase Pax7 expression at 7, 13 or 21 days after embryoid formation with hiPSCs in any of the tested ratios, while adult smooth muscle cells had minor effects at day 7 (**Supplementary Fig. 1b-e**). Interestingly, irradiated growth arrested embryonic fibroblasts (GAeFib), embryonic endothelial cells (eEC) and adult myoblasts (aMyo) in combination with hiPSCs lead to a 4- to 8-fold induction of Pax7 at day 7 and 13 (**Fig. 1b,c and Supplementary Fig. 1f,g**). To test for additive or synergistic effects we generated four-component embryoids of GAeFib, eEC, aMyo and hiPSCs.

However, we did not observe a significant increase in Pax7 expression compared to two-component embryoids containing hiPSCs with GAeFib, eEC or aMyo (**Supplementary Fig. 1h**). To reduce the probability of cross-inhibition by one of the cell types, we subsequently tested three-component embryoid conditions. No additive effects were observed for eEC and aMyo when combined with hiPSCs (**Supplementary Fig. 1i**). In contrast, the combination of GAeFib and aMyo in a 1:1:2 ratio with hiPSCs led to a more than 10-fold induction of Pax7 expression at day 7 and 13 (**Supplementary Fig. 1j**). Furthermore, GAeFib in combination with eEC and hiPSCs at a 1:1:2 ratio induced Pax7 expression at day 13 more than 30-fold (**Fig. 1d**). Thus, three-component embryoids (TCEs) of GAeFib, eEC and hiPSCs are most permissive for Pax7 induction.

Most established protocols for the derivation of MPs from hPSCs are performed in 2D culture and rely on activation of the Wnt-pathway through glycogen synthase kinase-3 (GSK3) inhibitors in the early stages of differentiation and subsequently switch to basic fibroblast growth factor (bFGF) stimulation[404, 408-412]. Suggesting increased differentiation at the expense of proliferation, Wnt pathway activation using CHIR99021 from day 1-7 of aggregation and bFGF stimulation from day 7-13, reduced TCE growth (**Fig. 1e and Supplementary Fig. 1k**).

Notably, expression analysis revealed an almost 2000-fold induction of Pax7 in Wnt/FGF pathway induced TCEs (**Fig. 1f**). At day 7 of this differentiation protocol, TCEs contained abundant epithelial-like structures with distinct domains of Pax7 positive (Pax7+) cells (**Fig. 1g**). TCEs also expressed high levels of the early mesoderm marker brachyury (T)[415], the paraxial mesoderm markers mesogenin 1 (Msgn1)[416] and T-box 6 (Tbx6)[417], and the dermomyotome marker Pax3[418] (**Fig 1h-k**). Between day 7 and 13 of the Wnt/FGF protocol, TCEs underwent an epithelial–mesenchymal transition-like process and invaginated (**Fig. 1l**). Pax7+ cells in day 13 TCEs were more evenly distributed than at day 7 and preferentially resided in actin-poor regions (**Fig. 1m**).

Expression of the myogenic commitment marker Myf5 increased in day 13 TCEs, while MyoD was not detectable (**Supplementary Fig. 1l,m**). Immunostainings revealed that TCEs contain copious amounts of the muscle niche extracellular matrix component laminin, while high numbers of Pax3 and homeobox 1 (Meox1)[419] positive cells confirmed mesoderm induction (**Fig. 1n,o**). In contrast to day 13, TCEs at day 7 stained positive for the primitive endoderm marker alpha-fetoprotein[420] (AFP) in their center while peripheral regions were positive for the mesoderm marker smooth muscle actin (SMA)[421] (**Fig. 1p**). A transient endoderm induction in day 7 TCEs was confirmed by Gata4[422] expression (**Supplementary Fig. 1n**).

The ectoderm marker fgf5[423] and the neural commitment marker Neurog1[424] were expressed at low levels in TCEs (**Supplementary Fig. 1o,p**). Immunostainings revealed that the center of TCEs contained small amounts of cells positive for the neuronal marker Tuj1[425], while no staining was observed for the neural progenitor markers nestin[426] or Sox2[427] (**Supplementary Fig. 1q**). In summary, hiPSC derivation in TCEs in combination with biochemical targeting of the WNT and FGF pathways induces efficient mesodermal commitment and leads to the generation of Pax7+ cells.

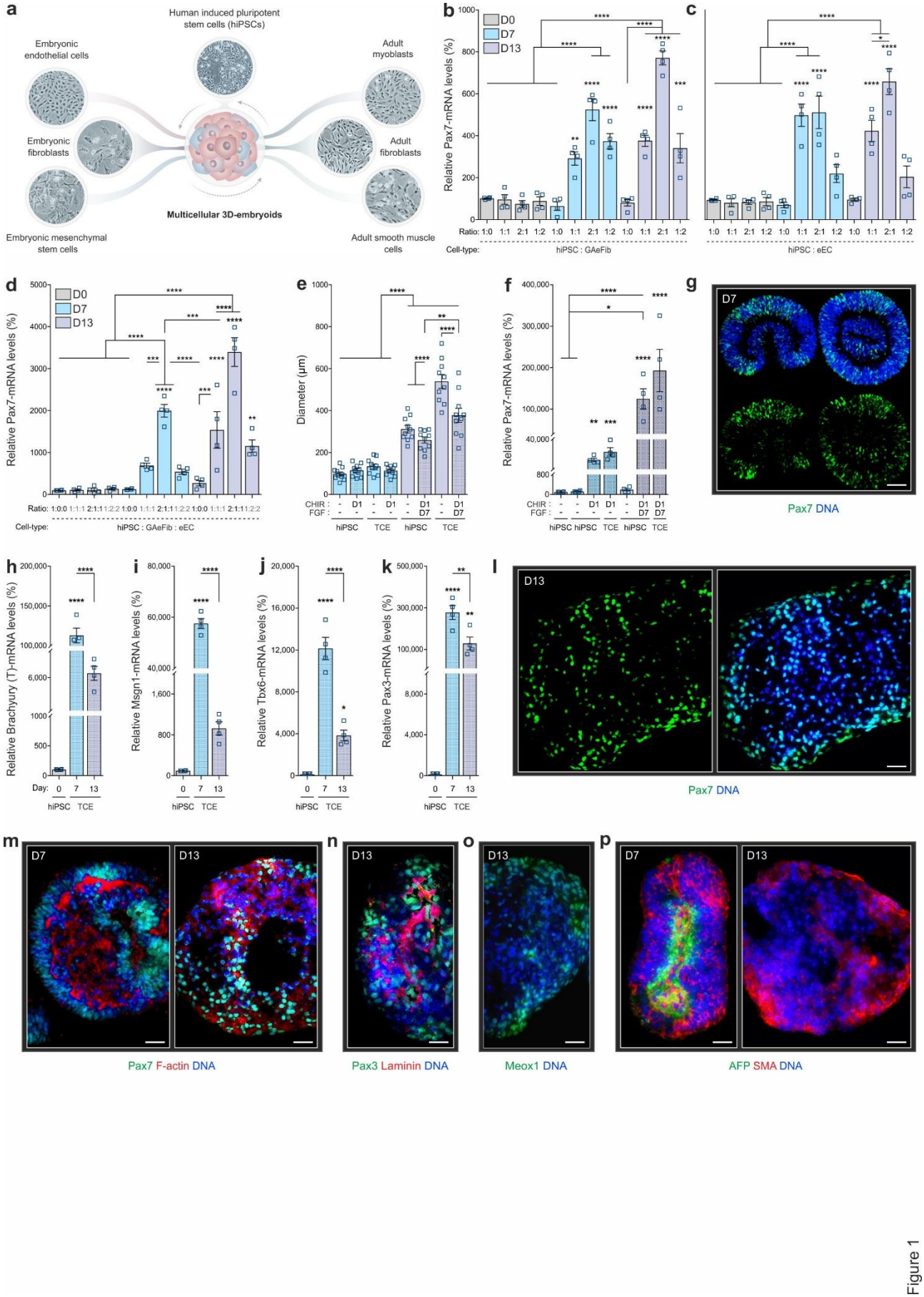
a
Human induced pluripotent stem cells (hiPSCs)
Embryonic endothelial cells
Adult myoblasts
Embryonic fibroblasts
Adult fibroblasts
Multicellular 3D-embryoids
Embryonic mesenchymal stem cells
Adult smooth muscle cells
b
D0
D7
D13
Relative Pax7-mRNA levels (%)
Ratio: 1:0 1:1 2:1 1:2 1:0 1:1 2:1 1:2 1:0 1:1 2:1 1:2
Cell-type: hiPSC : GAeFib
c
hiPSC : eEC
d
Relative Pax7-mRNA levels (%)
Ratio: 1:0:0 1:1:1 2:1:1 1:2:2 1:0:0 1:1:1 2:1:1 1:2:2 1:0:0 1:1:1 2:1:1 1:2:2
Cell-type: hiPSC : GAeFib : eEC
e
Diameter (µm)
CHIR : - D1 - D1 - D1 - D1
FGF : - - - - - D7 - D7
hiPSC TCE hiPSC TCE
f
Relative Pax7-mRNA levels (%)
hiPSC hiPSC TCE hiPSC TCE
g
D7
Pax7 DNA
h
Relative Brachyury (T)-mRNA levels (%)
Day: 0 7 13
hiPSC TCE
i
Relative Msgn1-mRNA levels (%)
j
Relative Tbx6-mRNA levels (%)
k
Relative Pax3-mRNA levels (%)
l
D13
Pax7 DNA
m
D7
D13
Pax7 F-actin DNA
n
D13
Pax3 Laminin DNA
o
D13
Meox1 DNA
p
D7
D13
AFP SMA DNA

Figure 1

Fig. 1: Three-component embryoids (TCEs) are highly permissive for myogenic specification. **a,** Schematic outlining the different embryonic and adult cell lines that were tested for their effects on the induction of the myogenic marker Pax7 in heterotypic human induced pluripotent stem cell (hiPSC) suspension embryoids. **b,c,** mRNA expression of Pax7 in embryoids containing different ratios of hiPSCs and growth arrested embryonic fibroblasts (GAeFib) or hiPSCs and embryonic endothelial cells (eEC). Mixtures of the respective cell types were analyzed immediately before (D0), and 7 and 13 days (D7 and D13) after aggregation. **d**, Pax7 mRNA expression in embryoids containing hiPSCs, GAeFib and eEC (TCEs). **e,f,** Size and Pax7 mRNA expression in embryoids containing only hiPSCs or in TCEs when combined with biochemical activation of the Wnt and FGF pathways. **g,** Representative Pax7 immunostaining of sections of Wnt/FGF induced D7 TCEs. **h-k,** mRNA expression of the mesoderm marker brachyury (T), the paraxial mesoderm markers Mesogenin 1 (Msgn1) and T-box 6 (Tbx6), and the dermomyotome marker Pax3 in hiPSCs and Wnt/FGF induced TCEs at D7 and D13. **l,** Representative Pax7 immunostaining of a Wnt/FGF induced D13 TCE. **m-p,** Representative stainings for actin, the extracellular matrix component laminin, the endoderm marker alpha-fetoprotein (AFP), and the mesoderm marker smooth muscle actin (SMA) in D7 or D13 TCEs stimulated using the Wnt/FGF induction protocol. **g,l,m-p** Scalebars = 25um. **b-f,h-k,** Data are represented as means ± S.E.M. p-values are *p<0.05, **p<0.01, ***p<0.001, ****p<0.0001 using an ANOVA followed by a Bonferroni post hoc test.

Enzymatic release of cells from Wnt/FGF stimulated day 13 embryoids and quantification by flow cytometry revealed ~50% more Pax7+ cells in TCEs when compared to hiPSCs alone (**Fig. 2a and Supplementary Fig. 2a**). Using hiPSC lines from two additional donors we confirmed a total yield of ~40-50% of Pax7+ cells from TCEs (**Supplementary Fig. 2b,c**). When GAeFib and eEC with hiPSCs where not aggregated but plated for 13 days in 2D and treated with the same Wnt/FGF scheme as TCEs, only 3.6% of the cells were observed to be Pax7+ positive (**Supplementary Fig. 2d**). Moreover, when two established biochemical 2D protocols[411, 428] were stopped after two weeks, no Pax7+ cells could be detected in the cultures (**Supplementary Fig. 2e,f**). Thus, the 3D context is essential for the improved efficiency of Pax7 induction in TCEs.

To interrogate the number of cells expressing the myogenic commitment markers Myf5 and MyoD, we used RNA fluorescence in situ hybridization (FISH). This revealed expression of Myf5 in around 16% of cells in TCEs, while MyoD was below 1% (**Fig. 2b, Supplementary Fig. 2g**). In contrast, myogenic progenitors isolated from adult human skeletal muscle (hskMPs) contain between 40 and 50% of Myf5/MyoD+ cells (**Fig. 2c**). This suggests that TCE derived Pax7+ cells resemble a largely uncommitted embryonic progenitor with a high stemness. To isolate live Pax7+ cells and examine their myogenic potential we tested a panel of cell surface markers previously reported to be expressed by adult or embryonic MPs by flow cytometry. The adult human MP marker CD56[429], as well as integrin α9[430], when used independently, detected around >85% of the Pax7+ cells enzymatically liberated from Wnt/FGF induced day 13 TCEs (**Fig. 2d,e**). Purity was lower when CD271[431], CD82[432], CD362[430] and CD54[430] were used (**Fig. 2f,i**). Pax7+ cells were also negative for the adipogenic marker CD34[433] and the neural crest marker CD57[434] (**Fig. 2j,k**). Notably, combination of CD56 and integrin α9 antibodies allowed for the isolation of a 99% pure population of Pax7+ cells (SEM = ± 0.231, n = 5 independent experiments) (**Fig. 2l**).

Following sorting of live CD56 and integrin α9 positive cells from Wnt/FGF induced TCEs using this strategy, the cells adhered most efficiently on vitronectin coated dishes compared to fibronectin, laminin, or gelatine (**Fig. 2m**). After isolation and 2D culture on vitronectin, most CD56 and integrin α9 positive embryonic-like myogenic progenitor cells (eMPs) sorted from Wnt/FGF induced TCEs stained positive for Pax7 but remained negative for the commitment marker MyoD (**Fig. 2n**). In growth factor depleted differentiation medium the number of eMPs expressing Pax7 dropped but was still higher than in proliferating hskMPs (**Fig. 2o,p**). While remaining lower than in hskMPs, MyoD positive cells became more abundant in eMPs in differentiation media (**Fig. 2o,q,r**). Under prolonged differentiation conditions, eMPs upregulated myosin heavy chain (MyHC) and formed multinucleated myotubes (**Fig. 2s**). With ~30%, the fusion index of eMPs was only slightly lower than hskMPs (**Fig. 2t**). Thus, eMPs are bona fide muscle progenitors capable of terminal differentiation.

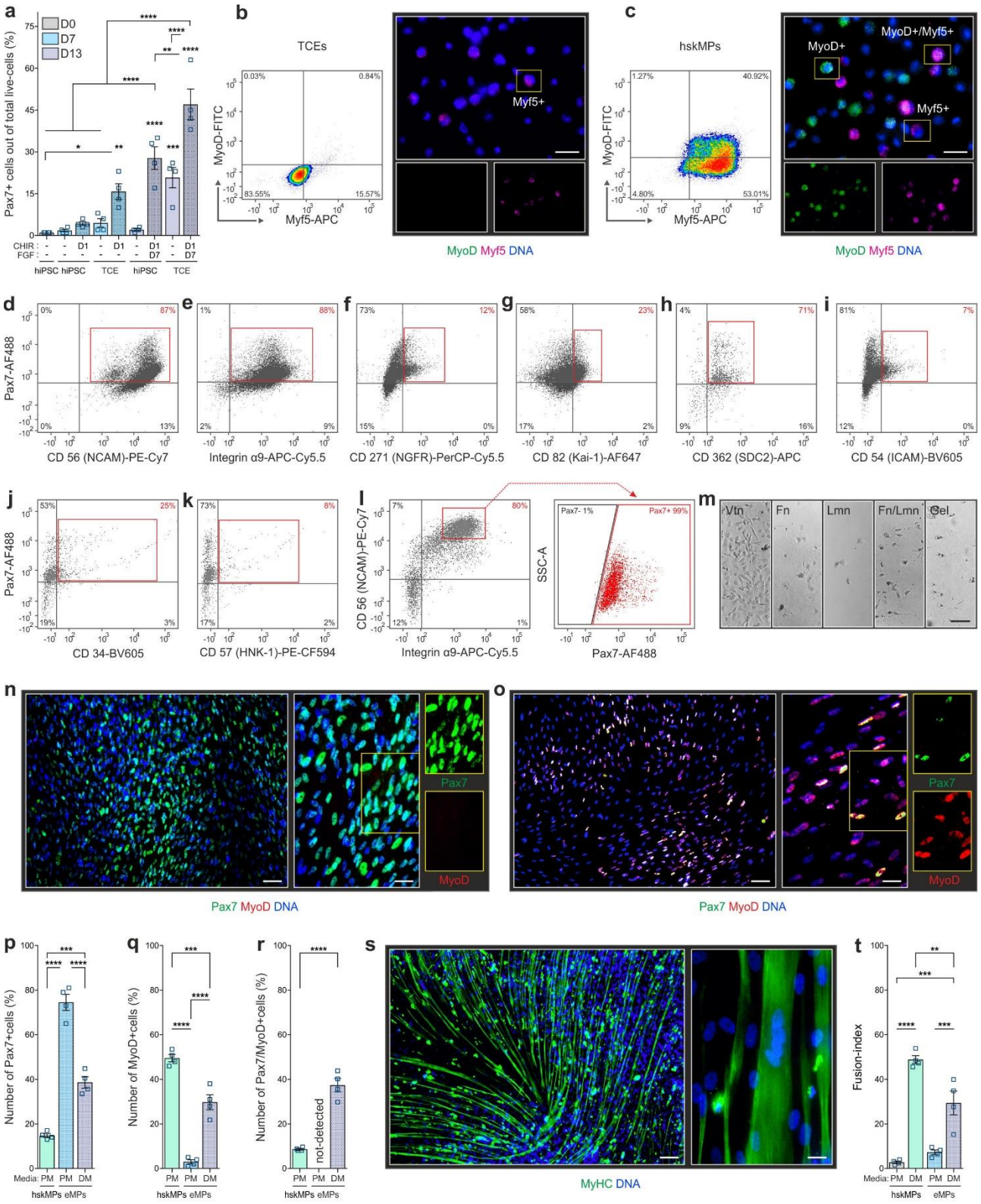
a
Pax7+ cells out of total live-cells (%)
D0
D7
D13
CHIR :
FGF :
hiPSC hiPSC TCE hiPSC TCE
b
TCEs
MyoD-FITC
Myf5-APC
Myf5+
MyoD Myf5 DNA
c
hskMPs
MyoD+
MyoD+/Myf5+
Myf5+
MyoD Myf5 DNA
d
Pax7-AF488
CD 56 (NCAM)-PE-Cy7
e
Integrin α9-APC-Cy5.5
f
CD 271 (NGFR)-PerCP-Cy5.5
g
CD 82 (Kai-1)-AF647
h
CD 362 (SDC2)-APC
i
CD 54 (ICAM)-BV605
j
CD 34-BV605
k
CD 57 (HNK-1)-PE-CF594
l
CD 56 (NCAM)-PE-Cy7
Integrin α9-APC-Cy5.5
SSC-A
Pax7- 1%
Pax7+ 99%
Pax7-AF488
m
Vtn
Fn
Lmn
Fn/Lmn
Gel
n
Pax7
MyoD
Pax7 MyoD DNA
o
Pax7
MyoD
Pax7 MyoD DNA
p
Number of Pax7+cells (%)
Media: PM PM DM
hskMPs eMPs
q
Number of MyoD+cells (%)
r
Number of Pax7/MyoD+cells (%)
not-detected
s
MyHC DNA
t
Fusion-index
Media: PM DM PM DM
hskMPs eMPs

Figure 2

Fig. 2: Characterization of TCE derived embryonic-like myogenic progenitors (eMPs). a, Flow cytometry quantification of the number of Pax7 positive cells in hiPSCs and TCEs at different stages of the Wnt/FGF differentiation protocol. **b,c,** RNA fluorescence in situ hybridization for the myogenic commitment markers Myf5 and MyoD in cells derived from D13 TCEs following Wnt/FGF induction (**b**) and primary adult human skeletal muscle myogenic progenitors (hskMPs) (**c**) by flow cytometry and in representative bulk post-sort cytospins. Scalebar = 25um. **d-i,** Flow cytometry quantification for Pax7 and myogenic progenitor surface markers in cells derived from Wnt/FGF induced D13 TCEs. **j,k,** Flow cytometry quantification of Pax7, the adipogenic marker CD34 and the neural crest marker CD57 in cells derived from Wnt/FGF induced D13 TCEs. **l,** Flow cytometry quantification of Pax7, integrin α9 and CD56 in cells isolated from Wnt/FGF induced D13 TCEs. **m,** Representative bright field images of the adhesion of integrin α9 and CD56 positive flow cytometrically sorted eMPs isolated from Wnt/FGF induced D13 TCEs on vitronectin (Vtn), fibronectin (Fn), Laminin (Lmn) and gelatine (Gel) in the presence of ROCK inhibitor. Scalebar = 40um. **n,** Representative immunostainings for Pax7 and MyoD in eMPs plated on Vtn and maintained in proliferation media (PM) after isolation. **o,** Representative immunostainings for Pax7 and MyoD in eMPs plated on Vtn that were first maintained in PM and then switched to differentiation media (DM). **p-r,** Quantification of the number of Pax7 (**p**), MyoD (**q**) and Pax7/MyoD double positive (**r**) cells in hskMPs and eMPs in PM and after switching to DM. **s,** Representative immunostaining for the muscle fiber marker myosin heavy chain (MyHC) of eMPs maintained in DM. **t,** Quantification of the fusion index of hskMPs and eMPs in PM and DM. **n,o,s,** Left-hand scalebar = 75um, right-hand scalebar = 50um. **a,p-r,t,** Data are represented as means ± S.E.M. p-values are *p<0.05, **p<0.01, ***p<0.001, ****p<0.0001 using an ANOVA followed by a Bonferroni post hoc test.

To test their ability to engraft in a cell therapy setting we injected freshly sorted eMPs into muscles of the mdx mouse model of Duchenne muscular dystrophy[435]. Compared to hskMPs, eMPs generated a larger number of dystrophin positive fibers in the host tissue 10 days after transplantation (**Fig. 3a, b**). Indicating an extensive migratory capacity in the host tissue, dystrophin positive fibers were more evenly distributed in the eMP injected muscles when compared to hskMPs (**Fig. 3a,c**)**.**

Staining for human nuclear Lamin A/C revealed that eMP derived cells frequently remained unfused and engrafted into the satellite cell position in the periphery of muscle fibers with restored dystrophin expression (**Fig. 3d**). Engraftment in the satellite cell position was rarely observed for hskMPs (**Supplementary Fig. 3a**). These observations show that eMPs are well-suited for cell therapy of recessive genetic muscle diseases and, through their ability to engraft into the host stem cell compartment, are likely to have sustained therapeutic effects.

Altogether, by mimicking the embryonic environment in heterotypic embryoids, we have significantly improved the efficiency and duration of established biochemical protocols for myogenic differentiation of hiPSCs. Our streamlined method allows for the two-week derivation of pure Pax7+ MPs from hiPSCs that have an engraftment potential superior to adult hskMPs. Notably, one of the primary reasons for the limited efficacy of hskMP transplantation in human trials is the use of adult donor hskMPs after prolonged 2D culture expansion[399, 436].

Adult hskMPs are strongly niche-dependent and *ex-vivo* proliferation impairs their stem cell character and engraftment potential. Given the high number of cells required for cell therapy treatments in humans, sufficient freshly isolated adult hskMPs are difficult to source. Our method provides a novel means to generate virtually unlimited amounts of myogenic progenitors with ideal stem cell characteristics in a biologically faithful 3D niche environment. Moreover, the scalability of embryoid suspension cultures allows for production at the bioreactor level and, next to much needed cell therapy applications for genetic SkM diseases, opens new avenues for disease modeling and biobanking (**Fig. 3e**).

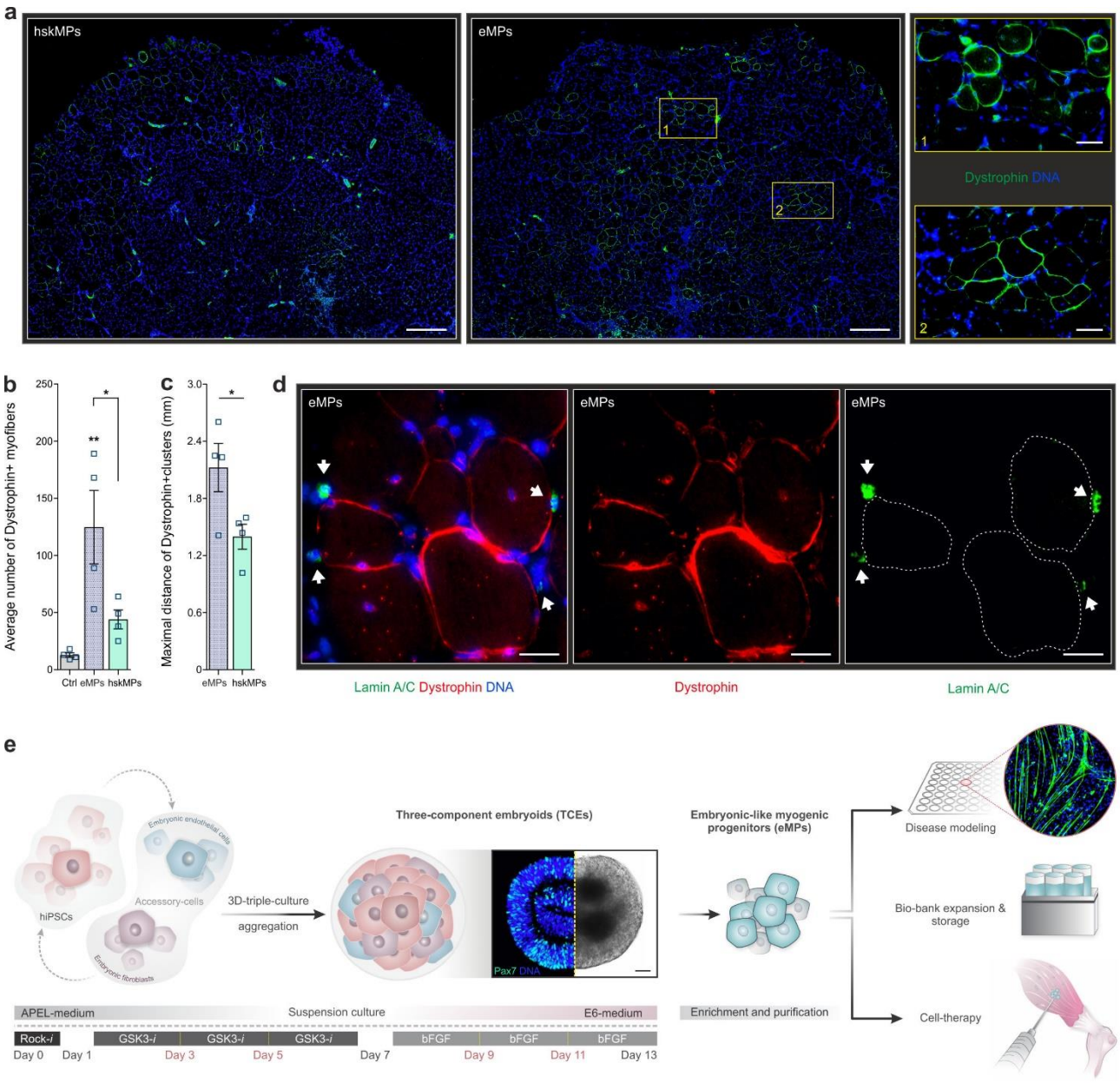
a
hskMPs
eMPs
1
2
Dystrophin DNA
b
Average number of Dystrophin+ myofibers
Ctrl eMPs hskMPs
c
Maximal distance of Dystrophin+clusters (mm)
eMPs hskMPs
d
eMPs
Lamin A/C Dystrophin DNA
Dystrophin
Lamin A/C
e
Embryonic endothelial cells
Accessory-cells
hiPSCs
Embryonic fibroblasts
3D-triple-culture aggregation
Three-component embryoids (TCEs)
Pax7 DNA
Embryonic-like myogenic progenitors (eMPs)
Enrichment and purification
Disease modeling
Bio-bank expansion & storage
Cell-therapy
APEL-medium
Suspension culture
E6-medium
Rock-i
GSK3-i
bFGF
Day 0 Day 1 Day 3 Day 5 Day 7 Day 9 Day 11 Day 13

Figure 3

Fig. 3: Engraftment of eMPs in diseased muscle. a, Representative immunostainings for dystrophin in cross-sections of muscles of mdx mice 10 days after transplantation of hskMPs or eMPs. Scalebars in the two left-hand side images = 300um. Scalebars in inserts 1 and 2 = 50um. **b,** Number of Dystrophin positive fibers in mdx muscles injected with vehicle (Ctrl), eMPs and hskMPs 10 days after transplantation**.** Data are represented as means ± S.E.M. p-values are *p<0.05, **p<0.01 using an ANOVA followed by a Bonferroni post hoc test. **c,** Maximal distance of clusters of dystrophin positive fibers in cross-sections of mdx muscles transplanted with eMPs and hskMPs. Data are represented as means ± S.E.M. p-value is *p<0.05 using a student's t-test. **d,** Representative immunostainings for the human nuclear marker lamin A/C and dystrophin in muscles of mdx mice 10 days after transplantation of eMPs. Arrows depict cells in the satellite cell position in the periphery of muscle fibers. Scalebars = 25um. **e,** Scheme summarizing the procedure for the generation of eMPs and downstream applications.

Acknowledgements

We are grateful to the Nestle Research community for fruitful discussion and support, in particular the Musculo-Skeletal Health group, Eric Rolland and Ed Baetge. We thank Alessio Palini and Federico Sizzano for expert advice on flow cytometry, J. Sanchez for help with mouse husbandry, and Sylviane Metairon, Frederic Raymond and Patrick Descombes for technical support with RNA extraction. O.M., J.N.F. and C.F.B are supported by the Fondation Suisse de Recherche sur les Maladies Musculaires (FSRMM). C.F.B. is supported by the Natural Sciences and Engineering Research Council of Canada (NSERC), the Fonds de recherche du Québec – Santé (FRQS), the ThéCell Network (supported by the FRQS), the Canadian Stem Cell Network, the CHUS Foundation, the Banting Research Foundation, a Research Chair of the Centre de recherche médicale de l'Université de Sherbrooke (CRMUS) and the Canadian Institutes of Health Research (CIHR).

Author contributions

O.M., C.F.B and J.N.F initiated and managed the project. O.M., S.K., P.S., G.D., and N.H. designed and conducted experiments, and analyzed data. F.D.F and J.M. provided technical support with imaging and flow cytometry. O.M., M.P.L., C.F.B. and JNF interpreted the results and wrote the manuscript.

Competing financial interests

All authors except M.P.L. are or were employees of Nestec S.A., Switzerland

Methods

Cell lines and 2D culture conditions

The human-induced pluripotent stem cell (hiPSC) line HYS0103 (ACS-1020) was obtained from ATCC and lines 603 and 482 were purchased from Fujifilm Cellular Dynamics, Inc (FCDI). Unless otherwise stated, experiments were performed using 603 cells. HYS0103 hiPSCs were initially cultured in pluripotent stem cell SFM XF/FF (ATCC ACS-3002) media on CellMatrix basement membrane gel (ATCC ACS-3035), then the medium was switched to essential-8 medium (A1517001, Thermo Fisher Scientific) on vitronectin (VTN-N, A14700, Thermo Fisher Scientific) coated dishes. hiPSCs from FCDI were cultivated in essential-8 medium (A1517001, Thermo Fisher Scientific) in vitronectin (VTN-N, A14700, Thermo Fisher Scientific) coated culture vessels. Human skeletal muscle cells (hskMPs, LZ-CC-2580, Lonza) were plated on fibronectin-coated (F2006, Sigma-Aldrich) dishes and expanded in skeletal muscle cell growth medium (SKM-M, AmsBio). Murine embryonic endothelial cells (eEC, C166, ATCC CRL-2581), murine adult myoblasts (aMyo, C2C12, ATCC CRL-1772), murine adult smooth muscle cells (aSMC, MOVAS, ATCC CRL-2797), murine embryonic fibroblasts (eFib, NIH-3T3, ATCC CRL-1658), murine adult fibroblasts (aFib, NOR-10, ATCC CCL-197), murine embryonic mesenchymal stem cells (eMSC, OP-9, ATCC CRL-2749) were obtained from ATCC, mitomycin C-treated murine embryonic fibroblasts (GAeFib, PMEF-CF-1) were purchased from Merck Millipore, and human neural progenitor cells (hNPCs, ReNcell VM, SCC008) were purchased from EMD Millipore. eEC, aMyo and eFib were cultured in DMEM-High Glucose 4.5 mg/l (11995065) supplemented with 10% fetal bovine serum (FBS, 10270098) and 1% antibiotic/antimycotic (15140122) solution (all from ThermoFisher Scientific). aSMC were cultured in DMEM-High Glucose 4.5 mg/l (11995065) supplemented with 0.2 mg/ml geneticin (G-418, 10131027), 10% fetal bovine serum (FBS, 10270098) and 1% antibiotic/antimycotic solution (all from ThermoFisher Scientific). aFib were cultured in DMEM containing 4.5 mg/l glucose (11995065) supplemented with 20% fetal bovine serum (FBS) and 1% antibiotic/antimycotic (15140122) solution (all from ThermoFisher Scientific). eMSC were cultured in alpha-minimum essential medium (α-MEM, without ribonucleosides and deoxyribonucleosides and with 2.2 g/L sodium bicarbonate, 12561056), supplemented with 20% fetal bovine serum (FBS, 10270098) and 1% antibiotic/antimycotic (15140122) solution (all from ThermoFisher Scientific). GAeFib were cultured in in DMEM with 2 mM L-glutamine (11965084) and 1% antibiotic/antimycotic (15140122) solution (all from ThermoFisher Scientific) on gelatin (G1393, Sigma-Aldrich) coated culture dishes. hNPCs were cultured in ReNcell NSC-maintenance media (SCM005, EMD Millipore), freshly supplemented 20 ng/mL EGF (PHG0311, Thermo Fisher Scientific), 20 ng/mL (FGF-2, PHG0023, Thermo Fisher Scientific), and 1% antibiotic/antimycotic (15140122, ThermoFisher Scientific) solution on laminin (LN-211, BioLamina) coated culture dishes. hNPCs differentiation was

induced by withdrawing the growth factors from the ReNcell NSC-maintenance media (SCM005, EMD Millipore). hiPSCs and hNPCs were passaged using the StemPro accutase (A1110501, Thermo Fisher Scientific). hskMPs and all murine cell lines were passaged using the TrypLE express enzyme (12605010, Thermo Fisher Scientific).

Embryoid formation and 3D culture conditions

hiPSCs alone or in combination with support cell types were prepared for 3D-aggregation by adding a total of 5.5×10^6 cells per-well in Corning Costar ultra-low attachment 6-well plates (CLS3471, Sigma-Aldrich) in STEMdiff APEL2 medium (05270, STEMCELL Technologies) supplemented with 10 mM ROCK inhibitor (Y-27632, 1254, Tocris Bioscience) with constant shaking (Orbi-Shaker CO2, Benchmark Scientific) at 95 rpm at 37 °C and 8% CO2 overnight. For Wnt/FGF pathway stimulation, the medium was then replaced with STEMdiff APEL2 medium (05270, STEMCELL Technologies), supplemented with 2.5 uM of GSK3-inhibitor CHIR99021 (Tocris Bioscience) for 6 days. On day 7 the embryoids were switched to essential 6 medium (A1516401, Thermo Fisher Scientific), supplemented with 20 ng/mL of bFGF (FGF-2, PHG0023, Thermo Fisher Scientific) until day 13. Culture medium was changed every other day. In conditions without Wnt/FGF pathway stimulation, DMSO was used as a vehicle-control.

2D myogenic differentiation of MPs

Integrin α9/CD56 positive flow cytometrically purified eMPs were plated on vitronectin (VTN-N, A14700, Thermo Fisher Scientific) coated plates in the presence of 10 mM ROCK inhibitor (Y-27632, 1254, Tocris Bioscience). eMPs were maintained in proliferation medium (PM, SkGM2 medium, CC-3160, Lonza) supplemented with 20ng/mL of bFGF (FGF-2, PHG0023, Thermo Fisher Scientific). For differentiation, following 11 days of maintenance in PM, the eMPs were switched to differentiation medium (DM, N2-media containing Insulin-Transferrin-Selenium, ITS-G, Thermo Fisher Scientific) and N-2 Supplement (17502048, Thermo Fisher Scientific) for 10 days. Extracellular matrix proteins other than vitronectin were fibronectin (F2006, Sigma-Aldrich), gelatin (G1393, Sigma-Aldrich), and laminin (LN-211, BioLamina). hskMP were obtained from adult human skeletal muscle (Lonza, LZ-CC-2580) and plated on fibronectin. hskMP were either maintained in PM (Skeletal Muscle Cell Growth Medium, AmsBio, SKM-M medium) or switched to DM (Dulbecco's Modified Eagle Medium/F-12, DMEM/F-12, 11320033, Thermo Fisher Scientific) supplemented with 2% horse serum (26050088, Thermo Fisher Scientific) for 4 days.

Immunocytochemistry

Cells were washed in PBS (10010023, Thermo Fisher Scientific) for 5 minutes before fixation in 4% paraformaldehyde (PFA, 28908, Thermo Fisher Scientific) for 15 minutes. Fixed cells were washed three times with PBS (10010023, Thermo Fisher Scientific) and permeabilized in 0.1% Triton X-100

(T8787, Sigma-Aldrich-Aldrich) for 15 minutes at room temperature. The cells were then blocked with 4% bovine serum albumin (BSA, 001000162, Jackson ImmunoResearch, IgG-free) in PBS (10010023, Thermo Fisher Scientific) and 4% goat-serum (16210064, Thermo Fisher Scientific) for 1 hour at room temperature. Samples were incubated with primary antibody at 4°C overnight or at room temperature for 2 hours. After three PBS (10010023, Thermo Fisher Scientific) washes, cells were incubated with corresponding secondary antibody and 40, 6-diamidino-2-phenylindole (DAPI, D1306, Thermo Fisher Scientific) for 45 minutes at room temperature. After PBS washing (10010023, Thermo Fisher Scientific), the sample was dried and mounted with mounting-buffer (ProLong Diamond Antifade Mountant, P36965, Thermo Fisher Scientific).

Immunohistochemistry of skeletal muscles

Tibialis anterior (TA) muscles were and frozen in isopentane cooled with liquid nitrogen. Cryosectioning was performed at 10 um. Sections were allowed to air-dry for 10 minutes, fixed during 10 minutes with 4% paraformaldehyde (PFA, 28908, Thermo Fisher Scientific) and subsequently permeabilized in 0.1% Triton X-100 (T8787, Sigma-Aldrich-Aldrich) for 15 minutes. After blocking in PBS (10010023, Thermo Fisher Scientific) with 4% goat-serum (16210064, Thermo Fisher Scientific) for 3 hours at room temperature, cryo-sections were incubated with primary-antibodies during 3 hours at room temperature in blocking solution. Slides were then incubated during 1 hour at room temperature with secondary antibodies and counterstained with DAPI (D1306, Thermo Fisher Scientific). For Pax7 staining, antigen retrieval was performed with two successive incubations of hot citric acid 0.01 M pH 6 for 10 minutes. The signal obtained from the Pax7 antibody was further amplified using a goat-anti mouse IgG1-biotin (115065205, Jackson ImmunoResearch) followed by a Streptavidin Alexa-555 (S32355, Life Tech) treatment, together with other secondary antibodies and the DAPI (D1306, Thermo Fisher Scientific) counterstain.

Immunohistochemistry of embryoids

Embryoids were washed with PBS (10010023, Thermo Fisher Scientific) and fixed with 4% paraformaldehyde (PFA, 28908, Thermo Fisher Scientific) for 30 minutes. Fixed samples were soaked in 30% sucrose for at least 24 hours at 4°C. For freezing embryoids were embedded in gelatin (G1393, Sigma-Aldrich-Aldrich) solution (15% sucrose, 7.5% gelatin in PBS). Samples were frozen at −50°C to −65°C in dry ice-cooled isopentane and stored at −80°C until sectioning. Cryosections of 10 um were stained using the same procedure for TA muscles above.

Imaging

Imaging was carried out using DMI6000 inverted microscope (Leica), a VS120 slide scanner (Olympus), or a DMI 4000B microscope (Leica) and analyzed either using the VS-ASW FL software measurement tools or the LAS AF software.

Antibodies and staining probes

The following antibodies and staining probes were used: Pax7 (34360, Abcam), Pax7 (528428, DHSB), Pax3 (381801, ThermoFisher Scientific), Meox1/Mox-1 (75895, Abcam), Tuj1/βIII-Tubulin (ectodermal), a-SMA (mesodermal), and AFP (endodermal) markers by using the 3-germ Layer immunocytochemistry kit (A25538, ThermoFisher Scientific), Tuj1/βIII-Tubulin (18207, Abcam), CytoPainter-Phalloidin-iFluor 488 reagent (176753, Abcam) which labels F-actin, MyoD (SC304, Santa Cruz), MyoD (PA523078, ThermoFisher Scientific), MyHC (MF20, MAB4470, R&D Systems), dystrophin (15277, Abcam), dystrophin (MANDYS106-clone 2C6) (MABT827, Millipore), Lamin A/C (clone JOL2, 40567, Abcam), Nestin (Rat-401) (6142, Abcam) and Sox2 (97959, Abcam). The following antibodies were used for flow cytometry: CD56 (clone B159, 555516, BD Biosciences), CD57 (Clone HNK-1, 562488, BD Biosciences), CD54 (ICAM, Clone HA58, 740404, BD Biosciences), CD271 (NGFR, Clone C40-1457, 560834, BD Biosciences), CD82 (Kai-1, 564341, BD Biosciences), CD34 (Clone 8G12-HPCA2, 745247, BD Biosciences), CD362 (SDC2, FAB29651G, R&D Systems) and Integrin α9 (clone Y9A2, 351602, BioLegend).

Fluorescence-activated cell sorting

Flow cytometric analysis and sorting were performed using an LSRFortessa SORP (H647800N0001, BD Biosciences) and a MoFlo Astrios EQ (106694, Beckman Coulter) respectively. The data on the LSRFortessa SORP were acquired and recorded with the BD FACSDiva software version 8.0.2. The data of the MoFlo Astrios EQ were acquired and recorded with the software Summit version 6.3.1.16945. All data were subsequently analyzed with FCSExpress Flow Cytometry version 6.06.0014 (4193, De Novo Software). Cell viability was assessed for all the experiments using the LIVE/DEAD fixable aqua dead cell stain kit (L34957, Thermo Fisher Scientific). The purity of sorted samples was verified by flow cytometric re-analysis.

RNA visualization

RNA visualization was performed using the PrimeFlow RNA Assay Kit (88-18009-204) from Thermo Fisher Scientific according to the manufacturer's instructions and was analysed using an LSR-Fortessa instrument (BD Biosciences). Briefly, dissociated-cells from embryoids and hskMPs, were fixed and permeabilized in Fixation Buffer 1 on ice for 30 minutes, followed by incubation in permeabilization-buffer on ice for 30 minutes. Then, samples were fixed in Fixation Buffer 2 at room temperature for 1 hour. To detect cellular RNA-targets, sequential hybridizations were performed in a dry incubator pre-calibrated to 40 °C. Target probe sets were hybridized for 2 hours and the signal was amplified using hybridizations with PreAmplifier and then Amplifier 1.5 hours each. Eventually, cells were hybridized with fluorochrome-conjugated Label Probes for 1 hour. Probes were: MyoD-AF488 (VA4-3082435), Myf5-AF647 (VA1-11144) and GADPH-AF750 (VA6-10337). For visualization stained cells were centrifuged onto a slide using a cytospin 4 (Thermo Fisher Scientific).

RNA extraction, quantification and quality control

RNA was extracted using the Agencourt-RNAdvance tissue kit (A32645, Beckman Coulter) following the manufacturer's instructions. Two rounds of cRNA synthesis starting with 5 ng of total RNA were performed using the MessageAmp II aRNA amplification kit (AM1751, Life Technologies) and MessageAmp II-biotin enhanced aRNA amplification kit (AM1791, Life Technologies) according to the manufacturer's instructions. RNA was quantified using the Quant-iT RiboGreen RNA Assay Kit (R11490, Invitrogen) using a Spectramax M2 (Molecular Devices). RNA quality assessment was performed using a Bioanalyzer 2100 with RNA 6000 Pico Kit (Agilent Technologies).

Quantitative RT-PCR

RNA samples were subjected to reverse transcription using Prime Script reverse transcriptase (2680B, Takara) with random 6-mer primers according to the manufacturer’s instructions using peqSTAR 96 universal gradient thermocycler (Peqlab). Quantitative reverse transcription PCR (qRT-PCR) performed by using the LightCycler 480 (Roche Diagnosis), 384-well PCR plates and the LightCycler 480 SYBR Green I Master kit (04707516001, Roche Diagnosis). All reactions were conducted in quadruplicate with each PCR consisting of 2 ul of the diluted cDNA, 0.5 um primers, and 2 ul LightCycler 480 SYBR-Green I master mix. The reaction volume was adjusted to 10 ul with nuclease-free water. The Non-template control (NTC) reactions contained water instead of cDNA as template. Taqman probes (ThermoFisher Scientific) were: Pax7 (Hs00242962_m1), Brachyury (T) (Hs00610080_m1), Msgn1 (Hs03405514_s1), Tbx6 (Hs00365539_m1), Pax3 (Hs00240950_m1), Myf5 (Hs00929416_g1), MyoD (Hs02330075_g1), Fgf5 (Hs03676587_s1), Gata4 (Hs00171403_m1), and Neurog1 (Hs01029249_s1).

Mice

All experiments were performed using male C57BL/10ScSn-Dmdmdx/J (Mdx mice) according to the Swiss regulation on animal experimentation for the care and use of laboratory animals and approved by the ethical committee of the canton de Vaud under licenses VD2620, VD2764, VD3002, VD3199 and VD3282. Mice had access to water and food ad libitum at all time. All the mice were studied between 4-8 weeks. Tacrolimus/FK-506 (S5003-500MG, Selleck Chemicals) was delivered continuously through a pre-equilibrated Alzet osmotic pump model 1002 (Charles River) implanted subcutaneously 5 days before cell transplant. Tacrolimus/FK-506 (S5003-500MG, Selleck Chemicals) was diluted in 70% EtOH and delivered at a dose of 2.5mg/kg/day and a delivery rate of 0.25 ul/hour. 2 days before transplantation, the TA-muscle of one leg was injected through the skin with 50 ul of 20 uM cardiotoxin (L8102, Latoxan). On the day of the transplantation, 25,000 integrin α9/CD56 positive flow cytometrically purified eMPs and 25,000 hskMPs were prepared under sterile

conditions and were injected into the injured TA-muscle in 50 ul of 0.9% NaCl. 10 days after cell-transplantation, muscles were collected for analysis.

Statistics and reproducibility

All mice were randomized according to body weight before interventions. Sample size determination was based on the expected effect size and variability that was previously observed for similar readouts in the investigators labs. *In-vivo* treatments were not blinded, but imaging readouts were analyzed in a blinded manner. All other statistical analyses were performed using GraphPad Prism (Version 7, GraphPad Software). A two-sample unpaired Student's t-test was used for two-group comparisons. For comparison of more than two groups, one-way or two-way ANOVAs were used, according to the experimental design, and followed by Bonferroni multiple-comparison testing. All data are expressed as mean ± S.E.M.

Supplementary Figures

An Engineered Multicellular Niche for the 3D Derivation of Human Myogenic Progenitors from iPSCs

Omid Mashinchian, Filippo De Franceschi, Joris Michaud, Sonia Karaz, Pascal Stuelsatz, Nagabhooshan Hegde, Gabriele Dammone, Matthias P. Lutolf, Jerome N. Feige, C. Florian Bentzinger

Supplementary Figures 1-3

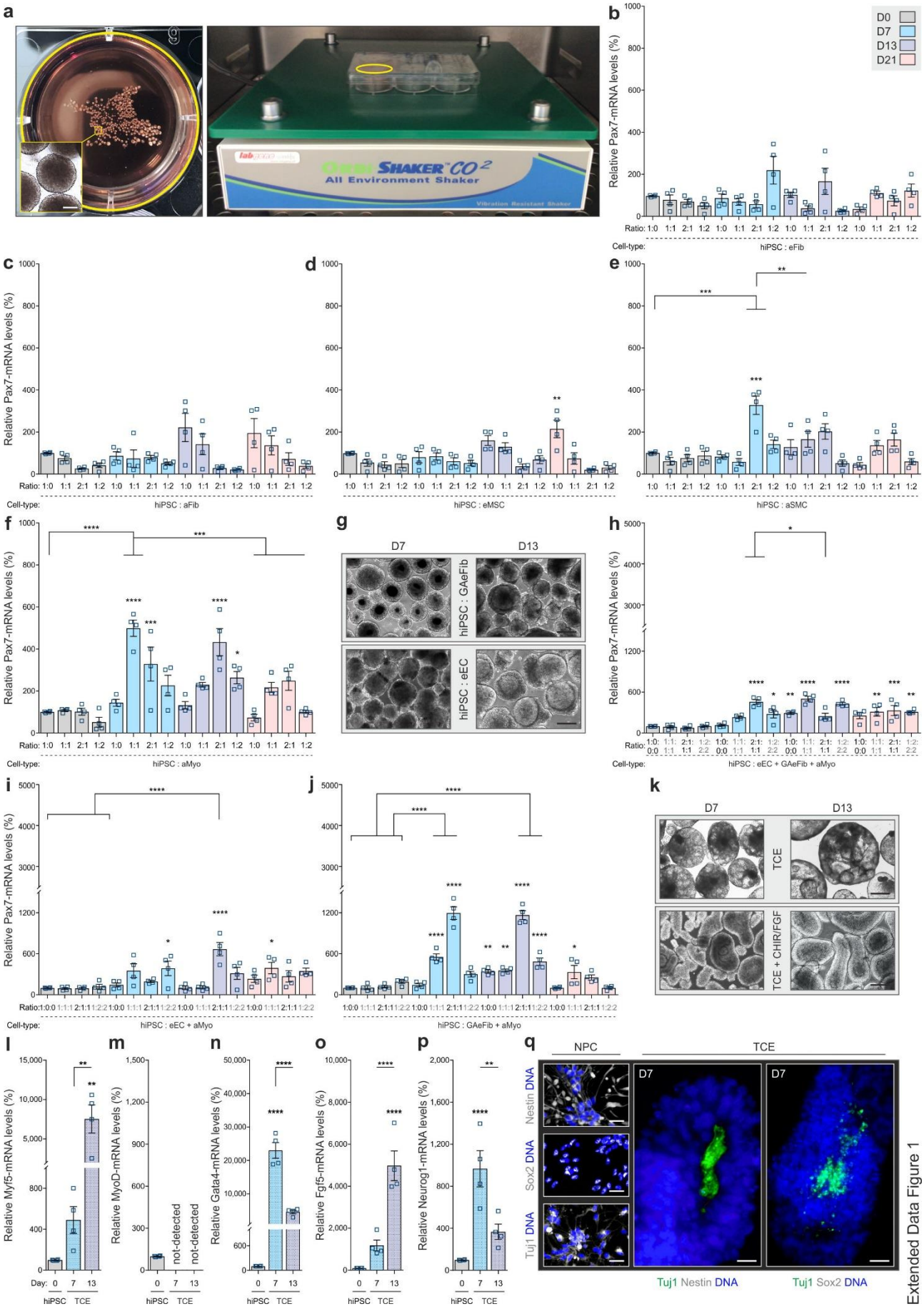

*Manuscript under revision (May 2019)

Extended Data Fig. 1: Characterization of multi-component embryoids. a, Horizontal shaker platform setup used to generate multi-component embryoids. **b-f,** mRNA expression of Pax7 in embryoids containing different ratios of hiPSCs and embryonic fibroblasts (eFib), adult fibroblasts (aFib), embryonic mesenchymal-like stem cells (eMSC), adult smooth muscle cells (aSMC) or adult myoblasts (aMyo). Mixtures of the respective cell types were interrogated immediately before (D0), and 7 and 13 days (D7 and D13) after aggregation. **g,** Representative bright field images of embryoids containing hiPSCs and embryonic endothelial cells (eEC) or growth arrested embryonic fibroblasts (GAeFib) in a 2:1 ratio. Scalebars = 125um. **h-j,** mRNA expression of Pax7 in embryoids containing different ratios of hiPSCs, GAeFib, eEC, aMyo. Mixtures of the respective cell types were interrogated immediately before (D0), and 7 and 13 days (D7 and D13) after aggregation. **k,** Representative bright field images of three-component embryoids (TCEs) containing hiPSCs, eEC and GAeFib in a 2:1:1 ratio with and without stimulation of the Wnt/FGF pathways. Scalebars = 125um. **l-p,** mRNA expression of the myogenic commitment markers Myf5 and MyoD, the endoderm marker Gata4, and the ectoderm markers Fgf5 and neurog1 in hiPSCs and Wnt/FGF induced TCEs at D7 and D13. **q,** Representative stainings for the neuronal progenitor markers Tuj1, Nestin and Sox2 in Wnt/FGF induced D7 TCEs. Human neural progenitor cells (NPCs) are shown as a positive control. Scalebars in the three left-hand side images = 25um, scalebar on the two larger right-hand side images = 20um. **b-f,h-p,** Data are represented as means ± S.E.M. p-values are *p<0.05, **p<0.01, ***p<0.001, ****p<0.0001 using an ANOVA followed by a Bonferroni post hoc test.

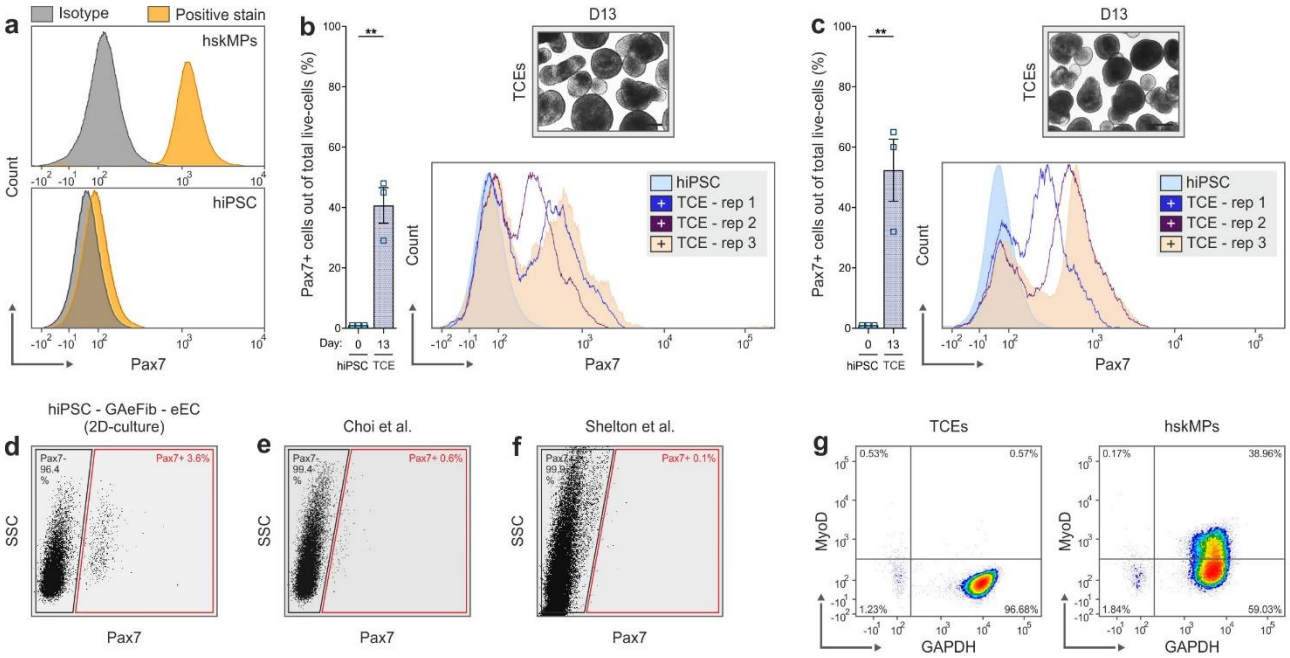

Extended Data Fig. 2: Technical validation and comparison of embryoid derivation to established protocols for myogenic hiPSCs differentiation. a, Flow cytometric validation of the Pax7 antibody in hiPSCs and hskMPs. **b,c,** Flow cytometry quantification of Pax7 positive cells from Wnt/FGF induced day 13 (D13) TCEs compared to hiPSCs, and representative images. Experiments in (**b**) and (**c**) were performed with hiPSC lines ACS-1020 and 482 generated from two donors that are biologically different from the one used in the main study. **d,** Flow cytometry quantification for Pax7 in hiPSCs co-cultured with GAeFib and eEC in 2D over two weeks. Wnt pathway activation was induced from day 1-7 and bFGF stimulation from day 7-13. **e,f,** Flow cytometry quantification for Pax7 in hiPSC cultures differentiated for two weeks according to Choi (32) or Shelton et al. (13). **g,** RNA fluorescence in situ hybridization for the myogenic commitment marker MyoD and the positive control GAPDH in hskMPs and cells derived from D13 TCEs following biochemical Wnt/FGF pathway stimulation quantified by flow cytometry. **b,c,** Data are represented as means ± S.E.M. p-value is *p<0.05 using a students t-test.

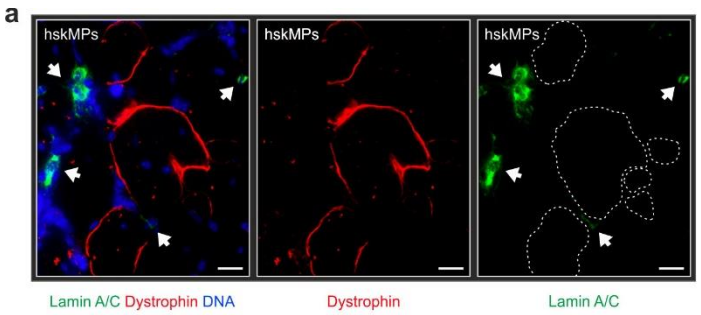

Extended Data Fig. 3: Engraftment of hskMPs in mdx mice. a, Representative immunostainings for the human nuclear marker lamin A/C and dystrophin in muscles of mdx mice 10 days after transplantation of hskMPs. Arrows depict cells in the satellite cell position in the periphery of muscle fibers. Scalebars = 20um.

Chapter 4:

In-vivo Transcriptomic Profiling of Systemic Aging using Stem Cell Encapsulation

Background & Rationale:

A surgical procedure developed more than a century ago which unites the vasculature of two living animals known as “parabiosis” has sourced a wealth of information towards a better understanding of different physiological states and how these communicate via the blood circulation [437]. In particular, this method has recently been extensively used to study the impact of an aged systemic environment on young tissues and vice versa.

However, parabiosis studies have triggered significant ethical concerns and authorities assessing animal protocols are very likely to challenge such experiments. Thus, an alternative approach to study systemic aging and its effect on different tissues and cell types would be of great interest for the field. In addition, current parabiosis based studies are largely limited to rodent models and conclusions are difficult to extrapolate to human cells and tissues.

Nevertheless, sustained exposure to a young systemic environment rejuvenates aged tissues and enhances stem cell function. However, due to the intrinsic complexity of tissues it remains challenging to pinpoint direct effects of circulating factors on specific cell populations from indirect effects where blood-borne factors interact with the tissue micro-environment.

In this chapter, we describe a novel method to mimic parabiosis by encapsulation of human stem cells in highly diffusible polyethersulfone hollow fiber capsules that can be used to profile the systemic environment independent of physical cellular interactions *in-vivo*.

Personal contribution:

Designing and performing encapsulation experiments *in-vitro*, analyzing the data, drafting the manuscript and leading the revision experiments.

Current status of the project*:

Manuscript under revision (since early February 2018)

*Manuscript under revision (February 2018)

In-vivo Transcriptomic Profiling of Systemic Aging using Stem-Cell Encapsulation

Xiaotong Hong[1]*, **Omid Mashinchian**[1,2,]* , Christophe Boss[1], Eugenia Migliavacca[1], Sylviane Metairon[1], Frederic Raymond[1], Patrick Descombes[1], Nicolas Bouche[1], Jerome N. Feige[1,2,#], C. Florian Bentzinger[1,3,#]

1. Nestle Institute of Health Sciences
   Innovation Park, Building H
   EPFL Campus, Lausanne, Switzerland

2. School of Life Sciences
   Ecole Polytechnique Federale de Lausanne (EPFL)
   Lausanne, Switzerland

3. Département de pharmacologie et physiologie
   Faculté de médecine et des sciences de la santé
   Université de Sherbrooke
   Sherbrooke, Canada

* / #: Equal contribution

Corresponding authors: C. Florian Bentzinger, *cf.bentzinger@usherbrooke.ca*
Jerome N. Feige, *Jerome.Feige@rd.nestle.com*

***Manuscript under revision (February 2018)**

Main

Declining stem cell function and regenerative failure are major hallmarks of aging in mammals. Parabiosis, a surgical technique developed more than a century ago, unites the vasculature of two living organisms [437]. In rodents, exposure to a young systemic environment through parabiotic pairing has been shown to restore stem cell function and enhance the regenerative capacity of aged tissues [438]. However, the characterization of the molecular mechanisms underlying the beneficial effects of parabiosis has proven to be highly complex. A major challenge arises from the fact that systemic factors do not always act in a direct manner on tissue resident stem cell populations, but can instead trigger paracrine propagation and modulation of signals through supportive cell types in the niche. In addition, significant differences in cell biology and physiology need to be taken into consideration when extrapolating results obtained from parabiosis experiments from animal models to humans.

Here we present a method that allows for the encapsulation of human stem cells in diffusible hollow fiber capsules that can be transplanted subcutaneously to profile the impact of the systemic environment in the absence of physical cellular interactions. Given their wide use in separation fields, their oxidative, thermal and hydrolytic stability, and their favorable mechanical properties we chose polyethersulfone (PES) hollow fiber membrane (HFM) tubes for encapsulation of human muscle progenitors (MP) [439]. Importantly, PES fibers are hemocompatible and become vascularized when subcutaneously implanted [440]. In order to maximize the number of encapsulated cells and, at the same time, allow for adequate oxygen diffusion throughout the capsule, we selected a tubular HFM with an outer diameter of 0.9 mm inner diameter of 0.7 mm. The spongy-like, cross-linked architecture of PES-HFM allows for the diffusion of molecules up to 1000 kDa freely through the membrane, but prevents infiltration by cells (**Fig. 1a**). To provide a suitable adhesion matrix for the cells in the fiber lumen, we chose Matrigel [441]. In contrast to inert agarose substrates, embedding MPs in Matrigel promoted cell spreading and the formation of protrusions (**Supplementary Fig. 1a**)**.** Following mounting of the HFM to an adaptor hub, the exposed end and the external hub interface were sealed using a bio-compatible photopolymerizing medical grade polyacrylate adhesive (**Fig. 1b and supplementary Fig. 1b**). Sealing of devices was verified using a submersion air pressure decay test. Assembled devices were then sterilized with ethylene oxide and all subsequent work was performed under antiseptic conditions. Trypsinized MPs mixed with Matrigel were injected into the capsule trough the adaptor hub using a Hamilton syringe. While cells were retained in the capsule, excess volume was ultrafiltrated through the porous membrane. The loaded capsule was then transferred onto a 3D printed autoclavable USP Class VI plastic cutting and sealing platform (**Supplementary Fig. 1c,d**). Following cutting of the adaptor hub, the loaded capsule was left protected in the UV blocking plastic device while the second adhesive seal was photopolymerized.

For validation of our experimental setup and to interrogate the behavior of encapsulated cells, we performed a series of *in-vitro* experiments. Loaded capsules were placed into culture dishes, immersed human myoblast growth media and maintained in a tissue culture incubator. TUNEL staining of cryosections from capsules that were kept in culture revealed that few cells did undergo cell death as an immediate consequence of the loading procedure (**Fig. 1c**)**.** Cell density initially increased in capsules in culture, but plateaued afterwards (**Fig. 1d**). Following ten days in culture, we observed a relatively homogeneous distribution of MPs in the capsules (**Fig. 1e**) and the cells remained positive for the myogenic marker MyoD (**Fig. 1f,g**). Growth factor deprivation over a typical four day differentiation period, induced a loss of MyoD positive MPs and an induction of the terminal differentiation marker myosin heavy chain (MHC) (**Fig. 1h-j**)**.** Collectively, these observations demonstrate that encapsulated human MPs remain viable and proliferative, maintain the expression of myogenic markers, and are capable to respond to pro-differentiative signals. Sufficient for downstream analysis, quantification of RNA isolated from whole homogenized capsules after ten days of culture under growth conditions revealed a yield averaging 296 ng per unit.

We next established the capsule implantation and recovery procedure using adult male mice. The animals were anesthetized and two incisions were made on the back slightly posterior to the scapulae (**Fig. 2a**). On one side, an osmotic pump supplying the immunosuppressant FK-506 was implanted through the incision so that it remained subcutaneously on the flank. On the other side, three capsules loaded with human MPs were implanted into the subcutaneous fascia over the rib cage separated by 1-2 mm from each other. Capsules were inserted using a stiff plastic applicator tube sliding over a metal plunger (**Supplementary Fig. 2a**). Following slow withdrawal of the tube covering the capsule that was held in place by the metal plunger, the applicator was removed and the incisions were closed. After ten days *in-vivo* the capsules showed vascularization and only minimal connective tissue build-up (**Fig. 2b**). TUNEL analysis of cross-sections from explanted capsules revealed that the MPs remained largely viable (**Fig. 2c,d**), and that MyoD and MHC was still expressed by the cells (**Fig. 2e-h**). Still satisfactory for downstream analysis, two pooled explanted units explanted from the same mouse yielded an average of ≥140 ng of RNA.

Finally, to exemplify an application of our systemic profiling protocol we implanted young and aged mice for ten days with capsules containing human MPs as established for adult mice. Likely as a consequence of inhibitory signals in the old systemic environment the RNA yield dropped significantly for the aged group (**Fig. 2i**). cDNA obtained from these samples was hybridized on microarrays covering the human 9 transcriptome (**Fig. 2j**), met quality control criteria, and showed a log2 expression range from 6-12. To exclude the detection of RNA from contaminating mouse cells, we analyzed connective tissue isolated in the immediate periphery of the implants from random animals in the young and aged groups using human-specific microarrays. No signal was detected in any of these samples, demonstrating that contamination

from mouse tissues does not bias the protocol. Expression analysis of capsule derived mRNAs revealed a highly specific signature of 157 genes that were differentially regulated (FDR<25%, |log2FC|>0.5) in cells exposed to an aged systemic environment when compared to the young condition (Fig. 2k). Reinforcing the notion that aged plasma generally represses MP function, about two thirds of these transcripts were downregulated. Gene set enrichment analysis using the hallmark database revealed pronounced anti-myogenic effects and changes in transcripts involved in the response to circulating hormones and cytokines in the aged condition (**Fig. 2l,m and Supplementary Table 1**).

Reduced levels of transcripts in the myogenesis, PI3K/Akt/mTOR and KRAS pathways in MPs extracted from capsules from aged mice fall well in line with the downregulation of sex hormones and the somatotroph axis in elderly humans, that is characterized by decreased levels of IGF-1 and growth hormone [442]. In addition, it has long been described that aging affects the immune system at multiple levels including decreased B and T cell production and altered lymphocyte function [443]. Our data shows that the resulting alterations in systemic cytokine levels affect a spectrum of pathways in MPs, including MYC, TNFα and NFκB signaling. Collectively, these results demonstrate a dominant involvement of altered levels of circulating hormones and cytokines in systemically imposed human stem cell aging. Finally, we set out to test whether processes affected by an aged systemic environment in encapsulated human MPs are also changed in tissues of mice undergoing heterochronic parabiosis. To this end, we compared gene ontology (GO) terms enriched in transcriptional profiling of brain tissue obtained from heterochronic relative to isochronic parabionts to our study [444]. This analysis revealed that GO terms for basic cellular processes such as ion homeostasis, immune response, peptidase activity and RNA processing, are significantly changed in both datasets (**Supplementary Table 2**). Thus, part of the transcriptional response to a differentially aged systemic environment is conserved across species and cell types.

Altogether, we demonstrate that our method allows for sensitive systemic profiling unbiased by cellular crosstalk that is not restricted by species barriers. The characterization of bona fide aging signatures in stem cell populations independent of heterogeneous cellular contexts, will allow for the identification of novel therapeutic targets for the systemic treatment of age-associated regenerative dysfunction. Moreover, in future applications, the combination encapsulation technology with induced pluripotent stem cell (iPSC) derived cells, will allow to study systemic effects at an unprecedented holistic level in humanized systems.

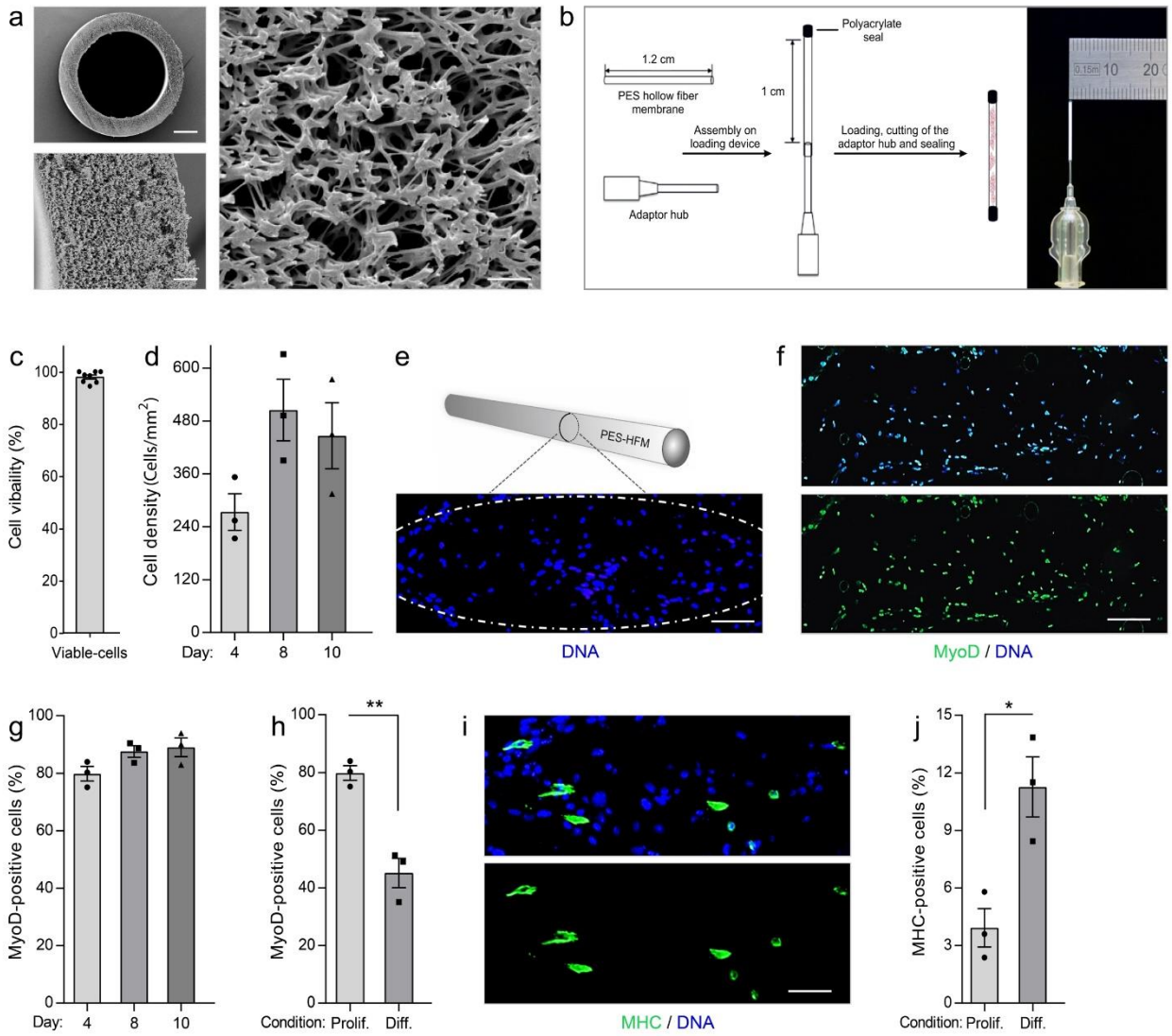
a
b
1.2 cm
PES hollow fiber membrane
1 cm
Polyacrylate seal
Assembly on loading device
Loading, cutting of the adaptor hub and sealing
Adaptor hub
c
Cell vibaility (%)
Viable-cells
d
Cell density (Cells/mm2)
Day: 4 8 10
e
PES-HFM
DNA
f
MyoD / DNA
g
MyoD-positive cells (%)
Day: 4 8 10
h
**
MyoD-positive cells (%)
Condition: Prolif. Diff.
i
MHC / DNA
j
*
MHC-positive cells (%)
Condition: Prolif. Diff.

FIGURE 1

Figure 1 | (**a**) Scanning electron micrographs of the polyethersulfone hollow fiber membrane. Scale bars: 200 µm, 20 µm and 5 µm from right to left. (**b**) Schematic outlining the capsule loading procedure and photograph of a polyethersulfone (PES) hollow fiber membrane mounted to the adaptor hub. (**c**) Quantification of TUNEL negative viable cells in capsules maintained growth media for one day after loading. (**d**) DNA staining based quantification of cell numbers in capsules maintained over a time course of ten days in growth media. (**e**) Representative DNA staining of a cross section from a capsule maintained ten days growth media. (**f**) Representative MyoD immunostaining of a cross section from a capsule maintained 10 days growth media. (**g**) Quantification of MyoD positive cells in capsules maintained for four days in growth media compared to differentiation media. (**i**) Representative myosin heavy chain (MHC) immunostaining of a cross section from a capsule maintained for 10 days growth media. (**j**) Quantification of MHC positive cells in capsules maintained for four days in growth media compared to differentiation media. Throughout, bars represent means + s.e.m. n≥3 cross sections from different capsules were quantified for each experiment and time-point. **P<0.01, *P<0.05; Two-way comparisons were made with a student's t–test and multiple comparisons by one–way ANOVA followed by Bonferroni post–test. (**e, f and I**) Scale bar: 250 µm.

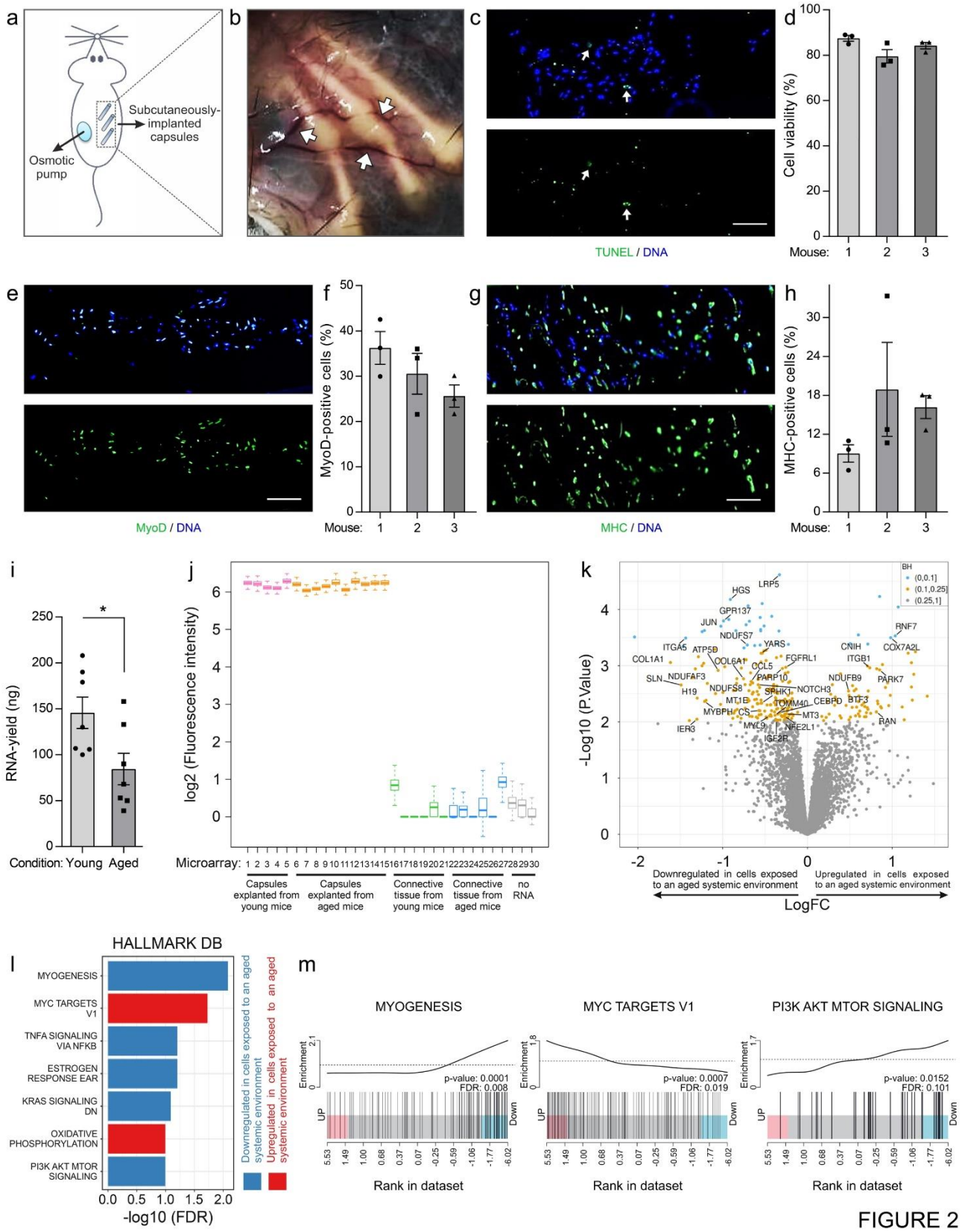
a
Subcutaneously-implanted capsules
Osmotic pump
b
c
TUNEL / DNA
d
Cell viability (%)
Mouse: 1 2 3
e
MyoD / DNA
f
MyoD-positive cells (%)
Mouse: 1 2 3
g
MHC / DNA
h
MHC-positive cells (%)
Mouse: 1 2 3
i
RNA-yield (ng)
Condition: Young Aged
j
log2 (Fluorescence intensity)
Microarray:
Capsules explanted from young mice
Capsules explanted from aged mice
Connective tissue from young mice
Connective tissue from aged mice
no RNA
k
-Log10 (P.Value)
Downregulated in cells exposed to an aged systemic environment
Upregulated in cells exposed to an aged systemic environment
LogFC
l
HALLMARK DB
MYOGENESIS
MYC TARGETS V1
TNFA SIGNALING VIA NFKB
ESTROGEN RESPONSE EAR
KRAS SIGNALING DN
OXIDATIVE PHOSPHORYLATION
PI3K AKT MTOR SIGNALING
-log10 (FDR)
m
MYOGENESIS
p-value: 0.0001
FDR: 0.008
MYC TARGETS V1
p-value: 0.0007
FDR: 0.019
PI3K AKT MTOR SIGNALING
p-value: 0.0152
FDR: 0.101
Enrichment
UP
Down
Rank in dataset

FIGURE 2

Figure 2 | (**a**) Schematic of the implantation strategy for the capsules and the osmotic pump. (**b**) Photograph of the capsules in the connective tissue under the skin ten days after implantation. Arrows are pointing at blood vessels in proximity of the capsules. (**c**) Representative TUNEL staining showing apoptotic nuclei in a cross section of a capsule after ten *in-vivo*. (**d**) Quantification of TUNEL negative viable cells in capsules after ten days *in-vivo*. (**e**) Representative immunostaining for MyoD in a cross section of a capsule after ten days *in-vivo*. (**f**) Quantification of MyoD positive cells in capsules after ten days *in-vivo*. (**g**) Representative immunostaining for MHC in a cross section of a capsule after ten days *in-vivo*. (**h**) Quantification of MHC positive cells in capsules after ten days *in-vivo*. (**i**) RNA yield from capsules after ten days *in-vivo* in young and aged mice. (**j**) Microarray control probes following hybridization with RNA derived samples from capsules explanted from young and aged mice after ten days. Each microarray was performed with RNA isolated from two pooled capsules explanted from individual mice. Array 5, 9 and 11 were excluded for downstream analysis due to missing control probe signals. Random samples of mouse connective tissues in the capsule periphery served as negative controls. (**k**) Volcano plot showing genes with a Benjamini-Hochberg false discovery rate <10% (blue) and <25% (Yellow) across the pooled microarray data from capsules explanted from young and aged mice after ten days. (**l and m**) Hallmark database pathway analysis based on gene ranks across the pooled microarray data from capsules explanted from young and aged mice after ten days. Throughout, bars represent means + s.e.m. (**d, f and h**) Cross sections of capsules explanted from n=3 mice were analyzed for each experiment. (**i-m**) Samples and data derived from capsules of n≥6 mice in each age group. *P<0.05; Two-way comparisons were made with a student's t–test and multiple comparisons by one–way ANOVA followed by Bonferroni post–test. (**c, e and g**) Scale bar: 250 µm.

Acknowledgements

We are grateful to the NIHS community for fruitful discussion and support, in particular the muscle aging group, Eric Rolland and Ed Baetge. We thank Phoukham Phothirath and Oliver Rizzo of the preclinical investigations group at the Nestlé Research Center (NRC) for expert advice and support with *in-vivo* experiments. O.M. and C.F.B are supported by the Fondation Suisse de Recherche sur les Maladies Musculaires (FSRMM). C.F.B. is supported by the Natural Sciences and Engineering Research Council of Canada (NSERC), the Fonds de recherche du Québec – Santé (FRQS), the CHUS Foundation, and the Banting Research Foundation.

Author Contributions

X.H., C.B., O.M. and N.B. contributed to experimental design, conducted experiments and analyzed results. E.M. performed data analysis. S.M., F.R. and P.D. developed the RNA isolation methodology and performed the Microarray experiments. J.N.F and C.F.B directed the study, designed experiments, analyzed results and wrote the manuscript.

Competing Financial Interests

X.H., C.B., O.M., E.M., S.M., F.R., P.D., N.B., J.N.F. and C.F.B. were or are employees of the Nestlé Institute of Health Sciences S.A., Switzerland

Methods

Cell culture

Human skeletal myoblasts (Lonza) isolated from donated human tissue after obtaining permission for their use in research applications by informed consent or legal authorization were used at passages 4-6. For *in-vitro* expansion, the cells were maintained in human skeletal muscle myoblast growth medium (Zenbio) and passaged once confluency reached 50%. For passaging, media was aspirated from the dishes, followed by a washing step with Dulbecco's phosphate buffered saline (Gibco) at room temperature. The cells were then treated with trypsin and kept in the incubator for 5 minutes until all cells were detached from the vessel. An appropriate amount of warm media (media: trypsin = 3:1) was added to the vessel to neutralize the effect of trypsin, the cells were transferred to a Falcon tube and centrifuged at 200 rcf for 5 minutes. The supernatant was then carefully aspirated and the cell pellet was resuspended in warm media. A desired amount of the mixture was transferred to a new dish with warm media and maintained in the incubator.

Matrigel embedding

Growth factor reduced Matrigel (Corning) was thawed at 4 °C and pipette tips were chilled at -20 °C before starting the experiment. All material was kept on ice or at 4 °C during the procedure to avoid undesired gelation of Matrigel. All mixing steps were carried out with caution to avoid the generation of bubbles. Cells were harvested with trypsin, numbers were quantified using a cell counter (Vi-CELL) and centrifuged at 200 rcf for 5 minutes. The pellet was resuspended in ice-cold medium at a concentration of 20k cells/µl and kept on ice. The cell mixture was mixed with 1 volume Matrigel by gentle pipetting, giving rise to a final concentration of 10k cells/µl.

Device mounting

Polyethersulfone (PES) hollow fiber membranes (HFM, AKZO NOBEL) were cut into pieces of 1 cm (Fig. 1a,b). The adaptor hub (Supplementary fig. 1b) was produced by assembling a plastic loading head (Neurotech Pharmaceuticals) with a piece of PEBAX single lumen tubing (Medical Extrusion Technologies). The piece of HFM was then assembled with one adaptor hub and sealed at the external interface with the PEBAX tube and at the exposed end using a bio-compatible photopolymerizing medical grade adhesive (Loctite, Henkel). Polymerization was induced using BlueWave LED Prime UVA high-intensity spot-curing system (Dymax) emitting two 5 second pulses of UV. The remaining empty lumen (1 cm) of the capsule holds a volume of 4 µL. Sealing of each device was verified using an air-leak test. While immerged in sterile double distilled water, filtered air was injected at a pressure of 17.58 hPa (2.5 Psi) for 5 s. Devices showing pressure decay greater than 100 Pa over 5 s were discarded. Assembled devices were sterilized with ethylene oxide gas before further use.

Cell encapsulation

10 µl of the cell-Matrigel mixture was loaded into each capsule using a Hamilton gastight syringe (50 µl) through the adaptor hub. Once the injected volume exceeded the inner volume of the device, a fraction of the total volume was ultrafiltrating through the porous membrane. The excess volume diffused from the membrane was removed by a piece of sterilized compress. The loaded capsule was transferred onto the 3D printed autoclavable USP Class VI plastic cutting and sealing platform (**Supplementary fig. 1c,d**), cut with a razor blade and sealed with the medical grade adhesive while left protected in the UV blocking plastic device. The capsule was then transferred to pre-warmed media and maintained on a shaker (80 rpm) in a 37°C, 5% CO2 incubator. Media was changed every day. For *in-vivo* studies, freshly loaded capsules were maintained in the incubator overnight before implantation.

In- and explantation surgery

All experiments were performed using male C57BL/6J mice (Janvier) in accordance with the Swiss regulation on animal experimentation and the European Community Council directive (86/609/EEC) for the care and use of laboratory animals. Mice had access to water and food ad libitum at all time. Adult mice were 6-month-old, young mice were 6-week-old and aged mice were 22-month-old. Before surgery, the mice were anesthetized using isoflurane and lidocaine was applied onto the skin. For the implantation of the preequilibrated Alzet osmotic pump model 1002 (Charles River) supplying 2.5 mg/kg of FK-506 in 70% ethanol (Selleck Chemicals) per day, a small incision was made on the back, slightly posterior to the scapulae.

One side of the incision was lifted with forceps and a subcutaneous pocket was created with a pair of sterile scissors. The pump was then inserted into this pocket using forceps. A second incision was introduced at the opposed side of the midline. Separated by 1-2 mm, 3 capsules were inserted through the incision into the subcutaneous fascia over the rip-cage using an applicator plastic tube sliding over a metal plunger (**Supplementary fig. 2**).

The metal plunger held the capsule in place while the plastic applicator tube was withdrawn over it. Subsequently the incisions were closed using surgical staples. Animals were first maintained in a heated recovery chamber before being moved to a cage. After surgery, the mice were kept in single housing with daily surveillance and bodyweight measurement. 10 d after implantation, the mice were sacrificed and the capsules were retrieved through manipulation at the rigid adhesive seals using forceps. Capsules were washed in warm PBS and incubated in 37 °C warm trypsin for 5 minutes and washed for further processing.

Cryo-sample preparation

Cultured capsules were washed three times with PBS before processing. Explanted capsules were washed with warm PBS, incubated 5 minutes in trypsin and washed a second time. Gelatin solution was heated up to and kept at 39 °C until completely melted. Firstly, a layer of gelatin was applied to the capsule sample using a plastic dropper. After the gel was solidified another layer of gelatin was applied to cover the entire capsule in a thin plastic mold. The sample was then kept at 4 °C for 5 minutes to ensure complete gelation. The sample was then snap frozen in a liquid nitrogen chilled isopentane slurry for 1 minute and transferred to dry ice.

Stainings

Capsule cryosections were washed in PBS for 5 minutes before fixation in 4% PFA (15 minutes). Fixed samples were washed three times with PBS and permeabilized in 0.1% Triton X-100 (Sigma-Aldrich) for 15 minutes at room temperature. The sections were then blocked with 4% BSA (Jackson ImmunoResearch, IgG-free) for 1 hour at room temperature. Samples were incubated with primary antibody at 4°C overnight or room temperature for 2 hours with the addition of mouse-on-mouse (M.O.M., Vector Laboratories) blocking reagent in the blocking buffer. After three PBS washes, cells were incubated with corresponding secondary antibody and 40, 6-diamidino-2-phenylindole (DAPI) for 45 minutes at room temperature. After three washing steps with PBS, the slide was dried and mounted with mounting buffer (ProLong Diamond Antifade Mountant) and a cover slide (Menzel-gläser, #1.5, Thermo Scientific). Imaging was carried out using DMI6000 inverted microscope (Leica) or VS120 slide scanner (Olympus). After the application of secondary antibody, all procedures were handled in darkness. Primary antibodies were Anti-MyoD antibody (C-20) (Santa Cruz Biotechnology, sc-304) and Anti-myosin heavy chain (Merck Millipore, A4.1025). TUNEL staining was performed using the In-Situ Cell Death Detection Kit (Roche) according to the manufacturer's instructions.

RNA extraction and microarray

Two devices from the same mouse were pooled and added to a Lysing Matrix D tube (MP Biomedicals, Santa Ana, California, USA) on ice. After addition of 450µL of lysis buffer (Agencourt RNAdvance Tissue Kit, Beckman Coulter, Indianapolis, Indiana, USA) the capsules were homogenized for 2x1 minute at speed 6.5 on a FastPrep-24 (MP Biomedicals, Santa Ana, California, USA). RNA was extracted using the Agencourt RNAdvance Tissue Kit (Beckman Coulter, Indianapolis, Indiana, USA) following the manufacturer's instructions.

Two rounds cRNA synthesis starting with 5 ng of total RNA were performed using the MessageAmp II aRNA amplification kit (AM1751) and MessageAmp II-biotin enhanced aRNA amplification kit (AM1791, Life Technologies, Carlsbad, California, USA) according to the manufacturer's instructions. RNA and cRNA were quantified using the Quant-iT RiboGreen RNA Assay Kit (Invitrogen, Carlsbad, California, USA) using a Spectramax M2 (Molecular Devices, Sunnyvale, California, USA). RNA quality assessment was performed using a Bioanalyzer 2100 with RNA 6000 Pico Kit (Agilent Technologies, Santa Clara, California, USA).

cRNA quality assessment was done using a Fragment Analyzer-96 with the Standard Sensitivity RNA Analysis Kit (15-nt) (Advanced Analytical, Technologies, Ankeny, Iowa, USA). Hybridization of 750ng of cRNA on Human HT-12 v4.0 Expression BeadChip (Illumina Inc., San Diego, California, USA), where performed according to the manufacturer's instructions. Scanning of the microarrays was performed on Illumina HiScan (Illumina Inc., San Diego, California, USA).

3D-printing

Design of the capsule cutting-sealing platform was carried out using Solidworks software (2014 version). Printing was done using the ProJet 3500 HDMax (3D systems) 3D printer. VisiJet M3 Crystal and VisiJet S300 (3D systems) served as printing material and support material, respectively. The printed pieces were incubated for 1-2 hours at 56°C in the oven and submerged for 1-2 hours in mineral oil at 56°C with ultrasonic cleaning in order to dissolve and remove the support material. The device was then incubated for 1-2 hours in isopropanol at room temperature with ultrasonic cleaning.

Statistics

After visual inspection and exclusion of microarrays presenting low signal (log2 median expression <5.8) or low variability (standard deviation <0.1), Illumina expression signals were quantile-normalized. We applied a nonspecific filter to discard probes with low average signal and retained 6892 Illumina probes whose mean expression was greater than the third quartile of expression of all of the probes. For differential expression analysis and pathway analyses, genes (represented by probes) were tested for differential expression using the moderated t-statistic as implemented in LIMMA. Gene Set Enrichment Analysis was performed using CAMERA and the hallmark gene set collection from MSigDB. All genome wide statistical analyses were performed using R version 3.3.3 and Bioconductor package LIMMA.

Accession codes

The data discussed in this publication have been deposited in NCBI's Gene Expression Omnibus and are accessible through GEO Series accession number GSE111401 (https://www.ncbi.nlm.nih.gov/geo/query/acc.cgi?acc=GSE111401).

Supplementary Figures

In-vivo Transcriptomic Profiling of Systemic Aging using Stem-Cell Encapsulation

Xiaotong Hong, **Omid Mashinchian**, Christophe Boss, Eugenia Migliavacca, Sylviane Metairon, Frederic Raymond, Patrick Descombes, Nicolas Bouche, Jerome N. Feige and C. Florian Bentzinger

Supplementary Information

Supplementary Figures 1-2

Supplementary Table 1

*****Manuscript under revision (February 2018)

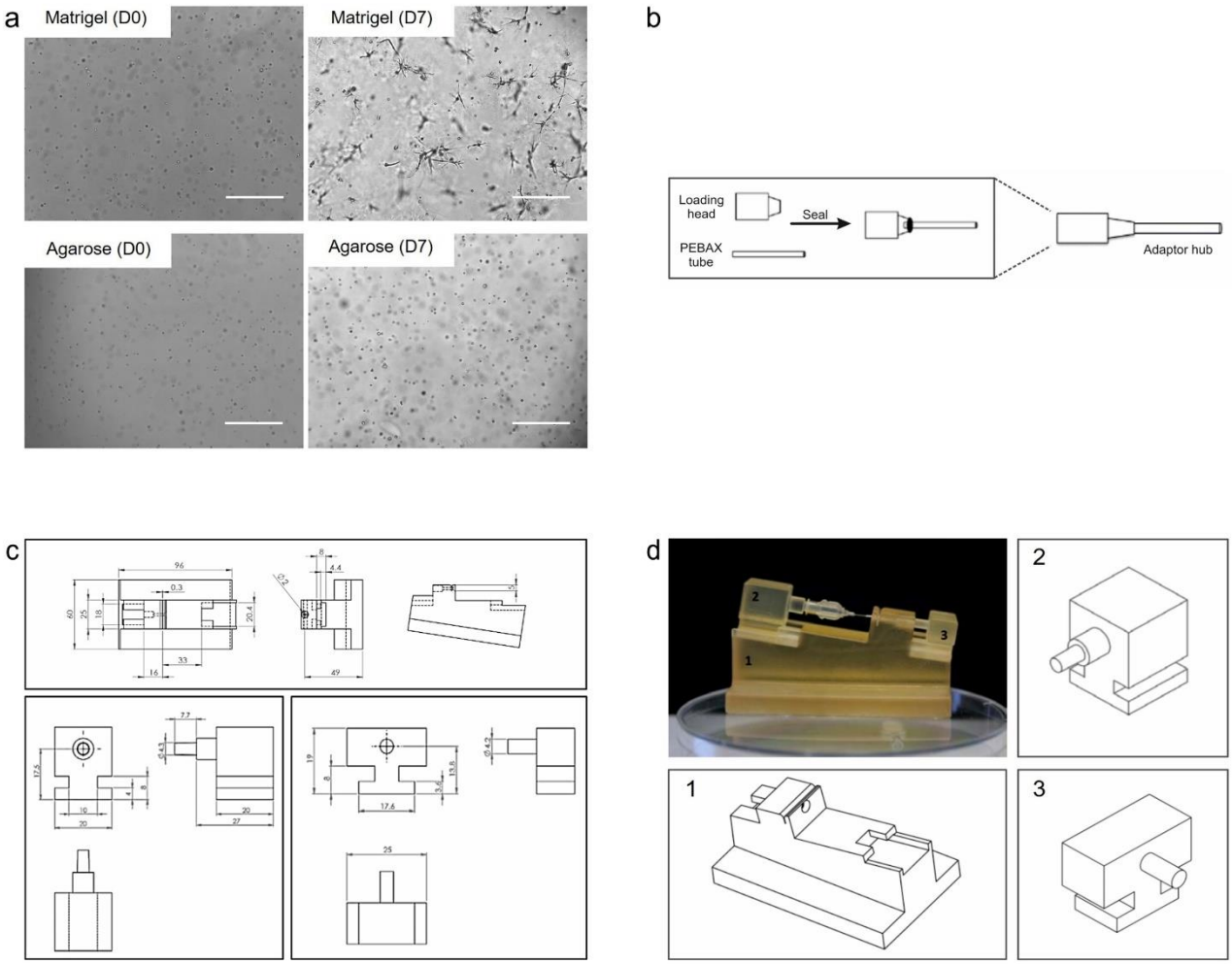

Supplementary figure 1 | (**a**) Light microscopy images revealing the morphology of human myoblasts in agarose or Matrigel at the day of embedding (D0) and after seven days in culture (D7). Scale bars: 250 µm (**b**) Schematic outlining the construction of the adaptor hub used for mounting and loading of the capsules. (**c and d**) Schematic of the parts of the 3D printed capsule cutting and sealing platform. The photograph in the upper left of (d) shows the assembled platform loaded with a capsule mounted to the adaptor hub.

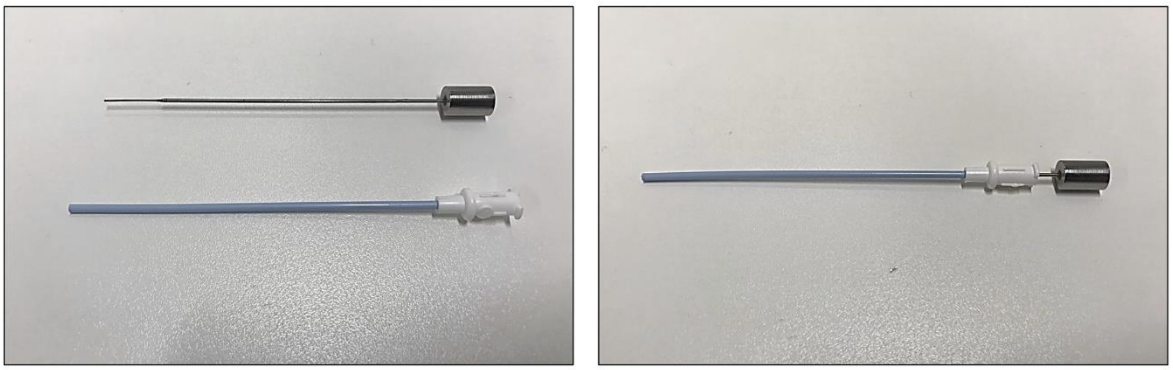

Supplementary figure 2 | The images show the capsule applicator composed of a stiff plastic tube freely sliding over a metal plunger. For implantation the applicator tube was loaded with a capsule on one end and the metal plunger was inserted from the other side. Once pushed into the subcutaneous fascia over the ribcage the plastic tube was withdrawn while the metal part kept the capsule in place.

Hallmark pahtway	Camera, ranks True, NGenes	Direction	PValue	FDR
HALLMARK_MYOGENESIS	99	Down	1.43E-04	7.14E-03
HALLMARK_MYC_TARGETS_V1	138	Up	1.63E-03	3.48E-02
HALLMARK_OXIDATIVE_PHOSPHORYLATION	118	Up	2.09E-03	3.48E-02
HALLMARK_PI3K_AKT_MTOR_SIGNALING	36	Down	4.59E-03	5.74E-02
HALLMARK_IL6_JAK_STAT3_SIGNALING	20	Down	1.28E-02	1.22E-01
HALLMARK_TNFA_SIGNALING_VIA_NFKB	81	Down	1.69E-02	1.22E-01
HALLMARK_INTERFERON_ALPHA_RESPONSE	47	Down	1.71E-02	1.22E-01
HALLMARK_ESTROGEN_RESPONSE_EARLY	65	Down	2.03E-02	1.27E-01
HALLMARK_INTERFERON_GAMMA_RESPONSE	77	Down	3.52E-02	1.82E-01
HALLMARK_NOTCH_SIGNALING	15	Down	3.99E-02	1.82E-01
HALLMARK_KRAS_SIGNALING_DN	29	Down	4.01E-02	1.82E-01
HALLMARK_FATTY_ACID_METABOLISM	66	Up	4.36E-02	1.82E-01
HALLMARK_INFLAMMATORY_RESPONSE	60	Down	5.53E-02	1.99E-01
HALLMARK_MITOTIC_SPINDLE	75	Down	5.57E-02	1.99E-01
HALLMARK_UV_RESPONSE_DN	59	Down	1.03E-01	3.42E-01
HALLMARK_PANCREAS_BETA_CELLS	7	Up	1.23E-01	3.86E-01
HALLMARK_COMPLEMENT	70	Down	1.62E-01	4.60E-01
HALLMARK_ESTROGEN_RESPONSE_LATE	70	Down	1.66E-01	4.60E-01
HALLMARK_APICAL_JUNCTION	98	Down	1.91E-01	5.03E-01
HALLMARK_HEDGEHOG_SIGNALING	9	Down	2.09E-01	5.04E-01
HALLMARK_APICAL_SURFACE	9	Down	2.12E-01	5.04E-01
HALLMARK_UNFOLDED_PROTEIN_RESPONSE	62	Down	2.48E-01	5.63E-01
HALLMARK_WNT_BETA_CATENIN_SIGNALING	19	Down	2.68E-01	5.82E-01
HALLMARK_ALLOGRAFT_REJECTION	60	Down	2.88E-01	5.99E-01
HALLMARK_MTORC1_SIGNALING	119	Down	3.02E-01	6.05E-01
HALLMARK_KRAS_SIGNALING_UP	60	Up	3.33E-01	6.29E-01
HALLMARK_HYPOXIA	112	Down	3.39E-01	6.29E-01
HALLMARK_APOPTOSIS	73	Down	3.57E-01	6.37E-01
HALLMARK_ANGIOGENESIS	20	Up	3.89E-01	6.70E-01
HALLMARK_E2F_TARGETS	64	Up	4.24E-01	6.92E-01
HALLMARK_EPITHELIAL_MESENCHYMAL_TRANSITION	128	Down	4.33E-01	6.92E-01
HALLMARK_UV_RESPONSE_UP	65	Down	4.57E-01	6.92E-01
HALLMARK_ADIPOGENESIS	90	Up	4.57E-01	6.92E-01
HALLMARK_P53_PATHWAY	91	Down	4.92E-01	7.06E-01
HALLMARK_IL2_STAT5_SIGNALING	75	Down	4.94E-01	7.06E-01
HALLMARK_G2M_CHECKPOINT	69	Up	5.17E-01	7.19E-01

HALLMARK_DNA_REPAIR	79	Down	5.32E-01	7.20E-01
HALLMARK_XENOBIOTIC_METABOLISM	69	Up	5.80E-01	7.64E-01
HALLMARK_PROTEIN_SECRETION	48	Up	6.01E-01	7.71E-01
HALLMARK_GLYCOLYSIS	97	Down	6.21E-01	7.76E-01
HALLMARK_SPERMATOGENESIS	20	Up	6.81E-01	8.09E-01
HALLMARK_TGF_BETA_SIGNALING	28	Down	6.89E-01	8.09E-01
HALLMARK_HEME_METABOLISM	69	Down	6.95E-01	8.09E-01
HALLMARK_PEROXISOME	30	Up	8.32E-01	9.29E-01
HALLMARK_CHOLESTEROL_HOMEOSTASIS	34	Up	8.52E-01	9.29E-01
HALLMARK_MYC_TARGETS_V2	30	Down	8.55E-01	9.29E-01
HALLMARK_BILE_ACID_METABOLISM	25	Down	9.02E-01	9.39E-01
HALLMARK_REACTIVE_OXIGEN_SPECIES_PATHWAY	31	Down	9.17E-01	9.39E-01
HALLMARK_COAGULATION	48	Up	9.20E-01	9.39E-01
HALLMARK_ANDROGEN_RESPONSE	42	Down	9.93E-01	9.93E-01

Supplementary table 1 | Hallmark database pathway analysis. FDR = False discovery rate

Relation to GO terms in hierarchical gene expression clusters changed in heterochronic mouse parabiosis	GO Term	Pvalue	FDR
Related to gene expression cluster III	GO_REGULATION_OF_METAL_ION_TRANSPORT	1.4E-03	4%
	GO_RESPONSE_TO_METAL_ION	3.4E-03	8%
	GO_HOMOTYPIC_CELL_CELL_ADHESION	5.6E-03	9%
Related to gene expression cluster IV	GO_REGULATION_OF_VASCULAR_ENDOTHELIAL_ GROWTH_FACTOR_RECEPTOR_SIGNALING_PATHWAY	7.7E-03	11%
Related to gene expression cluster VI	GO_VIRUS_RECEPTOR_ACTIVITY	1.4E-03	4%
	GO_RESPONSE_TO_VIRUS	8.4E-03	12%
	GO_RESPONSE_TO_TYPE_I_INTERFERON	6.6E-03	10%
Related to gene expression cluster VIII	GO_THREONINE_TYPE_PEPTIDASE_ACTIVITY	3.6E-03	8%
Related to gene expression cluster IX	GO_NCRNA_PROCESSING	1.6E-03	5%
	GO_NCRNA_METABOLIC_PROCESS	6.0E-04	3%
	GO_CLEAVAGE_INVOLVED_IN_RRNA_PROCESSING	9.6E-03	13%
	GO_RNA_PROCESSING	1.1E-03	4%
	GO_RESPONSE_TO_STEROL	1.8E-03	5%

Supplementary table 2 | Gene ontology (GO) terms perturbed in human encapsulated cells in the young and aged condition overlapping with those affected in tissues of heterochronic relative to isochronic mouse parabionts (Baruch et al. Science, 2014). FDR = False discovery rate.

Chapter 5:

Aging Disrupts Muscle Stem Cell Function by Impairing Matricellular WISP1 Secretion from Fibro-Adipogenic Progenitors

Background & Rationale:

Progenitor cells reside in the interstitial space between myofibers, and many new progenitor populations been recognized in the last decade. Among them, mesenchymal progenitor cells, known as FAPs [445] have received considerable attention and are recognized as primary mediators of fatty and fibrotic tissue-accumulation [446].

Numerous studies on age-related regenerative-failure of skeletal muscle have focused on the phenotypes of MuSCs. In contrast, the impact of aging on different accessory cells in the stem cell niche remains largely unexplored.

In order to address these questions, we studied the supporting role of FAPs in myogenesis, their cellular cross-talk with MuSCs, and how aging impacts the functional role of FAPs in skeletal muscle regeneration.

In the following chapter, we describe WISP1 as a FAP-derived matricellular signal which is lost during aging and required for efficient muscle regeneration.

Personal contribution:

Optimization of RNA fluorescence *in-situ* hybridization (RNA-FISH) experiment and performing in this project to elucidate where WISP1 is produced in skeletal muscle.

Current status of the project*:

Aging Disrupts Muscle Stem Cell Function by Impairing Matricellular WISP1 Secretion from Fibro-Adipogenic Progenitors. **Cell Stem Cell**. 24: 433-446; 2019

DOI: https://doi.org/10.1016/j.stem.2018.12.014. PMID: 3068676

*__Cell Stem Cell__. 24, 2019. Reprinted with permission from © Elsevier.

Article

Cell Stem Cell

Aging Disrupts Muscle Stem Cell Function by Impairing Matricellular WISP1 Secretion from Fibro-Adipogenic Progenitors

Graphical Abstract

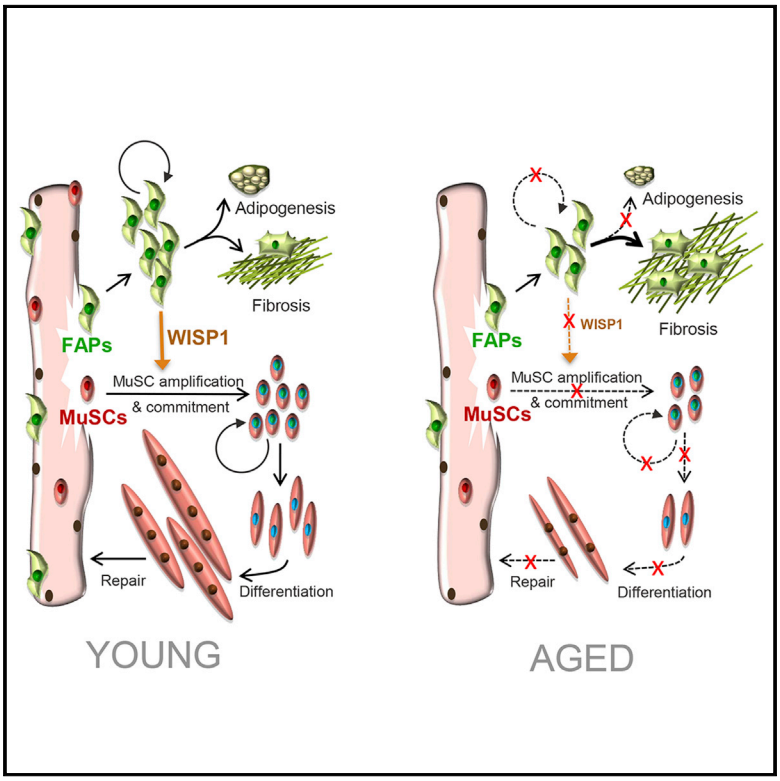

Authors

Laura Lukjanenko, Sonia Karaz, Pascal Stuelsatz, ..., Michael A. Rudnicki, C. Florian Bentzinger, Jerome N. Feige

Correspondence

jerome.feige@rd.nestle.com

In Brief

Feige and colleagues report that aging impairs matricellular signals in the skeletal muscle stem cell niche by affecting the function of fibro-adipogenic progenitors (FAPs). Aged FAPs secrete less matricellular WISP1, leading to impaired myogenic commitment of muscle stem cells (MuSCs). Restoration of WISP1 levels in the aged niche rejuvenates MuSCs and improves muscle regeneration.

Highlights

- Aging alters the myogenic support of FAPs to MuSCs
- Aged FAPs produce less matricellular WISP1
- FAP-derived WISP1 is required for MuSC expansion and commitment
- Restoring WISP1 levels rejuvenates the myogenic potential of aged MuSCs

Lukjanenko et al., 2019, Cell Stem Cell *24*, 433–446
March 7, 2019
https://doi.org/10.1016/j.stem.2018.12.014

CellPress

Cell Stem Cell
Article

Aging Disrupts Muscle Stem Cell Function by Impairing Matricellular WISP1 Secretion from Fibro-Adipogenic Progenitors

Laura Lukjanenko,[1,2,7] Sonia Karaz,[1,7] Pascal Stuelsatz,[1] Uxia Gurriaran-Rodriguez,[3,4] Joris Michaud,[1] Gabriele Dammone,[1] Federico Sizzano,[1] Omid Mashinchian,[1,2] Sara Ancel,[1,2] Eugenia Migliavacca,[1] Sophie Liot,[5] Guillaume Jacot,[1] Sylviane Metairon,[1] Frederic Raymond,[1] Patrick Descombes,[1] Alessio Palini,[1] Benedicte Chazaud,[5] Michael A. Rudnicki,[3,4] C. Florian Bentzinger,[1,6] and Jerome N. Feige[1,2,8,*]

[1]Nestlé Research, EPFL Innovation Park, 1015 Lausanne, Switzerland
[2]School of Life Sciences, Ecole Polytechnique Federale de Lausanne (EPFL), 1015 Lausanne, Switzerland
[3]Sprott Center for Stem Cell Research, Ottawa Hospital Research Institute, Ottawa, ON K1H8L6, Canada
[4]Department of Cellular and Molecular Medicine, Faculty of Medicine, University of Ottawa, Ottawa, ON, Canada
[5]Institut NeuroMyoGène, Université Claude Bernard Lyon 1, CNRS 5310, INSERM U1217, Lyon, France
[6]Département de pharmacologie et physiologie, Faculté de médecine et des sciences de la santé, Université de Sherbrooke, Sherbrooke, QC, Canada
[7]These authors contributed equally
[8]Lead Contact
*Correspondence: jerome.feige@rd.nestle.com
https://doi.org/10.1016/j.stem.2018.12.014

SUMMARY

Research on age-related regenerative failure of skeletal muscle has extensively focused on the phenotypes of muscle stem cells (MuSCs). In contrast, the impact of aging on regulatory cells in the MuSC niche remains largely unexplored. Here, we demonstrate that aging impairs the function of mouse fibro-adipogenic progenitors (FAPs) and thereby indirectly affects the myogenic potential of MuSCs. Using transcriptomic profiling, we identify WNT1 Inducible Signaling Pathway Protein 1 (WISP1) as a FAP-derived matricellular signal that is lost during aging. WISP1 is required for efficient muscle regeneration and controls the expansion and asymmetric commitment of MuSCs through Akt signaling. Transplantation of young FAPs or systemic treatment with WISP1 restores the myogenic capacity of MuSCs in aged mice and rescues skeletal muscle regeneration. Our work establishes that loss of WISP1 from FAPs contributes to MuSC dysfunction in aged skeletal muscles and demonstrates that this mechanism can be targeted to rejuvenate myogenesis.

INTRODUCTION

The regenerative capacity of skeletal muscle depends on the activity of tissue-resident muscle stem cells (MuSCs), also termed satellite cells. As a consequence of aging, the regenerative function of MuSCs is dramatically impaired, leading to inefficient muscle repair following injury (Almada and Wagers, 2016; Blau et al., 2015; Brack and Muñoz-Cánoves, 2016). The number of MuSCs decreases in aged muscle (Shefer et al., 2006), and remaining cells display impaired activation, adhesion, migration, proliferation, self-renewal, and differentiation and gradually switch to a senescent phenotype (Lukjanenko et al., 2016; Price et al., 2014; Sousa-Victor et al., 2014; Tierney et al., 2018). Alterations in both cellular signaling pathways and metabolism have been shown to impair MuSC function during aging. Aged MuSCs exhibit increased p38-mitogen-activated protein kinase (MAPK), ERK-MAPK, and JAK-STAT signaling (Bernet et al., 2014; Chakkalakal et al., 2012; Cosgrove et al., 2014; Price et al., 2014; Sousa-Victor et al., 2014), as well as Hoxa9 induction in response to epigenetic stress (Schwörer et al., 2016). In addition, impaired mitochondrial function as well as decreased autophagy perturb the physiology of MuSCs during aging and accelerate their transition toward senescence (García-Prat et al., 2016; Zhang et al., 2016). Importantly, recent studies have begun to elucidate the nature of the extracellular signals, which are disrupted in the niche and mediate some of these long-lasting intrinsic adaptations. For example, alterations in the levels of Fibronectin, Notch ligands, fibroblast growth factor (FGF)-2, Wnt ligand C1q, transforming growth factor β (TGF-β), oxytocin, or apelin have been reported to affect cellular aging pathways and thereby disturb MuSC function (Brack et al., 2007; Carlson et al., 2008; Chakkalakal et al., 2012; Elabd et al., 2014; Lukjanenko et al., 2016; Naito et al., 2012; Price et al., 2014; Vinel et al., 2018; Wang et al., 2015). Yet, in spite of these fundamental advancements in our understanding of the muscle stem cell niche, the cellular origin of extrinsic MuSC regulatory signals that are affected by the aging process remain largely enigmatic.

During adult myogenesis, MuSC function is under the control of a wide range of paracrine signals originating from different cell types in the niche (Mashinchian et al., 2018). The regulatory interplay between MuSCs, immune cells, fibrogenic cells, and adipogenic progenitors has emerged to be of particular complexity (Heredia et al., 2013; Varga et al., 2016; Verma et al., 2018). Reciprocal control of MuSCs and fibroblasts is indispensable for efficient expansion of the MuSC pool and for keeping

interstitial fibrosis in check (Fry et al., 2016; Murphy et al., 2011). Similarly, ablation of lineages with adipogenic potential leads to dysfunctional muscle repair (Liu et al., 2012). Both fibroblast-like cells and adipocytes residing in skeletal muscle are derived from a common bipotent mesenchymal fibro-adipogenic progenitor (FAP) marked by the expression of the platelet-derived growth factor receptor (PDGFR) α (Joe et al., 2010; Liu et al., 2012; Uezumi et al., 2010). Upon muscle injury, FAPs activate, enter a proliferative phase at the same time as MuSCs, and support myogenic commitment (Joe et al., 2010). Altered FAP lineage decisions during regeneration perturb extracellular matrix (ECM) remodeling and impair myogenesis (Fiore et al., 2016; Mozzetta et al., 2013). Permissive changes in the micro-environment of diseased muscle and altered FAP apoptosis in the late phase of regeneration promotes excessive differentiation toward fat or fibrotic tissue (Heredia et al., 2013; Lemos et al., 2015; Uezumi et al., 2010). One of the signals involved in fibrotic fate decisions of FAPs is platelet-derived growth factor (PDGF), which can be dynamically regulated by alternative processing of the *Pdgfra* mRNA in FAPs during muscle regeneration (Mueller et al., 2016). These observations demonstrate that FAPs orchestrate a plethora of processes involved in regenerative myogenesis and highlight the need for a better understanding of the signals controlling MuSC function.

Notably, aging affects mesenchymal progenitors in multiple tissues (Raggi and Berardi, 2012). Similarly, oxidative stress and other senescence-associated processes impair adipogenic progenitors in aged fat tissue (Tchkonia et al., 2010). These observations suggest that FAPs and their support function for myogenesis could also be deregulated by the aging process. Here, we set out to test this hypothesis and demonstrate that FAP activity is severely impaired as a consequence of old age. We describe that aged FAPs fail to support MuSCs due to reduced secretion of the matricellular protein WNT1 Inducible Signaling Pathway Protein 1 (WISP1). FAP-secreted WISP1 controls asymmetric MuSC commitment and activates the Akt pathway. Similar to aging, genetic deletion of WISP1 in mice perturbs the MuSC pool and impairs myogenesis. Conversely, systemic treatment of aged mice with recombinant WISP1, or transplantation of young but not aged or WISP1 knockout FAPs, rescues MuSC function, and rejuvenates the regenerative capacity of aged skeletal muscle. In summary, we demonstrate that the regenerative failure inherent to aged muscle can be ameliorated by targeting matricellular communication between FAPs and MuSCs.

RESULTS

Aging Affects FAP Function

Given the negative impact of aging on mesenchymal stem cells (Raggi and Berardi, 2012) and the pivotal role of FAPs as support cells in the MuSC niche (Joe et al., 2010; Lemos et al., 2015; Uezumi et al., 2010), we first asked whether FAP function is affected during aging. To address this question, we collected FAPs and MuSCs from muscles of 9- to 13-week-old young mice and 20- to 25-month-old pre-geriatric aged mice (Sousa-Victor et al., 2014) using fluorescence-activated cell sorting (FACS; Figure S1A). *Ex vivo* culture of MuSCs confirmed previously described aging defects that included impaired proliferation, reduced upregulation of the myogenic commitment factor MyoD, and inefficient differentiation of aged MuSCs (Figures S1B–S1E). Notably, we observed that aged FAPs also displayed a range of altered cellular phenotypes. In *ex vivo* culture, the number of FAPs isolated from aged mice was reduced, and they incorporated less 5-Ethynyl-2′-deoxyUridine (EdU) compared to young controls (Figures 1A–1C). Immunostaining for PDGFRα revealed lower numbers of FAPs in muscles of aged mice (Figures S1F and S1G). To investigate how aging affects FAP levels during regeneration, we analyzed muscles at different time points after injury. This revealed decreased numbers of aged FAPs at 4 days post-injury (dpi), that failed to be cleared from the tissue at 7 dpi (Figures S1H and S1I). Functional *ex vivo* analysis of aged FAPs demonstrated impaired growth factor induced (Figures 1D and 1E) and spontaneous (Figure S2A) adipogenesis. Clonal analysis of single aged FAPs showed that the capacity for expansion and the number of adipogenic clones are reduced compared to the young condition (Figure S2B). No difference in differentiation was observed between young and aged FAPs once the cells have taken a fate decision and an adipogenic clone had emerged (Figure S2C), indicating that aging affects fate decisions at the progenitor level. The impaired adipogenic potential of aged FAPs was reflected by reduced levels of oil red O positive intramuscular adipocytes at 14 dpi (Figures 1F, 1G, and S2D). This effect was also observed in H&E stainings (Figure S2E) and confirmed by the quantification of perilipin-positive adipocytes in cross-sections of aged muscles at 14 dpi (Figures S2F and S2G). In contrast, fibrogenic FAP differentiation to α-smooth muscle actin and collagenIα1 positive cells was higher in aged FAPs (Figures 1H, 1I, and S2H). In agreement with these findings, masson trichrome staining of muscle cross-sections of young and aged mice showed elevated fibrosis in aged muscle (Figures 1J and 1K). Gene expression profiling of young and aged FAPs isolated from injured muscles at 7 dpi further confirmed this finding and revealed increased mRNA expression of the gene ontology (GO) term "extracellular matrix" (Figures S2I and S2J). Fibrotic and adipogenic fate decisions in FAPs have been recently demonstrated to be mediated by alternative processing of the PDGFRα transcript (Mueller et al., 2016). An intronic variant of PDGFRα coding for a protein isoform with a truncated kinase domain acts as a decoy receptor to inhibit PDGF signaling and inhibit FAP differentiation into fibrotic cells. Interestingly, we observed that the relative amounts of this PDGFRα intronic variant (PDGFRα-In) is reduced after injury in aged muscles as well as in aged FAPs following FACS isolation (Figures 1L and 1M). Collectively, these data demonstrate that the function of aged FAPs is perturbed and that aging uncouples adipogenic from fibrogenic fate decisions at the progenitor level.

Aged FAPs Fail to Support MuSCs

Following injury, FAPs initially expand to support MuSC function (Fiore et al., 2016; Joe et al., 2010; Mozzetta et al., 2013). In order to characterize the cellular cross-talk between FAPs and MuSCs in a system where the age of each cell type can be uncoupled, we isolated MuSCs from tdTomato (Td) mice (Prigge et al., 2013), which constitutively express a nuclear red fluorescent protein (Figure S3A). The cells were then tracked based on the reporter in co-cultures with wild-type (WT) FAPs (Figures 2A and S3B). Aged FAPs displayed a reduced ability to support

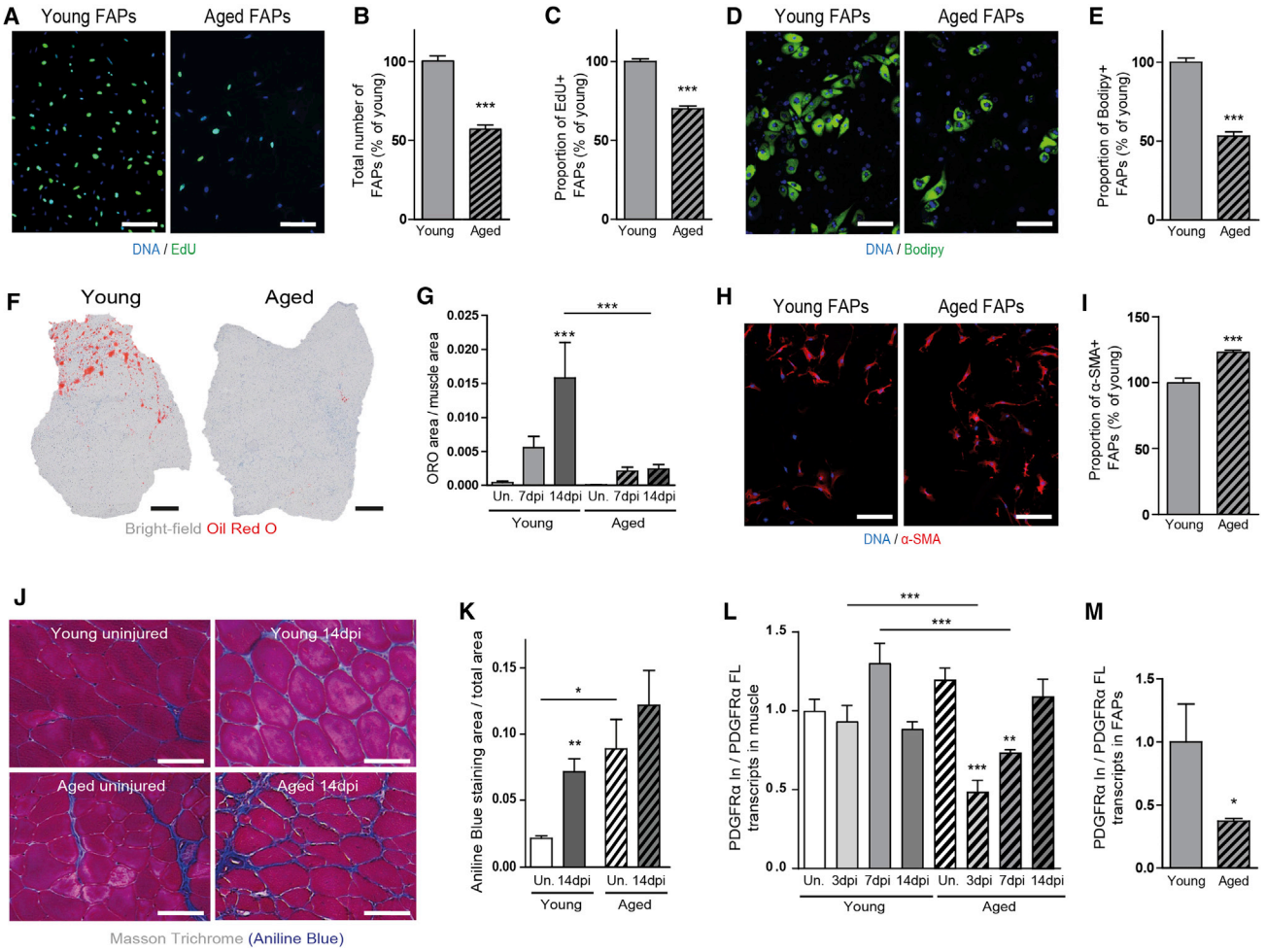

Figure 1. Aging Impairs FAP Function and Uncouples Adipogenic from Fibrogenic Fate Decisions

(A) Representative images of cell numbers and EdU incorporation of FAPs 6 days after isolation from uninjured muscles of young or aged mice. Scale bars, 100 μm.

(B) Quantification of the number of FAPs 6 days after isolation from uninjured muscles of young or aged mice.

(C) Quantification of the percentage of EdU$^+$ FAPs 6 days after isolation from young and aged uninjured muscles.

(D) Representative images of FAPs differentiated under pro-adipogenic conditions 13 days after isolation from uninjured muscles of young or aged mice. Lipid droplets were detected by bodipy staining. Scale bars, 100 μm.

(E) Quantification of the percentage of FAPs differentiated into bodipy$^+$ adipocytes under pro-adipogenic conditions 13 days after isolation from uninjured muscles of young or aged mice.

(F) Representative oil red O staining of muscle cross-sections from young and aged mice 14 days post-injury (dpi). Scale bars, 400 μm.

(G) Quantification of the oil red O covered area normalized to the total cross-sectional area of young and aged muscles under uninjured (Un.) conditions or at 7 and 14 dpi.

(H) Representative α-smooth muscle actin (α-SMA) immunostaining showing spontaneous fibrogenic differentiation of FAPs 6 days after isolation from uninjured muscles of young or aged mice. Scale bars, 100 μm.

(I) Quantification of the percentage of α-SMA$^+$ FAPs 6 days after isolation from uninjured muscles of young or aged mice.

(J) Representative Masson trichrome staining of cross-sections from muscles of young or aged mice under uninjured conditions or at 14 dpi. Fibrotic areas are labeled by the aniline blue component of the staining. Scale bars, 100 μm.

(K) Quantification of the aniline blue$^+$ fibrotic area of the Masson trichrome staining normalized to the total muscle area in cross-sections of young and aged muscles under uninjured conditions or at 14 dpi.

(L) qPCR quantification of the ratio of intronic (In) to full-length (FL) PDGFRα transcripts in young and aged muscle under uninjured conditions or at 3, 7, and 14 dpi.

(M) qPCR quantification of the ratio of In to FL PDGFRα transcripts in FAPs isolated from muscles of young or aged mice at 3 dpi.

In (B), (C), (E), and (I), cells were pooled from up to n = 3 mice and n ≥ 15 replicates per condition, repeated three times for each condition. (G, K, L, and M) n ≥ 6 mice per condition.

In (B), (C), (E), (G), (I), and (K)–(M), data are represented as means ± SEM; *p < 0.05, **p < 0.01, ***p < 0.001 using a Mann-Whitney test when comparing two conditions, and an ANOVA followed by a Bonferroni post hoc test when comparing multiple conditions.

See also Figures S1 and S2.

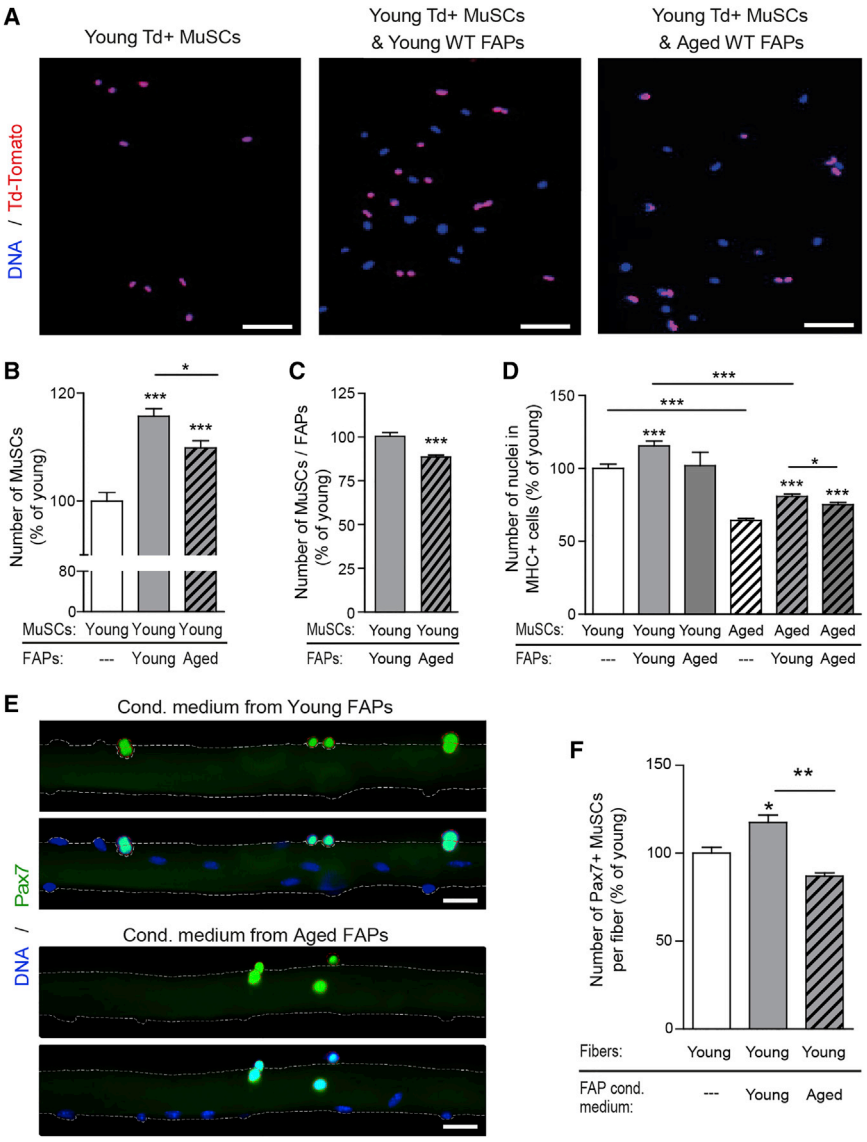

Figure 2. Aged FAPs Fail to Support MuSCs

(A) Representative images of MuSCs from uninjured muscles of young mice with constitutive nuclear TdTomato$^+$ (Td$^+$) expression, cultured alone or together with wild-type (WT) FAPs from uninjured young or aged muscles for 12 h after isolation. Scale bars, 50 μm.

(B) Quantification of the number of Td$^+$ MuSCs from uninjured muscles of young mice cultured alone or together with WT FAPs from young or aged uninjured muscles for 12 h after isolation.

(C) Quantification of the number of Td$^+$ MuSCs from young uninjured muscles relative to WT FAPs from young or aged uninjured muscles co-cultured for 12 h after isolation.

(D) Quantification of the number of nuclei in myosin heavy chain (MHC) positive cells generated by MuSCs from uninjured muscles from young or aged mice, alone or co-cultured with FAPs from young and aged uninjured muscles for 6 days after isolation. Cells pooled from up to n = 3 mice and n ≥ 13 replicates per condition, repeated three times for each condition.

(E) Representative Pax7 immunostaining of single extensor digitorum longus (EDL) myofibers that were cultured for 42 h after isolation from uninjured muscles of young mice with medium conditioned (Cond.) by FAPs isolated from uninjured muscles of young or aged mice. Scale bars, 25 μm.

(F) Quantification of Pax7$^+$ MuSCs on single myofibers that were cultured for 42 h after isolation from uninjured muscles of young mice with control medium or medium conditioned by FAPs isolated from uninjured muscles of young or aged mice. n = 3 mice per condition, n ≥ 30 fibers per mouse.

In (B) and (C), cells were pooled from up to n = 3 mice and n = 24 replicates per condition, repeated three times for each condition.

In (B), (C), (D), and (F), data are represented as means ± SEM; *p < 0.05, **p < 0.01, ***p < 0.001 using a Mann-Whitney test when comparing two conditions, and an ANOVA followed by a Bonferroni post hoc test when comparing multiple conditions.

See also Figure S3.

MuSC expansion and differentiation (Figures 2B–2D). The positive effect of FAPs on MuSC expansion correlated with the amount of FAPs (Figure S3C) and was not due to effects on the viability of MuSCs (Figure S3D). We next tested whether FAPs support MuSCs through soluble factors. Using single myofiber cultures, we demonstrated that the proliferation of MuSCs was increased in the presence of medium conditioned by young FAPs but was unaffected by medium conditioned by aged FAPs (Figures 2E and 2F). FAP conditioned culture medium was also able to promote the proliferation and differentiation of MuSCs *ex vivo* (Figures S3E and S3F). Thus, aging impairs the secretion of a soluble myogenic support signal from FAPs.

WISP1 Is Secreted by Activated FAPs and Is Lost during Aging

To uncover the molecular nature of the FAP-derived MuSC support signal lost during aging, we profiled the transcriptome of FAPs and MuSCs that were isolated in injured and uninjured muscles from young and aged mice. We first analyzed the GO terms enriched in FAPs compared to MuSCs and identified strong signatures of "organ development," "cell adhesion," and "extracellular matrix organization" in FAPs (Table S1). The fibrogenic nature of FAPs was highlighted by the higher expression of genes of the "extracellular matrix" GO term (Figure S4), and aging enhanced both molecular regulators of fibrosis in quiescent FAPs (Table S2) and ECM or fibrosis signatures at 7 dpi (Figures S2I and S2J). We next examined which transcripts coding for secreted proteins were upregulated in activated FAPs. Out of the 321 genes significantly upregulated with a fold change >2 during activation of young FAPs, we identified 20 secreted signaling proteins (Figure 3A). Genes upregulated in activated FAPs were then filtered for differential regulation with age and activation. The resulting 10 transcripts differentially regulated in aged activated FAPs contained a single secreted protein belonging to the Cyr61/CTGF/NOV (CCN) family of matricellular proteins and termed Wnt1 inducible signaling pathway protein 1

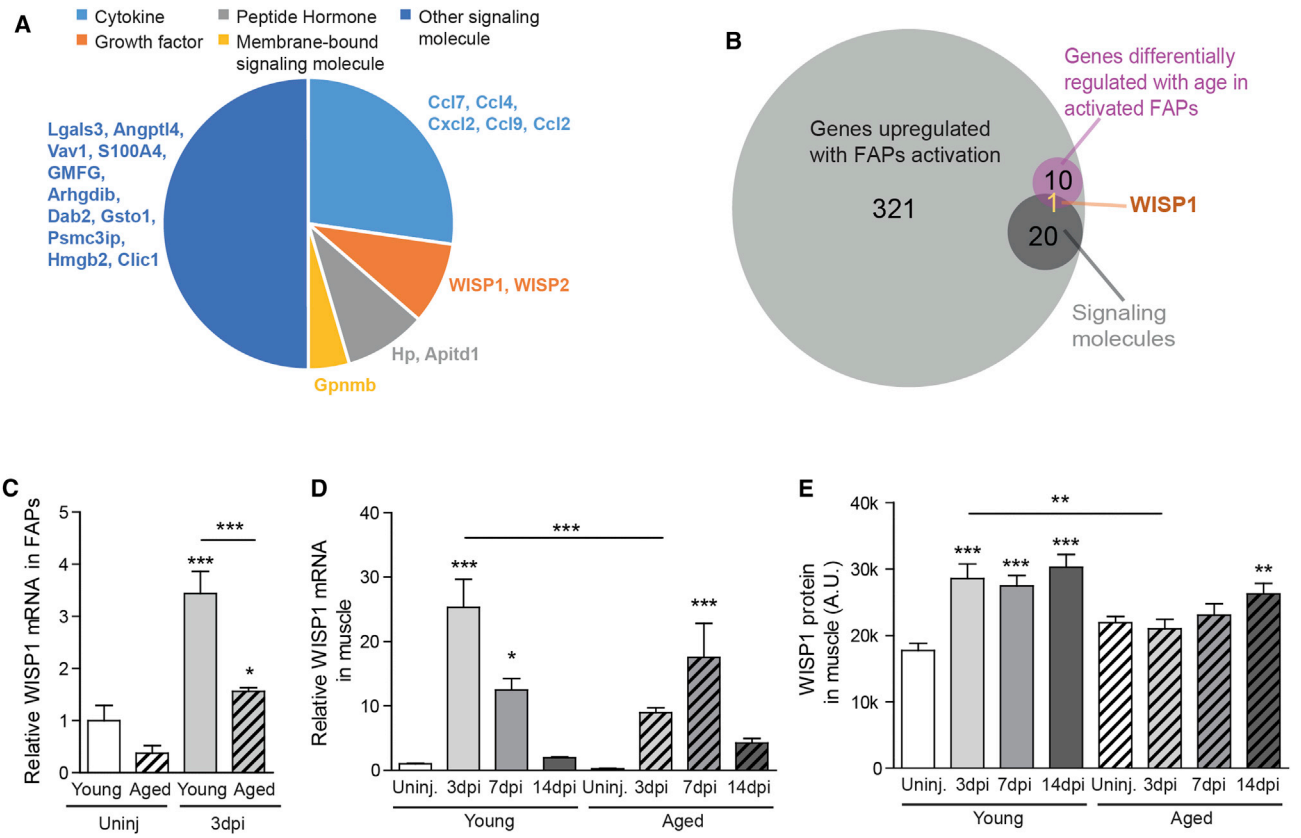

Figure 3. Identification of WISP1 as an Age-Affected Matricellular Factor Secreted by FAPs

(A) Pie chart of transcripts detected by genome-wide profiling that are upregulated in FAPs isolated from young muscles at 3 dpi compared to the uninjured condition and classified as secreted proteins.

(B) Venn diagram of genes induced in FAPs isolated from young muscles at 3 dpi compared to the uninjured condition (light gray), differentially regulated between FAPs isolated from young and aged muscles at 3 dpi (purple), and encoding proteins annotated as "signaling molecules" by the Panther database (dark gray).

(C) WISP1 mRNA levels measured by qPCR in FAPs isolated from young and aged muscles under uninjured conditions or at 3 dpi.

(D) WISP1 mRNA levels measured by qPCR in muscles from young and aged mice under uninjured conditions or at 3, 7, and 14 dpi (n = 8 mice per condition).

(E) WISP1 protein levels in regenerating muscles from young and aged mice under uninjured conditions or at 3, 7, and 14 dpi. n ≥ 5 mice per condition. Arbitrary units (A.U.).

In (A)–(C), n ≥ 5 replicates per condition, with cells pooled from multiple mice for each.

In (C)–(E), data are represented as means ± SEM; *p < 0.05, **p < 0.01, ***p < 0.001 using an ANOVA followed by a Bonferroni post hoc test.

See also Figures S4 and S5.

(WISP1/CCN4) (Figure 3B). WISP1 was also the most downregulated gene when aged activated FAPs were directly compared to young activated FAPs (Table S3). qPCR analysis confirmed that WISP1 is upregulated in young FAPs following muscle injury, and that this induction is blunted more than 2-fold in FAPs from aged mice (Figure 3C). In agreement with these observations, the upregulation of WISP1 mRNA and protein was blunted in regenerating tibialis anterior muscles of aged mice (Figures 3D and 3E).

To confirm that FAPs are the principal cell type in which aging affects WISP1 secretion, we interrogated different cell types found in quiescent and regenerating muscles. These included lineage positive cells (Lin^+), comprising immune, endothelial, and hematopoietic cells, MuSCs, FAPs, and $Sca1^+/CD34^+/PDGFR\alpha^-$ cells (hereafter called $PDGFR\alpha^-$). FAPs, MuSCs, and $PDGFR\alpha^-$ cells upregulated WISP1 expression following injury, while very low expression was observed in Lin^+ cells (Figure S5A). Notably, FAPs were the only cell type that displayed an age-dependent reduction in WISP1 expression. Since WISP1 is a secreted protein, RNA fluorescence in situ hybridization (FISH) was used to elucidate where WISP1 is produced in skeletal muscle. Consistent with the localization of FAPs, we observed an upregulation of WISP1 mRNA granules typical of RNA FISH experiments in the interstitial space of regenerating muscles (Figures S5B and S5C). No staining was detected in muscles of WISP1 knockout ($WISP1^{-/-}$) mice. We also observed that WISP1 mRNA was not directly associated with MuSCs but frequently localized to the vicinity of these cells (Figure S5D). These results identify WISP1 as a FAP-derived MuSC support signal that is impaired during aging.

Loss of WISP1 Impairs MuSC Function and Muscle Regeneration

We next asked whether the loss of WISP1 is sufficient to impair muscle regeneration independently of other age-induced

perturbations by analyzing *WISP1*$^{-/-}$ mice (Maeda et al., 2015). As expected, WISP1 mRNA was not detected in uninjured and regenerating *WISP1*$^{-/-}$ muscle (Figure S6A). We first assessed how loss of WISP1 affects the *ex vivo* phenotype of MuSCs and FAPs. While *WISP1*$^{-/-}$ MuSCs did not display an altered proliferation or differentiation potential (Figures S6B–S6D), FAPs isolated from *WISP1*$^{-/-}$ mice increased in number (Figure S6E). Despite this phenotype, *WISP1*$^{-/-}$ FAPs were not able to support MuSCs as efficiently as WT FAPs (Figure 4A). Following *in vivo* muscle injury, *WISP1*$^{-/-}$ muscles displayed reduced expression levels of myogenic markers such as Pax7, MyoD, and Myogenin (Figures 4B–4D). Histologically, we observed a prominent reduction in committed Pax7^{+}/MyoD^{+} MuSCs in muscle cross-sections of *WISP1*$^{-/-}$ mice at 3 dpi (Figures 4E and 4F). At later stages of regeneration, the architecture of *WISP1*$^{-/-}$ muscles was perturbed and showed abnormally small myofibers (Figures 4G and 4H). In contrast, myofiber size was not affected by loss of WISP1 in uninjured muscle (Figure S6F), demonstrating that WISP1 impairs myofiber repair without promoting atrophy of healthy fibers. In addition, *WISP1*$^{-/-}$ mice displayed similar expression profiles of macrophage, immune, endothelial, and fibroblast markers during regeneration (Figures S6G–S6J), suggesting that loss of WISP1 primarily affects the communication between FAPs and MuSCs. Altogether, these experiments demonstrate that loss of WISP1 from FAPs impairs MuSC function and recapitulates major age-associated phenotypes during skeletal muscle regeneration.

WISP1 Increases MuSC Commitment and Activates the Akt Pathway

Despite its matricellular nature, WISP1 is a soluble protein and can be detected in the systemic circulation (Maiese, 2014; Murahovschi et al., 2015). Addition of recombinant WISP1 to the culture medium increased the expansion and EdU incorporation of young and aged MuSCs *ex vivo* (Figures 5A–5C, S7A, and S7B) and promoted MuSC differentiation (Figure S7C). In contrast, WISP1 treatment did not affect FAP proliferation or myotube hypertrophy (Figures S7D and S7E). In order to interrogate effects on MuSC commitment, WISP1 was added to the medium of cultured single myofibers isolated from Myf5-Cre-ROSA26-YFP reporter mice (Kuang et al., 2007). In this paradigm, WISP1 promoted the generation of committed Pax7^{+}/Myf5^{+} MuSCs by stimulating the asymmetric division of Pax7^{+}/Myf5^{-} cells (Figures 5D and 5E). The Akt pathway has been implicated in asymmetric self-renewal defects of aged MuSCs (Rozo et al., 2016). Interestingly, WISP1 treatment of cultured myoblasts induced the phosphorylation of Akt (Figures 5F, 5G, and S7F). Supporting the notion that WISP1 exerts its effects through the Akt pathway, treatment of freshly isolated MuSCs with an Akt inhibitor abrogated the beneficial effects of WISP1 on MuSC proliferation (Figure 5H). In conclusion, by stimulating pathways involved in proliferation and myogenic commitment, WISP1 positively influences processes altered during MuSC aging.

Transplantation of Young FAPs Rejuvenates Aged MuSCs through WISP1

In order to demonstrate that WISP1 derived from FAPs stimulates MuSC function directly, we transplanted freshly isolated young, aged, or *WISP1*$^{-/-}$ FAPs into regenerating muscles of *WISP1*$^{-/-}$ mice (Figure 6A). Young FAPs increased the number of Pax7^{+}/MyoD^{+} MuSCs, while aged or *WISP1*$^{-/-}$ cells lost this ability (Figures 6B and 6C). Moreover, transplantation of young FAPs, but not aged or *WISP1*$^{-/-}$ FAPs, rescued the abundance of Pax7^{+}/MyoD^{+} MuSCs in aged mice (Figures 6D and 6E). In conclusion, these experiments demonstrate that FAP-derived WISP1 directly stimulates the myogenic commitment of aged MuSCs through paracrine communication.

Systemic WISP1 Treatment Rescues MuSC Function and Regeneration in Aged Mice

We next set out to test whether a restoration of WISP1 levels can ameliorate the impaired regeneration of aged muscles. To this end, mice were treated by systemic injections of either recombinant WISP1 or vehicle during muscle regeneration. mRNA levels of Pax7, MyoD, and Myogenin were significantly higher in WISP1-treated aged mice than in vehicle-treated animals at the myogenic peak of regeneration at 7dpi (Figures 7A–7C). In 3-dpi muscle cross-sections of aged mice treated with WISP1, the number of MuSCs positive for the proliferation marker Ki67 was significantly increased when compared to the vehicle control (Figures 7D and 7E). WISP1 also restored the number of committed MyoD^{+} MuSCs in aged muscle (Figure 7F). Systemic treatment of aged mice with recombinant WISP1 did not alter the induction of macrophage, immune, endothelial, and fibroblast markers during regeneration (Figures S7G–S7K). At later time points of muscle regeneration, systemic WISP1 treatment restored the amount of newly formed embryonic myosin heavy chain positive (eMHC) fibers to the levels observed in the young controls (Figures 7G and 7H). WISP1 treatment also improved the overall architecture of aged regenerating muscles (Figure 7I) and resulted in significantly larger regenerating fibers indicative of more efficient regeneration and terminal myogenesis (Figure 7J). However, systemic WISP1 did not promote muscle growth and anabolism in non-injured muscle as myofiber size was not affected in contra-lateral muscles of aged WISP1-treated mice (Figure S7L). Thus, systemic WISP1 treatment rejuvenates the myogenic function of aged MuSCs and boosts muscle repair.

DISCUSSION

In both mice and humans, aging leads to MuSC dysfunction and reduces the regenerative capacity of skeletal muscle (Almada and Wagers, 2016; Blau et al., 2015; Brack and Muñoz-Cánoves, 2016). Extensive efforts have aimed at understanding the mechanisms driving MuSC aging, which involve cell-autonomous processes and changes in the MuSC microenvironment (Bernet et al., 2014; Chakkalakal et al., 2012; Cosgrove et al., 2014; García-Prat et al., 2016; Mashinchian et al., 2018; Price et al., 2014; Sousa-Victor et al., 2014; Zhang et al., 2016). The MuSC niche is highly complex and contains a flux of different cell types in a tightly controlled spatiotemporal manner. The regulation of MuSCs by local secretion of growth factors, ECM, and the presentation of cell-cell receptors in the niche depends on the function and proliferation kinetics of these niche cell populations. Since aging has been shown to affect several critical niche components, it is likely that the local deposition of these cues by niche-resident cells is particularly susceptible to age-induced

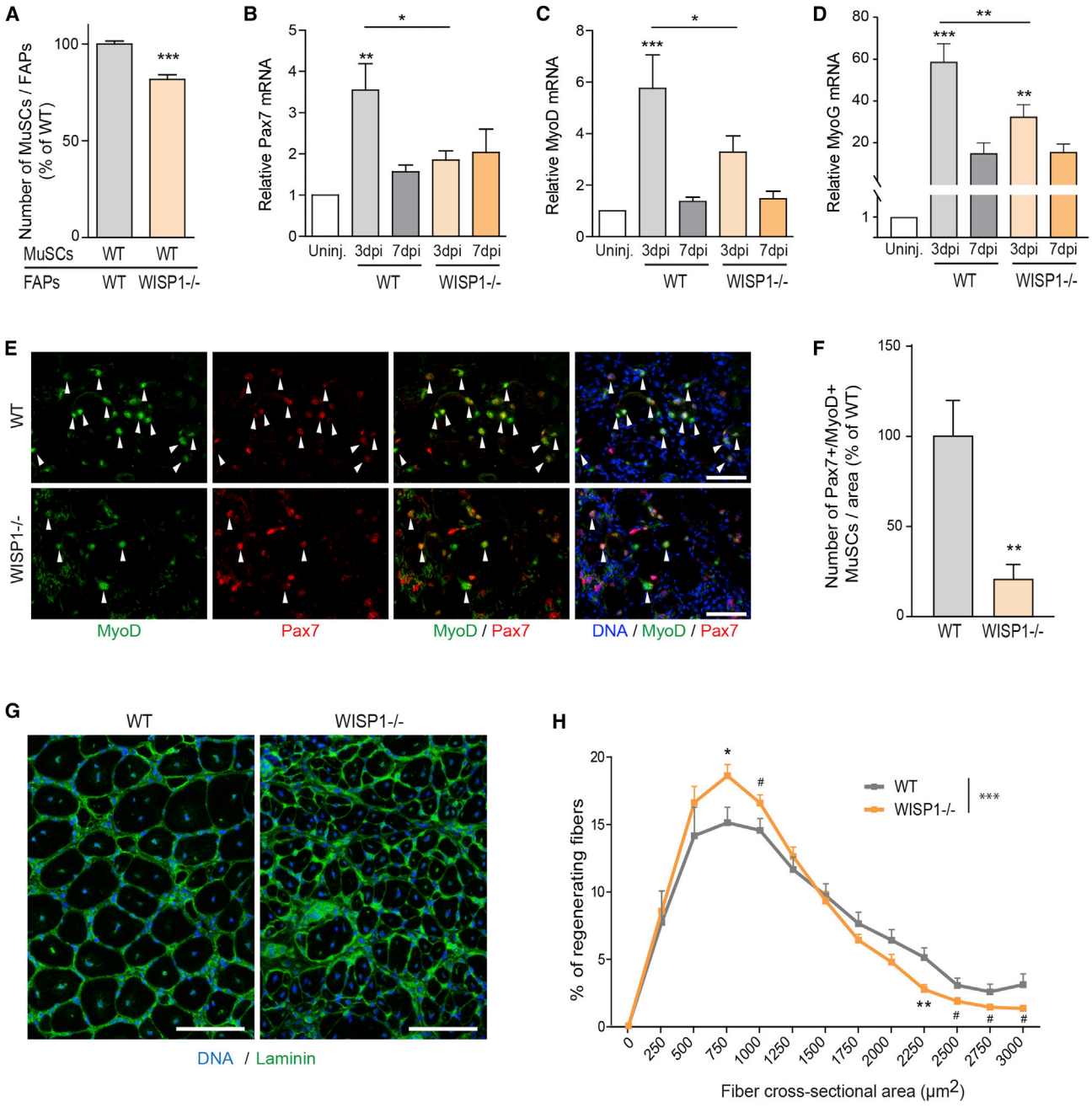

Figure 4. Impaired MuSC Commitment and Muscle Regeneration in WISP1 Knockout Mice

(A) Quantification of the number of Td^+ MuSCs from young uninjured muscles relative to co-cultured FAPs from wild-type (WT) or WISP1 knockout (*WISP1*$^{-/-}$) muscles for 12 h after isolation. n = 24 replicates per condition, repeated twice with cells from different mice for each condition.

(B–D) qPCR quantification of Pax7 (B), MyoD (C), and Myogenin (MyoG; D) mRNA from WT and *WISP1*$^{-/-}$ muscles under uninjured (uninj.) conditions or at 3 and 7 dpi.

(E) Representative Pax7 and MyoD immunostaining of WT and *WISP1*$^{-/-}$ muscle cross-sections at 3 dpi. White arrowheads indicate $Pax7^+$/$MyoD^+$ MuSCs. Scale bar, 100 μm.

(F) Quantification of the number of $Pax7^+$/$MyoD^+$ MuSCs in WT and *WISP1*$^{-/-}$ muscle cross-sections at 3 dpi.

(G) Representative Laminin immunostaining of WT and *WISP1*$^{-/-}$ muscle cross-sections at 14 dpi. Scale bar, 100 μm.

(H) Quantification of the cross-sectional area distribution of regenerating fibers with centralized nuclei in WT and *WISP1*$^{-/-}$ muscles at 14 dpi. (B–D, F, and H) n ≥ 5 mice per condition.

In (A)–(D), (F), and (H), data are represented as means ± SEM; *p < 0.05, **p < 0.01, ***p < 0.001, #p < 0.1 using a Mann-Whitney test when comparing two conditions, and ANOVA followed by a Bonferroni post hoc test when comparing multiple conditions, and a Kolmogorov-Smirnov test to assess fiber cross-sectional area distributions.

See also Figure S6.

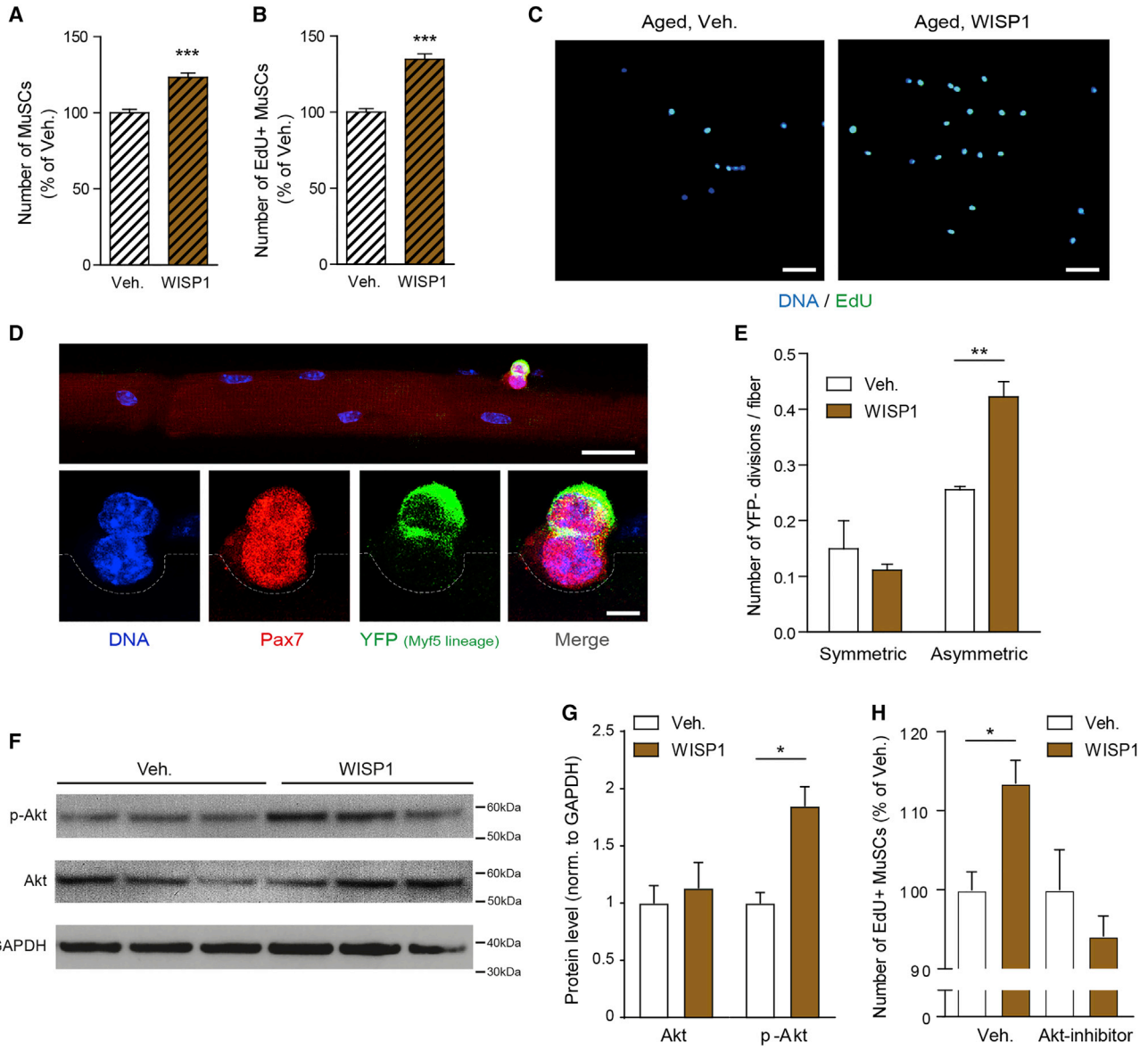

Figure 5. WISP1 Stimulates Asymmetric MuSC Commitment and Activates the Akt Pathway

(A) Quantification of the number of MuSCs cultured for 36 h after isolation from uninj.muscles of aged mice in media containing vehicle (Veh.) or 8 μg/mL WISP1.

(B) Quantification of the number of EdU$^+$ MuSCs cultured for 3 days after isolation from uninjured muscles of aged mice in media containing Veh. or WISP1.

(C) Representative images of EdU$^+$ MuSCs cultured for 3 days after isolation from uninjured muscles of aged mice in media containing Veh. or WISP1. Scale bars, 50 μm.

(D) Pax7 and YFP immunostaining of an asymmetric MuSC division on a single myofiber from a Myf5-Cre/R26R-YFP mouse. Scale bar, 25 μm (top) and 5 μm (bottom).

(E) Quantification of the number of symmetric (YFP$^-$/YFP$^-$) and asymmetric (YFP$^-$/YFP$^+$) divisions per single myofiber cultured in media containing Veh. or WISP1 for 42 h after isolation from adult uninjured EDL muscles of Myf5-Cre/R26R-YFP mice. n = 3 mice per condition, n ≥ 30 fibers analyzed per mouse.

(F and G) Primary myoblasts were treated with either Veh. or WISP1 for 24 h and phospho-Akt (p-Akt) and total Akt protein levels were quantified by western blot (F) and normalized to GAPDH (G). n = 3 replicates per condition.

(H) Quantification of the number of EdU$^+$ MuSCs cultured for 3 days after isolation from uninjured muscle of aged mice with media containing Veh. or WISP1 with or without 0.1 μM of the Akt inhibitor MK-2206.

In (A), (B), and (H), cells were pooled from up to 3 mice and n ≥ 16 replicates per condition, repeated twice for each condition.

In (A), (B), (E), (G), and (H), data are represented as means ± SEM; *p < 0.05, **p < 0.01, ***p < 0.001 using a Mann-Whitney test when comparing two conditions, and an ANOVA followed by a Bonferroni post hoc test when comparing multiple conditions.

See also Figure S7.

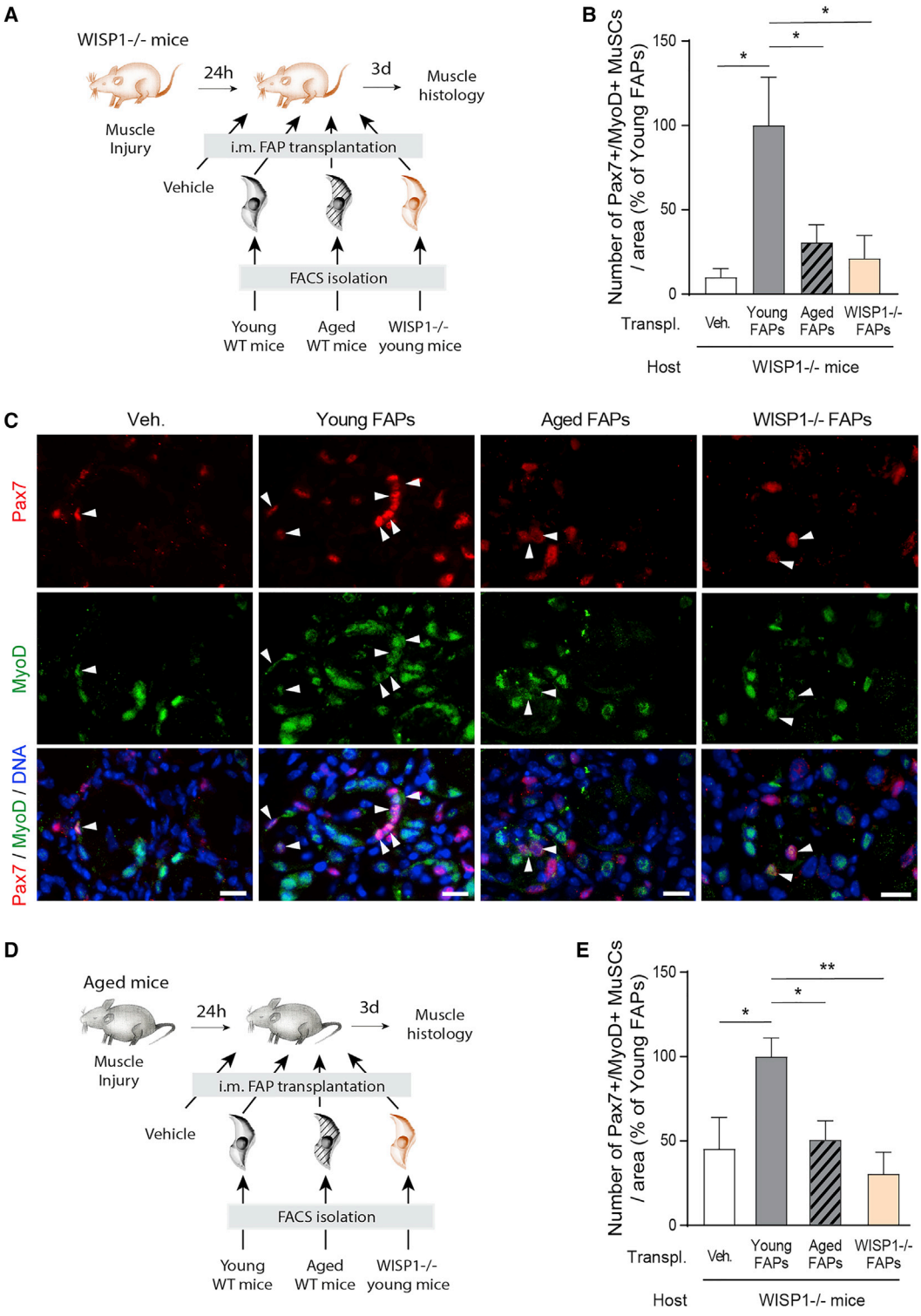

Figure 6. Paracrine WISP1 Secretion from Young FAPs Stimulates the Myogenic Commitment of Aged MuSCs

(A) Experimental overview of the *in vivo* transplantation of FAPs in *WISP1*$^{-/-}$ recipient mice.

(B and C) Quantification (B) and representative images (C) of Pax7^{+}/MyoD^{+} MuSCs by immunofluorescence in muscle cross-sections of *WISP1*$^{-/-}$ mice at 4dpi, after intra-muscular injection of Veh. or FAPs freshly isolated from young, aged, or *WISP1*$^{-/-}$ mice at 1 dpi. n $\geq$ 3 mice per condition.

(D) Experimental overview of the *in vivo* transplantation of FAPs in aged WT recipient mice.

(E) Quantification of the number of Pax7^{+}/MyoD^{+} MuSCs by immunofluorescence in muscle cross-sections of aged WT mice at 4dpi, after intra-muscular injection of Veh. or FAPs freshly isolated from young, aged, or *WISP1*$^{-/-}$ mice at 1 dpi. n $\geq$ 4 mice per condition.

In (B) and (E), data are represented as means ± SEM; *p < 0.05 and **p < 0.01 using an ANOVA followed by a Bonferroni post hoc test.

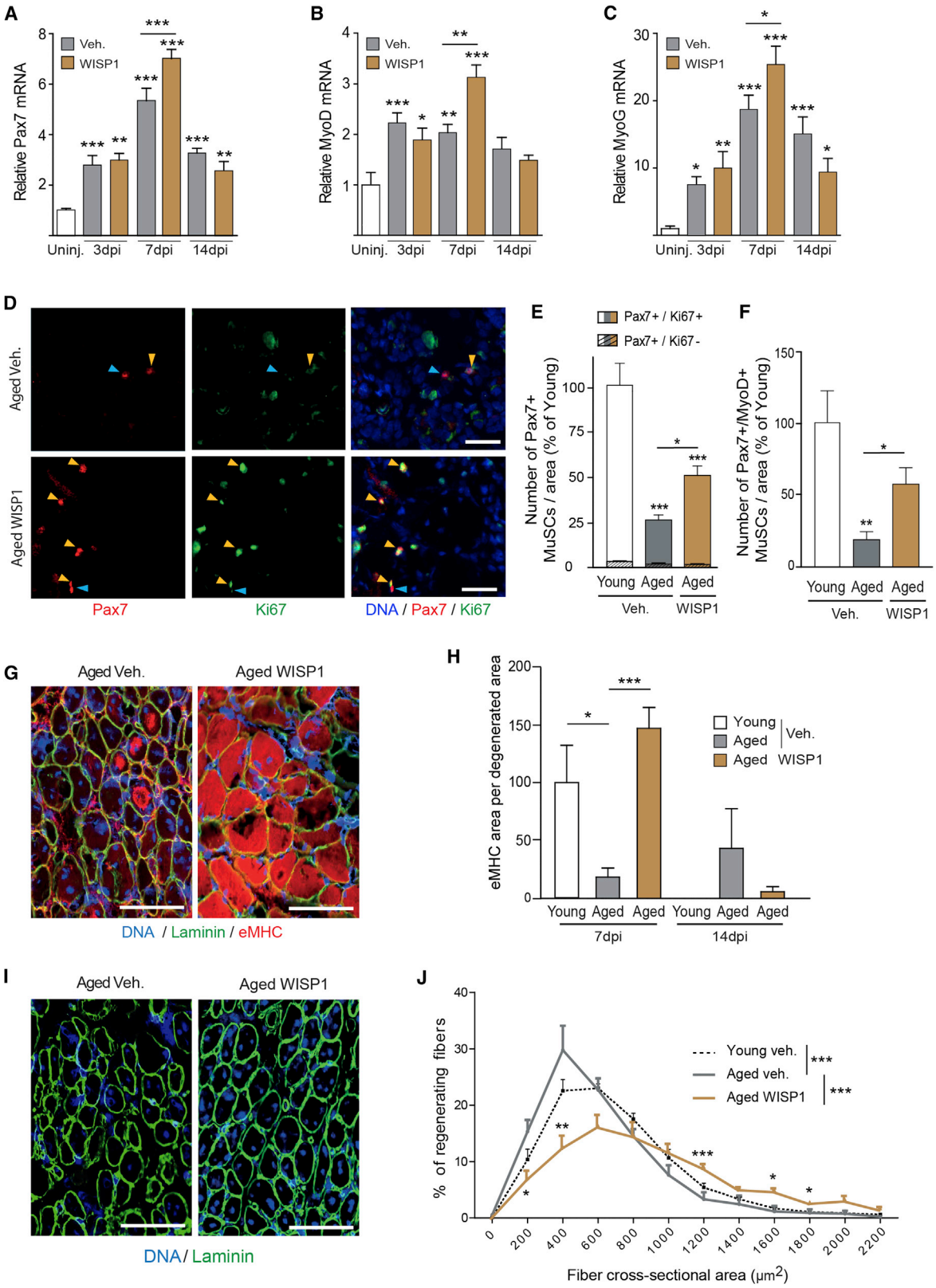

Figure 7. WISP1 Treatment Rejuvenates MuSC Function and Restores Muscle Regeneration

(A–C) qPCR quantification of Pax7 (A), MyoD (B), and MyoG (C) mRNA in muscles of aged mice treated with daily i.p. injection of Veh. or WISP1 at 1 mg/kg under uninjured conditions or at 3, 7, and 14 dpi.

(legend continued on next page)

stress. The identification of cell populations that fail to support MuSC function in aged muscles would allow for the development of targeted strategies to restore a youthful niche environment.

Here, we describe that aging severely perturbs the function of FAPs and their ability to support myogenesis. FAPs are less abundant and have an impaired proliferative capacity in aged muscle but accumulate during the late stages of regeneration when they are normally cleared by apoptosis (Lemos et al., 2015). Using transcriptomic profiling, we identified the matricellular protein WISP1 as a FAP-derived factor controlling MuSC expansion and commitment to myogenic differentiation. Age-induced loss of WISP1 is specific to the FAP population and directly deregulates MuSC function via paracrine signaling. Concomitantly, *WISP1*$^{-/-}$ mice phenocopy age-related defects of MuSC expansion, commitment, and muscle repair. WISP1 is part of the CCN family of matricellular proteins and has previously been involved in ECM remodeling and tissue repair in bone, cartilage, gut and lung epithelium, skin, and the cardiovascular system (Königshoff et al., 2009; Maeda et al., 2015; Maiese, 2014; Ono et al., 2018; Quiros et al., 2017; Wright et al., 2018; Yoshioka et al., 2016). At the cellular level, WISP1 modulates survival and proliferation in a spectrum of biological settings (Maiese, 2014; Ono et al., 2018). CCN proteins possess four conserved functional domains through which they interact with the ECM, growth factors, and cytokines (Maiese, 2014). Apart from their direct effects on cells, CCN proteins modulate the signaling efficiency of several growth factors (Maiese, 2014). These include VEGF and FGF (Lafont et al., 2005; Nishida et al., 2009), that have been shown to regulate MuSC function and muscle regeneration (Chakkalakal et al., 2012; Messina et al., 2007). Interestingly, WISP1 can interact with integrins via their cysteine-rich domains (Maiese, 2014; Ono et al., 2018). Integrin β1 activity is required for normal MuSC function and is deregulated during aging (Rozo et al., 2016). Moreover, CCN proteins can bind to the niche ECM component Fibronectin that is critical for adhesion, survival, and self-renewal of MuSCs and that is lost during regenerative remodeling of the aged stem cell niche (Bentzinger et al., 2013; Lukjanenko et al., 2016). Collectively, these observations suggest that FAP-derived matricellular WISP1 controls MuSC function in concert with growth factor signaling and the niche ECM.

Muscle regeneration associates with a transient ectopic adipocyte accumulation (Joe et al., 2010; Lukjanenko et al., 2013; Uezumi et al., 2010). Falling in line with the general paradigm that intra-muscular adipose tissue increases with advancing age and metabolic stress (Addison et al., 2014), fat infiltration following injury of aged muscle has also been proposed to become more abundant (Ikemoto-Uezumi et al., 2015). However, our data show that young mice with more efficient muscle repair activate stronger ectopic adipogenesis than aged mice. This observation is consistent with the reduced function of FAPs we observed in aged muscles. In line with our observation, aged mesenchymal progenitors from human white adipose tissue lose adipogenic potential (Tchkonia et al., 2010), and aged adipogenic progenitor senescence can be targeted to restore adipogenesis and metabolic homeostasis in adipose tissue (Xu et al., 2015). Interestingly, hind limb unloading after muscle injury impairs muscle regeneration, reduces ectopic adipogenesis, and lowers expression of PDGFRα (Pagano et al., 2015), suggesting that, similar to aging, a deregulation of FAPs can alter muscle plasticity during immobility. Next to adipogenic conversion, the degree of fibrogenic FAP differentiation has also been shown to be of critical importance for normal muscle regeneration (Fiore et al., 2016). We observed that aging increases the fibrogenic signature of FAPs and primes them for fibrosis by reducing expression of the PDGFRα-In anti-fibrotic isoform that acts as a decoy receptor for PDGF (Mueller et al., 2016). Several inflammatory processes have been implicated in fibrosis in skeletal muscle (Mann et al., 2011). Interestingly, the inability of aged FAPs to efficiently attract regulatory T cells through the secretion of IL-33 has recently been described during muscle regeneration (Kuswanto et al., 2016). An important question arising from these observations is whether aging also affects the function of differentiated descendants of FAPs. Our clonal analysis revealed that aged FAPs have a reduced capacity for clonal expansion and fate decisions. However, following lineage commitment, the differentiation efficiency of clones derived from young and aged FAPs was similar. This implies that aging perturbs FAP function at the progenitor level, and thereby leads to a deregulation of MuSC function and a concomitant imbalance of adipogenic and fibrogenic fate decisions that further exacerbates the regenerative dysfunction of aged muscles.

During normal muscle regeneration, MuSCs undergo asymmetric divisions producing cells that upregulate myogenic regulatory factors and become committed to terminal differentiation (Kuang et al., 2007). Lower Fibronectin levels in the aged MuSC niche lead to a loss of Integrin β1 activation and are accompanied by a reduced sensitivity of the integrin associated FGF receptor (Bernet et al., 2014; Cosgrove et al., 2014; Rozo et al., 2016). These changes at the receptor level lead to a dysregulation of Akt, ERK, and p38αβ MAPK pathways that impair the ability of aged MuSCs to undergo asymmetric commitment. Our

(D) Representative immunostainings for Pax7 and Ki67 of cross-sections of Veh. or WISP1-treated aged muscles at 3 dpi. Yellow and blue arrowheads show Pax7^{+}/Ki67^{+} and Pax7^{+}/Ki67^{-} MuSCs, respectively. Scale bars, 50 μm.

(E) Quantification of the number of Pax7^{+}/Ki67^{+} and Pax7^{+}/Ki67^{-} MuSCs in cross-sections of young and Veh. or WISP1-treated aged muscles at 3 dpi.

(F) Quantification of the number of Pax7^{+}/MyoD^{+} MuSCs in cross-sections of young and Veh. or WISP-treated aged muscles at 3 dpi.

(G) Representative Laminin and embryonic myosin heavy chain (eMHC) immunostainings of cross-sections of Veh. or WISP1-treated aged muscles at 7 dpi. Scale bars, 100 μm.

(H) Quantification of the area covered by eMHC positive fibers in sections of young and Veh. or WISP1-treated aged muscles at 7 and 14 dpi.

(I) Representative Laminin immunostainings of cross-sections of Veh. or WISP1-treated aged muscles at 7 dpi. Scale bars, 100 μm.

(J) Quantification of the cross-sectional area distribution of regenerating fibers with centralized nuclei in sections of young and aged Veh. or WISP1-treated muscles at 7 dpi. Inter-class statistics are compared to the aged Veh. group.

In (A)–(C), (E), (F), (H), and (J), $n \geq 4$ mice per condition. Data are represented as means ± SEM; *$p < 0.05$, **$p < 0.01$, ***$p < 0.001$ using an ANOVA followed by a Bonferroni post hoc test when comparing multiple conditions, and a Kolmogorov-Smirnov test to assess fiber cross-sectional area distributions.

See also Figure S7.

experiments revealed that FAP-derived WISP1 activates the Akt pathway and has the ability to rescue age-associated commitment defects of MuSCs via asymmetric division. WISP1 can act through both paracrine production and systemic inter-organ communication (Maiese, 2014). Local paracrine secretion of WISP1 from young FAPs exogenously transplanted in aged muscle rescues commitment defects in aged MuSC, but loss of WISP1 expression in aged or *WISP1*$^{-/-}$ FAPs impairs this cross-talk. Moreover, systemic delivery of recombinant WISP1 in aged mice is able to restore MuSC function and muscle regeneration. Importantly, neither loss of WISP1 in knockout mice, nor WISP1 treatment affected the size of fibers in muscles that were not regenerating. These data demonstrate that the function of FAP-derived WISP1 in skeletal muscle is specific to regenerative myogenesis. In humans and mice, WISP1 contains 367 amino acids and has a comparably low molecular weight of ~40 kDa. In light of our study demonstrating systemic efficacy of WISP1 on MuSC function and regeneration, these favorable properties discern WISP1 as an attractive target for the future development of biologics that promote skeletal muscle repair.

Altogether, we discovered a major age-induced defect in the FAP compartment of skeletal muscle. We characterize WISP1 as a FAP-secreted molecule involved in the regulation of MuSCs that is lost from the aged niche and that can be supplied systemically to rejuvenate muscle healing.

STAR★METHODS

Detailed methods are provided in the online version of this paper and include the following:

- KEY RESOURCE TABLE
- CONTACT FOR REAGENT AND RESOURCE SHARING
- EXPERIMENTAL MODELS
- METHOD DETAILS
  - *In vivo* procedures (muscle regeneration, FAP transplantation & WISP1 treatment)
  - Flow cytometry and progenitor cell isolation
  - Single fiber isolation and effect of FAP-conditioned medium on single fibers
  - *Ex vivo* assays
  - Myoblast culture and western blot
  - Immunocytochemistry and image analysis
  - Quantification of asymmetric MuSC divisions
  - Immunofluorescence and image analysis
  - Masson Trichrome staining
  - RNA fluorescent *in situ* hybridization (RNA-FISH)
  - Transcriptomic analysis
  - Quantitative PCR
  - Protein expression by slow off-rate modified aptamer assay
- QUANTIFICATION AND STATISTICAL ANALYSIS
- DATA AND SOFTWARE AVAILABILITY

SUPPLEMENTAL INFORMATION

Supplemental Information includes seven figures and three tables and can be found with this article online at https://doi.org/10.1016/j.stem.2018.12.014.

ACKNOWLEDGMENTS

We thank Marian Young (National Institute of Dental and Craniofacial Research, NIH, Bethesda) for sharing *WISP1*$^{-/-}$ mice and Edward Schmidt (Montana State University) for advice on the use of TdTomato mice. We are grateful to J. Sanchez (NIHS) for help with mouse husbandry and to the NIHS community for fruitful discussions and support. This work was funded by Nestec. O.M., J.N.F., and C.F.B. are supported by the Fondation Suisse de Recherche sur les Maladies Musculaires (FSRMM). C.F.B. is supported by the Natural Sciences and Engineering Research Council of Canada (NSERC), the Fonds de recherche du Québec - Santé (FRQS), the ThéCell Network (supported by the FRQS), the Canadian Stem Cell Network, the CHUS Foundation, the Banting Research Foundation, and a Research Chair of the Centre de recherche médicale de l'Université de Sherbrooke (CRMUS). M.A.R. holds the Canada Research Chair in Molecular Genetics. The studies from the laboratory of M.A.R. were carried out with support of grants from the U.S. NIH (R01AR044031), the Canadian Institutes of Health Research (FDN-148387), the Muscular Dystrophy Association, and the Stem Cell Network.

AUTHOR CONTRIBUTIONS

L.L. and J.N.F. initiated and managed the project. L.L., S.K., P.S., U.G.-R., J.M., G.D., F.S., O.M., S.A., S.L., and B.C. designed and conducted experiments and analyzed data. E.M. and F.R. performed genomic data analysis. S.M., G.J., A.P., and P.D. supported imaging, flow cytometry, or genomics. M.A.R. provided critical reagents and interpreted the results. L.L., P.S., C.F.B., and J.N.F. interpreted the results and wrote the manuscript.

DECLARATION OF INTERESTS

All authors except U.G.-R., S.L., B.C., and M.A.R. are or were employees of the Nestlé Institute of Health Sciences/Nestec S.A., Switzerland. L.L. and J.N.F. are inventors of patent WO2017207678A1 assigned to Nestec S.A.

Received: December 22, 2016
Revised: October 15, 2018
Accepted: December 17, 2018
Published: January 24, 2019

REFERENCES

Addison, O., Marcus, R.L., Lastayo, P.C., and Ryan, A.S. (2014). Intermuscular fat: A review of the consequences and causes. Int. J. Endocrinol. *2014*, 309570.

Almada, A.E., and Wagers, A.J. (2016). Molecular circuitry of stem cell fate in skeletal muscle regeneration, ageing and disease. Nat. Rev. Mol. Cell Biol. *17*, 267–279.

Bentzinger, C.F., Wang, Y.X., von Maltzahn, J., Soleimani, V.D., Yin, H., and Rudnicki, M.A. (2013). Fibronectin regulates Wnt7a signaling and satellite cell expansion. Cell Stem Cell *12*, 75–87.

Bernet, J.D., Doles, J.D., Hall, J.K., Kelly Tanaka, K., Carter, T.A., and Olwin, B.B. (2014). p38 MAPK signaling underlies a cell-autonomous loss of stem cell self-renewal in skeletal muscle of aged mice. Nat. Med. *20*, 265–271.

Blau, H.M., Cosgrove, B.D., and Ho, A.T. (2015). The central role of muscle stem cells in regenerative failure with aging. Nat. Med. *21*, 854–862.

Brack, A.S., and Muñoz-Cánoves, P. (2016). The ins and outs of muscle stem cell aging. Skelet. Muscle *6*, 1.

Brack, A.S., Conboy, M.J., Roy, S., Lee, M., Kuo, C.J., Keller, C., and Rando, T.A. (2007). Increased Wnt signaling during aging alters muscle stem cell fate and increases fibrosis. Science *317*, 807–810.

Brun, C.E., Wang, Y.X., and Rudnicki, M.A. (2018). Single EDL myofiber isolation for analyses of quiescent and activated muscle stem cells. Methods Mol. Biol. *1686*, 149–159.

Carlson, M.E., Hsu, M., and Conboy, I.M. (2008). Imbalance between pSmad3 and Notch induces CDK inhibitors in old muscle stem cells. Nature *454*, 528–532.

Chakkalakal, J.V., Jones, K.M., Basson, M.A., and Brack, A.S. (2012). The aged niche disrupts muscle stem cell quiescence. Nature *490*, 355–360.

Cosgrove, B.D., Gilbert, P.M., Porpiglia, E., Mourkioti, F., Lee, S.P., Corbel, S.Y., Llewellyn, M.E., Delp, S.L., and Blau, H.M. (2014). Rejuvenation of the muscle stem cell population restores strength to injured aged muscles. Nat. Med. *20*, 255–264.

Elabd, C., Cousin, W., Upadhyayula, P., Chen, R.Y., Chooljian, M.S., Li, J., Kung, S., Jiang, K.P., and Conboy, I.M. (2014). Oxytocin is an age-specific circulating hormone that is necessary for muscle maintenance and regeneration. Nat. Commun. *5*, 4082.

Fiore, D., Judson, R.N., Low, M., Lee, S., Zhang, E., Hopkins, C., Xu, P., Lenzi, A., Rossi, F.M., and Lemos, D.R. (2016). Pharmacological blockage of fibro/adipogenic progenitor expansion and suppression of regenerative fibrogenesis is associated with impaired skeletal muscle regeneration. Stem Cell Res. (Amst.) *17*, 161–169.

Fry, C.S., Kirby, T.J., Kosmac, K., McCarthy, J.J., and Peterson, C.A. (2016). Myogenic progenitor cells control extracellular matrix production by fibroblasts during skeletal muscle hypertrophy. Cell Stem Cell *20*, 56–69.

García-Prat, L., Martínez-Vicente, M., Perdiguero, E., Ortet, L., Rodríguez-Ubreva, J., Rebollo, E., Ruiz-Bonilla, V., Gutarra, S., Ballestar, E., Serrano, A.L., et al. (2016). Autophagy maintains stemness by preventing senescence. Nature *529*, 37–42.

Heredia, J.E., Mukundan, L., Chen, F.M., Mueller, A.A., Deo, R.C., Locksley, R.M., Rando, T.A., and Chawla, A. (2013). Type 2 innate signals stimulate fibro/adipogenic progenitors to facilitate muscle regeneration. Cell *153*, 376–388.

Hulsen, T., de Vlieg, J., and Alkema, W. (2008). BioVenn—A web application for the comparison and visualization of biological lists using area-proportional Venn diagrams. BMC Genomics *9*, 488.

Ikemoto-Uezumi, M., Uezumi, A., Tsuchida, K., Fukada, S., Yamamoto, H., Yamamoto, N., Shiomi, K., and Hashimoto, N. (2015). Pro-insulin-like growth factor-II ameliorates age-related inefficient regenerative response by orchestrating self-reinforcement mechanism of muscle regeneration. Stem Cells *33*, 2456–2468.

Joe, A.W., Yi, L., Natarajan, A., Le Grand, F., So, L., Wang, J., Rudnicki, M.A., and Rossi, F.M. (2010). Muscle injury activates resident fibro/adipogenic progenitors that facilitate myogenesis. Nat. Cell Biol. *12*, 153–163.

Königshoff, M., Kramer, M., Balsara, N., Wilhelm, J., Amarie, O.V., Jahn, A., Rose, F., Fink, L., Seeger, W., Schaefer, L., et al. (2009). WNT1-inducible signaling protein-1 mediates pulmonary fibrosis in mice and is upregulated in humans with idiopathic pulmonary fibrosis. J. Clin. Invest. *119*, 772–787.

Kuang, S., Kuroda, K., Le Grand, F., and Rudnicki, M.A. (2007). Asymmetric self-renewal and commitment of satellite stem cells in muscle. Cell *129*, 999–1010.

Kuswanto, W., Burzyn, D., Panduro, M., Wang, K.K., Jang, Y.C., Wagers, A.J., Benoist, C., and Mathis, D. (2016). Poor repair of skeletal muscle in aging mice reflects a defect in local, interleukin-33-dependent accumulation of regulatory T cells. Immunity *44*, 355–367.

Lafont, J., Thibout, H., Dubois, C., Laurent, M., and Martinerie, C. (2005). NOV/CCN3 induces adhesion of muscle skeletal cells and cooperates with FGF2 and IGF-1 to promote proliferation and survival. Cell Commun. Adhes. *12*, 41–57.

Lemos, D.R., Babaeijandaghi, F., Low, M., Chang, C.K., Lee, S.T., Fiore, D., Zhang, R.H., Natarajan, A., Nedospasov, S.A., and Rossi, F.M. (2015). Nilotinib reduces muscle fibrosis in chronic muscle injury by promoting TNF-mediated apoptosis of fibro/adipogenic progenitors. Nat. Med. *21*, 786–794.

Liu, W., Liu, Y., Lai, X., and Kuang, S. (2012). Intramuscular adipose is derived from a non-Pax3 lineage and required for efficient regeneration of skeletal muscles. Dev. Biol. *361*, 27–38.

Lukjanenko, L., Brachat, S., Pierrel, E., Lach-Trifilieff, E., and Feige, J.N. (2013). Genomic profiling reveals that transient adipogenic activation is a hallmark of mouse models of skeletal muscle regeneration. PLoS ONE *8*, e71084.

Lukjanenko, L., Jung, M.J., Hegde, N., Perruisseau-Carrier, C., Migliavacca, E., Rozo, M., Karaz, S., Jacot, G., Schmidt, M., Li, L., et al. (2016). Loss of fibronectin from the aged stem cell niche affects the regenerative capacity of skeletal muscle in mice. Nat. Med. *22*, 897–905.

Maeda, A., Ono, M., Holmbeck, K., Li, L., Kilts, T.M., Kram, V., Noonan, M.L., Yoshioka, Y., McNerny, E.M., Tantillo, M.A., et al. (2015). WNT1-induced Secreted Protein-1 (WISP1), a novel regulator of bone turnover and Wnt signaling. J. Biol. Chem. *290*, 14004–14018.

Maiese, K. (2014). WISP1: Clinical insights for a proliferative and restorative member of the CCN family. Curr. Neurovasc. Res. *11*, 378–389.

Mann, C.J., Perdiguero, E., Kharraz, Y., Aguilar, S., Pessina, P., Serrano, A.L., and Muñoz-Cánoves, P. (2011). Aberrant repair and fibrosis development in skeletal muscle. Skelet. Muscle *1*, 21.

Mashinchian, O., Pisconti, A., Le Moal, E., and Bentzinger, C.F. (2018). The Muscle Stem Cell Niche in Health and Disease. Curr. Top. Dev. Biol. *126*, 23–65.

Messina, S., Mazzeo, A., Bitto, A., Aguennouz, M., Migliorato, A., De Pasquale, M.G., Minutoli, L., Altavilla, D., Zentilin, L., Giacca, M., et al. (2007). VEGF overexpression via adeno-associated virus gene transfer promotes skeletal muscle regeneration and enhances muscle function in mdx mice. FASEB J. *21*, 3737–3746.

Mozzetta, C., Consalvi, S., Saccone, V., Tierney, M., Diamantini, A., Mitchell, K.J., Marazzi, G., Borsellino, G., Battistini, L., Sassoon, D., et al. (2013). Fibroadipogenic progenitors mediate the ability of HDAC inhibitors to promote regeneration in dystrophic muscles of young, but not old Mdx mice. EMBO Mol. Med. *5*, 626–639.

Mueller, A.A., van Velthoven, C.T., Fukumoto, K.D., Cheung, T.H., and Rando, T.A. (2016). Intronic polyadenylation of PDGFRα in resident stem cells attenuates muscle fibrosis. Nature *540*, 276–279.

Murahovschi, V., Pivovarova, O., Ilkavets, I., Dmitrieva, R.M., Döcke, S., Keyhani-Nejad, F., Gögebakan, Ö., Osterhoff, M., Kemper, M., Hornemann, S., et al. (2015). WISP1 is a novel adipokine linked to inflammation in obesity. Diabetes *64*, 856–866.

Murphy, M.M., Lawson, J.A., Mathew, S.J., Hutcheson, D.A., and Kardon, G. (2011). Satellite cells, connective tissue fibroblasts and their interactions are crucial for muscle regeneration. Development *138*, 3625–3637.

Naito, A.T., Sumida, T., Nomura, S., Liu, M.L., Higo, T., Nakagawa, A., Okada, K., Sakai, T., Hashimoto, A., Hara, Y., et al. (2012). Complement C1q activates canonical Wnt signaling and promotes aging-related phenotypes. Cell *149*, 1298–1313.

Nishida, T., Kondo, S., Maeda, A., Kubota, S., Lyons, K.M., and Takigawa, M. (2009). CCN family 2/connective tissue growth factor (CCN2/CTGF) regulates the expression of Vegf through Hif-1alpha expression in a chondrocytic cell line, HCS-2/8, under hypoxic condition. Bone *44*, 24–31.

Ono, M., Masaki, A., Maeda, A., Kilts, T.M., Hara, E.S., Komori, T., Pham, H., Kuboki, T., and Young, M.F. (2018). CCN4/WISP1 controls cutaneous wound healing by modulating proliferation, migration and ECM expression in dermal fibroblasts via α5β1 and TNFα. Matrix Biol. *68-69*, 533–546.

Pagano, A.F., Demangel, R., Brioche, T., Jublanc, E., Bertrand-Gaday, C., Candau, R., Dechesne, C.A., Dani, C., Bonnieu, A., Py, G., and Chopard, A. (2015). Muscle regeneration with intermuscular adipose tissue (IMAT) accumulation is modulated by mechanical constraints. PLoS ONE *10*, e0144230.

Price, F.D., von Maltzahn, J., Bentzinger, C.F., Dumont, N.A., Yin, H., Chang, N.C., Wilson, D.H., Frenette, J., and Rudnicki, M.A. (2014). Inhibition of JAK-STAT signaling stimulates adult satellite cell function. Nat. Med. *20*, 1174–1181.

Prigge, J.R., Wiley, J.A., Talago, E.A., Young, E.M., Johns, L.L., Kundert, J.A., Sonsteng, K.M., Halford, W.P., Capecchi, M.R., and Schmidt, E.E. (2013). Nuclear double-fluorescent reporter for in vivo and ex vivo analyses of biological transitions in mouse nuclei. Mamm. Genome *24*, 389–399.

Quiros, M., Nishio, H., Neumann, P.A., Siuda, D., Brazil, J.C., Azcutia, V., Hilgarth, R., O'Leary, M.N., Garcia-Hernandez, V., Leoni, G., et al. (2017). Macrophage-derived IL-10 mediates mucosal repair by epithelial WISP-1 signaling. J. Clin. Invest. *127*, 3510–3520.

Raggi, C., and Berardi, A.C. (2012). Mesenchymal stem cells, aging and regenerative medicine. Muscles Ligaments Tendons J. *2*, 239–242.

Rozo, M., Li, L., and Fan, C.M. (2016). Targeting β1-integrin signaling enhances regeneration in aged and dystrophic muscle in mice. Nat. Med. *22*, 889–896.

Schwörer, S., Becker, F., Feller, C., Baig, A.H., Köber, U., Henze, H., Kraus, J.M., Xin, B., Lechel, A., Lipka, D.B., et al. (2016). Epigenetic stress responses induce muscle stem-cell ageing by Hoxa9 developmental signals. Nature *540*, 428–432.

Shefer, G., Van de Mark, D.P., Richardson, J.B., and Yablonka-Reuveni, Z. (2006). Satellite-cell pool size does matter: Defining the myogenic potency of aging skeletal muscle. Dev. Biol. *294*, 50–66.

Sousa-Victor, P., Gutarra, S., García-Prat, L., Rodriguez-Ubreva, J., Ortet, L., Ruiz-Bonilla, V., Jardí, M., Ballestar, E., González, S., Serrano, A.L., et al. (2014). Geriatric muscle stem cells switch reversible quiescence into senescence. Nature *506*, 316–321.

Tallquist, M.D., Weismann, K.E., Hellström, M., and Soriano, P. (2000). Early myotome specification regulates PDGFA expression and axial skeleton development. Development *127*, 5059–5070.

Tchkonia, T., Morbeck, D.E., Von Zglinicki, T., Van Deursen, J., Lustgarten, J., Scrable, H., Khosla, S., Jensen, M.D., and Kirkland, J.L. (2010). Fat tissue, aging, and cellular senescence. Aging Cell *9*, 667–684.

Tierney, M.T., Stec, M.J., Rulands, S., Simons, B.D., and Sacco, A. (2018). Muscle stem cells exhibit distinct clonal dynamics in response to tissue repair and homeostatic aging. Cell Stem Cell *22*, 119–127.

Uezumi, A., Fukada, S., Yamamoto, N., Takeda, S., and Tsuchida, K. (2010). Mesenchymal progenitors distinct from satellite cells contribute to ectopic fat cell formation in skeletal muscle. Nat. Cell Biol. *12*, 143–152.

Varga, T., Mounier, R., Horvath, A., Cuvellier, S., Dumont, F., Poliska, S., Ardjoune, H., Juban, G., Nagy, L., and Chazaud, B. (2016). Highly dynamic transcriptional signature of distinct macrophage subsets during sterile inflammation, resolution, and tissue repair. J. Immunol. *196*, 4771–4782.

Verma, M., Asakura, Y., Murakonda, B.S.R., Pengo, T., Latroche, C., Chazaud, B., McLoon, L.K., and Asakura, A. (2018). Muscle satellite cell cross-talk with a vascular niche maintains quiescence via VEGF and notch signaling. Cell Stem Cell *23*, 530–543.

Vinel, C., Lukjanenko, L., Batut, A., Deleruyelle, S., Pradère, J.P., Le Gonidec, S., Dortignac, A., Geoffre, N., Pereira, O., Karaz, S., et al. (2018). The exerkine apelin reverses age-associated sarcopenia. Nat. Med. *24*, 1360–1371.

Wang, Y., Wehling-Henricks, M., Samengo, G., and Tidball, J.G. (2015). Increases of M2a macrophages and fibrosis in aging muscle are influenced by bone marrow aging and negatively regulated by muscle-derived nitric oxide. Aging Cell *14*, 678–688.

Wright, L.H., Herr, D.J., Brown, S.S., Kasiganesan, H., and Menick, D.R. (2018). Angiokine Wisp-1 is increased in myocardial infarction and regulates cardiac endothelial signaling. JCI Insight *3*, 3.

Xu, M., Palmer, A.K., Ding, H., Weivoda, M.M., Pirtskhalava, T., White, T.A., Sepe, A., Johnson, K.O., Stout, M.B., Giorgadze, N., et al. (2015). Targeting senescent cells enhances adipogenesis and metabolic function in old age. eLife *4*, e12997.

Yoshioka, Y., Ono, M., Maeda, A., Kilts, T.M., Hara, E.S., Khattab, H., Ueda, J., Aoyama, E., Oohashi, T., Takigawa, M., et al. (2016). CCN4/WISP-1 positively regulates chondrogenesis by controlling TGF-β3 function. Bone *83*, 162–170.

Zhang, H., Ryu, D., Wu, Y., Gariani, K., Wang, X., Luan, P., D'Amico, D., Ropelle, E.R., Lutolf, M.P., Aebersold, R., et al. (2016). NAD^+ repletion improves mitochondrial and stem cell function and enhances life span in mice. Science *352*, 1436–1443.

STAR★METHODS

KEY RESOURCE TABLE

REAGENT or RESOURCE	SOURCE	IDENTIFIER
Antibodies		
CD45	Invitrogen	#MCD4501 or #MCD4528
CD31	Invitrogen	#RM5201 or #RM5228
CD11b	Invitrogen	#RM2801 or #RM2828
CD34	BD Biosciences	#560230 or #560238
Ly-6A–Ly-6E	BD Biosciences	#561021
CD140a	eBioscience	#12–1401–81 or #17–1401–81
Laminin (mouse)	Sigma-Aldrich	#L9393
MyoD	Santa Cruz	#sc-304
MyoD	Abcam	#ab198251
eMHC	DSHB	#F1.652
Perilipin	Sigma-Aldrich	#P1873
Laminin (human)	Lifespan Bioscience	#LC-C96142-100
FAB	Jackson	#115-007-003
Pax7	DHSB	Self-produced and purified from hybridoma
Ki67	Abcam	#ab15580
IgG1-biotin	Jackson ImmunoResearch Laboratories	#115-065-205
Streptavidin Alexa555	Life Technologies / ThermoFisherScientic	#S-21381
α-smooth muscle actin	Sigma-Aldrich	#A5228
Collagen1A1	Abcam	#ab34710
Phospho-Akt (Ser473)	Cell Signaling	#4060
Akt	Cell Signaling	#9272
GAPDH	Cell Signaling	#5174
GFP	Abcam	#ab6556
Laminin (rat monoclonal clone AL-1) – used in Figure S1F	Abcam	#ab78287
PDGFRα (goat polyclonal) – used in Figure S1F	R&D Systems	#AF1062;
anti-goat FITC-conjugated – used in Figure S1F	Jackson ImmunoResearch	#705-095-147
anti-mouse Cy3-conjugated – used in Figure S1F	Jackson ImmunoResearch	#715-165-150
Biological Samples		
Mouse muscle samples (cryopreserved)	This study	See STAR Methods
Mouse muscle histology sections	This study	See STAR Methods
Mouse primary FAPs and MuSCs	This study	See STAR Methods
Chemicals, Peptides, and Recombinant Proteins		
Mouse recombinant WISP1 protein	R&D Systems	#1680-WS
Human recombinant WISP1 protein	Peprotech	#120-18
Cardiotoxin (from Naja pallida)	Latoxan	L8102
Streptavidin Alexa555	Life Technologies / ThermoFisherScientic	#S-21381
Dispase II	Roche	#04942078001
Collagenase B	Roche	#11088815001
Collagenase type I	Worthington Biochemical Corporation	#LS004196
bFGF	Invitrogen	#PMG0035
Bodipy 493/503	Life Technologies / ThermoFisherScientic	#D3922
RIPA lysis and extraction buffer	ThermoFisherScientic	#89901

(*Continued on next page*)

Continued

REAGENT or RESOURCE	SOURCE	IDENTIFIER
BCA protein assay kit	Pierce	N/A
Chick embryo extract (CEE)	Accurate Chemicals	#C3999
Protease and phosphatase inhibitor cocktail	ThermoFisherScientic	#78446
3%–12% Bis-Tris Protein gels	Novex	#BN1003
MK-2206	Selleckchem	#S1078
Gelatin	Sigma	#G1393
Collagen	Sigma	#C7774
Fibronectin	Sigma	#F2006
Matrigel	Corning	#354234
Skeletal Muscle Cell Growth Medium	AmsBio	#SKM-M medium
Fluorescent beads	ThermoFischer	#F8826
Critical Commercial Assays		
Click-iT assay	Molecular Probes	#C1033 or #C10340
RNeasy Micro Kit	QIAGEN	#74004
miRNeasy Mini Kit	QIAGEN	#217004
Quant-iT RiboGreen RNA Assay Kit	Life Technologies / ThermoFisherScientic	#R11490
High Capacity cDNA Reverse Transcription Kit	ABI / ThermoFisherScientic	#4368814
Light Cycler 480 SybR Green I master kit	Roche	#04887352001
HCS LIVE/DEAD® Green Kit	Life Technologies / ThermoFisherScientic	#H10290
Deposited Data		
Transcriptome MuSCs: raw and analyzed data	(Lukjanenko et al., 2016)	Gene Expression Omnibus: GSE81096
Transcriptome FAPs: raw and analyzed data	This paper	Gene Expression Omnibus: GSE92508
Experimental Models: Cell Lines		
Human Skeletal Muscle Cells	Lonza	#LZ-CC-2580
Experimental Models: Organisms/Strains		
Mus musculus C57BL/6JRj	Janvier labs	#SC-CJ (young) or #SA-CJ (aged)
Mus musculus B6;129S6-*Gt(ROSA)26Sor*$^{tm1(CAG-tdTomato*,-EGFP*)Ees}$/J	Jackson Labs	#023035 (Maeda et al., 2015)
Mus musculus B6;129S6/SvEv-(WISP1-PKG-Neo)	Dr. Marian Young	(Maeda et al., 2015)
Mus musculus B6;129S4-Myf5$^{tm3(cre)Sor}$/J	Jackson Labs	#007893
Mus musculus B6.129X1-*Gt(ROSA)26Sor*$^{tm1(EYFP)Cos}$/J	Jackson Labs	#006148
Sequence-Based Reagents		
MouseRef–8_V2 chips	Illumina	#BD-202-0202
Taqman primer for mouse *Ap1m1*	ThermoFisher Scientific	Mm00475912_m1, #4448489
Taqman primer for mouse *Ywhaq*	ThermoFisher Scientific	Mm01231061_g1, #4448489
Taqman primer for mouse *Wisp1*	ThermoFisher Scientific	Mm01200484_m1, #4331182
For SYBR Green qPCR primers	This paper; see Quantitative PCR in the STAR Methods	N/A
Mouse *Wisp-1* ViewRNA ISH Tissue Assay probe	ThermoFisher Scientific	VB1-10640
Software and Algorithms		
VS-ASW FL software measurement tools	Olympus	http://www.olympus-lifescience.com/en/microscopes/virtual/vs120/
LAS AF software	Leica	https://www.leica-microsystems.com/products/microscope-software/software-for-life-science-research/las-x-powerful-and-flexible/
MetaXpress software	Molecular Devices	N/A
R and Bioconductor packages	https://cran.r-project.org/bin/windows/base/old/3.1.3/	R version 3.1.3
GraphPad Prism Software	GraphPad	N/A

CONTACT FOR REAGENT AND RESOURCE SHARING

Further information and requests for resources and reagents should be directed to and will be fulfilled by Dr. Jerome N. Feige (jerome.feige@rd.nestle.com).

EXPERIMENTAL MODELS

Mice were housed under standard conditions and allowed access to food and water *ad libitum*. All wild-type (WT) mice were C57BL/6JRj males purchased at the relevant age from Janvier labs. Young male mice were between 9-13 weeks old and aged male mice were 20-25 months. Heterozygous ROSA-nTnG (B6;129S6-Gt(ROSA)26Sortm4(CAG-tdTomato*,-EGFP*)Ees/J), hereafter called TdTomato mice were purchased from Jackson Labs and crossed onto a pure C57BL/6J genetic background to obtain homozygous mice used for isolation of MuSCs bearing a nuclear TdTomato fluorescent marker (Prigge et al., 2013). Heterozygous WISP1 (+/−) mice (B6; 129S6/SvEv-(WISP1-PKG-Neo)) were provided by Dr Marian Young (Maeda et al., 2015) and rederived by in vitro fertiliztaion of C57Bl/6N oocyte from *WISP1*$^{+/-}$ sperm straws. Heterozygous mice (95% pure) were then crossed together to obtain WISP1−/− mice and their WISP1+/+ littermate controls. Male adult Myf5-Cre/ROSA26-YFP mice (8 weeks of age) were obtained by crossing the knock-in Myf5-Cre (Tallquist et al., 2000) heterozygous mice with ROSA26-YFP homozygous reporter mice. Experiments with these latter mice were performed at the University of Ottawa, and all experimental procedures were approved by the University of Ottawa according to guidelines of the Canadian Council for Animal Care (CCAC). All other *in vivo* experiments were performed following the regulations of the Swiss Animal Experimentation Ordinance and approved by the ethical committee of the canton de Vaud under licenses VD2620, VD3002 and VD3199.

METHOD DETAILS

In vivo procedures (muscle regeneration, FAP transplantation & WISP1 treatment)

Muscle regeneration was induced by intramuscular injection of 50 μL of 50% v/v glycerol into tibialis anterior (TA) muscles (experiments with WT mice) or 50 μL of cardiotoxin 10 μM (experiments with *WISP1*$^{-/-}$ mice, *in vivo* FAP quantification or FAP transplantation), and mice were sacrificed 3, 4, 7 or 14 days post-injury (dpi). For isolation of muscle activated progenitors used for transcriptomics, tibialis anterior, quadriceps and gastrocnemius muscles were intramuscularly injected to maximize the number of cells collected, with 50 μl, 50 μL and 100 μL of 50% v/v glycerol, respectively. For *in vivo* WISP1 treatment, mouse recombinant WISP1 protein (R&D # 1680-WS) was administered daily by intra-peritoneal injections at 1mg/kg per day during the course of muscle regeneration after injury. Young and aged control mice received an equivalent volume of PBS using the same dosing scheme. For *in vivo* FAP transplantation, FAPs were freshly isolated from uninjured muscles by flow cytometry and directly transplanted into regenerating tibialis anterior muscles by intra-muscular injection. 60'000 FAPs per mouse were co-injected with 0.02% w/v of fluorescent beads to label the injection site. Injections were performed using a 50 μL Hamilton syringe 24h after intra-muscular injection of 50 μL of cardiotoxin 10 μM.

Flow cytometry and progenitor cell isolation

For isolation of cell populations, tibialis anterior, quadriceps and gastrocnemius muscles were collected uninjured or 3 days after glycerol injection and digested with Dispase II (2.5 U/ml) (Roche), Collagenase B (0.2%) (Roche) and MgCl2 (5 mM) at 37°C. Cells were then incubated at 4°C for 30 min with antibodies against CD45 (Invitrogen, MCD4501 or MCD4528; dilution for both 1/25), CD31 (Invitrogen, RM5201 or RM5228; dilution for both 1/25), CD11b (Invitrogen, RM2801 or RM2828; dilution for both 1/25), CD34 (BD Biosciences, 560230 or 560238; dilution for both 1/60), Ly-6A–Ly-6E (Sca1) (BD Biosciences, 561021; dilution 1/150), α7-integrin (R&D, FAB3518N; dilution 1/30) and CD140a (eBioscience, 12–1401–81 or 17–1401–81; dilution for both 1/30). Antibody validation is provided on the manufacturer's website. Specific cell subsets were isolated with a Beckman Coulter Astrios Cell sorter as described below and represented in supplementary Figures S1 and S3A. MuSCs were identified as CD31$^-$/CD11b$^-$/CD45$^-$/Sca1$^-$/CD34$^+$/Integrin α7$^+$ and Fibro/Adipogenic progenitors (FAPs) were identified as CD31$^-$/CD11b$^-$/CD45$^-$/Sca1$^+$/CD34$^+$/PDGFRα$^+$. Lineage positive cells (Lin+) were identified as: CD31$^+$/CD11b$^+$/CD45$^+$. CD31$^-$/CD11b$^-$/CD45$^-$/Sca1$^+$/CD34$^+$/PDGFRα$^-$ cells were also collected and named PDGFRα$^-$ cells.

Single fiber isolation and effect of FAP-conditioned medium on single fibers

Single myofibers were isolated and cultured *ex vivo* from the EDL muscles as previously described (Brun et al., 2018). Briefly, EDL muscles were harvested intact from tendon to tendon and enzymatically digested for 1h at 37C° with collagenase I (Worthington). Afterward, single myofibers were manually separated and cultured in suspension in FAP-conditioned medium in 12-well plates, previously coated with horse serum to prevent fiber attachment. FAP-conditioned medium was prepared from young and aged FAPs isolated as described above,and cultured in fresh myofiber medium (15% FBS and 1% chick embryo extract (Accurate Chemicals)) in DMEM containing 2% L-glutamine, 4,5% glucose, and 110mg/ml sodium pyruvate at a density of 85000 FAPs/ml, for 24h before the medium was harvested to be used for single myofiber cultures. After 42h in culture, myofibers were then fixed with PFA 2%/PBS 1X for 10min at room temperature and then washed 3 times in PBS for 5min. Later myofibers were permeabilized for 10min with 0.1% Triton X-100, 0.1M Glycine in PBS 1X and followed by blocking solution for 2h at room temperature with 5% horse serum,

2% BSA, 0.1% Triton X-100 in PBS 1X. Incubation with undiluted Pax7 primary antibody (DHSB) was performed overnight. The following day, myofibers were washed 3 times in PBS for 5min and incubated with anti-mouse IgG1 in PBS for 1h at room temperature. Finally, myofibers were mounted with Mowiol medium containing Hoechst (10μL of Hoechst 1μg/μL). Total counting of Pax7+ and DAPI+ nuclei per myofiber was performed manually using an epifluorescent microscope Zeiss AxioObserver Z1. Digital images were taking using the same microscope.

Ex vivo assays

MuSCs and FAPs were isolated by flow cytometry as described above, and unless otherwise mentioned, were directly plated into gelatin-coated 96 well plates and grown in 20mM glucose DMEM, 20% heat-inactivated FBS, 10% inactivated horse serum, 2.5ng/ml bFGF (Invitrogen), 1% P/S + 1% L-Glutamine, 1% Na-pyruvate (Invitrogen), referred later as "growth medium." MuSC viability was assessed at 12h post isolation using the HCS LIVE/DEAD Green Kit (Life Technologies). To asses MuSC cell cycle entry, 1 μM EdU was added to the medium directly after cell sorting for 36h. To assess MuSC and FAP proliferation, 1 μM EdU was added in the medium the third day after sorting for 3h, and the sixth day after sorting for 5h, respectively. MuSC differentiation was induced after four days of growth, by switching to differentiation medium (20mM glucose DMEM, 5% inactivated horse serum, 1% P/S) for 2 days. To test for adipogenic potential, FAPs were plated into Matrigel-coated 96 well plates and were either let to spontaneously differentiate for 13 days in growth medium, or switched to adipogenic differentiation medium on the sixth day for another seven days (20mM glucose DMEM, 20% heat-inactivated FBS, 1% P/S, 0,25μM dexamethasone, 1μg/ml insulin, 5μM troglitazone, 0.5mM isobutylmethylxanthine). To assess fibrogenic capacity, FAPs were grown for 6 days (α-SMA) or 10 days (Col1a1) in growth medium. For co-cultures, unless stated otherwise, the same number of MuSCs and FAPs/MuSCs were seeded in wells. When conditioned medium was used, all cells were freshly isolated the same day, and transfer of conditioned medium to MuSCs was performed after 1 day, then daily during the entire protocol. For WISP1 *ex vivo* treatment experiments, 8 μg/mL of mouse recombinant WISP1 protein (R&D # 1680-WS) or human recombinant WISP1 protein (Peprotech, # 120-18), or equal amount of vehicle was added in the medium. Medium containing WISP1 or vehicle was changed daily. To avoid batch to batch variation in the efficacy of recombinant WISP1, all new commercial batches were first tested for effects on proliferation of WT MuSC and batches without efficacy were discarded. For Akt-inhibitor experiments, MuSCs were directly plated in growth medium containing 0.1μM of Akt inhibitor (MK-2206, Selleckchem, # S1078) or equal amount of vehicle (DMSO) and 2 hours after plating, 8 μg/mL of human recombinant WISP1 protein (Peprotech, # 120-18) or equal amount of vehicle were added to the medium. The medium was thereafter changed daily using fresh WISP1 and Akt-inhibitor. MuSCs were grown for 3 days and 1 μM EdU was added to the medium 3 hours before fixing the cells. For FAP clonal assay, FAPs were directly plated in Matrigel-coated 96 well plates at 1 cell per well in growth medium and grown for 3 weeks with medium change every 3 days.

Myoblast culture and western blot

Human Skeletal Muscle Cells (Lonza, # LZ-CC-2580) were plated on fibronectin-coated 6 wells plate at a density of 100 000 cells per well. Cells were grown for 48h in Skeletal Muscle Cell Growth Medium (AmsBio, SKM-M medium). Cells were treated with WISP1 by adding 8 μg/mL of human recombinant WISP1 protein (Peprotech, # 120-18) in medium that was exchanged daily. Proteins were extracted in RIPA lysis and extraction buffer (Thermofisher, #89901) supplemented with protease and phosphatase inhibitor cocktail (ThermoFisher, #78446). Protein concentration was determined by a BCA assay (Pierce), and samples were diluted at 1.3 ug/mL and boiled 5 min in Laemmli buffer. Samples were run on 4%–12% Bis-Tris Protein gels (Novex, # BN1003) and then transferred using the wet system from Life Technologies. Antibodies used were phospho-Akt (Ser473) Antibody (Cell Signaling, #4060, 1/1000), Akt Antibody (Cell Signaling, #9272, 1/1000) and GAPDH (Cell Signaling, #5174, 1/1000).

Immunocytochemistry and image analysis

EdU incorporation was revealed using the Click-iT assay (Molecular Probes) according to manufacturer's instruction. Briefly, cells were fixed during 15 minutes in 4% PFA, permeabilized during 20 minutes in PBTX 0.5%, stained with the Click-iT reaction mix and counterstained with DAPI. For MyHC staining, cells were fixed during 10 minutes in 4% PFA, permeabilized using cold EtOH/MetOH (v/v) during 5 min, incubated during 1h with the primary antibody anti-MHC 1/200 (Millipore clone A4.1025) in PBS, 1% Horse Serum at room temperature, and incubated during 30min with the secondary antibody Alexa488 anti-mouse IgG diluted at 1/1000 (Life Tech. A-10680) and Hoeschst 33342 in PBS, 1% Horse Serum at room temperature. For Pax7 and MyoD immunostaining, cells were blocked for 1–2 h in 5% goat serum, 1% BSA and 0.2% PBTX, before incubation with primary mouse anti-mouse Pax7 (DHSB, purified, 2.5 μg/ml), rabbit-anti mouse MyoD antibody (Santa-Cruz #sc-304, 1/100) and secondary antibodies. For α-SMA staining used to asses fibrogenic conversion, FAPs were fixed and permeabilized, blocked in PBS, 5% GS, 1% BSA, and incubated with a mouse IgG2a anti-mouse α-smooth muscle actin antibody (#Sigma A5228, 1/150). For collagen1a1 staining, cells were fixed 10min with 4% PFA, permeabilized 10min with PBS 0.5% Triton X-100 and blocked overnight at 4°C in PBS 5% NGS, 1% BSA. The primary Col1a1 antibody and the secondary antibody were successively incubated 2h at room temperature in PBS 5% NGS (Normal Goat Serum), 1% BSA at dilutions of 1/200 and 1/1000, respectively. For adipogenic differentiation, cells were fixed for 10 minutes in PFA 4%, then incubated with Bodipy 493/503 (LifeTechnologies, 1/1000 of the 1mg/ml stock solution of bodipy in ethanol), and counterstained with Hoechst 33342. Image acquisition was performed using the ImageXpress (Molecular Devices) platform. Quantifications were performed with the MetaXpress software using the Multi-Wavelength Cell Scoring or Cell Scoring application modules, or an automated image processing algorithm developed internally.

Quantification of asymmetric MuSC divisions

Single myofibers were isolated and cultured *ex vivo* from the EDL muscles of Myf5-Cre/ROSA26-YFP uninjured mice as described above. Myofibers were cultured for 42h in DMEM media with 15% FBS and 1% chick embryo extract (Accurate Chemicals) and treated with 8 μg/mL of mouse recombinant WISP1 protein or vehicle. After 42h, myofibers were fixed with PFA 2%/PBS 1X for 10min at room temperature and then washed 3 times in PBS for 5 min. Myofibers were then permeabilized for 10min with 0.1% Triton X-100, 0.1M Glycine in PBS 1X and followed by blocking solution for 2h at room temperature with 5% horse serum, 2% BSA, 0.1% Triton X-100 in PBS 1X. Incubation with undiluted anti-Pax7 (DHSB) and anti-GFP (1:1000) primary antibodies was performed overnight. The next day, day myofibers were washed 3 times in PBS for 5 min and incubated with anti-mouse IgG1 and anti-chicken IgG secondary antibodies in PBS for 1h at room temperature. Finally, myofibers were mounted with mounting medium containing Hoechst (10uL of Hoechst 1ug/uL). MuSCs divisions were quantified based on the expression or absence of YFP on Pax7+ doublets ($Pax7^+/YFP^-$-$Pax7^+/YFP^+$ asymmetric or $Pax7^+/YFP^-$-$Pax7^+/YFP^-$ symmetric). Quantifications were done manually using an epifluorescent microscope Zeiss AxioObserver Z1. Digital images were taking using the same microscope.

Immunofluorescence and image analysis

TA muscles were frozen in isopentane cooled with liquid nitrogen, and further sectioned at 10μm using a cryostat. Hematoxylin and Eosin (H&E) staining was performed by placing the dried slides in Harris-hematoxylin during 1min, followed by differentiation in 1% acid-alcohol and washing, and 1min bath in eosine-phloxine (10 g/L). Oil Red O staining was performed on air-dried slides by incubating them in 50% ethanol during 30min, followed by 15min incubation in 2.5g/L oil red O solution in 70% ethanol, 1 min washing in 50% ethanol then water; and slides were counterstained with Mayer's hematoxylin. For laminin-eMHC immunostaining, cryosections were allowed to dry for 10 minutes and blocked for 45 minutes at room temperature in blocking solution (PBS, 4% BSA, 1% FBS). Cryosections were stained for 3 hours at room temperature using monoclonal anti-laminin antibody produced in rabbit (Sigma-Aldrich #L9393) and anti-eMHC produced in mouse (DSHB, #F1.652) diluted at 1/100 and 1/500 in the blocking solution, respectively. For perilipin staining, sections were fixed during 10 minutes with PFA 4%, permeabilized during 10 minutes in PBTX 0,5%, blocked in PBS, 4% Goat-serum. A rabbit polyclonal anti-mouse perilipin antibody (Sigma #P1873) and a chicken polyclonal anti-human laminin antibody (Lifespan Bioscience #LC-C96142-100) were then incubated on the sections during 3h at room temperature, diluted 1/300 and 1/200 in the blocking solution, respectively. Slides were then incubated during 1 hour at room temperature with secondary antibodies and counterstained with Hoechst 33342. For Pax7, MyoD and Ki67 stainings, slides were fixed with PFA 4%, and permeabilized in cold methanol. Antigen retrieval was performed with two successive incubations of hot citric acid 0.01M pH 6 during 10min, and sections were further blocked in PBS, 4% BSA during 3h, followed by 30 minutes blocking with a goat-anti-mouse FAB diluted 1/50 (Jackson #115-007-003). Mouse anti-mouse Pax7 (DHSB, purified), rabbit-anti mouse MyoD antibody (Santa-Cruz #sc-304 or Abcam # ab198251), rabbit-anti mouse Ki67 (Abcam #ab15580) and chicken anti-human laminin (Lifespan Bioscience #LC-C96142-100) antibodies were used at 2.5 μg/ml, 1/100, 1/100 and 1/200 in blocking solution, respectively. Pax7 signal was further amplified using a goat-anti mouse IgG1-biotin (1/1000, Jackson ImmunoResearch #115-065-205) followed by a Streptavidin Alexa555 (1/2000) (Life Tech. S-21381) treatment, together with other secondary antibodies and Hoechst counterstain. Stained tissues were imaged using an Olympus VS120 slide scanner or a Leica DMI 4000B microscope and analyzed either using the VS-ASW FL software measurement tools or the LAS AF software. The number of Pax7, MyoD and Ki67 positive cells was determined manually by counting of immunostainings in muscle sections in random areas of the injured region, and the area covered by eMHC-positive fibers and degenerated area was determined manually across the entire sections. For FAP transplantation experiments, the quantification of Pax7 and MyoD immunostainings was restricted to the regenerating regions surrounding the sites of injection identified by the fluorescent beads (ThermoFischer #F8826). The size of myofibers with centralized nuclei was calculated from laminin/DAPI stainings on all fibers of the section, and Oil Red O positive structures segmentation and area determination were performed across the entire sections, using an automated image processing algorithm developed internally using the MetaXpress software (Molecular Devices). For FAP staining, 8 μm cryosections were labeled with antibodies against PDGFRα overnight at 4°C and Laminin counter-staining was performed for 2h at 37°C. Secondary antibodies were coupled to FITC and Cy3. Images were recorded with a DMI 6000 Leica microscope connected to a Coolsnap camera at 20X magnification. For each condition of each experiment, at least 8-10 fields chosen randomly were counted. The number of labeled $PDGFR\alpha^+$ cells was calculated using the cell tracker tool in ImageJ.

Masson Trichrome staining

Frozen sections were dried and fixed 1h with 4% PFA and then incubated overnight in Bouin solution. Slides were rinsed in water for 1min and stained in Weigert solution for 5 min. Slides were successively dipped in water for 1 min, 1% HCl diluted in 100% Ethanol for 3 s, again for 10 min in water and in 1% acetic acid for 1 min. Slides were then stained in 1% Biebrich scarlet-acid fuchsin solution for 5 min. Slides were successively incubated in 1% acetic acid for 2 min, 5% phosphomolybdic-phosphotungstic acid solution for 10min and in 1% acetic acid for 2 min. Slides were stained in 3% Aniline blue for 5 min and differentiated in 1% acetic acid for 2min. Finally, slides were dehydrated in Ethanol 100% for 2 min and cleared in Xylene for 2 min before being mounted with Eukitt mounting medium.

RNA fluorescent *in situ* hybridization (RNA-FISH)

Frozen muscle samples were sectioned using a cryo-microtome (Leica-1850 UV) and *Wisp1*-mRNA expression in muscle cross sections was analyzed using the ViewRNA ISH Tissue Assay Kit and Fast red substrate following the manufacturer's instructions

(ThermoFisher Scientific, USA). Wisp1 was detected using the VIEWRNA type-1 probe-set for *Mus musculus Wisp-1* (VB1-10640) and nuclei were detected with DAPI. Images were acquired using an Olympus-VS120 slide scanner. Image overlay with Pax7 was performed by merging the RNA FISH and Pax7 immunofluorescence on adjacent serial sections and overlapping morphological structures and selected DAPI-positive nuclei.

Transcriptomic analysis

RNA was extracted from freshly sorted MuSCs and FAPs using the RNeasy Micro Kit (QIAGEN). RNA samples were quality controlled and then subjected to 3′ microarray analysis on Illumina MouseRef–8_V2 chips. 3ng of total RNA were used to produce cRNA in a two-round amplification protocol, using first Messageamp II aRNA amplification kit (AM1751, Life Technologies, Inc.) followed by Messageamp II–biotin enhanced aRNA amplification kit (AM1791, Life Technologies, Inc.). 750ng of cRNA were hybridized for 16h at 55°C on Illumina MouseRef–8 v2 microarrays. Quality of total RNA was checked by using the Bioanalyzer 2100 with Total RNA Pico kit, and quality of cRNA was checked by using the Bioanalyzer 2100 with the Total RNA Nano kit (Agilent Technologies). Quantifications were done using the Quant-iT RiboGreen RNA Assay Kit (Life Technologies, Inc.). Illumina expression signals were quantile-normalized. We applied a nonspecific filter to discard probes with low variability and retained 12,848 Illumina probe whose standard deviation was greater than the median of the s.d. of all of the probe. For differential expression analysis and pathway analyses, genes (represented by probes) were tested for differential expression using the moderated t-statistic as implemented in LIMMA44 for both datasets. Venn diagrams where built from differentially expressed genes (https://www.cmbi.ru.nl/cdd/biovenn/index.php)(Hulsen et al., 2008). We used the Pantherdb platform to identify protein classes (signaling molecules) within lists of differentially expressed genes (http://pantherdb.org/).

Quantitative PCR

RNA was extracted from frozen muscles or freshly sorted cells using miRNeasy Mini Kit or RNeasy Micro Kit (QIAGEN), respectively. RNA samples were subjected to reverse transcription using random primers (High Capacity cDNA Reverse Transcription Kit, ABI). Quantitative PCR on full muscle was performed using the SYBR Green I master kit (Roche) on a LightCycler 480. Reference genes (ATP5b, EIF2a and PSMB4) were selected based on their stability across time points of regeneration from micro-array data. Quantification of PDGFRα variants both in full muscles and freshly isolated FAPs were performed using the SYBR Green method, and primers amplifying the intronic variant number 16 were designed as previously described (PDGFRα In) (Mueller et al., 2016). Other qPCR reactions performed using SYBR assays were performed with the following primers (5′-3′): ATP5b forward: ACCTCGGTGCAGGCTATCTA; ATP5b reverse: AATAGCCCGGGACAACACAG; CD11b forward: GCCTGTGAAGTACGCCATCT; CD11b reverse: GCCCAGGTTGTTGAACTGGT; CD11c forward: ACACTGAGTGATGCCACTGT; CD11c reverse: TTCGGAGGT CACCTAGTTGGG; CD31 forward: CACACCGAGAGCTACGTCAT; CD31 reverse: TTGGATACGCCATGCACCTT; EIF2a forward: CACGGTGCTTCCCAGAGAAT; EIF2a reverse: TGCAGTAGTCCCTTGTTAGCG; F4/80 forward: CTCTTCTGGGGCTTCAGTGG; F4/80 reverse: TGTCAGTGCAGGTGGCATAA; PSMB4 forward: GCGAGTCAACGACAGCACTA; PSMB4 reverse: TCATCAATCAC CATCTGGCCG; Pax7 forward: AAGTTCGGGAAGAAAGAGGACGAC; Pax7 reverse: GAGGTCGGGTTCTGATTCCACATC; MyoD forward: GCAGATGCACCACCAGAGTC; MyoD reverse: GCACCTGATAAATCGCATTGG; Myog forward: GTGCCCAGTGAATG CAACTC; Myog reverse: CGCGAGCAAATGATCTCCTG; PDGFRα In forward: AAAAGTGCCCATGCTCATTC; PDGFRα In reverse: GCTTGGCAGAGCTACCTGTC; PDGFRα FL forward: AGTGGCTACATCATCCCCCT; PDGFRα FL reverse: CCGAAGTCTGT GAGCTGTGT; TCF4 forward: GGCGATGAGAACCTGCAAGA; TCF4 reverse: GGTCCTCATCATCGTTATTGCTAGA; WISP1 forward: CAGTGAGCCCAAGAGTCAGG; WISP1 reverse: TCGTCTCTGTCAGCTTGCAC; WISP1 forward (for KO experiment): ATCGCCC GAGGTACGCAATAGG; WISP1 reverse (for KO experiment): CAGCCCACCGTGCCATCAATG; PDGFRα forward: AGTGGCTACAT CATCCCCCT; PDGFRα reverse: CCGAAGTCTGTGAGCTGTGT. Quantitative PCRs on isolated progenitors was performed using Taqman probes (ABI) on a LightCycler 480. Reference genes (Ap1m1 and Ywhaq) were selected based on their stability across cell types and states from micro-array data. Taqman probes used for real-time PCR were mWISP1 (ThermoFisher Scientific, Mm01200484_m1, #4331182), mAp1m1 (ThermoFisher Scientific, Mm00475912_m1, #4448489) and mYwhaq (ThermoFisher Scientific, Mm01231061_g1, #4448489).

Protein expression by slow off-rate modified aptamer assay

Muscle samples were pulverized using the cryoPREP impactor system (Covaris). The muscle powder was then subjected to mechanical lysis using a Polytron homogenizer and proteins were extracted in 50 mM Tris (pH 7.5), 150 mM NaCl, 50 mM NaF, 1 mM EDTA, 0.5% TritonX. Protein concentration was determined by a BCA assay and samples were diluted at 250ug/mL. Protein extracts were analyzed using DNA aptamer-based recognition on the SOMAscan platform (Somalogic, Boulder, CO, USA). Median normalized relative fluorescence units (RFU) were log2 transformed before applying principal component analysis and linear models.

QUANTIFICATION AND STATISTICAL ANALYSIS

All mice were randomized according to body weight before interventions. Sample size determination was based on the expected effect size and variability that was previously observed for similar readouts in the investigators' labs. *In vivo* treatments were not blinded, but imaging readouts were analyzed in a blinded manner. Genome-wide statistical analyses and Kolmogorov–Smirnov tests were performed using R version 3.1.3 and relevant Bioconductor packages. GO terms were tested on genes differentially expressed

in the indicated conditions using a Benjamini-Hochberg adjusted p value < 0.05. Genes upregulated during FAP activation were filtered as: Benjamini-Hochberg adjusted p value < 0.001, Fold-change > 2. Genes differentially upregulated in FAPs during activation with age were filtered as: Benjamini-Hochberg adjusted p value [Activation young] < 0.001, Fold-change [Activation young] > 2; Benjamini-Hochberg adjusted p value [interaction: Activation*Age] < 0.25; Benjamini-Hochberg adjusted p value [aged activated FAPs versus young activated FAPs] < 0.1. All other statistical analyses were performed using GraphPad Prism (GraphPad Software). Statistical significance for binary comparisons was assessed by a Mann-Whitney test. All exploratory and signaling experiments were analyzed by using two-tailed tests. For comparison of more than two groups, one-way or two-way ANOVAs were used, according to the experimental design, and followed by Bonferroni multiple-comparison testing. Comparison of distributions were performed by a Kolmogorov-Smirnov test. All data are expressed as mean + SEM.

DATA AND SOFTWARE AVAILABILITY

The genomics data from this study have been submitted to the NCBI Gene Expression Omnibus (GEO) (https://www.ncbi.nlm.nih.gov/geo) under accession numbers GEO: GSE92508 and GEO: GSE81096. All software used were freely or commercially available.

Cell Stem Cell, Volume *24*

Supplemental Information

Aging Disrupts Muscle Stem Cell Function by Impairing Matricellular WISP1 Secretion from Fibro-Adipogenic Progenitors

Laura Lukjanenko, Sonia Karaz, Pascal Stuelsatz, Uxia Gurriaran-Rodriguez, Joris Michaud, Gabriele Dammone, Federico Sizzano, Omid Mashinchian, Sara Ancel, Eugenia Migliavacca, Sophie Liot, Guillaume Jacot, Sylviane Metairon, Frederic Raymond, Patrick Descombes, Alessio Palini, Benedicte Chazaud, Michael A. Rudnicki, C. Florian Bentzinger, and Jerome N. Feige

Figure S1 (related to figure 1). Effects of aging on MuSCs and FAPs

(A) Fluorescent-Activated Cell Sorting (FACS) isolation of FAPs and MuSCs from skeletal muscles of WT mice. Forward scatter area (FSC-A), forward scatter width (FSC-W), side scatter height (SSC-H), Alexa Fluor 700 (Alexa700), fluorescein isothiocyanate (FITC), phycoerythrin-cyanine 7 (PC7), allophycocyanin (APC), Fluorescence Minus One (FMO) control. CD31+/CD11b+/CD45+ cells are jointly detected using Pacific Blue and referred to as "lineage". (B) Quantification of the percentage of EdU+ MuSCs 36 h after isolation from young and aged uninjured muscles. (C) Quantification of the percentage of Pax7+/MyoD-, Pax7+/MyoD+ and Pax7-/MyoD+ 36 h after isolation from young and aged uninjured muscles. (D) Quantification of the percentage of EdU+ MuSCs 3 d after isolation from young and aged uninjured muscles. (E) Quantification of the number of nuclei in Myosin Heavy Chain (MHC) positive cells 6 d after MuSC isolation from young and aged uninjured muscles. (F) Representative PDGFRα immunostaining in uninjured young and aged muscle cross sections. Scale bar = 50 μm. (G) Quantification of the number of PDGFRα+/DAPI+ FAPs in uninjured young and aged muscle cross sections. n≥10 mice per condition. (H) Representative PDGFRα immunostaining in young and aged muscle cross sections at 7dpi. Scale bar = 50 μm. (I) Quantification of the number of PDGFRα+/DAPI+ FAPs in young and aged muscle cross sections at 4dpi, 7dpi and 28dpi; n≥3 mice at 4dpi, n≥4 mice at 7dpi and n≥8 mice at 28dpi. (B-E) n≥6 replicates per condition, replicated three times with cells from different mice. Data are represented as means ± S.E.M. p-values are *p<0.05, **p<0.01, ***p<0.001 using a Mann-Whitney test when comparing two conditions, and an ANOVA followed by a Bonferroni post hoc test when comparing multiple conditions.

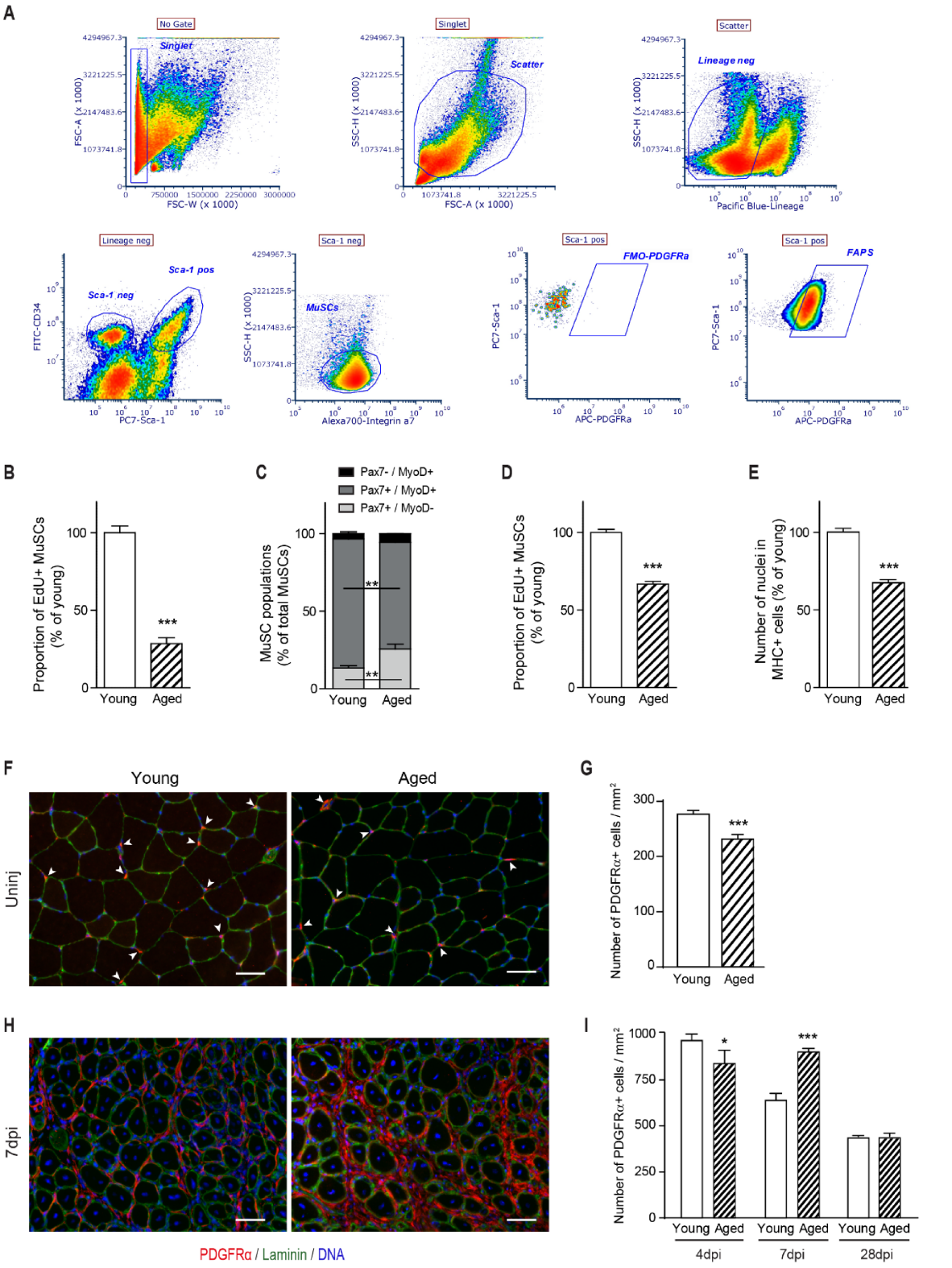
A
No Gate
Singlet
FSC-A (x 1000)
FSC-W (x 1000)
Singlet
Scatter
SSC-H (x 1000)
FSC-A (x 1000)
Scatter
Lineage neg
SSC-H (x 1000)
Pacific Blue-Lineage
Lineage neg
Sca-1 pos
Sca-1 neg
FITC-CD34
PC7-Sca-1
Sca-1 neg
MuSCs
SSC-H (x 1000)
Alexa700-Integrin a7
Sca-1 pos
FMO-PDGFRa
PC7-Sca-1
APC-PDGFRa
Sca-1 pos
FAPS
PC7-Sca-1
APC-PDGFRa
B
Proportion of EdU+ MuSCs (% of young)
Young
Aged
***
C
Pax7- / MyoD+
Pax7+ / MyoD+
Pax7+ / MyoD-
MuSC populations (% of total MuSCs)
Young
Aged
**
**
D
Proportion of EdU+ MuSCs (% of young)
Young
Aged
***
E
Number of nuclei in MHC+ cells (% of young)
Young
Aged
***
F
Young
Aged
Uninj
G
Number of PDGFRα+ cells / mm²
Young
Aged
***
H
7dpi
PDGFRα / Laminin / DNA
I
Number of PDGFRα+ cells / mm²
*
***
Young Aged
Young Aged
Young Aged
4dpi
7dpi
28dpi

Fig. S1

Figure S2 (related to figure 1). Effects of aging on FAP fate

(A) Quantification of the percentage of FAPs spontaneously differentiated into bodipy+ adipocytes in growth medium 13 d after isolation from uninjured muscles of young or aged mice. Cells pooled from up to n=3 mice and n≥12 replicates per condition, repeated three times for each condition. (B) Pie charts showing the clonal efficiency of single FAPs and their spontaneous adipogenic potential quantified by bodipy staining 21 d after isolation from uninjured muscles of young or aged mice. n≥384 cells per condition, isolated from pooled cell isolation of two mice per condition. (C) Proportion of bodipy+ adipogenic cells in adipogenic clones from single FAPs 21 d after isolation from uninjured muscles of young or aged mice. (D) Quantification of the Oil-red O positive area normalized to the total regenerating area containing fibers with centralized nuclei of young and aged muscles at 3, 7 and 14 dpi. (E) Representative hematoxylin/eosin staining of cross sections from muscles of young or aged mice at 14 dpi. Scale bar = 100 μm. (F) Representative Perilipin and Laminin immunostainings of cross-sections from muscles of young or aged mice at 14 dpi. Scale bar = 100 μm. (G) Quantification of the area covered by Perilipin staining in cross-sections from muscles of young or aged mice at 14 dpi. (H) Quantification of the percentage of collagenIα1 (Col1a1) positive FAPs 10 d after isolation from uninjured muscles of young or aged mice. Cells were pooled from n=4 mice and n≥40 replicates per condition. (I) Table of the 10 most significantly regulated GO categories in aged FAPs compared to young FAPs freshly isolated from regenerating muscles at 7dpi. P-values were computed with Fisher statistics. (J) Heatmap of mRNA expression of the GO term “Extracellular matrix” significantly regulated in aged FAPs compared to young FAPs freshly isolated from regenerating muscles at 7dpi. (D and G) Data from n≥6 mice per condition. (I and J) Data from n=3 replicates per condition with cells pooled from 2 mice per replicate. Data are represented as means ± S.E.M. p-values are *p<0.05, **p<0.01, ***p<0.001 using a Mann-Whitney test when comparing two conditions, and an ANOVA followed by a Bonferroni post hoc test when comparing multiple conditions.

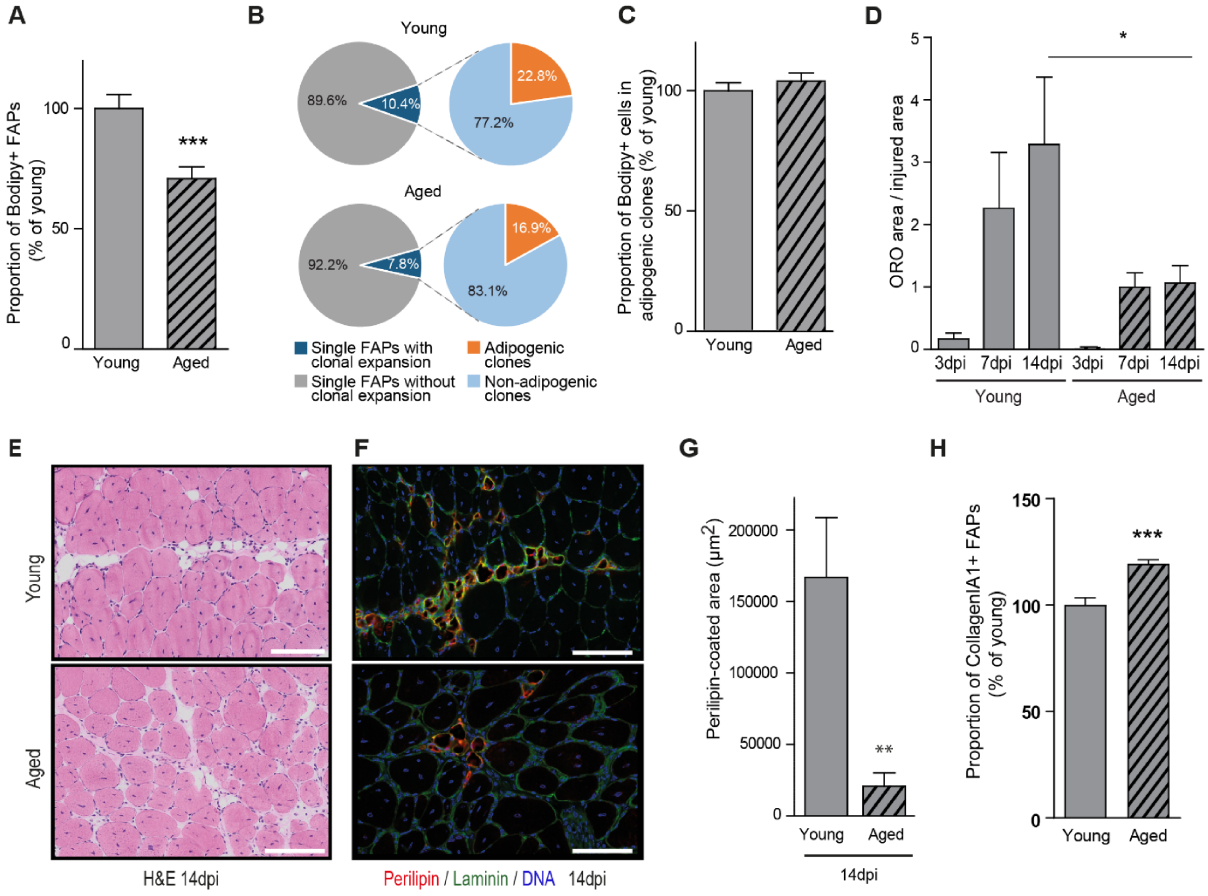

I

Rank	GO ID	GO Term	p-value
1	GO:0005576	extracellular region	1.4E-15
2	GO:0044421	extracellular region part	2.2E-15
3	GO:0005615	extracellular space	1.0E-13
4	GO:0031012	extracellular matrix	6.2E-12
5	GO:0005578	proteinaceous extracellular matrix	2.4E-11
6	GO:0043230	extracellular organelle	4.4E-10
7	GO:0031982	vesicle	8.0E-10
8	GO:1903561	extracellular vesicle	1.2E-09
9	GO:0071944	cell periphery	2.2E-09
10	GO:0070062	extracellular exosome	4.7E-09

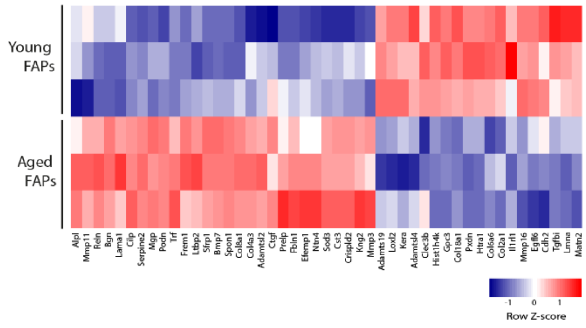

Fig. S2

Figure S3 (related to figure 2). Modulation of MuSC Function by FAPs

(A) FACS strategy for isolation of FAPs and MuSCs from mice constitutively expressing Td-Tomato+. (B) Schematic representation of the study design for testing FAP effects on MuSCs in ex vivo co-culture. Td-Tomato+ (Td+). (C) Quantification of the number EdU+/Td+ MuSCs from uninjured muscles of young mice and cultured for 3 d alone or together with increasing amounts of WT FAPs isolated from young uninjured muscles. (D) Quantification of the number of non-viable Td+ MuSCs incorporating DEAD green dye 12h after isolation from uninjured muscles of young mice and cultured alone or with WT FAPs isolated from young uninjured muscles. (E) Quantification of the number EdU+/Td+ MuSCs from uninjured muscles of young mice cultured for 3 d after isolation in medium conditioned by young FAPs. (F) Quantification of the number of nuclei in Myosin Heavy Chain (MHC) positive cells generated by MuSCs from uninjured muscles from young mice and cultured for 6 d after isolation in control medium or medium conditioned by young FAPs. (C-F) Cells pooled from up to n=5 mice and n≥8 replicates per condition, repeated three times for each condition. Data are represented as means ± S.E.M. p-values are *$p<0.05$, **$p<0.01$, ***$p<0.001$ using a Mann-Whitney test when comparing two conditions, and an ANOVA followed by a Bonferroni post hoc test when comparing multiple conditions.

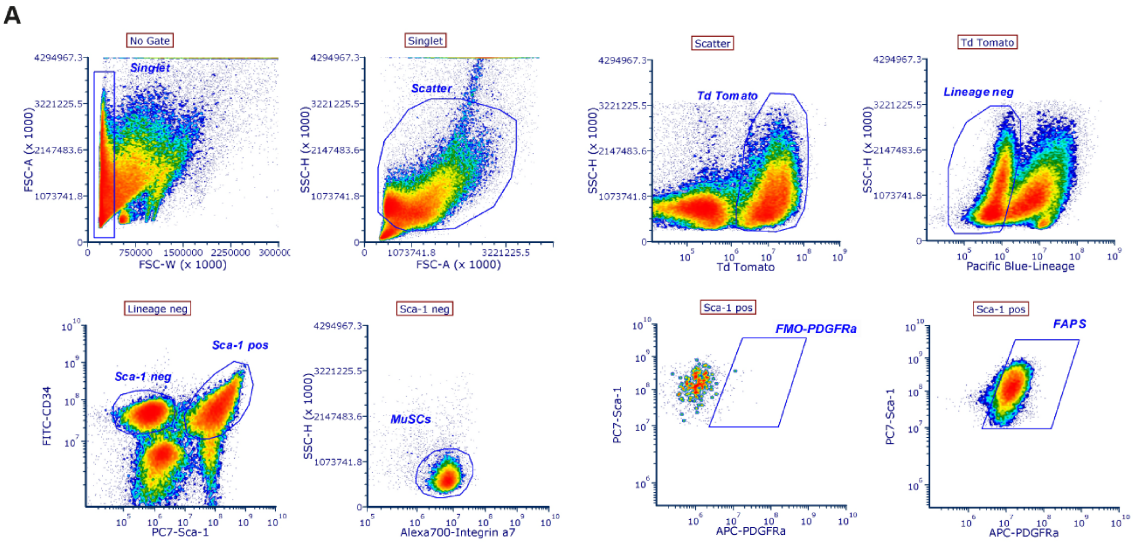
A
No Gate
Singlet
FSC-A (x 1000)
FSC-W (x 1000)
Singlet
Scatter
SSC-H (x 1000)
FSC-A (x 1000)
Scatter
Td Tomato
SSC-H (x 1000)
Td Tomato
Td Tomato
Lineage neg
SSC-H (x 1000)
Pacific Blue-Lineage
Lineage neg
Sca-1 pos
Sca-1 neg
FITC-CD34
PC7-Sca-1
Sca-1 neg
MuSCs
SSC-H (x 1000)
Alexa700-Integrin a7
Sca-1 pos
FMO-PDGFRa
PC7-Sca-1
APC-PDGFRa
Sca-1 pos
FAPS
PC7-Sca-1
APC-PDGFRa

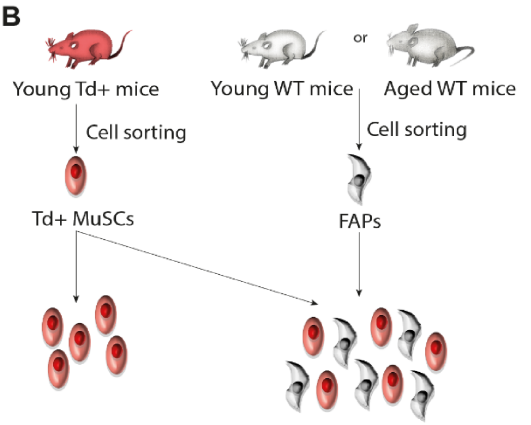
B
Young Td+ mice
Young WT mice
or
Aged WT mice
Cell sorting
Cell sorting
Td+ MuSCs
FAPs

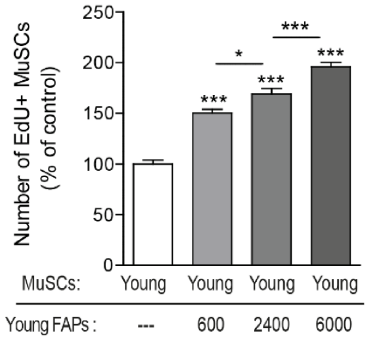
C
Number of EdU+ MuSCs (% of control)
250
200
150
100
50
0
***
*
***
***
***
MuSCs: Young Young Young Young
Young FAPs : --- 600 2400 6000

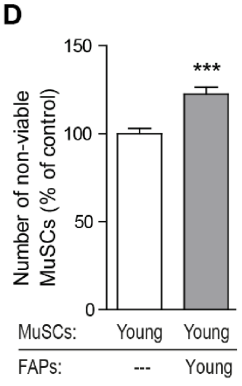
D
Number of non-viable MuSCs (% of control)
150
100
50
0
***
MuSCs: Young Young
FAPs: --- Young

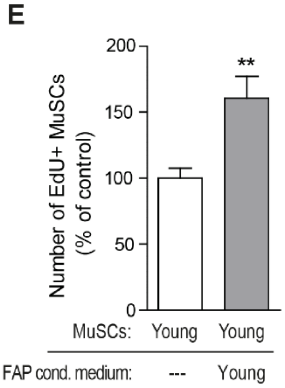
E
Number of EdU+ MuSCs (% of control)
200
150
100
50
0
**
MuSCs: Young Young
FAP cond. medium: --- Young

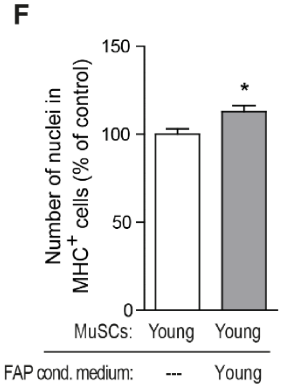
F
Number of nuclei in MHC+ cells (% of control)
150
100
50
0
*
MuSCs: Young Young
FAP cond. medium: --- Young

Fig. S3

Figure S4 (related to figure 3). Expression of Extracellular Matrix Genes in FAPs and MuSCs

Heatmap of mRNA expression for the gene ontology (GO) term “Extracellular matrix” significantly regulated in young FAPs compared to MuSCs isolated from uninjured muscles. n=6 replicates per condition, with cells pooled from multiple mice for each.

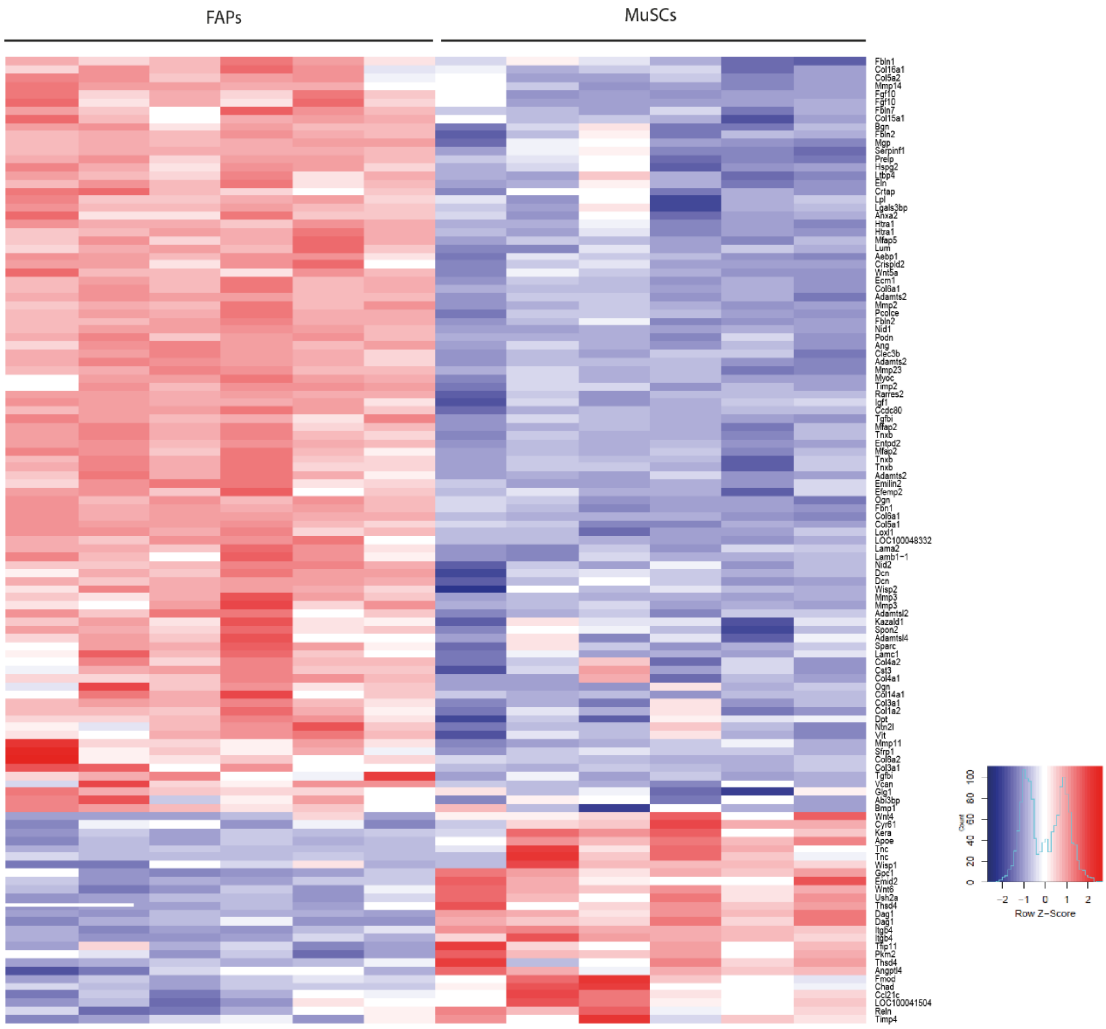

Figure S5 (related to figure 3). WISP1 Expression in Cell Types of the Muscle Stem Cell Niche

(A) qPCR quantification of WISP1 mRNA in Lineage positive cells (Lin+, CD31+/CD11b+/CD45+), MuSCs, FAPs, and Sca1+/PDGFRα- cells (CD31-/CD11b-/CD45-/Sca1+/CD34+/PDGFRα-) isolated from muscles of young and aged mice in uninjured conditions or at 3 dpi. n≥5 mice per condition. Data are normalized to MuSCs isolated from young uninjured muscles and are represented as means ± S.E.M. p-values are *p<0.05, **p<0.01, ***p<0.001 using an ANOVA followed by a Bonferroni post hoc test. (B) Representative RNA fluorescent in situ hybridization (FISH) staining of cross sections from muscles of young WT mice under uninjured conditions using a WISP1 anti-sense probe or a negative control without the target RNA probe. (C) Representative RNA FISH staining of cross sections from muscles of young WT or WISP1-/- mice under uninjured conditions or at 3 dpi using a WISP1 probe. (D) Representative RNA FISH staining of cross sections from muscles of young WT mice at 3 dpi using the WISP1 probe combined with a Pax7 immunostaining. (B-D) Scale bars = 100 μm.

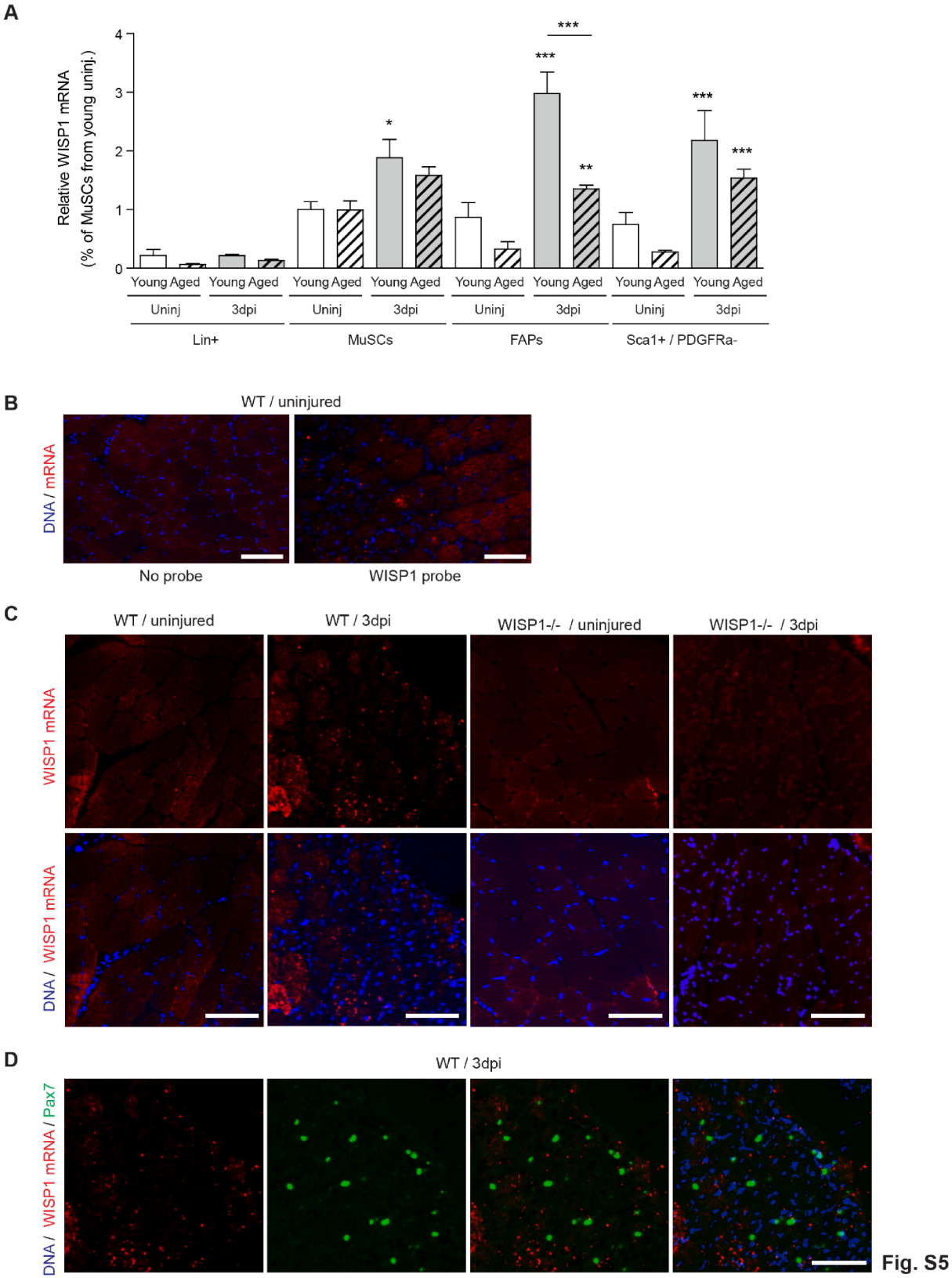
A
Relative WISP1 mRNA
(% of MuSCs from young uninj.)
0
1
2
3
4
***
***
*
**
***
***
Young Aged
Uninj
3dpi
Lin+
MuSCs
FAPs
Sca1+ / PDGFRa-
B
WT / uninjured
DNA / mRNA
No probe
WISP1 probe
C
WT / uninjured
WT / 3dpi
WISP1-/- / uninjured
WISP1-/- / 3dpi
WISP1 mRNA
DNA / WISP1 mRNA
D
WT / 3dpi
DNA / WISP1 mRNA / Pax7

Fig. S5

Figure S6 (related to figure 4). Characterization of FAPs and Muscle in WISP1-/- mice

(A) qPCR quantification of WISP1 mRNA in muscles of WT or WISP1-/- mice under uninjured (uninj.) conditions or at 3, and 7 dpi. (B) Quantification of the number of MuSCs from uninjured muscles of young WT or WISP1-/- mice cultured for 12 h after isolation. n≥24 replicates per condition. (C) Quantification of the percentage of EdU+ MuSCs from uninjured muscles of young WT or WISP1-/- mice cultured for 72 h after isolation. n≥39 replicates per condition. (D) Quantification of the number of nuclei in Myosin Heavy Chain (MHC) positive cells generated by MuSCs from uninjured muscles of young WT or WISP1-/- mice cultured for 6 d after isolation. n≥11 replicates per condition. (B-D) Data are normalized to MuSCs isolated from young uninjured muscles. (E) Quantification of the number of FAPs from uninjured muscles of young WT or WISP1-/- mice cultured with Td+ MuSCs from uninjured muscles for 12 h after isolation. n=24 replicates per condition, repeated twice for each condition. (F) Quantification of the myofiber cross-sectional area distribution quantified from a laminin staining of uninjured muscles of WT or WISP1-/- mice. (G-J) qPCR quantification of F4/80, CD11b, CD31 and TCF4 mRNA in muscles of WT or WISP1-/- mice under uninjured conditions or at 3, and 7 dpi. (A and E-J) n≥5 mice per condition. (A-J) Data are represented as means ± S.E.M. p-values are *$p<0.05$, **$p<0.01$, ***$p<0.001$ using a Mann-Whitney test when comparing two conditions, and an ANOVA followed by a Bonferroni post hoc test when comparing multiple conditions.

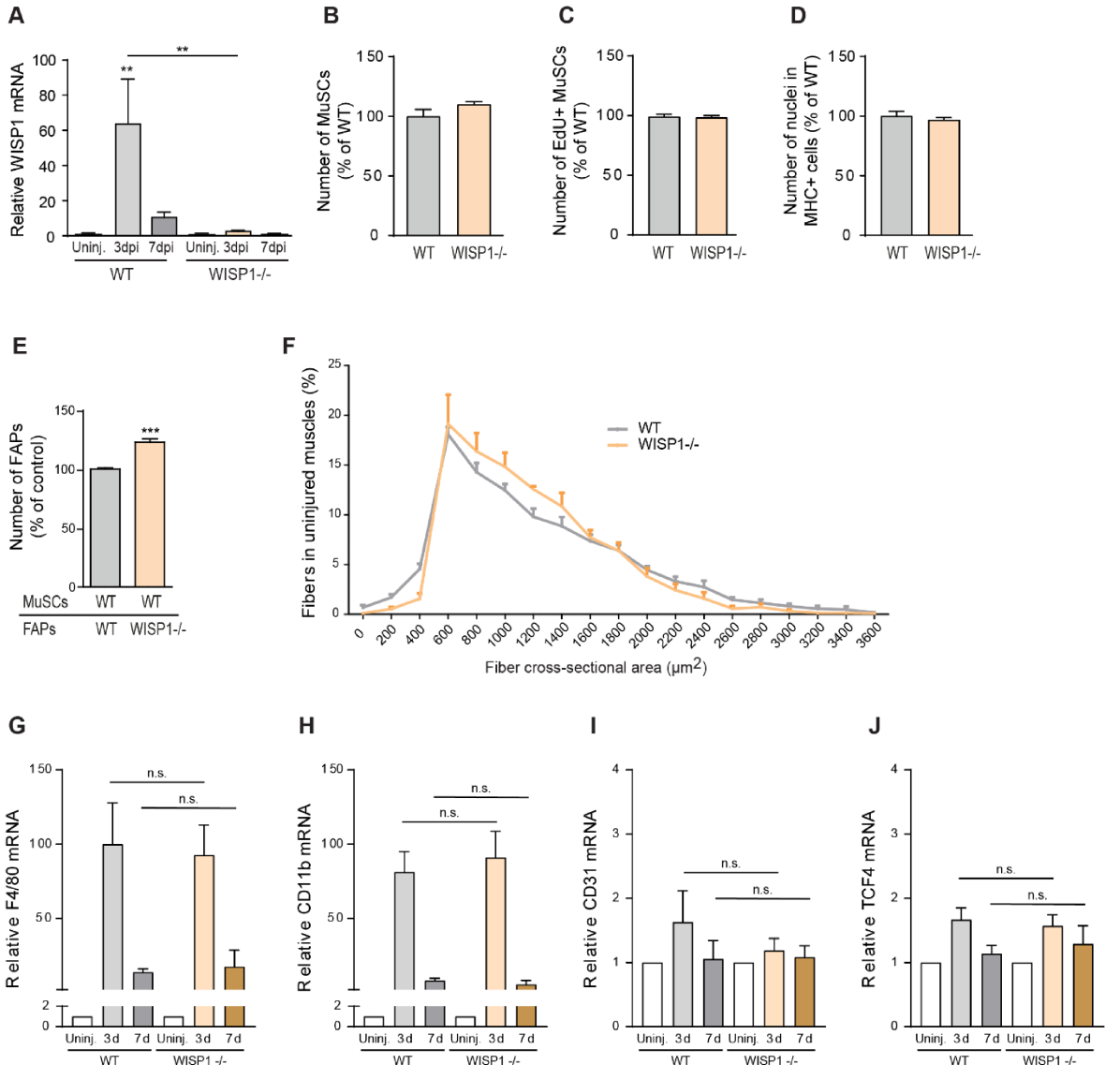
A
Relative WISP1 mRNA
Uninj. 3dpi 7dpi Uninj. 3dpi 7dpi
WT
WISP1-/-
B
Number of MuSCs (% of WT)
WT WISP1-/-
C
Number of EdU+ MuSCs (% of WT)
WT WISP1-/-
D
Number of nuclei in MHC+ cells (% of WT)
WT WISP1-/-
E
Number of FAPs (% of control)
MuSCs WT WT
FAPs WT WISP1-/-
F
Fibers in uninjured muscles (%)
WT
WISP1-/-
Fiber cross-sectional area (μm2)
G
Relative F4/80 mRNA
H
Relative CD11b mRNA
I
Relative CD31 mRNA
J
Relative TCF4 mRNA
n.s.
Uninj. 3 d 7 d Uninj. 3 d 7 d
WT
WISP1 -/-

Fig. S6

Figure S7 (related to figures 5 and 7). Effects of WISP1 Treatment on MuSCs and FAPs (A-F) and on Muscles of Aged mice (G-L).

(A) Quantification of the number MuSCs from uninjured muscles of young mice treated with Veh. or 8µg/mL WISP1 for 36 h after isolation. (B) Quantification of the number of EdU+ MuSCs from uninjured muscles of young mice treated with Veh. or WISP1 for 3 d after isolation. Cells pooled from up to n=6 mice and n≥20 replicates per condition, repeated three times for each condition. (C) Quantification of the number of nuclei in Myosin Heavy Chain (MHC) positive cells generated by MuSCs from uninjured muscles of young mice 6 d after isolation and treated with Veh. or WISP1 for the final 2 d of differentiation. (D) Quantification of the percentage of EdU+ FAPs 6 d after isolation from young uninjured muscles treated with Veh. or WISP1. Cells pooled from n=3 mice and n=20 replicates per condition, repeated two times for each condition. (E) Quantification of the myotube width generated by MuSCs from uninjured muscles of young mice 6 d after isolation and treated with Veh. or WISP1 for the final 2 d of differentiation. (F) Raw scans of western blots of primary myoblasts treated with either Veh. or WISP1 for 24h. (G-K) qPCR quantification of F4/80, CD11b, CD11c, CD31 and TCF4 mRNA in muscles of young Veh. treated mice and aged mice treated with daily i.p. injection of vehicle (Veh.) or WISP1 under uninjured conditions or at 3, 7 and 14 dpi. Statistical significances are reported relative to the uninjured control of the same group. (L) Quantification of the myofiber cross-sectional area distribution quantified from laminin stainings of uninjured muscles of young and aged Veh. or WISP1 treated muscles. n≥5 mice per condition. (A, C and E) Cells pooled from up to n=6 mice and n=24 replicates per condition. (A-L) Data are represented as means ± S.E.M. p-values are *$p<0.05$, **$p<0.01$, ***$p<0.001$ using a Mann-Whitney test when comparing two conditions, and an ANOVA followed by a Bonferroni post hoc test when comparing multiple conditions.

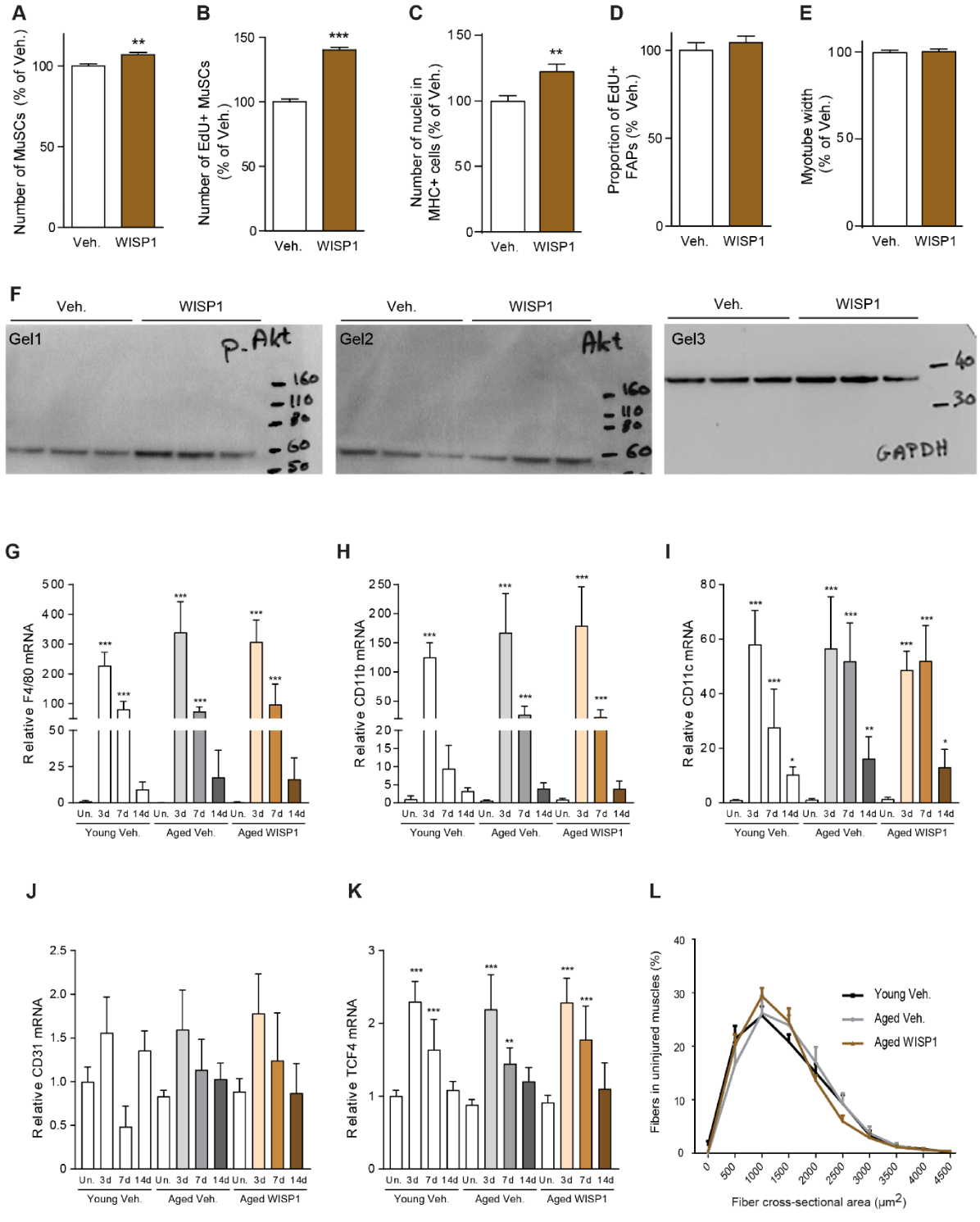
A
Number of MuSCs (% of Veh.)
Veh.
WISP1
B
Number of EdU+ MuSCs (% of Veh.)
C
Number of nuclei in MHC+ cells (% of Veh.)
D
Proportion of EdU+ FAPs (% Veh.)
E
Myotube width (% of Veh.)
F
Gel1
p-Akt
Gel2
Akt
Gel3
GAPDH
G
Relative F4/80 mRNA
H
Relative CD11b mRNA
I
Relative CD11c mRNA
J
Relative CD31 mRNA
K
Relative TCF4 mRNA
Un. 3d 7d 14d
Young Veh.
Aged Veh.
Aged WISP1
L
Fibers in uninjured muscles (%)
Young Veh.
Aged Veh.
Aged WISP1
Fiber cross-sectional area (μm2)

Fig. S7

Table S1 (related to figure 3). Top GO Term in FAPs vs. MuSCs, cell type effect. Top Gene Ontology (GO) terms of genes regulated in young quiescent FAPs vs. young quiescent MuSCs.

GO.ID	Term	Annotated	Significant	Expected	classicFisher
GO:0044707	single-multicellular organism process	3763	580	407.01	1.80E-26
GO:0032501	multicellular organismal process	3835	583	414.8	5.60E-25
GO:0048731	system development	2580	428	279.06	2.40E-24
GO:0048513	organ development	1894	335	204.86	4.60E-23
GO:0044767	single-organism developmental process	3432	523	371.21	9.20E-22
GO:0032502	developmental process	3452	525	373.37	1.20E-21
GO:0007275	multicellular organismal development	2949	462	318.97	4.40E-21
GO:0048856	anatomical structure development	3088	478	334	7.70E-21
GO:0007155	cell adhesion	679	148	73.44	9.50E-18
GO:0030198	extracellular matrix organization	157	57	16.98	1.90E-17
GO:0009888	tissue development	1137	214	122.98	2.00E-17
GO:0043062	extracellular structure organization	158	57	17.09	2.60E-17
GO:0022610	biological adhesion	687	148	74.31	2.90E-17
GO:0016477	cell migration	745	154	80.58	3.10E-16
GO:0072358	cardiovascular system development	699	147	75.6	3.40E-16
GO:0072359	circulatory system development	699	147	75.6	3.40E-16
GO:0044699	single-organism process	8387	1031	907.15	1.20E-15
GO:0048870	cell motility	790	159	85.45	1.20E-15
GO:0051674	localization of cell	790	159	85.45	1.20E-15
GO:0040011	locomotion	918	177	99.29	1.80E-15
GO:0009653	anatomical structure morphogenesis	1597	267	172.73	8.90E-15

Table S2 (related to figure 3). Top GO Term in FAPs, age effect. Top Gene Ontology (GO) terms of genes regulated in old quiescent FAPs *vs*. young quiescent FAPs.

GO.ID	Term	Annotated	Significant	Expected	classicFisher
GO:0065007	biological regulation	6584	48	32.7	4.20E-05
GO:0050794	regulation of cellular process	5944	45	29.52	4.70E-05
GO:0050678	regulation of epithelial cell proliferation	208	7	1.03	7.30E-05
GO:0050789	regulation of biological process	6311	46	31.35	1.00E-04
GO:0070228	regulation of lymphocyte apoptotic proces	51	4	0.25	1.20E-04
GO:0044092	negative regulation of molecular function	604	11	3	1.60E-04
GO:0001525	angiogenesis	320	8	1.59	1.70E-04
GO:0050673	epithelial cell proliferation	240	7	1.19	1.80E-04
GO:0043433	negative regulation of sequence-specific DNA binding transcription factor activity	110	5	0.55	2.10E-04
GO:0007179	transforming growth factor beta receptor signaling	114	5	0.57	2.50E-04
GO:0070887	cellular response to chemical stimulus	1239	16	6.15	2.60E-04
GO:0070227	lymphocyte apoptotic process	63	4	0.31	2.60E-04
GO:0042221	response to chemical	1820	20	9.04	3.30E-04
GO:0001568	blood vessel development	456	9	2.26	3.90E-04
GO:0071559	response to transforming growth factor beta	130	5	0.65	4.60E-04
GO:0071560	cellular response to transforming growth factor	130	5	0.65	4.60E-04

Table S3 (related to figure 3). Identification of genes both significantly regulated in Old activated FAPs vs. Young activated FAPs and significantly upregulated with activation in young FAPs.

adj. p-value [Activation young] < 0.001, Fold-change [Activation young] > 2; adj. p-value [interaction: Activation*Age] < 0.25; adj. p-value [old activated FAPs *vs*. young activated FAPs] < 0.1. Y = young, O = old, Q = quiescent, A =activated, F = FAPs, FC = fold-change. Arg1: arginase 1 liver, Birc5 : Baculoviral IAP Repeat-Containing 5, Gpr176 : G protein-coupled receptor 176, Cdc20 : cell division cycle 20 homolog (S. cerevisiae), N6amt2 : N-6 adenine-specific DNA methyltransferase 2, Cenpp : centromere protein P, Actn1 : actinin alpha 1, Fkbp11 : FK506 binding protein 11, Aldh1l2 : aldehyde dehydrogenase 1 family, member L2, WISP1 : WNT1 inducible signaling pathway protein 1.

				YAF vs. YQF Activation effect			Interaction Age * Treatment			OAF vs. YAF Effect of age in activated FAPs		
Probe Id	Accession	Symbol	Amean	log_2(FC)	p-value	BH adj. p-value	log_2(FC)	p-value	BH adj. p-value	log_2(FC)	p-value	BH adj. p-value
ILMN_2952275	NM_007482.2	**Arg1**	7.774136	1.57418	1.61E-07	5.37E-06	1.110655	0.001121808	0.179146479	1.130296667	2.04E-05	0.020123961
ILMN_2632712	NM_009689.2	**Birc5**	7.391934	1.546418333	8.11E-14	1.30E-10	-0.50471167	0.001089471	0.178674974	-0.44682	0.000107574	0.051584051
ILMN_2742912	NM_201367.2	**Gpr176**	7.259477	1.439868333	3.49E-09	2.67E-07	-0.77940833	0.001608279	0.199178049	-0.622685	0.000516491	0.080925328
ILMN_2612206	NM_023223.1	**Cdc20**	7.414382	1.724106667	1.83E-12	9.41E-10	-0.80067	0.000143918	0.092453149	-0.62642833	4.38E-05	0.031814026
ILMN_1235697	NM_026526.2	**N6amt2**	9.317762	1.575351667	4.93E-09	3.58E-07	-0.89838	0.001204227	0.179609402	-0.706145	0.000438063	0.080118423
ILMN_2970623	NM_025495.1	**Cenpp**	7.221673	1.366705	2.53E-08	1.25E-06	-0.94690167	0.000460104	0.147785252	-0.76514333	0.000109332	0.051584051
ILMN_2844996	NM_134156.1	**Actn1**	11.03137	1.121933333	2.16E-06	4.48E-05	-1.06105	0.000334277	0.134212027	-0.83001667	0.000110836	0.051584051
ILMN_1224635	NM_024169.3	**Fkbp11**	10.729	2.33442	7.83E-12	2.45E-09	-0.918625	0.001551561	0.199178049	-0.89775	5.34E-05	0.036133989
ILMN_2898319	NM_153543.1	**Aldh1l2**	7.424884	1.291073333	3.45E-08	1.62E-06	-1.12440667	4.37E-05	0.043221189	-1.14651167	2.44E-07	0.001042847
ILMN_2492264	NM_018865.2	**Wisp1**	7.972638	2.15291	1.92E-08	1.01E-06	-1.20416167	0.002757801	0.243394442	-1.52888167	4.22E-06	0.009030832

Chapter 6:

Conclusion & Perspective

General Considerations

The recent discovery of “cellular reprograming” and “induced pluripotent stem cells” has led to open a new window to bypass the need for donor tissue derived muscle stem cells for cell-therapy of muscular dystrophies [447]. Pluripotent stem cells (e.g., ES and iPSC cells) by using directed-differentiation protocols could allow for the generation of virtually unlimited amounts of MuSCs. Most importantly, by stopping the differentiation stage at the right moment, MuSCs with a higher stemness than adult cells which resembling uncommitted embryonic fetal progenitors, could be obtained.

Alternatively, other methods rely on the overexpression of transgenes (e.g., Pax3/7 or MyoD) to force cellular reprogramming towards the myogenic lineage. The disadvantage of this strategy to chemically-directed differentiation approaches for the clinical translation is that, next to the lengthy differentiation procedure, the need for introduction of foreign DNA/RNA and potential reactivation of vectors and the risk of insertional-mutagenesis using viral vectors is a strong concern for regulatory agencies.

Stem cell differentiation through chemical induction is controllable and small molecular drugs can be washed out subsequently from culture condition before transplantation in a clinical-setting. Unfortunately, present published-protocols take 30-50 days or more. In addition, adherent cells require a large culture vessel surface, which makes clinical scale-up production very challenging.

Thesis Main Outcome

In the **1st study** of this thesis, we addressed both the problem of “terminal stem cell commitment” associated with 2D culture and the “time-consuming nature” with published protocols for generation of muscle progenitors from human iPSCs[448].

First, we chose a non-adherent 3D-condition to allow for scalable production, by using hiPSC-aggregates formed in a suspension in low-adhesion plates on a horizontal shaker-platform. Second, we investigated whether some of the widely available immortalized cell lines, resembling the function of niche’s support cells involved in embryonic/fetal specification of muscle, could enhance the efficiency of hiPSC towards myogenic-derivation in the 3D-aggregates and ultimately maintain the cells at a stemness level suitable for cell-therapy.

After extensive trials of permutations of up to three different cell lines simultaneously, we identified a particular "triple" aggregate condition containing endothelial cells and growth arrested fibroblasts, which led the differentiation to a strong induction of Pax7 in three-component embryoids (TCEs) within two weeks. Notably, we could significantly boost the efficiency of Pax7 expression to higher levels when combined TCEs with the GSK3β inhibitor (CHIR) which promotes early mesoderm specification in pluripotent stem cells. Flow-cytometry results revealed a very high myogenic efficiency as ~50% of hiPSC (3 different lines) were derived to Pax7-positive progenitors using our

aggregation-system. Interestingly, when instead of using the suspension aggregate paradigm, the accessory cells were co-cultured in 2D-condition with hiPSCs, only a very low amount of Pax7-positive cells were detected. This observation demonstrates that the 3D-context is essential for the efficiency of our novel derivation protocol. TCEs exhibited remarkable 3D-self-organizing structures which beautifully corresponding early embryonic development. They also expressed high levels of developmental markers of the mesodermal and myogenic lineages, which were progressively regulated in a time-dependent fashion during the 3D-differentiation.

In order to isolate live myogenic progenitors from TCEs for transplantation, we tested a panel of cell-surface markers by flow cytometry. A combination of the CD56 and α9-integrin enriched for 99% pure Pax7+progenitors from enzymatically digested embryoids. Also, RNA-FISH experiment revealed a high stemness stage of sorted cells by showing very low amounts of the commitment markers Myf5 and MyoD. Immunostaining of sorted myogenic progenitor cells in differentiated cultures (2D) revealed the presence of (I) self-renewing MuSCs that remained Pax7 positive, (II) cells expressing the myogenic activation and proliferation marker MyoD, and (III) differentiating or differentiated cells expressing Myogenin (MyoG) and the muscle fiber structural protein myosin heavy chain (MyHC). CD56 and integrin α9 positive embryonic-like myogenic progenitor cells (eMPs) displayed a striking efficiency in generating dystrophin positive muscle fibers when compared to 2D cultured human myoblasts after transplantation into immunosuppressed Duchenne muscular dystrophy mdx mice. Most interestingly, transplanted eMPs were also more evenly distributed in the host tissue and frequently occupied the satellite cell stem cell position in the periphery of dystrophin+ fibers. In conclusion, our experiments in this study will provide a much needed protocol for the derivation of uncommitted myogenic progenitors from human iPS cells for therapeutic applications, as well as a unique *in-vitro* organoid-like system for the interrogation of human stem cell biology.

In the **2nd study**, we engineered a novel platform for encapsulation of human myogenic progenitor cells in order to implant in mice to study an aged systemic environment. These highly diffusible polyethersulfone hollow fiber capsules can be implanted subcutaneously into young and old mice, and become vascularized over a time-course of ten days. The porous structure of the capsule wall allows molecules up to 1000 kDa to diffuse freely through the membrane, but prevents infiltration by cells. Encapsulated human stem cells retain their proliferation and differentiation potential, and can readily be extracted from the capsules following explantation from their hosts for subsequent molecular profiling. Human RNA yield and quality are sufficient for downstream transcriptomic profiling and do not show contamination by mouse transcripts. For proof-of-concept we analyzed RNA from encapsulated human muscle stem cells that were exposed to the systemic environment in 6- or 22-month-old mice for 10 days. We were able to identify highly specific transcriptional signature induced by systemic aging that covers a wide range of novel age affected factors, as well as pathways previously characterized to be deregulated during aging including Akt/mTOR and

cytokine signaling. Overall, this novel bioengineered-platform as a mimetic-model of parabiosis represents an innovative and important step forward in the aging and stem cell fields by capturing the isolated systemic molecular signatures.

Finally, the **3rd study** opened a new opportunity for us to target MuSCs interactions with their niche-resident cell types as a promising strategy in order to restore their regenerative function in skeletal muscle. In this story, we showed that aging strongly perturbs the function of fibro/adipogenic progenitors (FAPs) and their ability to support myogenesis. We illuminated the communication of FAPs with MuSCs through paracrine signaling using transcriptomic profiling. Our work demonstrates that loss of matricellular protein WNT1 Inducible Signaling Pathway Protein 1 (WISP1) from FAPs contributes to MuSC dysfunction in aged skeletal muscles and this novel mechanism can be targeted to rejuvenate myogenesis. Interestingly, aged population of FAPs have a reduced capacity for clonal expansion and also fate decisions. This strongly indicates that aging perturbs FAP function at the progenitor stage, and consequently leads to a deregulation of MuSC function and eventually a concomitant imbalance of adipogenic and fibrogenic fate decisions which further intensifies the regenerative dysfunction of aged muscles.

Perspectives

This thesis presents a variety of applications at the interface of “bioengineering” and “stem cell biology”. Importantly, through a better understanding of the biology of the niche (**Chapters 4 & 5**), we presented our novel “organoid-like approach” for the derivation of muscle stem cells which represents an incremental step forward for stem cell therapy of degenerative skeletal muscle disease.

As we have described in the first and main study of this thesis, within a two-week time-window, we are able to generate uncommitted myogenic progenitor cells in 3D-scale with an unprecedented stem cell character from iPSCs in suspension embryoids. The fact that our protocol is entirely performed in solution will facilitate scaling to the bioreactor-level and allow for efficient clinical translation. Our work established a more optimistic outlook by providing a potential resource of real stem cells for “personalized” cellular therapy of patients with dystrophinopathies.

As a future perspective for regenerative medicine, patient-specific iPSCs-derived progenitor cells produced with our model can be used for a variety of applications including *in-vitro* assessment of true myogenic capacity, drug screening, modeling muscle diseases and identification of pathologic-features or etiologies. Although cell therapy illuminates a promising-forecast for practical setting in the near future, it is -so far- far from being applied in the clinic due to major bottlenecks, which we tried to unlock them with our technology:

(I) *High-variability on the production of real and safe progenitors*: We addressed this issue by our 3D-directed "controllable" differentiation protocol and subsequent purification by flow-cytometer along with the identified specific surface-markers to purify myogenic progenitors

(II) *Identification of the ideal cell-population for transplantation*: Our embryonic-like myogenic progenitor cells (eMPs) crossed the barriers toward interstitial muscle space and successfully engrafted into the injured dystrophic muscle fibers.

Morover, purified-eMPs can be used in "combinatorial therapies" together with current running treatments such as physical-therapies for increasing range of muscle motion/growth and corticosteroids therapy for improving muscle strength and functional abilities in the case of Duchenne muscular dystrophy [449]. Importantly, the implications of our novel protocol are not limited to cell-therapy alone. The availability of a virtually unlimited source of uncommitted human muscle progenitors will allow for disease modelling and screening at a whole new level. Patient specific eMPs-high-throughput drug screening will allow us for the study of disease pathways and also could provide a platform for testing the safety and efficacy of new chemical/drug candidates when paired with *in-vivo* models.

Nonetheless, future prospective analysis will be necessary to better dissect the eMPs mechanistically using the new technologies such as "single-cell RNA sequencing" as to probe the identity and physiology of individual cells. We recently started to decode the transcriptional signatures of our 3D-derived progenitors as well as relative transcriptional alteration during the differentiation, the description of signaling pathways associated with cell's state transitions and 3D-cell differentiation trajectories *in-vitro* and eventually exploring the dynamics of muscle/lineage specific gene expression within single cells over time (data not shown in the thesis).

Furthermore, our encapsulation study can be used as a biocompatible engineered-platform to expose the patient specific eMPs derived from iPSC into systemic environment and aging process *in-vivo*, independent of any physical cellular interactions. This unique device can be effective for serving as "vascular" model [450] as our engineered hollow fiber capsules become vascularized when subcutaneously implanted in short duration. Absence of a developed vasculature is one of the main limitations in the disease modeling and synergistic bioengineering [451, 452]. Lastly, we identified a niche-resident cell type that fail to support MuSC function in aged muscles. This would allow us to develop a targeted strategy to restore a "youthful-niche" environment and it can build a perspective and substantial insights for other scientists to systematically decode other tissue-specific stem cell niches and their supporting compounds on diagnostic and therapeutic potentials.

It is hoped that the technological advances reported in this doctoral-thesis will support the emerging fields of personalized medicine and cell therapy in the field of muscle disease treatments.

Chapter 7:

Scientific Outputs Published during the PhD Study (2015-2019): Not-Included in the Thesis

Editorial & Book Chapter:

1. S. Tavakol*****, S. Jalili-Firoozinezhad*****, **O. Mashinchian*** and M. Mahmoudi. Bioinspired Nanotechnologies for Skin Regeneration. **Book Chapter in Nanoscience in Dermatology. Elsevier, Inc**. 2016

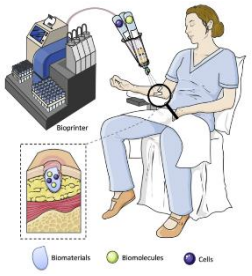

2. S. Moayyedi, **O. Mashinchian** and R. Dinarvand. Osmolarity: A Hidden Factor in Nanotoxicology. **DARU Journal of Pharmaceutical Sciences**. 2016, 24 (9).

Original Research Paper:

3. T. Heydari*, M. Heidari*, **O. Mashinchian***, M. Wojcik, K. Xu, M. Dalby, M. Mahmoudi and M. R. Ejtehadi. Development of a Virtual Cell Model to Predict Cell Response to Substrate Topography. **ACS Nano**. 2017, 11 (9). Impact Factor: **13.7**
#Highlighted in Nanowerk

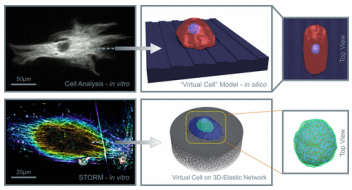

4. S. A. Hosseini, M. Abdolahad, S. Zanganeh, M. Dahmardeh, M. Gharooni, H. Abiri, A. Alikhani, S. Mohajerzadeh and **O. Mashinchian***. Nanoelectromechanical Chip (NELMEC) Combination of Nanoelectronics and Microfluidics to Diagnose Epithelial and Mesenchymal Circulating Tumor Cells from Leukocytes. **Small**. 2016, 12 (7). Impact Factor: **9.5**

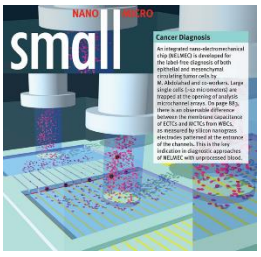

5. S. Bonakdar, M. Mahmoudi, L. Montazeri, M. Taghipoor, A. Bertsch, M. A. Shokrgozar, S. Sharifi, M. Majidi, **O. Mashinchian**, M. H. Sekachaei, P. Zolfaghari, and P. Renaud. Cell-Imprinted Substrates Modulate Differentiation, Redifferentiation, and Transdifferentiation. **ACS Applied Materials and Interfaces**. 2016, 8 (22). Impact Factor: **8**

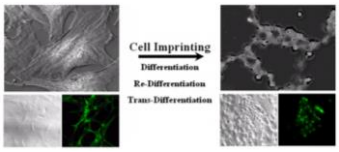

6. B. Ghaemi*, **O. Mashinchian***, T. Mousavi, R. Karimi, S. Kharrazi and Amir Amani. Harnessing the Cancer Radiation Therapy by Lanthanide-Doped Zinc Oxide Based Theranostic Nanoparticles. **ACS Applied Materials and Interfaces**. 2016, 8 (5). Impact Factor: **8**

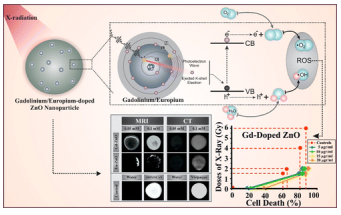

7. M. Namiri, M. K. Ashtiani, **O. Mashinchian**, M. M. Hasani-Sadrabadi, M. Mahmoudi, N. Aghdami and H. Baharvand. Engineering Natural Heart Valves: Possibilities and Challenges. **Journal of Tissue Engineering and Regenerative Medicine**. 2016. Impact Factor: **4**

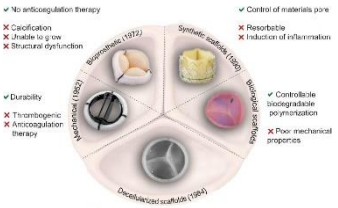

8. F. Esfandiari*, **O. Mashinchian***, M. K. Ashtiani, M. H. Ghanian, K. Hayashi, A. A. Saei, M. Mahmoudi and Hossein Baharvand. Possibilities in Germ Cell Research: An Engineering Insight. **Trends in Biotechnology**. 2015, 33 (12). Impact Factor: **13.5**

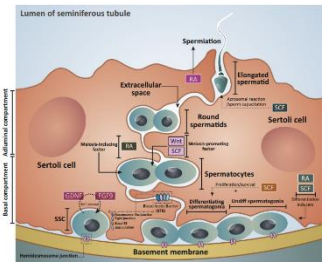

Patent:

9. O. Mashinchian, J. N. Feige and C. F. Bentzinger. *In-vitro* Production of Muscle Stem Cells. **European Patent Office (nm: WO2018091282)**. 2018

Chapter 8:

Bibliography

Bibliography

1. Waterlow, J.C. The extent of protein synthesis in muscle in man. *Hum Nutr Clin Nutr* **38**, 151-154 (1984).
2. Hoppeler, H. & Fluck, M. Normal mammalian skeletal muscle and its phenotypic plasticity. *J Exp Biol* **205**, 2143-2152 (2002).
3. Schnyder, S. & Handschin, C. Skeletal muscle as an endocrine organ: PGC-1alpha, myokines and exercise. *Bone* **80**, 115-125 (2015).
4. Janssen, I., Heymsfield, S.B., Wang, Z.M. & Ross, R. Skeletal muscle mass and distribution in 468 men and women aged 18-88 yr. *J Appl Physiol (1985)* **89**, 81-88 (2000).
5. Silva, A.M. et al. Ethnicity-related skeletal muscle differences across the lifespan. *Am J Hum Biol* **22**, 76-82 (2010).
6. Demontis, F., Piccirillo, R., Goldberg, A.L. & Perrimon, N. Mechanisms of skeletal muscle aging: insights from Drosophila and mammalian models. *Dis Model Mech* **6**, 1339-1352 (2013).
7. Montero-Fernandez, N. & Serra-Rexach, J.A. Role of exercise on sarcopenia in the elderly. *Eur J Phys Rehabil Med* **49**, 131-143 (2013).
8. Cooper, S.T. & McNeil, P.L. Membrane Repair: Mechanisms and Pathophysiology. *Physiol Rev* **95**, 1205-1240 (2015).
9. Wang, Y.X. & Rudnicki, M.A. Satellite cells, the engines of muscle repair. *Nature reviews* **13**, 127-133 (2011).
10. Rochlin, K., Yu, S., Roy, S. & Baylies, M.K. Myoblast fusion: when it takes more to make one. *Developmental biology* **341**, 66-83 (2010).
11. Mauro, A. Satellite cell of skeletal muscle fibers. *The Journal of biophysical and biochemical cytology* **9**, 493-495 (1961).
12. Scharner, J. & Zammit, P.S. The muscle satellite cell at 50: the formative years. *Skelet Muscle* **1**, 28 (2011).
13. Kuang, S., Gillespie, M.A. & Rudnicki, M.A. Niche regulation of muscle satellite cell self-renewal and differentiation. *Cell stem cell* **2**, 22-31 (2008).
14. Bentzinger, C.F., Wang, Y.X. & Rudnicki, M.A. Building muscle: molecular regulation of myogenesis. *Cold Spring Harbor perspectives in biology* **4** (2012).
15. Ali, S. & Garcia, J.M. Sarcopenia, cachexia and aging: diagnosis, mechanisms and therapeutic options - a mini-review. *Gerontology* **60**, 294-305 (2014).
16. Petis, S., Howard, J.L., Lanting, B.L. & Vasarhelyi, E.M. Surgical approach in primary total hip arthroplasty: anatomy, technique and clinical outcomes. *Can J Surg* **58**, 128-139 (2015).
17. Serrano, A.L. & Munoz-Canoves, P. Fibrosis development in early-onset muscular dystrophies: Mechanisms and translational implications. *Semin Cell Dev Biol* **64**, 181-190 (2017).
18. Schofield, R. The relationship between the spleen colony-forming cell and the haemopoietic stem cell. *Blood Cells* **4**, 7-25 (1978).
19. Scadden, D.T. The stem-cell niche as an entity of action. *Nature* **441**, 1075-1079 (2006).
20. Gokhin, D.S., Ward, S.R., Bremner, S.N. & Lieber, R.L. Quantitative analysis of neonatal skeletal muscle functional improvement in the mouse. *J Exp Biol* **211**, 837-843 (2008).
21. Allbrook, D.B., Han, M.F. & Hellmuth, A.E. Population of muscle satellite cells in relation to age and mitotic activity. *Pathology* **3**, 223-243 (1971).
22. Schultz, E. A quantitative study of the satellite cell population in postnatal mouse lumbrical muscle. *The Anatomical record* **180**, 589-595 (1974).
23. Tierney, M.T. et al. Autonomous Extracellular Matrix Remodeling Controls a Progressive Adaptation in Muscle Stem Cell Regenerative Capacity during Development. *Cell reports* **14**, 1940-1952 (2016).
24. Urciuolo, A. et al. Collagen VI regulates satellite cell self-renewal and muscle regeneration. *Nature communications* **4**, 1964 (2013).
25. Bentzinger, C.F. et al. Fibronectin regulates Wnt7a signaling and satellite cell expansion. *Cell Stem Cell* **12**, 75-87 (2013).

26. Burkin, D.J. & Kaufman, S.J. The alpha7beta1 integrin in muscle development and disease. *Cell and tissue research* **296**, 183-190 (1999).
27. Gnocchi, V.F., White, R.B., Ono, Y., Ellis, J.A. & Zammit, P.S. Further characterisation of the molecular signature of quiescent and activated mouse muscle satellite cells. *PloS one* **4**, e5205 (2009).
28. Cornelison, D.D., Filla, M.S., Stanley, H.M., Rapraeger, A.C. & Olwin, B.B. Syndecan-3 and syndecan-4 specifically mark skeletal muscle satellite cells and are implicated in satellite cell maintenance and muscle regeneration. *Developmental biology* **239**, 79-94 (2001).
29. Lukjanenko, L. et al. Loss of fibronectin from the aged stem cell niche affects the regenerative capacity of skeletal muscle in mice. *Nature medicine* **22**, 897-905 (2016).
30. Rozo, M., Li, L. & Fan, C.M. Targeting beta1-integrin signaling enhances regeneration in aged and dystrophic muscle in mice. *Nature medicine* **22**, 889-896 (2016).
31. Garcion, E., Halilagic, A., Faissner, A. & ffrench-Constant, C. Generation of an environmental niche for neural stem cell development by the extracellular matrix molecule tenascin C. *Development* **131**, 3423-3432 (2004).
32. Nakamura-Ishizu, A. et al. Extracellular matrix protein tenascin-C is required in the bone marrow microenvironment primed for hematopoietic regeneration. *Blood* **119**, 5429-5437 (2012).
33. Young, H.E., Carrino, D.A. & Caplan, A.I. Change in synthesis of sulfated glycoconjugates during muscle development, maturation and aging in embryonic to senescent CBF-1 mouse. *Mech Ageing Dev* **53**, 179-193 (1990).
34. Pannerec, A., Formicola, L., Besson, V., Marazzi, G. & Sassoon, D.A. Defining skeletal muscle resident progenitors and their cell fate potentials. *Development* **140**, 2879-2891 (2013).
35. Formicola, L., Marazzi, G. & Sassoon, D.A. The extraocular muscle stem cell niche is resistant to ageing and disease. *Frontiers in aging neuroscience* **6**, 328 (2014).
36. Mitchell, K.J. et al. Identification and characterization of a non-satellite cell muscle resident progenitor during postnatal development. *Nature cell biology* **12**, 257-266 (2010).
37. Mathew, S.J. et al. Connective tissue fibroblasts and Tcf4 regulate myogenesis. *Development* **138**, 371-384 (2011).
38. Sarelius, I.H., Damon, D.N. & Duling, B.R. Microvascular adaptations during maturation of striated muscle. *Am J Physiol* **241**, H317-324 (1981).
39. Christov, C. et al. Muscle satellite cells and endothelial cells: close neighbors and privileged partners. *Mol Biol Cell* **18**, 1397-1409 (2007).
40. Kostallari, E. et al. Pericytes in the myovascular niche promote post-natal myofiber growth and satellite cell quiescence. *Development* **142**, 1242-1253 (2015).
41. Abou-Khalil, R., Mounier, R. & Chazaud, B. Regulation of myogenic stem cell behavior by vessel cells: the "menage a trois" of satellite cells, periendothelial cells and endothelial cells. *Cell cycle Georgetown, Tex* **9**, 892-896 (2010).
42. Liu, W., Wei-LaPierre, L., Klose, A., Dirksen, R.T. & Chakkalakal, J.V. Inducible depletion of adult skeletal muscle stem cells impairs the regeneration of neuromuscular junctions. *Elife* **4** (2015).
43. Redfern, P.A. Neuromuscular transmission in new-born rats. *J Physiol* **209**, 701-709 (1970).
44. Alonso-Martin, S. et al. Gene Expression Profiling of Muscle Stem Cells Identifies Novel Regulators of Postnatal Myogenesis. *Front Cell Dev Biol* **4**, 58 (2016).
45. Stark, D.A., Karvas, R.M., Siegel, A.L. & Cornelison, D.D. Eph/ephrin interactions modulate muscle satellite cell motility and patterning. *Development* **138**, 5279-5289 (2011).
46. Ladi, E. et al. The divergent DSL ligand Dll3 does not activate Notch signaling but cell autonomously attenuates signaling induced by other DSL ligands. *J Cell Biol* **170**, 983-992 (2005).
47. Geffers, I. et al. Divergent functions and distinct localization of the Notch ligands DLL1 and DLL3 in vivo. *J Cell Biol* **178**, 465-476 (2007).
48. Delfini, M.C., Hirsinger, E., Pourquie, O. & Duprez, D. Delta 1-activated notch inhibits muscle differentiation without affecting Myf5 and Pax3 expression in chick limb myogenesis. *Development* **127**, 5213-5224 (2000).

49. Hirsinger, E. et al. Notch signalling acts in postmitotic avian myogenic cells to control MyoD activation. *Development* **128**, 107-116 (2001).
50. Schuster-Gossler, K., Cordes, R. & Gossler, A. Premature myogenic differentiation and depletion of progenitor cells cause severe muscle hypotrophy in Delta1 mutants. *Proc Natl Acad Sci U S A* **104**, 537-542 (2007).
51. Vasyutina, E. et al. RBP-J (Rbpsuh) is essential to maintain muscle progenitor cells and to generate satellite cells. *Proc Natl Acad Sci U S A* **104**, 4443-4448 (2007).
52. Mourikis, P., Gopalakrishnan, S., Sambasivan, R. & Tajbakhsh, S. Cell-autonomous Notch activity maintains the temporal specification potential of skeletal muscle stem cells. *Development* **139**, 4536-4548 (2012).
53. Brohl, D. et al. Colonization of the satellite cell niche by skeletal muscle progenitor cells depends on Notch signals. *Developmental cell* **23**, 469-481 (2012).
54. Tajbakhsh, S. Skeletal muscle stem cells in developmental versus regenerative myogenesis. *Journal of internal medicine* **266**, 372-389 (2009).
55. White, R.B., Bierinx, A.S., Gnocchi, V.F. & Zammit, P.S. Dynamics of muscle fibre growth during postnatal mouse development. *BMC developmental biology* **10**, 21 (2010).
56. Katz, B. The Terminations of the Afferent Nerve Fibre in the Muscle Spindle of the Frog. *Philosophical Transactions of the Royal Society of London. Series B, Biological Sciences* **243**, 221-240 (1961).
57. Cheung, T.H. & Rando, T.A. Molecular regulation of stem cell quiescence. *Nature reviews* **14**, 329-340 (2013).
58. Holmberg, J. & Durbeej, M. Laminin-211 in skeletal muscle function. *Cell Adh Migr* **7**, 111-121 (2013).
59. Kohfeldt, E., Sasaki, T., Gohring, W. & Timpl, R. Nidogen-2: a new basement membrane protein with diverse binding properties. *J Mol Biol* **282**, 99-109 (1998).
60. Fox, J.W. et al. Recombinant nidogen consists of three globular domains and mediates binding of laminin to collagen type IV. *EMBO J* **10**, 3137-3146 (1991).
61. Ghadiali, R.S., Guimond, S.E., Turnbull, J.E. & Pisconti, A. Dynamic changes in heparan sulfate during muscle differentiation and ageing regulate myoblast cell fate and FGF2 signalling. *Matrix Biol* **59**, 54-68 (2017).
62. Gohring, W., Sasaki, T., Heldin, C.H. & Timpl, R. Mapping of the binding of platelet-derived growth factor to distinct domains of the basement membrane proteins BM-40 and perlecan and distinction from the BM-40 collagen-binding epitope. *Eur J Biochem* **255**, 60-66 (1998).
63. Cohn, R.D. et al. Disruption of DAG1 in differentiated skeletal muscle reveals a role for dystroglycan in muscle regeneration. *Cell* **110**, 639-648 (2002).
64. Blanco-Bose, W.E., Yao, C.C., Kramer, R.H. & Blau, H.M. Purification of mouse primary myoblasts based on alpha 7 integrin expression. *Experimental cell research* **265**, 212-220 (2001).
65. Dumont, N.A. et al. Dystrophin expression in muscle stem cells regulates their polarity and asymmetric division. *Nature medicine* **21**, 1455-1463 (2015).
66. Nunes, A.M. et al. Impaired fetal muscle development and JAK-STAT activation mark disease onset and progression in a mouse model for merosin-deficient congenital muscular dystrophy. *Hum Mol Genet* **26**, 2018-2033 (2017).
67. Vachon, P.H. et al. Integrins (alpha7beta1) in muscle function and survival. Disrupted expression in merosin-deficient congenital muscular dystrophy. *J Clin Invest* **100**, 1870-1881 (1997).
68. Rooney, J.E. et al. Severe muscular dystrophy in mice that lack dystrophin and alpha7 integrin. *J Cell Sci* **119**, 2185-2195 (2006).
69. Fukada, S. et al. Molecular signature of quiescent satellite cells in adult skeletal muscle. *Stem Cells* **25**, 2448-2459 (2007).
70. Xian, X., Gopal, S. & Couchman, J.R. Syndecans as receptors and organizers of the extracellular matrix. *Cell and tissue research* **339**, 31-46 (2010).
71. Carey, D.J. Syndecans: multifunctional cell-surface co-receptors. *Biochem J* **327 (Pt 1)**, 1-16 (1997).

72. Cornelison, D.D. et al. Essential and separable roles for Syndecan-3 and Syndecan-4 in skeletal muscle development and regeneration. *Genes & development* **18**, 2231-2236 (2004).
73. Pisconti, A. et al. Loss of niche-satellite cell interactions in syndecan-3 null mice alters muscle progenitor cell homeostasis improving muscle regeneration. *Skelet Muscle* **6**, 34 (2016).
74. Shea, K.L. et al. Sprouty1 regulates reversible quiescence of a self-renewing adult muscle stem cell pool during regeneration. *Cell Stem Cell* **6**, 117-129 (2010).
75. Pallafacchina, G. et al. An adult tissue-specific stem cell in its niche: a gene profiling analysis of in vivo quiescent and activated muscle satellite cells. *Stem cell research* **4**, 77-91 (2010).
76. Quarta, M. et al. An artificial niche preserves the quiescence of muscle stem cells and enhances their therapeutic efficacy. *Nat Biotechnol* **34**, 752-759 (2016).
77. Irintchev, A., Zeschnigk, M., Starzinski-Powitz, A. & Wernig, A. Expression pattern of M-cadherin in normal, denervated, and regenerating mouse muscles. *Developmental dynamics : an official publication of the American Association of Anatomists* **199**, 326-337 (1994).
78. Bornemann, A. & Schmalbruch, H. Immunocytochemistry of M-cadherin in mature and regenerating rat muscle. *The Anatomical record* **239**, 119-125 (1994).
79. Beauchamp, J.R. et al. Expression of CD34 and Myf5 defines the majority of quiescent adult skeletal muscle satellite cells. *J Cell Biol* **151**, 1221-1234 (2000).
80. Hollnagel, A., Grund, C., Franke, W.W. & Arnold, H.H. The cell adhesion molecule M-cadherin is not essential for muscle development and regeneration. *Mol Cell Biol* **22**, 4760-4770 (2002).
81. Krauss, R.S. Regulation of promyogenic signal transduction by cell-cell contact and adhesion. *Experimental cell research* **316**, 3042-3049 (2010).
82. Goel, A.J., Rieder, M.-K., Arnold, H.-H., Radice, G.L. & Krauss, R.S. Niche cadherins control the quiescence-to-activation transition in muscle stem cells. *Cell reports* **21**, 2236-2250 (2017).
83. Yamaguchi, M. et al. Calcitonin Receptor Signaling Inhibits Muscle Stem Cells from Escaping the Quiescent State and the Niche. *Cell reports* **13**, 302-314 (2015).
84. Bjornson, C.R. et al. Notch signaling is necessary to maintain quiescence in adult muscle stem cells. *Stem Cells* **30**, 232-242 (2012).
85. Wen, Y. et al. Constitutive Notch activation upregulates Pax7 and promotes the self-renewal of skeletal muscle satellite cells. *Mol Cell Biol* **32**, 2300-2311 (2012).
86. Pisconti, A., Cornelison, D.D., Olguin, H.C., Antwine, T.L. & Olwin, B.B. Syndecan-3 and Notch cooperate in regulating adult myogenesis. *J Cell Biol* **190**, 427-441 (2010).
87. Kim, J.H. et al. Sex hormones establish a reserve pool of adult muscle stem cells. *Nature cell biology* **18**, 930-940 (2016).
88. Baghdadi, M.B. et al. Reciprocal signalling by Notch–Collagen V–CALCR retains muscle stem cells in their niche. *Nature* **557**, 714 (2018).
89. Abou-Khalil, R. et al. Autocrine and paracrine angiopoietin 1/Tie-2 signaling promotes muscle satellite cell self-renewal. *Cell Stem Cell* **5**, 298-309 (2009).
90. Lukjanenko, L., Brachat, S., Pierrel, E., Lach-Trifilieff, E. & Feige, J.N. Genomic profiling reveals that transient adipogenic activation is a hallmark of mouse models of skeletal muscle regeneration. *PloS one* **8**, e71084 (2013).
91. Hardy, D. et al. Comparative Study of Injury Models for Studying Muscle Regeneration in Mice. *PloS one* **11**, e0147198 (2016).
92. Bischoff, R. Interaction between satellite cells and skeletal muscle fibers. *Development* **109**, 943-952 (1990).
93. Caldwell, C.J., Mattey, D.L. & Weller, R.O. Role of the basement membrane in the regeneration of skeletal muscle. *Neuropathol Appl Neurobiol* **16**, 225-238 (1990).
94. Koskinen, S.O. et al. Short-term effects of forced eccentric contractions on collagen synthesis and degradation in rat skeletal muscle. *Pflugers Arch* **444**, 59-72 (2002).
95. Schmalbruch, H. The morphology of regeneration of skeletal muscles in the rat. *Tissue Cell* **8**, 673-692 (1976).

96. Vracko, R. & Benditt, E.P. Basal lamina: the scaffold for orderly cell replacement. Observations on regeneration of injured skeletal muscle fibers and capillaries. *J Cell Biol* **55**, 406-419 (1972).
97. Webster, M.T., Manor, U., Lippincott-Schwartz, J. & Fan, C.M. Intravital Imaging Reveals Ghost Fibers as Architectural Units Guiding Myogenic Progenitors during Regeneration. *Cell Stem Cell* **18**, 243-252 (2016).
98. Sanes, J.R., Marshall, L.M. & McMahan, U.J. Reinnervation of muscle fiber basal lamina after removal of myofibers. Differentiation of regenerating axons at original synaptic sites. *J Cell Biol* **78**, 176-198 (1978).
99. Siegel, A.L., Atchison, K., Fisher, K.E., Davis, G.E. & Cornelison, D.D. 3D timelapse analysis of muscle satellite cell motility. *Stem Cells* **27**, 2527-2538 (2009).
100. Goetsch, S.C., Hawke, T.J., Gallardo, T.D., Richardson, J.A. & Garry, D.J. Transcriptional profiling and regulation of the extracellular matrix during muscle regeneration. *Physiological genomics* **14**, 261-271 (2003).
101. Kherif, S. et al. Expression of matrix metalloproteinases 2 and 9 in regenerating skeletal muscle: a study in experimentally injured and mdx muscles. *Developmental biology* **205**, 158-170 (1999).
102. Mann, C.J. et al. Aberrant repair and fibrosis development in skeletal muscle. *Skelet Muscle* **1**, 21 (2011).
103. Tidball, J.G., Dorshkind, K. & Wehling-Henricks, M. Shared signaling systems in myeloid cell-mediated muscle regeneration. *Development* **141**, 1184-1196 (2014).
104. Tidball, J.G. & Villalta, S.A. Regulatory interactions between muscle and the immune system during muscle regeneration. *American journal of physiology* **298**, R1173-1187 (2010).
105. Hindi, S.M. & Kumar, A. Toll-like receptor signalling in regenerative myogenesis: friend and foe. *J Pathol* **239**, 125-128 (2016).
106. Niethammer, P., Grabher, C., Look, A.T. & Mitchison, T.J. A tissue-scale gradient of hydrogen peroxide mediates rapid wound detection in zebrafish. *Nature* **459**, 996-999 (2009).
107. Brigitte, M. et al. Muscle resident macrophages control the immune cell reaction in a mouse model of notexin-induced myoinjury. *Arthritis and rheumatism* **62**, 268-279 (2010).
108. Zhang, J. et al. CD8 T cells are involved in skeletal muscle regeneration through facilitating MCP-1 secretion and Gr1(high) macrophage infiltration. *J Immunol* **193**, 5149-5160 (2014).
109. Sun, D. et al. Bone marrow-derived cell regulation of skeletal muscle regeneration. *FASEB J* **23**, 382-395 (2009).
110. Stoick-Cooper, C.L., Moon, R.T. & Weidinger, G. Advances in signaling in vertebrate regeneration as a prelude to regenerative medicine. *Genes & development* **21**, 1292-1315 (2007).
111. Heredia, J.E. et al. Type 2 innate signals stimulate fibro/adipogenic progenitors to facilitate muscle regeneration. *Cell* **153**, 376-388 (2013).
112. Arnold, L. et al. Inflammatory monocytes recruited after skeletal muscle injury switch into antiinflammatory macrophages to support myogenesis. *The Journal of experimental medicine* **204**, 1057-1069 (2007).
113. Varga, T. et al. Highly Dynamic Transcriptional Signature of Distinct Macrophage Subsets during Sterile Inflammation, Resolution, and Tissue Repair. *J Immunol* **196**, 4771-4782 (2016).
114. Saclier, M. et al. Differentially activated macrophages orchestrate myogenic precursor cell fate during human skeletal muscle regeneration. *Stem Cells* **31**, 384-396 (2013).
115. Tidball, J.G. Inflammatory processes in muscle injury and repair. *American journal of physiology* **288**, R345-353 (2005).
116. Palacios, D. et al. TNF/p38alpha/polycomb signaling to Pax7 locus in satellite cells links inflammation to the epigenetic control of muscle regeneration. *Cell Stem Cell* **7**, 455-469 (2010).
117. Acharyya, S. et al. TNF inhibits Notch-1 in skeletal muscle cells by Ezh2 and DNA methylation mediated repression: implications in duchenne muscular dystrophy. *PloS one* **5**, e12479 (2010).

118. Jennische, E., Ekberg, S. & Matejka, G.L. Expression of hepatocyte growth factor in growing and regenerating rat skeletal muscle. *Am J Physiol* **265**, C122-128 (1993).
119. Allen, R.E., Sheehan, S.M., Taylor, R.G., Kendall, T.L. & Rice, G.M. Hepatocyte growth factor activates quiescent skeletal muscle satellite cells in vitro. *J Cell Physiol* **165**, 307-312 (1995).
120. Tatsumi, R., Anderson, J.E., Nevoret, C.J., Halevy, O. & Allen, R.E. HGF/SF is present in normal adult skeletal muscle and is capable of activating satellite cells. *Developmental biology* **194**, 114-128 (1998).
121. Filippin, L.I. et al. Nitric oxide regulates the repair of injured skeletal muscle. *Nitric Oxide* **24**, 43-49 (2011).
122. Yamada, M. et al. Matrix metalloproteinase-2 mediates stretch-induced activation of skeletal muscle satellite cells in a nitric oxide-dependent manner. *Int J Biochem Cell Biol* **40**, 2183-2191 (2008).
123. Rodgers, J.T. et al. mTORC1 controls the adaptive transition of quiescent stem cells from G0 to G(Alert). *Nature* **510**, 393-396 (2014).
124. Rodgers, J.T., Schroeder, M.D., Ma, C. & Rando, T.A. HGFA Is an Injury-Regulated Systemic Factor that Induces the Transition of Stem Cells into GAlert. *Cell reports* **19**, 479-486 (2017).
125. Alfaro, L.A. et al. CD34 promotes satellite cell motility and entry into proliferation to facilitate efficient skeletal muscle regeneration. *Stem Cells* **29**, 2030-2041 (2011).
126. Suelves, M. et al. Plasmin activity is required for myogenesis in vitro and skeletal muscle regeneration in vivo. *Blood* **99**, 2835-2844 (2002).
127. Lluis, F. et al. Urokinase-dependent plasminogen activation is required for efficient skeletal muscle regeneration in vivo. *Blood* **97**, 1703-1711 (2001).
128. Alameddine, H.S. & Morgan, J.E. Matrix Metalloproteinases and Tissue Inhibitor of Metalloproteinases in Inflammation and Fibrosis of Skeletal Muscles. *J Neuromuscul Dis* **3**, 455-473 (2016).
129. Bobadilla, M. et al. MMP-10 is required for efficient muscle regeneration in mouse models of injury and muscular dystrophy. *Stem Cells* **32**, 447-461 (2014).
130. Nicholson, R., Murphy, G. & Breathnach, R. Human and rat malignant-tumor-associated mRNAs encode stromelysin-like metalloproteinases. *Biochemistry* **28**, 5195-5203 (1989).
131. Nakamura, H., Fujii, Y., Ohuchi, E., Yamamoto, E. & Okada, Y. Activation of the precursor of human stromelysin 2 and its interactions with other matrix metalloproteinases. *Eur J Biochem* **253**, 67-75 (1998).
132. Singh, P., Carraher, C. & Schwarzbauer, J.E. Assembly of fibronectin extracellular matrix. *Annual review of cell and developmental biology* **26**, 397-419 (2010).
133. Yennek, S., Burute, M., Thery, M. & Tajbakhsh, S. Cell adhesion geometry regulates non-random DNA segregation and asymmetric cell fates in mouse skeletal muscle stem cells. *Cell reports* **7**, 961-970 (2014).
134. Bernet, J.D. et al. p38 MAPK signaling underlies a cell-autonomous loss of stem cell self-renewal in skeletal muscle of aged mice. *Nature medicine* **20**, 265-271 (2014).
135. Le Grand, F., Jones, A.E., Seale, V., Scime, A. & Rudnicki, M.A. Wnt7a activates the planar cell polarity pathway to drive the symmetric expansion of satellite stem cells. *Cell Stem Cell* **4**, 535-547 (2009).
136. Gilbert, P.M. et al. Substrate elasticity regulates skeletal muscle stem cell self-renewal in culture. *Science (New York, N.Y* **329**, 1078-1081 (2010).
137. Yin, H., Price, F. & Rudnicki, M.A. Satellite cells and the muscle stem cell niche. *Physiol Rev* **93**, 23-67 (2013).
138. DiMario, J., Buffinger, N., Yamada, S. & Strohman, R.C. Fibroblast growth factor in the extracellular matrix of dystrophic (mdx) mouse muscle. *Science (New York, N.Y* **244**, 688-690 (1989).
139. Anderson, J.E., Mitchell, C.M., McGeachie, J.K. & Grounds, M.D. The time course of basic fibroblast growth factor expression in crush-injured skeletal muscles of SJL/J and BALB/c mice. *Experimental cell research* **216**, 325-334 (1995).
140. Chakkalakal, J.V., Jones, K.M., Basson, M.A. & Brack, A.S. The aged niche disrupts muscle stem cell quiescence. *Nature* **490**, 355-360 (2012).

141. Rao, N. et al. Fibroblasts influence muscle progenitor differentiation and alignment in contact independent and dependent manners in organized co-culture devices. *Biomed Microdevices* **15**, 161-169 (2013).
142. Hannon, K., Kudla, A.J., McAvoy, M.J., Clase, K.L. & Olwin, B.B. Differentially expressed fibroblast growth factors regulate skeletal muscle development through autocrine and paracrine mechanisms. *J Cell Biol* **132**, 1151-1159 (1996).
143. Flanagan-Steet, H., Hannon, K., McAvoy, M.J., Hullinger, R. & Olwin, B.B. Loss of FGF receptor 1 signaling reduces skeletal muscle mass and disrupts myofiber organization in the developing limb. *Developmental biology* **218**, 21-37 (2000).
144. Rapraeger, A.C., Krufka, A. & Olwin, B.B. Requirement of heparan sulfate for bFGF-mediated fibroblast growth and myoblast differentiation. *Science (New York, N.Y* **252**, 1705-1708 (1991).
145. Allen, R.E. & Boxhorn, L.K. Regulation of skeletal muscle satellite cell proliferation and differentiation by transforming growth factor-beta, insulin-like growth factor I, and fibroblast growth factor. *J Cell Physiol* **138**, 311-315 (1989).
146. Musaro, A. et al. Localized Igf-1 transgene expression sustains hypertrophy and regeneration in senescent skeletal muscle. *Nature genetics* **27**, 195-200 (2001).
147. Machida, S., Spangenburg, E.E. & Booth, F.W. Forkhead transcription factor FoxO1 transduces insulin-like growth factor's signal to p27Kip1 in primary skeletal muscle satellite cells. *J Cell Physiol* **196**, 523-531 (2003).
148. Chakravarthy, M.V., Abraha, T.W., Schwartz, R.J., Fiorotto, M.L. & Booth, F.W. Insulin-like growth factor-I extends in vitro replicative life span of skeletal muscle satellite cells by enhancing G1/S cell cycle progression via the activation of phosphatidylinositol 3'-kinase/Akt signaling pathway. *The Journal of biological chemistry* **275**, 35942-35952 (2000).
149. Chazaud, B. et al. Satellite cells attract monocytes and use macrophages as a support to escape apoptosis and enhance muscle growth. *J Cell Biol* **163**, 1133-1143 (2003).
150. Cheng, M., Nguyen, M.H., Fantuzzi, G. & Koh, T.J. Endogenous interferon-gamma is required for efficient skeletal muscle regeneration. *Am J Physiol Cell Physiol* **294**, C1183-1191 (2008).
151. Londhe, P. & Davie, J.K. Interferon-gamma resets muscle cell fate by stimulating the sequential recruitment of JARID2 and PRC2 to promoters to repress myogenesis. *Sci Signal* **6**, ra107 (2013).
152. Burzyn, D. et al. A special population of regulatory T cells potentiates muscle repair. *Cell* **155**, 1282-1295 (2013).
153. Kuswanto, W. et al. Poor Repair of Skeletal Muscle in Aging Mice Reflects a Defect in Local, Interleukin-33-Dependent Accumulation of Regulatory T Cells. *Immunity* **44**, 355-367 (2016).
154. Tidball, J.G. Regulation of muscle growth and regeneration by the immune system. *Nat Rev Immunol* **17**, 165-178 (2017).
155. Perdiguero, E. et al. p38/MKP-1-regulated AKT coordinates macrophage transitions and resolution of inflammation during tissue repair. *J Cell Biol* **195**, 307-322 (2011).
156. Tonkin, J. et al. Monocyte/Macrophage-derived IGF-1 Orchestrates Murine Skeletal Muscle Regeneration and Modulates Autocrine Polarization. *Mol Ther* **23**, 1189-1200 (2015).
157. Deng, B., Wehling-Henricks, M., Villalta, S.A., Wang, Y. & Tidball, J.G. IL-10 triggers changes in macrophage phenotype that promote muscle growth and regeneration. *J Immunol* **189**, 3669-3680 (2012).
158. Murphy, M.M., Lawson, J.A., Mathew, S.J., Hutcheson, D.A. & Kardon, G. Satellite cells, connective tissue fibroblasts and their interactions are crucial for muscle regeneration. *Development (Cambridge, England)* **138**, 3625-3637 (2011).
159. Joe, A.W. et al. Muscle injury activates resident fibro/adipogenic progenitors that facilitate myogenesis. *Nature cell biology* **12**, 153-163 (2010).
160. Uezumi, A., Fukada, S., Yamamoto, N., Takeda, S. & Tsuchida, K. Mesenchymal progenitors distinct from satellite cells contribute to ectopic fat cell formation in skeletal muscle. *Nature cell biology* **12**, 143-152 (2010).

161. Fiore, D. et al. Pharmacological blockage of fibro/adipogenic progenitor expansion and suppression of regenerative fibrogenesis is associated with impaired skeletal muscle regeneration. *Stem cell research* **17**, 161-169 (2016).
162. Scholz, D., Thomas, S., Sass, S. & Podzuweit, T. Angiogenesis and myogenesis as two facets of inflammatory post-ischemic tissue regeneration. *Mol Cell Biochem* **246**, 57-67 (2003).
163. Luque, E., Pena, J., Martin, P., Jimena, I. & Vaamonde, R. Capillary supply during development of individual regenerating muscle fibers. *Anatomia, histologia, embryologia* **24**, 87-89 (1995).
164. Wagatsuma, A. Endogenous expression of angiogenesis-related factors in response to muscle injury. *Mol Cell Biochem* **298**, 151-159 (2007).
165. Rhoads, R.P. et al. Satellite cell-mediated angiogenesis in vitro coincides with a functional hypoxia-inducible factor pathway. *Am J Physiol Cell Physiol* **296**, C1321-1328 (2009).
166. Birbrair, A. et al. Pericytes: multitasking cells in the regeneration of injured, diseased, and aged skeletal muscle. *Frontiers in aging neuroscience* **6**, 245 (2014).
167. Gutierrez, J. & Brandan, E. A novel mechanism of sequestering fibroblast growth factor 2 by glypican in lipid rafts, allowing skeletal muscle differentiation. *Mol Cell Biol* **30**, 1634-1649 (2010).
168. Brandan, E. & Gutierrez, J. Role of skeletal muscle proteoglycans during myogenesis. *Matrix Biol* **32**, 289-297 (2013).
169. Florini, J.R. et al. "Spontaneous" differentiation of skeletal myoblasts is dependent upon autocrine secretion of insulin-like growth factor-II. *The Journal of biological chemistry* **266**, 15917-15923 (1991).
170. Stewart, C.E., James, P.L., Fant, M.E. & Rotwein, P. Overexpression of insulin-like growth factor-II induces accelerated myoblast differentiation. *J Cell Physiol* **169**, 23-32 (1996).
171. Duan, C., Ren, H. & Gao, S. Insulin-like growth factors (IGFs), IGF receptors, and IGF-binding proteins: roles in skeletal muscle growth and differentiation. *Gen Comp Endocrinol* **167**, 344-351 (2010).
172. Varga, T. et al. Macrophage PPARgamma, a Lipid Activated Transcription Factor Controls the Growth Factor GDF3 and Skeletal Muscle Regeneration. *Immunity* **45**, 1038-1051 (2016).
173. Lemos, D.R. et al. Nilotinib reduces muscle fibrosis in chronic muscle injury by promoting TNF-mediated apoptosis of fibro/adipogenic progenitors. *Nature medicine* **21**, 786-794 (2015).
174. Dellavalle, A. et al. Pericytes of human skeletal muscle are myogenic precursors distinct from satellite cells. *Nature cell biology* **9**, 255-267 (2007).
175. Dellavalle, A. et al. Pericytes resident in postnatal skeletal muscle differentiate into muscle fibres and generate satellite cells. *Nature communications* **2**, 499 (2011).
176. Birbrair, A. et al. Role of pericytes in skeletal muscle regeneration and fat accumulation. *Stem Cells Dev* **22**, 2298-2314 (2013).
177. Pannerec, A., Marazzi, G. & Sassoon, D. Stem cells in the hood: the skeletal muscle niche. *Trends in molecular medicine* **18**, 599-606 (2012).
178. Goodell, M.A. & Rando, T.A. Stem cells and healthy aging. *Science (New York, N.Y* **350**, 1199-1204 (2015).
179. Blau, H.M., Cosgrove, B.D. & Ho, A.T. The central role of muscle stem cells in regenerative failure with aging. *Nature medicine* **21**, 854 (2015).
180. Lightfoot, A.P., McCormick, R., Nye, G.A. & McArdle, A. Mechanisms of skeletal muscle ageing; avenues for therapeutic intervention. *Curr Opin Pharmacol* **16**, 116-121 (2014).
181. Renault, V., Thornell, L.E., Eriksson, P.O., Butler-Browne, G. & Mouly, V. Regenerative potential of human skeletal muscle during aging. *Aging Cell* **1**, 132-139 (2002).
182. Day, K., Shefer, G., Shearer, A. & Yablonka-Reuveni, Z. The depletion of skeletal muscle satellite cells with age is concomitant with reduced capacity of single progenitors to produce reserve progeny. *Developmental biology* **340**, 330-343 (2010).
183. Shefer, G., Van de Mark, D.P., Richardson, J.B. & Yablonka-Reuveni, Z. Satellite-cell pool size does matter: defining the myogenic potency of aging skeletal muscle. *Developmental biology* **294**, 50-66 (2006).

184. Brack, A.S., Bildsoe, H. & Hughes, S.M. Evidence that satellite cell decrement contributes to preferential decline in nuclear number from large fibres during murine age-related muscle atrophy. *J Cell Sci* **118**, 4813-4821 (2005).
185. Verdijk, L.B. et al. Satellite cell content is specifically reduced in type II skeletal muscle fibers in the elderly. *Am J Physiol Endocrinol Metab* **292**, E151-157 (2007).
186. Shefer, G., Rauner, G., Yablonka-Reuveni, Z. & Benayahu, D. Reduced satellite cell numbers and myogenic capacity in aging can be alleviated by endurance exercise. *PloS one* **5**, e13307 (2010).
187. Sajko, S. et al. Frequency of M-cadherin-stained satellite cells declines in human muscles during aging. *J Histochem Cytochem* **52**, 179-185 (2004).
188. Fry, C.S. et al. Inducible depletion of satellite cells in adult, sedentary mice impairs muscle regenerative capacity without affecting sarcopenia. *Nature medicine* **21**, 76-80 (2015).
189. Collins, C.A., Zammit, P.S., Ruiz, A.P., Morgan, J.E. & Partridge, T.A. A population of myogenic stem cells that survives skeletal muscle aging. *Stem Cells* **25**, 885-894 (2007).
190. Collins, C.A. et al. Stem cell function, self-renewal, and behavioral heterogeneity of cells from the adult muscle satellite cell niche. *Cell* **122**, 289-301 (2005).
191. Hall, J.K., Banks, G.B., Chamberlain, J.S. & Olwin, B.B. Prevention of muscle aging by myofiber-associated satellite cell transplantation. *Sci Transl Med* **2**, 57ra83 (2010).
192. Fry, C.S., Kirby, T.J., Kosmac, K., McCarthy, J.J. & Peterson, C.A. Myogenic Progenitor Cells Control Extracellular Matrix Production by Fibroblasts during Skeletal Muscle Hypertrophy. *Cell Stem Cell* **20**, 56-69 (2017).
193. Sousa-Victor, P. & Munoz-Canoves, P. Regenerative decline of stem cells in sarcopenia. *Mol Aspects Med* **50**, 109-117 (2016).
194. Pawlikowski, B., Pulliam, C., Betta, N.D., Kardon, G. & Olwin, B.B. Pervasive satellite cell contribution to uninjured adult muscle fibers. *Skelet Muscle* **5**, 42 (2015).
195. Keefe, A.C. et al. Muscle stem cells contribute to myofibres in sedentary adult mice. *Nature communications* **6**, 7087 (2015).
196. Rando, T.A. Stem cells, ageing and the quest for immortality. *Nature* **441**, 1080-1086 (2006).
197. Ponsot, E., Lexell, J. & Kadi, F. Skeletal muscle telomere length is not impaired in healthy physically active old women and men. *Muscle Nerve* **37**, 467-472 (2008).
198. Li, J., Han, S., Cousin, W. & Conboy, I.M. Age-specific functional epigenetic changes in p21 and p16 in injury-activated satellite cells. *Stem Cells* **33**, 951-961 (2015).
199. Price, F.D. et al. Inhibition of JAK-STAT signaling stimulates adult satellite cell function. *Nature medicine* **20**, 1174-1181 (2014).
200. Tierney, M.T. et al. STAT3 signaling controls satellite cell expansion and skeletal muscle repair. *Nature medicine* **20**, 1182-1186 (2014).
201. Cosgrove, B.D. et al. Rejuvenation of the muscle stem cell population restores strength to injured aged muscles. *Nature medicine* **20**, 255-264 (2014).
202. Carlson, B.M. & Faulkner, J.A. Muscle transplantation between young and old rats: age of host determines recovery. *Am J Physiol* **256**, C1262-1266 (1989).
203. Conboy, I.M. et al. Rejuvenation of aged progenitor cells by exposure to a young systemic environment. *Nature* **433**, 760-764 (2005).
204. Conboy, I.M., Conboy, M.J., Smythe, G.M. & Rando, T.A. Notch-mediated restoration of regenerative potential to aged muscle. *Science (New York, N.Y* **302**, 1575-1577 (2003).
205. Corbu, A. et al. Satellite cell characterization from aging human muscle. *Neurol Res* **32**, 63-72 (2010).
206. Alsharidah, M. et al. Primary human muscle precursor cells obtained from young and old donors produce similar proliferative, differentiation and senescent profiles in culture. *Aging Cell* **12**, 333-344 (2013).
207. Carlson, M.E., Hsu, M. & Conboy, I.M. Imbalance between pSmad3 and Notch induces CDK inhibitors in old muscle stem cells. *Nature* **454**, 528-532 (2008).
208. Carlson, M.E. et al. Relative roles of TGF-beta1 and Wnt in the systemic regulation and aging of satellite cell responses. *Aging Cell* **8**, 676-689 (2009).
209. Egerman, M.A. et al. GDF11 Increases with Age and Inhibits Skeletal Muscle Regeneration. *Cell Metab* **22**, 164-174 (2015).

210. Hinken, A.C. et al. Lack of evidence for GDF 11 as a rejuvenator of aged skeletal muscle satellite cells. *Aging cell* **15**, 582-584 (2016).
211. Sinha, M. et al. Restoring systemic GDF11 levels reverses age-related dysfunction in mouse skeletal muscle. *Science (New York, N.Y* **344**, 649-652 (2014).
212. Jamaiyar, A. et al. The versatility and paradox of GDF 11. *Pharmacology & therapeutics* **175**, 28-34 (2017).
213. Schafer, M.J. et al. Quantification of GDF11 and myostatin in human aging and cardiovascular disease. *Cell metabolism* **23**, 1207-1215 (2016).
214. Turnbull, J., Powell, A. & Guimond, S. Heparan sulfate: decoding a dynamic multifunctional cell regulator. *Trends Cell Biol* **11**, 75-82 (2001).
215. Brack, A.S. et al. Increased Wnt signaling during aging alters muscle stem cell fate and increases fibrosis. *Science (New York, N.Y* **317**, 807-810 (2007).
216. Stearns-Reider, K.M. et al. Aging of the skeletal muscle extracellular matrix drives a stem cell fibrogenic conversion. *Aging Cell* **16**, 518-528 (2017).
217. Mueller, A.A., van Velthoven, C.T., Fukumoto, K.D., Cheung, T.H. & Rando, T.A. Intronic polyadenylation of PDGFRalpha in resident stem cells attenuates muscle fibrosis. *Nature* **540**, 276-279 (2016).
218. Hearon, C.M., Jr. & Dinenno, F.A. Regulation of skeletal muscle blood flow during exercise in ageing humans. *J Physiol* **594**, 2261-2273 (2016).
219. Le Moal, E. et al. Redox Control of Skeletal Muscle Regeneration. *Antioxid Redox Signal* (2017).
220. Brune, B. et al. Redox control of inflammation in macrophages. *Antioxid Redox Signal* **19**, 595-637 (2013).
221. Franceschi, C. & Campisi, J. Chronic inflammation (inflammaging) and its potential contribution to age-associated diseases. *J Gerontol A Biol Sci Med Sci* **69 Suppl 1**, S4-9 (2014).
222. Coletti, D., Moresi, V., Adamo, S., Molinaro, M. & Sassoon, D. Tumor necrosis factor-alpha gene transfer induces cachexia and inhibits muscle regeneration. *Genesis* **43**, 120-128 (2005).
223. Coletti, D., Yang, E., Marazzi, G. & Sassoon, D. TNFalpha inhibits skeletal myogenesis through a PW1-dependent pathway by recruitment of caspase pathways. *EMBO J* **21**, 631-642 (2002).
224. Guttridge, D.C., Mayo, M.W., Madrid, L.V., Wang, C.Y. & Baldwin, A.S., Jr. NF-kappaB-induced loss of MyoD messenger RNA: possible role in muscle decay and cachexia. *Science (New York, N.Y* **289**, 2363-2366 (2000).
225. Miller, S.C., Ito, H., Blau, H.M. & Torti, F.M. Tumor necrosis factor inhibits human myogenesis in vitro. *Mol Cell Biol* **8**, 2295-2301 (1988).
226. Degens, H. The role of systemic inflammation in age-related muscle weakness and wasting. *Scand J Med Sci Sports* **20**, 28-38 (2010).
227. McKay, B.R. et al. Elevated SOCS3 and altered IL-6 signaling is associated with age-related human muscle stem cell dysfunction. *Am J Physiol Cell Physiol* **304**, C717-728 (2013).
228. Paliwal, P., Pishesha, N., Wijaya, D. & Conboy, I.M. Age dependent increase in the levels of osteopontin inhibits skeletal muscle regeneration. *Aging (Albany NY)* **4**, 553-566 (2012).
229. Brack, A.S., Conboy, I.M., Conboy, M.J., Shen, J. & Rando, T.A. A temporal switch from notch to Wnt signaling in muscle stem cells is necessary for normal adult myogenesis. *Cell stem cell* **2**, 50-59 (2008).
230. Conboy, I.M., Conboy, M.J., Smythe, G.M. & Rando, T.A. Notch-mediated restoration of regenerative potential to aged muscle. *Science (New York, N.Y* **302**, 1575-1577 (2003).
231. Brack, A.S. et al. Increased Wnt signaling during aging alters muscle stem cell fate and increases fibrosis. *Science (New York, N.Y* **317**, 807-810 (2007).
232. Bouché, M., Muñoz-Cánoves, P., Rossi, F. & Coletti, D. Inflammation in muscle repair, aging, and myopathies. *BioMed research international* **2014** (2014).
233. Sousa-Victor, P. et al. Geriatric muscle stem cells switch reversible quiescence into senescence. *Nature* **506**, 316 (2014).

234. Cosgrove, B.D. et al. Rejuvenation of the muscle stem cell population restores strength to injured aged muscles. *Nature medicine* **20**, 255 (2014).
235. Chakkalakal, J.V., Jones, K.M., Basson, M.A. & Brack, A.S. The aged niche disrupts muscle stem cell quiescence. *Nature* **490**, 355 (2012).
236. Sahenk, Z. & Mendell, J.R. The muscular dystrophies: distinct pathogenic mechanisms invite novel therapeutic approaches. *Curr Rheumatol Rep* **13**, 199-207 (2011).
237. Tidball, J.G. & Wehling-Henricks, M. Damage and inflammation in muscular dystrophy: potential implications and relationships with autoimmune myositis. *Curr Opin Rheumatol* **17**, 707-713 (2005).
238. Dadgar, S. et al. Asynchronous remodeling is a driver of failed regeneration in Duchenne muscular dystrophy. *J Cell Biol* **207**, 139-158 (2014).
239. Myllyla, R., Myllyla, V.V., Tolonen, U. & Kivirikko, K.I. Changes in collagen metabolism in diseased muscle. I. Biochemical studies. *Arch Neurol* **39**, 752-755 (1982).
240. Peltonen, L., Myllyla, R., Tolonen, U. & Myllyla, V.V. Changes in collagen metabolism in diseased muscle. II. Immunohistochemical studies. *Arch Neurol* **39**, 756-759 (1982).
241. Ionasescu, V. & Ionasescu, R. Increased collagen synthesis by Duchenne myogenic clones. *J Neurol Sci* **54**, 79-87 (1982).
242. Caceres, S. et al. Synthesis of proteoglycans is augmented in dystrophic mdx mouse skeletal muscle. *Eur J Cell Biol* **79**, 173-181 (2000).
243. Alvarez, K., Fadic, R. & Brandan, E. Augmented synthesis and differential localization of heparan sulfate proteoglycans in Duchenne muscular dystrophy. *J Cell Biochem* **85**, 703-713 (2002).
244. von Moers, A. et al. Increased mRNA expression of tissue inhibitors of metalloproteinase-1 and -2 in Duchenne muscular dystrophy. *Acta Neuropathol* **109**, 285-293 (2005).
245. Sun, G.L., Zhao, S., Li, P. & Jiang, H.K. Expression of tissue inhibitor of metalloproteinase-1 in progression muscular dystrophy. *Neurosci Bull* **22**, 85-90 (2006).
246. Fukushima, K. et al. Activation and localization of matrix metalloproteinase-2 and -9 in the skeletal muscle of the muscular dystrophy dog (CXMDJ). *BMC Musculoskelet Disord* **8**, 54 (2007).
247. Heydemann, A. et al. Latent TGF-beta-binding protein 4 modifies muscular dystrophy in mice. *J Clin Invest* **119**, 3703-3712 (2009).
248. Arecco, N. et al. Elastase levels and activity are increased in dystrophic muscle and impair myoblast cell survival, proliferation and differentiation. *Sci Rep* **6**, 24708 (2016).
249. Suelves, M. et al. uPA deficiency exacerbates muscular dystrophy in MDX mice. *J Cell Biol* **178**, 1039-1051 (2007).
250. Ardite, E. et al. PAI-1-regulated miR-21 defines a novel age-associated fibrogenic pathway in muscular dystrophy. *J Cell Biol* **196**, 163-175 (2012).
251. Yoshida, T. et al. Angiotensin II inhibits satellite cell proliferation and prevents skeletal muscle regeneration. *The Journal of biological chemistry* **288**, 23823-23832 (2013).
252. Painemal, P., Acuna, M.J., Riquelme, C., Brandan, E. & Cabello-Verrugio, C. Transforming growth factor type beta 1 increases the expression of angiotensin II receptor type 2 by a SMAD- and p38 MAPK-dependent mechanism in skeletal muscle. *Biofactors* **39**, 467-475 (2013).
253. Vial, C. et al. Skeletal muscle cells express the profibrotic cytokine connective tissue growth factor (CTGF/CCN2), which induces their dedifferentiation. *J Cell Physiol* **215**, 410-421 (2008).
254. Meyer-Hoffert, U. & Wiedow, O. Neutrophil serine proteases: mediators of innate immune responses. *Curr Opin Hematol* **18**, 19-24 (2011).
255. Clancy, D.M., Henry, C.M., Sullivan, G.P. & Martin, S.J. Neutrophil extracellular traps can serve as platforms for processing and activation of IL-1 family cytokines. *FEBS J* (2017).
256. Chevessier, F., Hantai, D. & Verdiere-Sahuque, M. Expression of the thrombin receptor (PAR-1) during rat skeletal muscle differentiation. *J Cell Physiol* **189**, 152-161 (2001).
257. Chinni, C. et al. Protease-activated receptor-2 mediates proliferative responses in skeletal myoblasts. *J Cell Sci* **113 Pt 24**, 4427-4433 (2000).

258. Viloria, K. & Hill, N.J. Embracing the complexity of matricellular proteins: the functional and clinical significance of splice variation. *Biomol Concepts* **7**, 117-132 (2016).
259. Holland, A. et al. Label-free mass spectrometric analysis of the mdx-4cv diaphragm identifies the matricellular protein periostin as a potential factor involved in dystrophinopathy-related fibrosis. *Proteomics* **15**, 2318-2331 (2015).
260. Holland, A., Murphy, S., Dowling, P. & Ohlendieck, K. Pathoproteomic profiling of the skeletal muscle matrisome in dystrophinopathy associated myofibrosis. *Proteomics* **16**, 345-366 (2016).
261. Thakur, R. & Mishra, D.P. Matrix reloaded: CCN, tenascin and SIBLING group of matricellular proteins in orchestrating cancer hallmark capabilities. *Pharmacol Ther* **168**, 61-74 (2016).
262. Lorts, A., Schwanekamp, J.A., Baudino, T.A., McNally, E.M. & Molkentin, J.D. Deletion of periostin reduces muscular dystrophy and fibrosis in mice by modulating the transforming growth factor-beta pathway. *Proc Natl Acad Sci U S A* **109**, 10978-10983 (2012).
263. Riquelme, C. et al. Antisense inhibition of decorin expression in myoblasts decreases cell responsiveness to transforming growth factor beta and accelerates skeletal muscle differentiation. *The Journal of biological chemistry* **276**, 3589-3596 (2001).
264. Cabello-Verrugio, C. & Brandan, E. A novel modulatory mechanism of transforming growth factor-beta signaling through decorin and LRP-1. *The Journal of biological chemistry* **282**, 18842-18850 (2007).
265. Goetsch, K.P. & Niesler, C.U. The extracellular matrix regulates the effect of decorin and transforming growth factor beta-2 (TGF-beta2) on myoblast migration. *Biochem Biophys Res Commun* **479**, 351-357 (2016).
266. Miura, T. et al. Decorin binds myostatin and modulates its activity to muscle cells. *Biochem Biophys Res Commun* **340**, 675-680 (2006).
267. Gutierrez, J., Osses, N. & Brandan, E. Changes in secreted and cell associated proteoglycan synthesis during conversion of myoblasts to osteoblasts in response to bone morphogenetic protein-2: role of decorin in cell response to BMP-2. *J Cell Physiol* **206**, 58-67 (2006).
268. Vial, C., Gutierrez, J., Santander, C., Cabrera, D. & Brandan, E. Decorin interacts with connective tissue growth factor (CTGF)/CCN2 by LRR12 inhibiting its biological activity. *The Journal of biological chemistry* **286**, 24242-24252 (2011).
269. Vidal, B. et al. Amelioration of Duchenne muscular dystrophy in mdx mice by elimination of matrix-associated fibrin-driven inflammation coupled to the alphaMbeta2 leukocyte integrin receptor. *Hum Mol Genet* **21**, 1989-2004 (2012).
270. Villalta, S.A., Rosenberg, A.S. & Bluestone, J.A. The immune system in Duchenne muscular dystrophy: Friend or foe. *Rare Dis* **3**, e1010966 (2015).
271. McArdle, A., Foxley, A., Edwards, R.H. & Jackson, M.J. Prostaglandin metabolism in dystrophin-deficient MDX mouse muscle. *Biochem Soc Trans* **19**, 177S (1991).
272. Okinaga, T. et al. Induction of hematopoietic prostaglandin D synthase in hyalinated necrotic muscle fibers: its implication in grouped necrosis. *Acta Neuropathol* **104**, 377-384 (2002).
273. Nakagawa, T. et al. A prostaglandin D2 metabolite is elevated in the urine of Duchenne muscular dystrophy patients and increases further from 8 years old. *Clin Chim Acta* **423**, 10-14 (2013).
274. Kuru, S. et al. Expression of tumor necrosis factor-alpha in regenerating muscle fibers in inflammatory and non-inflammatory myopathies. *Acta Neuropathol* **105**, 217-224 (2003).
275. Kumar, A. & Boriek, A.M. Mechanical stress activates the nuclear factor-kappaB pathway in skeletal muscle fibers: a possible role in Duchenne muscular dystrophy. *FASEB J* **17**, 386-396 (2003).
276. Messina, S. et al. Activation of NF-kappaB pathway in Duchenne muscular dystrophy: relation to age. *Acta Myol* **30**, 16-23 (2011).
277. Villalta, S.A. et al. Interleukin-10 reduces the pathology of mdx muscular dystrophy by deactivating M1 macrophages and modulating macrophage phenotype. *Hum Mol Genet* **20**, 790-805 (2011).
278. Villalta, S.A., Nguyen, H.X., Deng, B., Gotoh, T. & Tidball, J.G. Shifts in macrophage phenotypes and macrophage competition for arginine metabolism affect the severity of muscle pathology in muscular dystrophy. *Hum Mol Genet* **18**, 482-496 (2009).

279. Acharyya, S. et al. Interplay of IKK/NF-kappaB signaling in macrophages and myofibers promotes muscle degeneration in Duchenne muscular dystrophy. *J Clin Invest* **117**, 889-901 (2007).
280. Radley, H.G., Davies, M.J. & Grounds, M.D. Reduced muscle necrosis and long-term benefits in dystrophic mdx mice after cV1q (blockade of TNF) treatment. *Neuromuscul Disord* **18**, 227-238 (2008).
281. Villalta, S.A., Deng, B., Rinaldi, C., Wehling-Henricks, M. & Tidball, J.G. IFN-gamma promotes muscle damage in the mdx mouse model of Duchenne muscular dystrophy by suppressing M2 macrophage activation and inhibiting muscle cell proliferation. *J Immunol* **187**, 5419-5428 (2011).
282. Wehling-Henricks, M. et al. Major basic protein-1 promotes fibrosis of dystrophic muscle and attenuates the cellular immune response in muscular dystrophy. *Hum Mol Genet* **17**, 2280-2292 (2008).
283. Wehling, M., Spencer, M.J. & Tidball, J.G. A nitric oxide synthase transgene ameliorates muscular dystrophy in mdx mice. *J Cell Biol* **155**, 123-131 (2001).
284. Muller, C. & Kapr, J. [Deepening of the socialist model of physician-patient relations]. *Cesk Zdrav* **23**, 68-71 (1975).
285. Wehling-Henricks, M., Lee, J.J. & Tidball, J.G. Prednisolone decreases cellular adhesion molecules required for inflammatory cell infiltration in dystrophin-deficient skeletal muscle. *Neuromuscul Disord* **14**, 483-490 (2004).
286. Hussein, M.R. et al. The effects of glucocorticoid therapy on the inflammatory and dendritic cells in muscular dystrophies. *Int J Exp Pathol* **87**, 451-461 (2006).
287. Manzur, A.Y., Kuntzer, T., Pike, M. & Swan, A. Glucocorticoid corticosteroids for Duchenne muscular dystrophy. *Cochrane Database Syst Rev*, CD003725 (2008).
288. D'Souza, D.M., Al-Sajee, D. & Hawke, T.J. Diabetic myopathy: impact of diabetes mellitus on skeletal muscle progenitor cells. *Front Physiol* **4**, 379 (2013).
289. Nguyen, M.H., Cheng, M. & Koh, T.J. Impaired muscle regeneration in ob/ob and db/db mice. *ScientificWorldJournal* **11**, 1525-1535 (2011).
290. Peterson, J.M., Bryner, R.W. & Alway, S.E. Satellite cell proliferation is reduced in muscles of obese Zucker rats but restored with loading. *Am J Physiol Cell Physiol* **295**, C521-528 (2008).
291. Krause, M.P. et al. Impaired macrophage and satellite cell infiltration occurs in a muscle-specific fashion following injury in diabetic skeletal muscle. *PloS one* **8**, e70971 (2013).
292. Krause, M.P., Moradi, J., Nissar, A.A., Riddell, M.C. & Hawke, T.J. Inhibition of plasminogen activator inhibitor-1 restores skeletal muscle regeneration in untreated type 1 diabetic mice. *Diabetes* **60**, 1964-1972 (2011).
293. Aragno, M. et al. Oxidative stress impairs skeletal muscle repair in diabetic rats. *Diabetes* **53**, 1082-1088 (2004).
294. Jeong, J., Conboy, M.J. & Conboy, I.M. Pharmacological inhibition of myostatin/TGF-beta receptor/pSmad3 signaling rescues muscle regenerative responses in mouse model of type 1 diabetes. *Acta Pharmacol Sin* **34**, 1052-1060 (2013).
295. Nunan, R., Harding, K.G. & Martin, P. Clinical challenges of chronic wounds: searching for an optimal animal model to recapitulate their complexity. *Dis Model Mech* **7**, 1205-1213 (2014).
296. Henriksen, E.J., Diamond-Stanic, M.K. & Marchionne, E.M. Oxidative stress and the etiology of insulin resistance and type 2 diabetes. *Free Radic Biol Med* **51**, 993-999 (2011).
297. Zou, M.H., Shi, C. & Cohen, R.A. Oxidation of the zinc-thiolate complex and uncoupling of endothelial nitric oxide synthase by peroxynitrite. *J Clin Invest* **109**, 817-826 (2002).
298. Berria, R. et al. Increased collagen content in insulin-resistant skeletal muscle. *Am J Physiol Endocrinol Metab* **290**, E560-565 (2006).
299. Richardson, D.K. et al. Lipid infusion decreases the expression of nuclear encoded mitochondrial genes and increases the expression of extracellular matrix genes in human skeletal muscle. *The Journal of biological chemistry* **280**, 10290-10297 (2005).
300. Hong, E.G. et al. Interleukin-10 prevents diet-induced insulin resistance by attenuating macrophage and cytokine response in skeletal muscle. *Diabetes* **58**, 2525-2535 (2009).

301. Watts, R., McAinch, A.J., Dixon, J.B., O'Brien, P.E. & Cameron-Smith, D. Increased Smad signaling and reduced MRF expression in skeletal muscle from obese subjects. *Obesity (Silver Spring)* **21**, 525-528 (2013).
302. Chiu, C.Y. et al. Advanced glycation end-products induce skeletal muscle atrophy and dysfunction in diabetic mice via a RAGE-mediated, AMPK-down-regulated, Akt pathway. *J Pathol* **238**, 470-482 (2016).
303. Morley, J.E., Thomas, D.R. & Wilson, M.M. Cachexia: pathophysiology and clinical relevance. *Am J Clin Nutr* **83**, 735-743 (2006).
304. Kuschel, R., Yablonka-Reuveni, Z. & Bornemann, A. Satellite cells on isolated myofibers from normal and denervated adult rat muscle. *J Histochem Cytochem* **47**, 1375-1384 (1999).
305. Verdijk, L.B. et al. Reduced satellite cell numbers with spinal cord injury and aging in humans. *Med Sci Sports Exerc* **44**, 2322-2330 (2012).
306. Mitchell, P.O. & Pavlath, G.K. Skeletal muscle atrophy leads to loss and dysfunction of muscle precursor cells. *Am J Physiol Cell Physiol* **287**, C1753-1762 (2004).
307. Ferreira, R. et al. Skeletal muscle atrophy increases cell proliferation in mice gastrocnemius during the first week of hindlimb suspension. *Eur J Appl Physiol* **97**, 340-346 (2006).
308. He, W.A. et al. NF-kappaB-mediated Pax7 dysregulation in the muscle microenvironment promotes cancer cachexia. *J Clin Invest* **123**, 4821-4835 (2013).
309. Acharyya, S. et al. Dystrophin glycoprotein complex dysfunction: a regulatory link between muscular dystrophy and cancer cachexia. *Cancer Cell* **8**, 421-432 (2005).
310. Schakman, O., Kalista, S., Barbe, C., Loumaye, A. & Thissen, J.P. Glucocorticoid-induced skeletal muscle atrophy. *Int J Biochem Cell Biol* **45**, 2163-2172 (2013).
311. Brzeszczynska, J. et al. Loss of oxidative defense and potential blockade of satellite cell maturation in the skeletal muscle of patients with cancer but not in the healthy elderly. *Aging (Albany NY)* **8**, 1690-1702 (2016).
312. Murphy, K.T. et al. Antibody-directed myostatin inhibition enhances muscle mass and function in tumor-bearing mice. *American journal of physiology* **301**, R716-726 (2011).
313. Zhou, X. et al. Reversal of cancer cachexia and muscle wasting by ActRIIB antagonism leads to prolonged survival. *Cell* **142**, 531-543 (2010).
314. Anker, S.D. et al. Prognostic importance of weight loss in chronic heart failure and the effect of treatment with angiotensin-converting-enzyme inhibitors: an observational study. *Lancet* **361**, 1077-1083 (2003).
315. Sanders, P.M., Russell, S.T. & Tisdale, M.J. Angiotensin II directly induces muscle protein catabolism through the ubiquitin-proteasome proteolytic pathway and may play a role in cancer cachexia. *Br J Cancer* **93**, 425-434 (2005).
316. Beutler, B., Mahoney, J., Le Trang, N., Pekala, P. & Cerami, A. Purification of cachectin, a lipoprotein lipase-suppressing hormone secreted by endotoxin-induced RAW 264.7 cells. *The Journal of experimental medicine* **161**, 984-995 (1985).
317. Di Francescomarino, S., Sciartilli, A., Di Valerio, V., Di Baldassarre, A. & Gallina, S. The effect of physical exercise on endothelial function. *Sports Med* **39**, 797-812 (2009).
318. Groen, B.B. et al. Skeletal muscle capillary density and microvascular function are compromised with aging and type 2 diabetes. *J Appl Physiol (1985)* **116**, 998-1005 (2014).
319. Ryan, N.A. et al. Lower skeletal muscle capillarization and VEGF expression in aged vs. young men. *J Appl Physiol (1985)* **100**, 178-185 (2006).
320. Franzoni, F. et al. Effects of age and physical fitness on microcirculatory function. *Clin Sci (Lond)* **106**, 329-335 (2004).
321. Green, D.J., Maiorana, A., O'Driscoll, G. & Taylor, R. Effect of exercise training on endothelium-derived nitric oxide function in humans. *J Physiol* **561**, 1-25 (2004).
322. Sessa, W.C. Molecular control of blood flow and angiogenesis: role of nitric oxide. *J Thromb Haemost* **7 Suppl 1**, 35-37 (2009).
323. Nyberg, M. et al. Lifelong physical activity prevents an age-related reduction in arterial and skeletal muscle nitric oxide bioavailability in humans. *J Physiol* **590**, 5361-5370 (2012).
324. Gustafsson, T. & Kraus, W.E. Exercise-induced angiogenesis-related growth and transcription factors in skeletal muscle, and their modification in muscle pathology. *Front Biosci* **6**, D75-89 (2001).

325. Reuben, D.B., Judd-Hamilton, L., Harris, T.B., Seeman, T.E. & MacArthur Studies of Successful, A. The associations between physical activity and inflammatory markers in high-functioning older persons: MacArthur Studies of Successful Aging. *J Am Geriatr Soc* **51**, 1125-1130 (2003).
326. Hollander, J. et al. Superoxide dismutase gene expression is activated by a single bout of exercise in rat skeletal muscle. *Pflugers Arch* **442**, 426-434 (2001).
327. McArdle, A. & Jackson, M.J. Exercise, oxidative stress and ageing. *J Anat* **197 Pt 4**, 539-541 (2000).
328. Dennis, R.A. et al. Aging alters gene expression of growth and remodeling factors in human skeletal muscle both at rest and in response to acute resistance exercise. *Physiological genomics* **32**, 393-400 (2008).
329. Han, X.Y. et al. Increased mRNAs for procollagens and key regulating enzymes in rat skeletal muscle following downhill running. *Pflugers Arch* **437**, 857-864 (1999).
330. Kjaer, M. et al. Extracellular matrix adaptation of tendon and skeletal muscle to exercise. *J Anat* **208**, 445-450 (2006).
331. Rullman, E. et al. A single bout of exercise activates matrix metalloproteinase in human skeletal muscle. *J Appl Physiol (1985)* **102**, 2346-2351 (2007).
332. Garg, K. & Boppart, M.D. Influence of exercise and aging on extracellular matrix composition in the skeletal muscle stem cell niche. *J Appl Physiol (1985)* **121**, 1053-1058 (2016).
333. Kovanen, V. & Suominen, H. Effects of age and life-long endurance training on the passive mechanical properties of rat skeletal muscle. *Compr Gerontol A* **2**, 18-23 (1988).
334. Lacraz, G. et al. Correction: Increased Stiffness in Aged Skeletal Muscle Impairs Muscle Progenitor Cell Proliferative Activity. *PloS one* **11**, e0167661 (2016).
335. Gosselin, L.E., Adams, C., Cotter, T.A., McCormick, R.J. & Thomas, D.P. Effect of exercise training on passive stiffness in locomotor skeletal muscle: role of extracellular matrix. *J Appl Physiol (1985)* **85**, 1011-1016 (1998).
336. Biressi, S., Miyabara, E.H., Gopinath, S.D., Carlig, P.M. & Rando, T.A. A Wnt-TGFbeta2 axis induces a fibrogenic program in muscle stem cells from dystrophic mice. *Sci Transl Med* **6**, 267ra176 (2014).
337. Li, H. et al. Customized platelet-rich plasma with transforming growth factor beta1 neutralization antibody to reduce fibrosis in skeletal muscle. *Biomaterials* **87**, 147-156 (2016).
338. Cabrera, D. et al. Andrographolide attenuates skeletal muscle dystrophy in mdx mice and increases efficiency of cell therapy by reducing fibrosis. *Skelet Muscle* **4**, 6 (2014).
339. Gosselin, L.E., Williams, J.E., Personius, K. & Farkas, G.A. A comparison of factors associated with collagen metabolism in different skeletal muscles from dystrophic (mdx) mice: impact of pirfenidone. *Muscle Nerve* **35**, 208-216 (2007).
340. Morales, M.G. et al. Reducing CTGF/CCN2 slows down mdx muscle dystrophy and improves cell therapy. *Hum Mol Genet* **22**, 4938-4951 (2013).
341. Murphy, A.M., Wong, A.L. & Bezuhly, M. Modulation of angiotensin II signaling in the prevention of fibrosis. *Fibrogenesis Tissue Repair* **8**, 7 (2015).
342. Elbaz, M. et al. Losartan, a therapeutic candidate in congenital muscular dystrophy: studies in the dy(2J) /dy(2J) mouse. *Ann Neurol* **71**, 699-708 (2012).
343. Bish, L.T. et al. Chronic losartan administration reduces mortality and preserves cardiac but not skeletal muscle function in dystrophic mice. *PloS one* **6**, e20856 (2011).
344. Spurney, C.F. et al. Losartan decreases cardiac muscle fibrosis and improves cardiac function in dystrophin-deficient mdx mice. *J Cardiovasc Pharmacol Ther* **16**, 87-95 (2011).
345. Meinen, S., Lin, S. & Ruegg, M.A. Angiotensin II type 1 receptor antagonists alleviate muscle pathology in the mouse model for laminin-alpha2-deficient congenital muscular dystrophy (MDC1A). *Skelet Muscle* **2**, 18 (2012).
346. Cohn, R.D. et al. Angiotensin II type 1 receptor blockade attenuates TGF-beta-induced failure of muscle regeneration in multiple myopathic states. *Nature medicine* **13**, 204-210 (2007).
347. Rafael-Fortney, J.A. et al. Early treatment with lisinopril and spironolactone preserves cardiac and skeletal muscle in Duchenne muscular dystrophy mice. *Circulation* **124**, 582-588 (2011).
348. Angelini, C. The role of corticosteroids in muscular dystrophy: a critical appraisal. *Muscle Nerve* **36**, 424-435 (2007).

349. Anderson, J.E., Weber, M. & Vargas, C. Deflazacort increases laminin expression and myogenic repair, and induces early persistent functional gain in mdx mouse muscular dystrophy. *Cell Transplant* **9**, 551-564 (2000).
350. Ermolova, N.V. et al. Long-term administration of the TNF blocking drug Remicade (cV1q) to mdx mice reduces skeletal and cardiac muscle fibrosis, but negatively impacts cardiac function. *Neuromuscul Disord* **24**, 583-595 (2014).
351. Hodgetts, S., Radley, H., Davies, M. & Grounds, M.D. Reduced necrosis of dystrophic muscle by depletion of host neutrophils, or blocking TNFalpha function with Etanercept in mdx mice. *Neuromuscul Disord* **16**, 591-602 (2006).
352. Meador, B.M. et al. The Green Tea Polyphenol Epigallocatechin-3-Gallate (EGCg) Attenuates Skeletal Muscle Atrophy in a Rat Model of Sarcopenia. *J Frailty Aging* **4**, 209-215 (2015).
353. Cesari, M. et al. Antioxidants and physical performance in elderly persons: the Invecchiare in Chianti (InCHIANTI) study. *Am J Clin Nutr* **79**, 289-294 (2004).
354. Coto-Montes, A., Boga, J.A., Tan, D.X. & Reiter, R.J. Melatonin as a Potential Agent in the Treatment of Sarcopenia. *Int J Mol Sci* **17** (2016).
355. Dorchies, O.M. et al. Green tea extract and its major polyphenol (-)-epigallocatechin gallate improve muscle function in a mouse model for Duchenne muscular dystrophy. *Am J Physiol Cell Physiol* **290**, C616-625 (2006).
356. Nakae, Y. et al. Quantitative evaluation of the beneficial effects in the mdx mouse of epigallocatechin gallate, an antioxidant polyphenol from green tea. *Histochem Cell Biol* **137**, 811-827 (2012).
357. Hibaoui, Y., Reutenauer-Patte, J., Patthey-Vuadens, O., Ruegg, U.T. & Dorchies, O.M. Melatonin improves muscle function of the dystrophic mdx5Cv mouse, a model for Duchenne muscular dystrophy. *J Pineal Res* **51**, 163-171 (2011).
358. Passerieux, E. et al. Effects of vitamin C, vitamin E, zinc gluconate, and selenomethionine supplementation on muscle function and oxidative stress biomarkers in patients with facioscapulohumeral dystrophy: a double-blind randomized controlled clinical trial. *Free Radic Biol Med* **81**, 158-169 (2015).
359. Tonon, E. et al. Ascorbic acid protects the diaphragm muscle against myonecrosis in mdx mice. *Nutrition* **28**, 686-690 (2012).
360. Zuo, L. & Pannell, B.K. Redox Characterization of Functioning Skeletal Muscle. *Front Physiol* **6**, 338 (2015).
361. Buyse, G.M. et al. Efficacy of idebenone on respiratory function in patients with Duchenne muscular dystrophy not using glucocorticoids (DELOS): a double-blind randomised placebo-controlled phase 3 trial. *Lancet* **385**, 1748-1757 (2015).
362. Handschin, C. Caloric restriction and exercise "mimetics": Ready for prime time? *Pharmacol Res* **103**, 158-166 (2016).
363. Niks, E.H. & Aartsma-Rus, A. Exon skipping: a first in class strategy for Duchenne muscular dystrophy. *Expert Opin Biol Ther* **17**, 225-236 (2017).
364. Bello, L. & Pegoraro, E. Genetic diagnosis as a tool for personalized treatment of Duchenne muscular dystrophy. *Acta Myol* **35**, 122-127 (2016).
365. Aartsma-Rus, A., Ginjaar, I.B. & Bushby, K. The importance of genetic diagnosis for Duchenne muscular dystrophy. *J Med Genet* **53**, 145-151 (2016).
366. Araki, R. et al. Negligible immunogenicity of terminally differentiated cells derived from induced pluripotent or embryonic stem cells. *Nature* **494**, 100-104 (2013).
367. Sincennes, M.-C., Brun, C.E. & Rudnicki, M.A. Concise Review: Epigenetic Regulation of Myogenesis in Health and Disease. *Stem Cells Translational Medicine*, sctm. 2015-0266 (2016).
368. Tedesco, F.S. et al. Transplantation of genetically corrected human iPSC-derived progenitors in mice with limb-girdle muscular dystrophy. *Science translational medicine* **4**, 140ra189-140ra189 (2012).
369. Chal, J. et al. Differentiation of pluripotent stem cells to muscle fiber to model Duchenne muscular dystrophy. *Nature biotechnology* (2015).

370. Hicks, M.R. et al. ERBB3 and NGFR mark a distinct skeletal muscle progenitor cell in human development and hPSCs. *Nature cell biology* **20**, 46 (2018).
371. Ohlstein, B., Kai, T., Decotto, E. & Spradling, A. The stem cell niche: theme and variations. *Current opinion in cell biology* **16**, 693-699 (2004).
372. Thomas, K., Engler, A.J. & Meyer, G.A. Extracellular matrix regulation in the muscle satellite cell niche. *Connective tissue research* **56**, 1-8 (2015).
373. Scadden, D.T. The stem-cell niche as an entity of action. *Nature* **441**, 1075-1079 (2006).
374. Rezza, A., Sennett, R. & Rendl, M. Adult stem cell niches: cellular and molecular components. *Curr. Top. Dev. Biol* **107**, 333-372 (2014).
375. Sousa-Victor, P., García-Prat, L., Serrano, A.L., Perdiguero, E. & Muñoz-Cánoves, P. Muscle stem cell aging: regulation and rejuvenation. *Trends in Endocrinology & Metabolism* **26**, 287-296 (2015).
376. Christov, C. et al. Muscle satellite cells and endothelial cells: close neighbors and privileged partners. *Molecular biology of the cell* **18**, 1397-1409 (2007).
377. Murphy, M.M., Lawson, J.A., Mathew, S.J., Hutcheson, D.A. & Kardon, G. Satellite cells, connective tissue fibroblasts and their interactions are crucial for muscle regeneration. *Development* **138**, 3625-3637 (2011).
378. Partridge, T., Morgan, J., Coulton, G., Hoffman, E. & Kunkel, L. Conversion of mdx myofibres from dystrophin-negative to-positive by injection of normal myoblasts. *Nature* **337**, 176 (1989).
379. Skuk, D., Goulet, M., Roy, B. & Tremblay, J.P. Myoblast transplantation in whole muscle of nonhuman primates. *Journal of Neuropathology & Experimental Neurology* **59**, 197-206 (2000).
380. Skuk, D., Goulet, M., Roy, B. & Tremblay, J.P. Efficacy of myoblast transplantation in nonhuman primates following simple intramuscular cell injections: toward defining strategies applicable to humans. *Experimental neurology* **175**, 112-126 (2002).
381. Jankowski, R., Deasy, B. & Huard, J. Muscle-derived stem cells. *Gene therapy* **9**, 642 (2002).
382. Law, P. et al. Dystrophin production induced by myoblast transfer therapy in Duchenne muscular dystrophy. *The Lancet* **336**, 114-115 (1990).
383. Partridge, T., Lu, Q.L., Morris, G. & Hoffman, E. Is myoblast transplantation effective? *Nature medicine* **4**, 1208 (1998).
384. Mouly, V. et al. Myoblast transfer therapy: is there any light at the end of the tunnel? *Acta myologica: myopathies and cardiomyopathies: official journal of the Mediterranean Society of Myology/edited by the Gaetano Conte Academy for the study of striated muscle diseases* **24**, 128-133 (2005).
385. Bentzinger, C.F., Wang, Y.X., von Maltzahn, J. & Rudnicki, M.A. The emerging biology of muscle stem cells: implications for cell-based therapies. *Bioessays* **35**, 231-241 (2013).
386. Negroni, E., Butler-Browne, G. & Mouly, V. Myogenic stem cells: regeneration and cell therapy in human skeletal muscle. *Pathologie Biologie* **54**, 100-108 (2006).
387. Blau, H.M. & Daley, G.Q. Stem Cells in the Treatment of Disease. *New England Journal of Medicine* **380**, 1748-1760 (2019).
388. Rowe, R.G. & Daley, G.Q. Induced pluripotent stem cells in disease modelling and drug discovery. *Nature Reviews Genetics*, 1 (2019).
389. Darabi, R. et al. Assessment of the myogenic stem cell compartment following transplantation of Pax3/Pax7-induced embryonic stem cell-derived progenitors. *Stem cells* **29**, 777-790 (2011).
390. Darabi, R. et al. Human ES-and iPS-derived myogenic progenitors restore DYSTROPHIN and improve contractility upon transplantation in dystrophic mice. *Cell stem cell* **10**, 610-619 (2012).
391. Xu, C. et al. A zebrafish embryo culture system defines factors that promote vertebrate myogenesis across species. *Cell* **155**, 909-921 (2013).
392. Borchin, B., Chen, J. & Barberi, T. Derivation and FACS-mediated purification of PAX3+/PAX7+ skeletal muscle precursors from human pluripotent stem cells. *Stem cell reports* **1**, 620-631 (2013).

393. Shelton, M. et al. Derivation and expansion of PAX7-positive muscle progenitors from human and mouse embryonic stem cells. *Stem cell reports* **3**, 516-529 (2014).
394. Maffioletti, S.M. et al. Three-dimensional human iPSC-derived artificial skeletal muscles model muscular dystrophies and enable multilineage tissue engineering. *Cell reports* **23**, 899-908 (2018).
395. Takahashi, K. & Yamanaka, S. Induction of pluripotent stem cells from mouse embryonic and adult fibroblast cultures by defined factors. *cell* **126**, 663-676 (2006).
396. Pan, L. et al. Stem cell aging is controlled both intrinsically and extrinsically in the Drosophila ovary. *Cell stem cell* **1**, 458-469 (2007).
397. Boyle, M., Wong, C., Rocha, M. & Jones, D.L. Decline in self-renewal factors contributes to aging of the stem cell niche in the Drosophila testis. *Cell stem cell* **1**, 470-478 (2007).
398. Chal, J. & Pourquie, O. Making muscle: skeletal myogenesis in vivo and in vitro. *Development* **144**, 2104-2122 (2017).
399. Skuk, D. & Tremblay, J.P. Cell therapy in muscular dystrophies: many promises in mice and dogs, few facts in patients. *Expert Opin Biol Ther* **15**, 1307-1319 (2015).
400. Gawlik, K.I. At the Crossroads of Clinical and Preclinical Research for Muscular Dystrophy-Are We Closer to Effective Treatment for Patients? *Int J Mol Sci* **19** (2018).
401. Darabi, R. et al. Human ES- and iPS-derived myogenic progenitors restore DYSTROPHIN and improve contractility upon transplantation in dystrophic mice. *Cell Stem Cell* **10**, 610-619 (2012).
402. Tedesco, F.S. et al. Transplantation of genetically corrected human iPSC-derived progenitors in mice with limb-girdle muscular dystrophy. *Sci Transl Med* **4**, 140ra189 (2012).
403. Abujarour, R. et al. Myogenic differentiation of muscular dystrophy-specific induced pluripotent stem cells for use in drug discovery. *Stem Cells Transl Med* **3**, 149-160 (2014).
404. Chal, J. et al. Generation of human muscle fibers and satellite-like cells from human pluripotent stem cells in vitro. *Nat Protoc* **11**, 1833-1850 (2016).
405. Rao, L. et al. Highly efficient derivation of skeletal myotubes from human embryonic stem cells. *Stem Cell Rev* **8**, 1109-1119 (2012).
406. Albini, S. et al. Epigenetic reprogramming of human embryonic stem cells into skeletal muscle cells and generation of contractile myospheres. *Cell reports* **3**, 661-670 (2013).
407. Shoji, E. et al. Early pathogenesis of Duchenne muscular dystrophy modelled in patient-derived human induced pluripotent stem cells. *Sci Rep* **5**, 12831 (2015).
408. Yu, J. et al. Induced pluripotent stem cell lines derived from human somatic cells. *Science (New York, N.Y* **318**, 1917-1920 (2007).
409. Barberi, T. et al. Derivation of engraftable skeletal myoblasts from human embryonic stem cells. *Nature medicine* **13**, 642-648 (2007).
410. Caron, L. et al. A Human Pluripotent Stem Cell Model of Facioscapulohumeral Muscular Dystrophy-Affected Skeletal Muscles. *Stem Cells Transl Med* **5**, 1145-1161 (2016).
411. Shelton, M. et al. Derivation and expansion of PAX7-positive muscle progenitors from human and mouse embryonic stem cells. *Stem Cell Reports* **3**, 516-529 (2014).
412. Chal, J. et al. Differentiation of pluripotent stem cells to muscle fiber to model Duchenne muscular dystrophy. *Nat Biotechnol* **33**, 962-969 (2015).
413. Simunovic, M. & Brivanlou, A.H. Embryoids, organoids and gastruloids: new approaches to understanding embryogenesis. *Development* **144**, 976-985 (2017).
414. Bryson-Richardson, R.J. & Currie, P.D. The genetics of vertebrate myogenesis. *Nat Rev Genet* **9**, 632-646 (2008).
415. Showell, C., Binder, O. & Conlon, F.L. T-box genes in early embryogenesis. *Developmental dynamics : an official publication of the American Association of Anatomists* **229**, 201-218 (2004).
416. Chalamalasetty, R.B. et al. Mesogenin 1 is a master regulator of paraxial presomitic mesoderm differentiation. *Development* **141**, 4285-4297 (2014).
417. Chapman, D.L., Agulnik, I., Hancock, S., Silver, L.M. & Papaioannou, V.E. Tbx6, a mouse T-Box gene implicated in paraxial mesoderm formation at gastrulation. *Developmental biology* **180**, 534-542 (1996).

418. Goulding, M., Lumsden, A. & Paquette, A.J. Regulation of Pax-3 expression in the dermomyotome and its role in muscle development. *Development* **120**, 957-971 (1994).
419. Candia, A.F. et al. Mox-1 and Mox-2 define a novel homeobox gene subfamily and are differentially expressed during early mesodermal patterning in mouse embryos. *Development* **116**, 1123-1136 (1992).
420. Kwon, G.S. et al. Tg(Afp-GFP) expression marks primitive and definitive endoderm lineages during mouse development. *Developmental dynamics : an official publication of the American Association of Anatomists* **235**, 2549-2558 (2006).
421. Bharathan, S.P. et al. Systematic evaluation of markers used for the identification of human induced pluripotent stem cells. *Biol Open* **6**, 100-108 (2017).
422. Narita, N., Bielinska, M. & Wilson, D.B. Wild-type endoderm abrogates the ventral developmental defects associated with GATA-4 deficiency in the mouse. *Developmental biology* **189**, 270-274 (1997).
423. Hebert, J.M., Boyle, M. & Martin, G.R. mRNA localization studies suggest that murine FGF-5 plays a role in gastrulation. *Development* **112**, 407-415 (1991).
424. Ma, Q., Chen, Z., del Barco Barrantes, I., de la Pompa, J.L. & Anderson, D.J. neurogenin1 is essential for the determination of neuronal precursors for proximal cranial sensory ganglia. *Neuron* **20**, 469-482 (1998).
425. Easter, S.S., Jr., Ross, L.S. & Frankfurter, A. Initial tract formation in the mouse brain. *J Neurosci* **13**, 285-299 (1993).
426. Frederiksen, K. & McKay, R.D. Proliferation and differentiation of rat neuroepithelial precursor cells in vivo. *J Neurosci* **8**, 1144-1151 (1988).
427. Ellis, P. et al. SOX2, a persistent marker for multipotential neural stem cells derived from embryonic stem cells, the embryo or the adult. *Dev Neurosci* **26**, 148-165 (2004).
428. Choi, I.Y. et al. Concordant but Varied Phenotypes among Duchenne Muscular Dystrophy Patient-Specific Myoblasts Derived using a Human iPSC-Based Model. *Cell reports* **15**, 2301-2312 (2016).
429. Schubert, W., Zimmermann, K., Cramer, M. & Starzinski-Powitz, A. Lymphocyte antigen Leu-19 as a molecular marker of regeneration in human skeletal muscle. *Proc Natl Acad Sci U S A* **86**, 307-311 (1989).
430. Magli, A. et al. PAX7 Targets, CD54, Integrin alpha9beta1, and SDC2, Allow Isolation of Human ESC/iPSC-Derived Myogenic Progenitors. *Cell reports* **19**, 2867-2877 (2017).
431. Hicks, M.R. et al. ERBB3 and NGFR mark a distinct skeletal muscle progenitor cell in human development and hPSCs. *Nature cell biology* **20**, 46-57 (2018).
432. Uezumi, A. et al. Cell-Surface Protein Profiling Identifies Distinctive Markers of Progenitor Cells in Human Skeletal Muscle. *Stem Cell Reports* **7**, 263-278 (2016).
433. Pisani, D.F. et al. Isolation of a highly myogenic CD34-negative subset of human skeletal muscle cells free of adipogenic potential. *Stem Cells* **28**, 753-764 (2010).
434. Lipinski, M., Braham, K., Caillaud, J.M., Carlu, C. & Tursz, T. HNK-1 antibody detects an antigen expressed on neuroectodermal cells. *The Journal of experimental medicine* **158**, 1775-1780 (1983).
435. Sicinski, P. et al. The molecular basis of muscular dystrophy in the mdx mouse: a point mutation. *Science (New York, N.Y* **244**, 1578-1580 (1989).
436. Bentzinger, C.F., Wang, Y.X., von Maltzahn, J. & Rudnicki, M.A. The emerging biology of muscle stem cells: implications for cell-based therapies. *Bioessays* **35**, 231-241 (2013).
437. Bert, P. Expériences et Considérations Sur la Greffe Animale. *J. Anatomie Physiologie* **1**, 69–87 (1864).
438. Conboy, I.M., Conboy, M.J. & Rebo, J. Systemic Problems: A perspective on stem cell aging and rejuvenation. *Aging (Albany NY)* **7**, 754-765 (2015).
439. Zhao, C., Xue, J., Ran, F. & Sun, S. Modification of polyethersulfone membranes – A review of methods. *Progress in Materials Science* **58**, 76-150 (2013).
440. Hunter, S.K., Kao, J.M., Wang, Y., Benda, J.A. & Rodgers, V.G. Promotion of neovascularization around hollow fiber bioartificial organs using biologically active substances. *ASAIO J* **45**, 37-40 (1999).

441. Kleinman, H.K. et al. Isolation and characterization of type IV procollagen, laminin, and heparan sulfate proteoglycan from the EHS sarcoma. *Biochemistry* **21**, 6188-6193 (1982).
442. Lombardi, G., Di Somma, C., Rota, F. & Colao, A. Associated hormonal decline in aging: is there a role for GH therapy in aging men? *J Endocrinol Invest* **28**, 99-108 (2005).
443. Montecino-Rodriguez, E., Berent-Maoz, B. & Dorshkind, K. Causes, consequences, and reversal of immune system aging. *J Clin Invest* **123**, 958-965 (2013).
444. Baruch, K. et al. Aging-induced type I interferon response at the choroid plexus negatively affects brain function. *Science (New York, N.Y* **346**, 89-93 (2014).
445. Joe, A.W. et al. Muscle injury activates resident fibro/adipogenic progenitors that facilitate myogenesis. *Nature cell biology* **12**, 153 (2010).
446. Uezumi, A. et al. Fibrosis and adipogenesis originate from a common mesenchymal progenitor in skeletal muscle. *J Cell Sci* **124**, 3654-3664 (2011).
447. Takahashi, K. & Yamanaka, S. Induction of pluripotent stem cells from mouse embryonic and adult fibroblast cultures by defined factors. *Cell* **126**, 663-676 (2006).
448. Kodaka, Y., Rabu, G. & Asakura, A. Skeletal Muscle Cell Induction from Pluripotent Stem Cells. *Stem Cells Int* **2017**, 1376151 (2017).
449. Emery, A.E. The muscular dystrophies. *The Lancet* **359**, 687-695 (2002).
450. Takebe, T., Zhang, B. & Radisic, M. Synergistic engineering: organoids meet organs-on-a-chip. *Cell Stem Cell* **21**, 297-300 (2017).
451. Le Bras, A. A new organoid model to study diabetic vasculopathy. *Nature Reviews Cardiology* **16**, 131 (2019).
452. Lancaster, M.A. Brain organoids get vascularized. *Nature biotechnology* **36**, 407 (2018).

Chapter 9:

Curriculum vitae

Omid Mashinchian

Nestlé Research, Nestlé Institute of Health Sciences (NIHS)
Campus EPFL, EPFL-Innovation Park, Building-H
1015 Lausanne, Switzerland
Tel: +41-21-632-6335
Email: Omid.Mashinchian@rd.nestle.com
Omid.Mashinchian@epfl.ch

1. EDUCATION

- **Doctor of Philosophy (PhD) in Biotechnology & Bioengineering (EDBB)** **2015-2019**

  Swiss Federal Institute of Technology (EPFL) / Nestle Institute of Health Sciences, Switzerland

  PhD-Thesis: *Bioengineering the Human Muscle Stem-Cell Niche for Therapeutic Applications*

- **Innosuisse-Fellow on Business Concept (A Federal Program for Startup Founders)** **Feb. to June 2018**

  Founder of Start-up Project on Personalized-Medicine; EPFL-Innovation Park in Western Switzerland

- **Master of Science (MSc) in Medical-Nanotechnology (Ranked #1: 18.66/20)** **2012-2014**

  Tehran University of Medical Sciences, Iran

  MSc-Thesis: *Cell-Imprinted Substrates Act as an Artificial Niche for Skin Regeneration*

- **Bio-Medical Science (BMed)** **2008-2012**

  Tabriz University of Medical Sciences, Iran
  BMed-Thesis: *Novel Thermosensitive Poly (N-isopropylacrylamide-co-vinylpyrrolidone-co-methacrylic acid) Nanosystems for Delivery of Natural Products*

2. WORK EXPERIENCE & SHORT-TERM VISITING

- **Nestlé Research, Nestlé Institute of Health Sciences (NIHS)**, Switzerland **2015-2019**

  Host Lab.: **Dr. Jérome Feige**
  I am responsible for a cross-functional bioengineering project between the lab of Matthias Lütolf (EPFL), and Jérome Feige at Musculo-Skeletal Health Department, NIHS. In the past three years, I have optimized 3D derivation platform of human muscle stem cells (MuSCs) from human induced pluripotent stem cells (h-iPSCs) in a biologically faithful 3D environment.

- **Université de Mons, Université libre de Bruxelles (ULB) and CMMI**, Belgium **2013**

  Host Lab.: **Dr. Sophie Laurent** and **Dr. Robert N. Muller**
  I developed novel bioinspired materials which can mimic the stem cell environment and modulate stem cell differentiation and proliferation by cell-imprinted substrates based on mature human keratinocyte morphological templates.

- **Stanford University**, CA, US **2012-2014**

  Host Lab.: **Dr. Morteza Mahmoudi (**Now at **Brigham and Women's Hospital**, **Harvard Medical School**, MA, US**)**
  I was involved on several projects for developing an imprinting technique as an effective and promising way to regulate any cell phenotype *in-vitro* with significant potential applications in regenerative medicine and cell-based therapies.

3. SCIENTIFIC OUTPUT

- Number of publication: **24** Total-citation: **501** h-index: **12**
- **Most impactful publication (Full-listed at the end):**

1. **O. Mashinchian**, F. De Franceschi, J. Michaud, S. Karaz, P. Stuelsatz, N. Hegde, G. Dammone, M. P. Lutolf, J. N. Feige* and C. F. Bentzinger*. An Engineered Multicellular Stem Cell Niche for the 3D Derivation of Human Myogenic Progenitors from iPSCs. Under-review at **Nature Methods**
   **Contributed equally to this work*

2. L. Lukjanenko*, S. Karaz*, U. Gurriaran-Rodriguez, P. Stuelsatz, **O. Mashinchian**, G. Dammone, E. Migliavacca, F. Sizzano, J. Michaud, G. Jacot, S. Metairon, F. Raymond, P. Descombes, A. Palini, M. A. Rudnicki, C. F. Bentzinger and J. N. Feige. Aging Disrupts Muscle Stem Cell Function by Impairing Matricellular WISP1 Signals from Fibro-Adipogenic Progenitors. **Cell Stem Cell**. 2019. Impact Factor: **23.290**

3. **O. Mashinchian**, S. Bonakdar, H. Taghinejad, V. Satarifard, M. Heidari, M. Majidi, S. Sharifi, A. Peirovi, S. Saffar, M. Taghinejad, M. Abdolahad, S. Mohajerzadeh, M. A. Shokrgozar, S. M. Rezayat, M. R. Ejtehadi, M. J. Dalby and M. Mahmoudi. Cell-Imprinted Substrates Act as an Artificial Niche for Skin Regeneration. **ACS Applied Materials and Interfaces**. 2014, 6 (15). Impact Factor: **8.097**
Highlighted in Nanowerk

- **Patents**

1. **O. Mashinchian**, J. N. Feige and C. F. Bentzinger. *In-vitro* Production of Muscle Stem Cells. **European Patent Office (nm: WO2018091282)**. 2018
2. H. Aghaverdi, **O. Mashinchian**, M. Mahmoudi and R. Sakhtianchi. Smart Substrates for Stem Cell Differentiation. **Iranian Patent (nm: 81859)**. 2014
3. **O. Mashinchian**, S. Davaran, A. Aghanejad, R. Salehi, M. Moghoe and G. Dehghan. Design and Development of Polymeric Nanoparticles for Targeted Cancer Therapy. **Iranian Patent (nm: 56417)** and **Iranian Research Organization for Science & Technology (IROST) (nm: 415.1445)**. 2009

- **Conference presentation (**Selected from 25 Poster/Oral Talks**)**

1. Oral-Talk & Poster: Myogenesis-Gordon Research Seminar (GRS), Renaissance Tuscany Il Ciocco, **Lucca (Barga), Italy** (June 11-16, 2017)
2. Poster:13th Annual Swiss Stem Cell Network Meeting, **Lausanne, Switzerland** (5th September 2017)
3. Poster:10-years of iPSCs (Cell Symposium), **Berkeley, CA, USA** (25–27 September 2016)
4. Oral-Talk: 12th Horizons in Molecular Biology Conference, **Göttingen, Germany** (14-17 September 2015)
5. Poster: 25th European Students' Conference (ESC), **Berlin, Germany** (17-20th September 2014)
6. Oral-Talk & Poster: UEGW 2012, Amsterdam, **The Netherlands** (20-24th October 2012)

4. HONORS AND AWARDS

- **Nestlé - Awarded Certificate in Recognition of Proactive Collaboration** with Stem Cell Group at **2016, 2017** and **2018**, Nestlé Institute of Health Sciences (NIHS), **Switzerland**, **2018**
- **Certificate-Award on Innosuisse Start-up Training Business Concept** (A Federal program for startup founders) of 14-week training program**, Switzerland**, **2018**
- **Awarded Student Talk, 14th Horizons in Molecular Biology Symposium,** Göttingen, **Germany**, **2017**
- **Awarded Student Talk, 12th Horizons in Molecular Biology Symposium,** Göttingen, **Germany**, **2015**
- **Graduate Research and Teaching Assistantship (GRA/GTA)**, **Northeastern University**, MA, United States, **2015-2019**
- **Distinguished Thesis Award (1st Rank), The 1st Avicenna Student Festival,** Tehran University of Medical Sciences, **Iran, 2014**
- **First Prize for Business Plan**, 7th Asia Nanotech Camp (ANC2014), Tehran, **Iran, 2014**
- **Ranked #1** Among the Medical Nanotechnology Students (**MSc** Degree), Tehran University of Medical Sciences (TUMS), **2014**
- Award of the **International Scholarship** for Postgraduate Teaching Program and **Travel Grant**, UEGW, Amsterdam, **The Netherlands**, **2012**
- **Ranked 16th/2000** Among the Biomedical Students in the **University Entrance National Exam** for **MSc** Degree, **2012**
- **UEGW 2011 Travel Award**, Stockholm, **Sweden**, **2011**
- Award of the **Young Investigator Competition** and **Congress Bursary**, 16th World Congress of Basic and Clinical Pharmacology (WorldPharma2010), Copenhagen, **Denmark**, **2010**
- Award of **Student Membership**, American College of Clinical Pharmacology (ACCP) for **2010-2011** Year
- Award of **3rd Prize** for the **Best Oral Lecture**, 1st Student Congress on New Perspectives in Health System Arena, Urmia, **Iran**, **2009**

5. SOCIAL & NETWORKING ACTIVITIES

- **Founder and President of Student Association**, Nestlé Institute of Health Sciences, Lausanne, Switzerland, **2016-2018**
- **Leading the Nestlé Corporate Official Instagram Account** for One Week **2018**
- **Highlighting for Global Youth Initiative at Nestle official page for Facebook, Twitter and LinkedIn 2018**
- **Coordinating more than 20-Events (Visiting, Workshop and Career Event) with EPFL-PhD/PostDoc Association 2018**

6. PUBLICATIONS (Full-list)

BOOK CHAPTERS

1. S. Tavakol*, S. Jalili-Firoozinezhad*, **O. Mashinchian*** and M. Mahmoudi. **Bioinspired Nanotechnologies for Skin Regeneration**. *Book Chapter in Nanoscience in Dermatology*. **Elsevier, Inc**. 2016
2. **O. Mashinchian**, A. M. Alkilany, M. J. Hajipour and S. Tavakol. **Gold Nanoparticles for Biomedical Imaging and their Biological Response**. *Book Chapter in New Developments in Gold Nanomaterials Research*. **Nova Science Publishers, Inc**. 2016
3. **O. Mashinchian**, S. Bonakdar, S. Sharifi and M. Mahmoudi. **Stem Cell Nanoengineering from Bench to Bed**; Commercial Strategies in Nano Tissue Engineering and Clinical Applications (Including Different Regulatory Agencies and Public Information Sites, Commercialization). *Book Chapter in Stem Cell NanoEngineering*. **John Wiley & Sons, Inc**. 2015
4. *S. Bonakdar and ***O. Mashinchian**. **Toxicity of Nanobiomaterials**. *Book Chapter in Stem Cell NanoEngineering*. **John Wiley & Sons, Inc**. 2015

ARTICLES in SCIENTIFIC JOURNALS

5. **O. Mashinchian***, A. Pisconti*, E. L. Moal* and C. F. Bentzinger. The Muscle Stem Cell Niche in Health and Disease. **Current Topics in Developmental Biology**. 2018, 126. Impact Factor: **4.677**
   *Featured in **Science***
6. L. Lukjanenko*, S. Karaz*, U. Gurriaran-Rodriguez, P. Stuelsatz, **O. Mashinchian**, G. Dammone, E. Migliavacca, F. Sizzano, J. Michaud, G. Jacot, S. Metairon, F. Raymond, P. Descombes, A. Palini, M. A. Rudnicki, C. F. Bentzinger and J. N. Feige. Aging Disrupts Muscle Stem Cell Function by Impairing Matricellular WISP1 Signals from Fibro-Adipogenic Progenitors. **Cell Stem Cell**. 2018, 24 (3). Impact Factor: **23.290**
7. T. Heydari*, M. Heidari*, **O. Mashinchian***, M. Wojcik, K. Xu, M. Dalby, M. Mahmoudi and M. R. Ejtehadi. Development of a Virtual Cell Model to Predict Cell Response to Substrate Topography. **ACS Nano**. 2017, 11 (9). Impact Factor: **13.709**
   Highlighted in Nanowerk
8. S. A. Hosseini, M. Abdolahad, S. Zanganeh, M. Dahmardeh, M. Gharooni, H. Abiri, A. Alikhani, S. Mohajerzadeh and **O. Mashinchian***. Nanoelectromechanical Chip (NELMEC) Combination of Nanoelectronics and Microfluidics to Diagnose Epithelial and Mesenchymal Circulating Tumor Cells from Leukocytes. **Small**. 2016, 12 (7). Impact Factor: **9.590**
9. S. Bonakdar, M. Mahmoudi, L. Montazeri, M. Taghipoor, A. Bertsch, M. A. Shokrgozar, S. Sharifi, M. Majidi, **O. Mashinchian**, M. H. Sekachaei, P. Zolfaghari, and P. Renaud. Cell-Imprinted Substrates Modulate Differentiation, Redifferentiation, and Transdifferentiation. **ACS Applied Materials and Interfaces**. 2016, 8 (22). Impact Factor: **8.097**
10. B. Ghaemi*, **O. Mashinchian***, T. Mousavi, R. Karimi, S. Kharrazi and Amir Amani. Harnessing the Cancer Radiation Therapy by Lanthanide-Doped Zinc Oxide Based Theranostic Nanoparticles. **ACS Applied Materials and Interfaces**. 2016, 8 (5). Impact Factor: **8.097**
11. M. Namiri, M. K. Ashtiani, **O. Mashinchian**, M. M. Hasani-Sadrabadi, M. Mahmoudi, N. Aghdami and H. Baharvand. Engineering Natural Heart Valves: Possibilities and Challenges. **Journal of Tissue Engineering and Regenerative Medicine**. 2016. Impact Factor: **4.089**
12. S. Moayyedi, **O. Mashinchian** and R. Dinarvand. Osmolarity: A Hidden Factor in Nanotoxicology. **DARU Journal of Pharmaceutical Sciences**. 2016, 24 (9). Impact Factor: **2.667**
13. F. Esfandiari*, **O. Mashinchian***, M. K. Ashtiani, M. H. Ghanian, K. Hayashi, A. A. Saei, M. Mahmoudi and Hossein Baharvand. Possibilities in Germ Cell Research: An Engineering Insight. **Trends in Biotechnology**. 2015, 33 (12). Impact Factor: **13.578**
14. **O. Mashinchian**, L. A. Turner, M. J. Dalby, S. Laurent, M. A. Shokrgozar, S. Bonakdar, M. Imani and M. Mahmoudi. Regulation of Stem Cell Fate by Nano-Material Substrates. **Nanomedicine**. 2015, 10 (5). Impact Factor: **5.005**

15. M. J. Hajipour, J. Raheb, O. Akhavan, S. Arjmand, **O. Mashinchian**, M. Rahman, M. Abdolahad, V. Serpooshan, S. Laurent, and M. Mahmoudi. Personalized, Disease-Specific Protein Corona Influences the Therapeutic Impact of Graphene Oxide. **Nanoscale**. 2015, 19 (7). Impact Factor: **7.233**

16. M. Abdolahad, A. Saeedi, M. Janmaleki, **O. Mashinchian**, M. Taghinejad, H. Taghinejad, S. Azimi, M. Mahmoudi and S. Mohajerzadeh. A Single-Cell Correlative Nanoelectromechanosensing Approach to Detect Cancerous Transformation: Monitoring the Function of F-actin Microfilaments in the Modulation of the Ion Channel Activity. **Nanoscale**. 2015, 5 (7). Impact Factor: **7.233**
Highlighted in Nanowerk

17. **O. Mashinchian**, S. Bonakdar, H. Taghinejad, V. Satarifard, M. Heidari, M. Majidi, S. Sharifi, A. Peirovi, S. Saffar, M. Taghinejad, M. Abdolahad, S. Mohajerzadeh, M. A. Shokrgozar, S. M. Rezayat, M. R. Ejtehadi, M. J. Dalby and M. Mahmoudi. Cell-Imprinted Substrates Act as an Artificial Niche for Skin Regeneration. **ACS Applied Materials and Interfaces**. 2014, 6 (15). Impact Factor: **8.097**
Highlighted in Nanowerk

18. T. Norizadeh-Abbariki*, **O. Mashinchian***, M. A. Shokrgozar, N. Haghighipour, T. Sen and M. Mahmoudi. Superparamagnetic Nanoparticles Direct Differentiation of Embryonic Stem Cells into Skeletal Muscle Cells. **Journal of Biomaterials and Tissue Engineering**. 2014, 4 (7). Impact Factor: **1.383**

19. **O. Mashinchian**, M. Johari-Ahar, B. Ghaemi, M. Rashidi, J. Barar and Y. Omidi. Impacts of Quantum Dots in Molecular Detection and Bioimaging of Cancer. **Bioimpacts**. 2014, 4 (3).

20. J. Ezzati Nazhad Dolatabadi, **O. Mashinchian**, B. Ayoubi, A. A. Jamali, A. Mobed, D. Losic, Y. Omidi and M. de la Guardia. Optical and Electrochemical DNA Nanobiosensors. **TrAC Trends in Analytical Chemistry**. 2011, 30 (3). Impact Factor : **7.034**
Top 25 Most Downloaded Article

21. M. Ebrahimi, M. Johari-Ahar, H. Hamzeiy, J. Barar, **O. Mashinchian** and Y. Omidi. Electrochemical Impedance Spectroscopic Sensing of Methamphetamine by a Specific Aptamer. **Bioimpacts**. 2012, 2 (2).

22. **O. Mashinchian**, R. Salehi, G. Dehghan, A. Aganejad, S. Davaran and Y. Omidi. Novel Thermosensitive Poly (N-isopropylacrylamide-co-vinylpyrrolidone-co-methacrylic acid) Nanosystems for Delivery of Natural Products. **International Journal of Drug Delivery**. 2011, 2 (4).

7. REFERENCES

- **Dr. Jérome Feige** Jerome.Feige@rd.nestle.com
  Nestlé Research, Campus-EPFL, EPFL-Innovation Park, Building-H, 1015 Lausanne, Switzerland
- **Dr. Florian Bentzinger** cf.bentzinger@usherbrooke.ca
  Département de pharmacologie et physiologie, Faculté de médecine et des sciences de la santé, Université de Sherbrooke, Qc, Canada
- **Dr. Matthias Lütolf** Matthias.Lutolf@epfl.ch
  Institute of Bioengineering, School of Life Sciences, Ecole Polytechnique Fédérale de Lausanne (EPFL), CH-1015 Lausanne, Switzerland

Chapter 10:

Appendix

ELSEVIER LICENSE
TERMS AND CONDITIONS

Feb 20, 2019

This Agreement between Omid Mashinchian ("You") and Elsevier ("Elsevier") consists of your license details and the terms and conditions provided by Elsevier and Copyright Clearance Center.

The publisher has provided special terms related to this request that can be found at the end of the Publisher's Terms and Conditions.

License Number	4533000939975
License date	Feb 20, 2019
Licensed Content Publisher	Elsevier
Licensed Content Publication	Elsevier Books
Licensed Content Title	Current Topics in Developmental Biology
Licensed Content Author	Omid Mashinchian,Addolorata Pisconti,Emmeran Le Moal,C. Florian Bentzinger
Licensed Content Date	Jan 1, 2018
Licensed Content Volume	126
Licensed Content Issue	n/a
Licensed Content Pages	43
Start Page	23
End Page	65
Type of Use	reuse in a thesis/dissertation
I am an academic or government institution with a full-text subscription to this journal and the audience of the material consists of students and/or employees of this institute?	No
Portion	full chapter
Circulation	1
Format	electronic
Are you the author of this Elsevier chapter?	Yes
Will you be translating?	No
Title of your thesis/dissertation	Generation of Uncommitted Human iPSC Derived Muscle Stem Cells for Therapeutic Applications
Expected completion date	Mar 2019
Estimated size (number of pages)	150
Requestor Location	Omid Mashinchian NIHS, Campus EPFL, EPFL-Innovation Park BUILDING-H

	Lausanne, Vaud 1015 Switzerland Attn: Omid Mashinchian
Publisher Tax ID	GB 494 6272 12
Billing Type	Invoice
Billing Address	Omid Mashinchian NIHS, Campus EPFL, EPFL-Innovation Park BUILDING-H Lausanne, Switzerland 1015 Attn: Omid Mashinchian
Total	0.00 CHF

Terms and Conditions

INTRODUCTION

1. The publisher for this copyrighted material is Elsevier. By clicking "accept" in connection with completing this licensing transaction, you agree that the following terms and conditions apply to this transaction (along with the Billing and Payment terms and conditions established by Copyright Clearance Center, Inc. ("CCC"), at the time that you opened your Rightslink account and that are available at any time at http://myaccount.copyright.com).

GENERAL TERMS

2. Elsevier hereby grants you permission to reproduce the aforementioned material subject to the terms and conditions indicated.
3. Acknowledgement: If any part of the material to be used (for example, figures) has appeared in our publication with credit or acknowledgement to another source, permission must also be sought from that source. If such permission is not obtained then that material may not be included in your publication/copies. Suitable acknowledgement to the source must be made, either as a footnote or in a reference list at the end of your publication, as follows:
"Reprinted from Publication title, Vol /edition number, Author(s), Title of article / title of chapter, Pages No., Copyright (Year), with permission from Elsevier [OR APPLICABLE SOCIETY COPYRIGHT OWNER]." Also Lancet special credit - "Reprinted from The Lancet, Vol. number, Author(s), Title of article, Pages No., Copyright (Year), with permission from Elsevier."
4. Reproduction of this material is confined to the purpose and/or media for which permission is hereby given.
5. Altering/Modifying Material: Not Permitted. However figures and illustrations may be altered/adapted minimally to serve your work. Any other abbreviations, additions, deletions and/or any other alterations shall be made only with prior written authorization of Elsevier Ltd. (Please contact Elsevier at permissions@elsevier.com). No modifications can be made to any Lancet figures/tables and they must be reproduced in full.
6. If the permission fee for the requested use of our material is waived in this instance, please be advised that your future requests for Elsevier materials may attract a fee.
7. Reservation of Rights: Publisher reserves all rights not specifically granted in the combination of (i) the license details provided by you and accepted in the course of this licensing transaction, (ii) these terms and conditions and (iii) CCC's Billing and Payment terms and conditions.
8. License Contingent Upon Payment: While you may exercise the rights licensed immediately upon issuance of the license at the end of the licensing process for the transaction, provided that you have disclosed complete and accurate details of your proposed use, no license is finally effective unless and until full payment is received from you (either by publisher or by CCC) as provided in CCC's Billing and Payment terms and conditions. If full payment is not received on a timely basis, then any license preliminarily granted shall be deemed automatically revoked and shall be void as if never granted. Further, in the event

that you breach any of these terms and conditions or any of CCC's Billing and Payment terms and conditions, the license is automatically revoked and shall be void as if never granted. Use of materials as described in a revoked license, as well as any use of the materials beyond the scope of an unrevoked license, may constitute copyright infringement and publisher reserves the right to take any and all action to protect its copyright in the materials.

9. Warranties: Publisher makes no representations or warranties with respect to the licensed material.

10. Indemnity: You hereby indemnify and agree to hold harmless publisher and CCC, and their respective officers, directors, employees and agents, from and against any and all claims arising out of your use of the licensed material other than as specifically authorized pursuant to this license.

11. No Transfer of License: This license is personal to you and may not be sublicensed, assigned, or transferred by you to any other person without publisher's written permission.

12. No Amendment Except in Writing: This license may not be amended except in a writing signed by both parties (or, in the case of publisher, by CCC on publisher's behalf).

13. Objection to Contrary Terms: Publisher hereby objects to any terms contained in any purchase order, acknowledgment, check endorsement or other writing prepared by you, which terms are inconsistent with these terms and conditions or CCC's Billing and Payment terms and conditions. These terms and conditions, together with CCC's Billing and Payment terms and conditions (which are incorporated herein), comprise the entire agreement between you and publisher (and CCC) concerning this licensing transaction. In the event of any conflict between your obligations established by these terms and conditions and those established by CCC's Billing and Payment terms and conditions, these terms and conditions shall control.

14. Revocation: Elsevier or Copyright Clearance Center may deny the permissions described in this License at their sole discretion, for any reason or no reason, with a full refund payable to you. Notice of such denial will be made using the contact information provided by you. Failure to receive such notice will not alter or invalidate the denial. In no event will Elsevier or Copyright Clearance Center be responsible or liable for any costs, expenses or damage incurred by you as a result of a denial of your permission request, other than a refund of the amount(s) paid by you to Elsevier and/or Copyright Clearance Center for denied permissions.

LIMITED LICENSE

The following terms and conditions apply only to specific license types:

15. **Translation**: This permission is granted for non-exclusive world **English** rights only unless your license was granted for translation rights. If you licensed translation rights you may only translate this content into the languages you requested. A professional translator must perform all translations and reproduce the content word for word preserving the integrity of the article.

16. **Posting licensed content on any Website**: The following terms and conditions apply as follows: Licensing material from an Elsevier journal: All content posted to the web site must maintain the copyright information line on the bottom of each image; A hyper-text must be included to the Homepage of the journal from which you are licensing at http://www.sciencedirect.com/science/journal/xxxxx or the Elsevier homepage for books at http://www.elsevier.com; Central Storage: This license does not include permission for a scanned version of the material to be stored in a central repository such as that provided by Heron/XanEdu.

Licensing material from an Elsevier book: A hyper-text link must be included to the Elsevier homepage at http://www.elsevier.com . All content posted to the web site must maintain the copyright information line on the bottom of each image.

Posting licensed content on Electronic reserve: In addition to the above the following clauses are applicable: The web site must be password-protected and made available only to

bona fide students registered on a relevant course. This permission is granted for 1 year only. You may obtain a new license for future website posting.

17. **For journal authors:** the following clauses are applicable in addition to the above:

Preprints:

A preprint is an author's own write-up of research results and analysis, it has not been peer-reviewed, nor has it had any other value added to it by a publisher (such as formatting, copyright, technical enhancement etc.).

Authors can share their preprints anywhere at any time. Preprints should not be added to or enhanced in any way in order to appear more like, or to substitute for, the final versions of articles however authors can update their preprints on arXiv or RePEc with their Accepted Author Manuscript (see below).

If accepted for publication, we encourage authors to link from the preprint to their formal publication via its DOI. Millions of researchers have access to the formal publications on ScienceDirect, and so links will help users to find, access, cite and use the best available version. Please note that Cell Press, The Lancet and some society-owned have different preprint policies. Information on these policies is available on the journal homepage.

Accepted Author Manuscripts: An accepted author manuscript is the manuscript of an article that has been accepted for publication and which typically includes author-incorporated changes suggested during submission, peer review and editor-author communications.

Authors can share their accepted author manuscript:

- immediately
    - via their non-commercial person homepage or blog
    - by updating a preprint in arXiv or RePEc with the accepted manuscript
    - via their research institute or institutional repository for internal institutional uses or as part of an invitation-only research collaboration work-group
    - directly by providing copies to their students or to research collaborators for their personal use
    - for private scholarly sharing as part of an invitation-only work group on commercial sites with which Elsevier has an agreement
- After the embargo period
    - via non-commercial hosting platforms such as their institutional repository
    - via commercial sites with which Elsevier has an agreement

In all cases accepted manuscripts should:

- link to the formal publication via its DOI
- bear a CC-BY-NC-ND license - this is easy to do
- if aggregated with other manuscripts, for example in a repository or other site, be shared in alignment with our hosting policy not be added to or enhanced in any way to appear more like, or to substitute for, the published journal article.

Published journal article (JPA): A published journal article (PJA) is the definitive final record of published research that appears or will appear in the journal and embodies all value-adding publishing activities including peer review co-ordination, copy-editing, formatting, (if relevant) pagination and online enrichment.

Policies for sharing publishing journal articles differ for subscription and gold open access articles:

Subscription Articles: If you are an author, please share a link to your article rather than the full-text. Millions of researchers have access to the formal publications on ScienceDirect, and so links will help your users to find, access, cite, and use the best available version.

Theses and dissertations which contain embedded PJAs as part of the formal submission can be posted publicly by the awarding institution with DOI links back to the formal

publications on ScienceDirect.
If you are affiliated with a library that subscribes to ScienceDirect you have additional private sharing rights for others' research accessed under that agreement. This includes use for classroom teaching and internal training at the institution (including use in course packs and courseware programs), and inclusion of the article for grant funding purposes.
Gold Open Access Articles: May be shared according to the author-selected end-user license and should contain a CrossMark logo, the end user license, and a DOI link to the formal publication on ScienceDirect.
Please refer to Elsevier's posting policy for further information.
18. **For book authors** the following clauses are applicable in addition to the above: Authors are permitted to place a brief summary of their work online only. You are not allowed to download and post the published electronic version of your chapter, nor may you scan the printed edition to create an electronic version. **Posting to a repository:** Authors are permitted to post a summary of their chapter only in their institution's repository.
19. **Thesis/Dissertation**: If your license is for use in a thesis/dissertation your thesis may be submitted to your institution in either print or electronic form. Should your thesis be published commercially, please reapply for permission. These requirements include permission for the Library and Archives of Canada to supply single copies, on demand, of the complete thesis and include permission for Proquest/UMI to supply single copies, on demand, of the complete thesis. Should your thesis be published commercially, please reapply for permission. Theses and dissertations which contain embedded PJAs as part of the formal submission can be posted publicly by the awarding institution with DOI links back to the formal publications on ScienceDirect.

Elsevier Open Access Terms and Conditions
You can publish open access with Elsevier in hundreds of open access journals or in nearly 2000 established subscription journals that support open access publishing. Permitted third party re-use of these open access articles is defined by the author's choice of Creative Commons user license. See our open access license policy for more information.
Terms & Conditions applicable to all Open Access articles published with Elsevier:
Any reuse of the article must not represent the author as endorsing the adaptation of the article nor should the article be modified in such a way as to damage the author's honour or reputation. If any changes have been made, such changes must be clearly indicated.
The author(s) must be appropriately credited and we ask that you include the end user license and a DOI link to the formal publication on ScienceDirect.
If any part of the material to be used (for example, figures) has appeared in our publication with credit or acknowledgement to another source it is the responsibility of the user to ensure their reuse complies with the terms and conditions determined by the rights holder.
Additional Terms & Conditions applicable to each Creative Commons user license:
CC BY: The CC-BY license allows users to copy, to create extracts, abstracts and new works from the Article, to alter and revise the Article and to make commercial use of the Article (including reuse and/or resale of the Article by commercial entities), provided the user gives appropriate credit (with a link to the formal publication through the relevant DOI), provides a link to the license, indicates if changes were made and the licensor is not represented as endorsing the use made of the work. The full details of the license are available at http://creativecommons.org/licenses/by/4.0.
CC BY NC SA: The CC BY-NC-SA license allows users to copy, to create extracts, abstracts and new works from the Article, to alter and revise the Article, provided this is not done for commercial purposes, and that the user gives appropriate credit (with a link to the formal publication through the relevant DOI), provides a link to the license, indicates if changes were made and the licensor is not represented as endorsing the use made of the work. Further, any new works must be made available on the same conditions. The full details of the license are available at http://creativecommons.org/licenses/by-nc-sa/4.0.

CC BY NC ND: The CC BY-NC-ND license allows users to copy and distribute the Article, provided this is not done for commercial purposes and further does not permit distribution of the Article if it is changed or edited in any way, and provided the user gives appropriate credit (with a link to the formal publication through the relevant DOI), provides a link to the license, and that the licensor is not represented as endorsing the use made of the work. The full details of the license are available at http://creativecommons.org/licenses/by-nc-nd/4.0. Any commercial reuse of Open Access articles published with a CC BY NC SA or CC BY NC ND license requires permission from Elsevier and will be subject to a fee.
Commercial reuse includes:

- Associating advertising with the full text of the Article
- Charging fees for document delivery or access
- Article aggregation
- Systematic distribution via e-mail lists or share buttons

Posting or linking by commercial companies for use by customers of those companies.

20. **Other Conditions**: Posting of the full chapter online by the author is not permitted. You may post a summary of the book with a link to the Elsevier website www.elsevier.com , or to the chapter on ScienceDirect if it is available on that platform.

v1.9

Questions? customercare@copyright.com or +1-855-239-3415 (toll free in the US) or +1-978-646-2777.

PRIZE ESSAY

FINALIST
C. Florian Bentzinger
C. Florian Bentzinger received his master's and Ph.D. degrees from the University of Basel in Switzerland. Following his postdoctoral studies at the Ottawa Hospital Research Institute, Dr. Bentzinger joined the Nestlé Institute of Health Sciences. In 2016, he was appointed as an assistant professor at the Université de Sherbrooke and as an investigator at the Centre de recherche du CHUS in Canada, where he is conducting research on the skeletal muscle stem cell niche.
www.sciencemag.org/content/363/6431/1051.3

REGENERATIVE MEDICINE

Best supporting actors

Nearby cells help boost stem cell–mediated skeletal muscle repair

By **C. Florian Bentzinger**

Skeletal muscle stem cells (MuSCs) are critically dependent on their microenvironment, the so-called "stem cell niche." The niche contains a multitude of cellular and acellular elements that regulate MuSC functions, including quiescence, proliferation, self-renewal, and differentiation (Fig. 1). By spatiotemporally controlling MuSCs, the components of the niche ultimately determine the regenerative capacity of skeletal muscle (SkM) tissue.

Upon SkM injury, certain cell types, such as fibroblasts, vascular cells, and immune cells, become highly abundant in the stem cell niche and play particularly important roles in regulating MuSCs. These supportive cell types interact with MuSCs by presenting cell-cell contacts, secreting growth factors, and providing various structural components to the extracellular matrix (ECM) (*1*, *2*). Regulatory interactions of supportive cell types with MuSCs can be severely perturbed in aging and neuromuscular disorders (*2*–*4*).

Impaired MuSC-niche interactions represent a root cause of regenerative failure of SkM tissue, and restoring microenvironmental signals can improve its healing capacity, thus slowing or stopping disease progression. Given its fundamental importance for regenerative medicine, it is imperative to study the cellular dynamics and molecular signals in the MuSC niche. In the long run, this research will pave the way for the development of novel therapies for degenerative SkM diseases.

In early studies, we investigated the regenerative deficit that accompanies a rare form of muscular dystrophy called congenital muscular dystrophy type 1A (MDC1A). This work revealed that a lack of the muscle fiber–derived ECM component laminin-α2 in the niche severely impairs muscle healing in a mouse model of MDC1A and must therefore be essential for MuSC function (*4*). Reactivation of laminin receptors using transgenic expression of a miniaturized ligand restores the regenerative capacity of SkM tissue, slows the disease, and prolongs the life of the animals.

Subsequently, we identified a novel receptor complex that integrates Wnt signals and the ECM component fibronectin (FN) to control MuSC self-renewal in the regenerative niche (*5*). MuSCs express the Wnt receptor Frizzled-7 (Fzd7), which binds to the plasma membrane proteoglycan syndecan-4 to form a receptor complex co-activated by Wnt7a and FN ligands. When Wnt7a was administered to a mouse model of Duchenne muscular dystrophy (DMD), a disorder associated with SkM degeneration and impaired regeneration, the treatment restored MuSC function and enhanced tissue repair (*6*, *7*).

A follow-up study demonstrated that in vitro administration of Wnt7a to MuSCs before transplantation into DMD SkM greatly enhanced their engraftment and led to a remarkable mitigation of the disease (*8*). Not only were the Wnt7a-treated donor MuSCs more abundant following transplantation, we also observed improved migration of these cells into the host tissue. In addition, we discovered an unexpected role for Wnt7a: the regulation of postnatal growth of muscle fibers through the mTOR-AKT pathway (*9*). Thus, Wnt7a and FN appear to boost SkM regeneration through two different mechanisms: (i) by stimulating MuSC function and (ii) by increasing the growth rate of muscle fibers.

To exploit the potential of Wnt7a as a therapeutic agent, we developed a truncated variant with increased solubility, in which the C-terminal 137 amino acids lack the conserved palmitoylation sites (*10*). This mini-Wnt7a has full biological activity on MuSCs and is highly efficient in inducing muscle fiber hypertrophy. These properties make Wnt7a and its derivatives attractive candidates for developing drugs that stimulate SkM growth and regeneration. Several patents regarding therapeutic use of Wnt7a for SkM disease have been filed because of these discoveries (*11*–*13*).

Département de Pharmacologie-Physiologie, Université de Sherbrooke, Sherbrooke, Quebec J1H 5N4, Canada.
Email: cf.bentzinger@usherbrooke.ca

PHOTO: COURTESY OF C. FLORIAN BENTZINGER

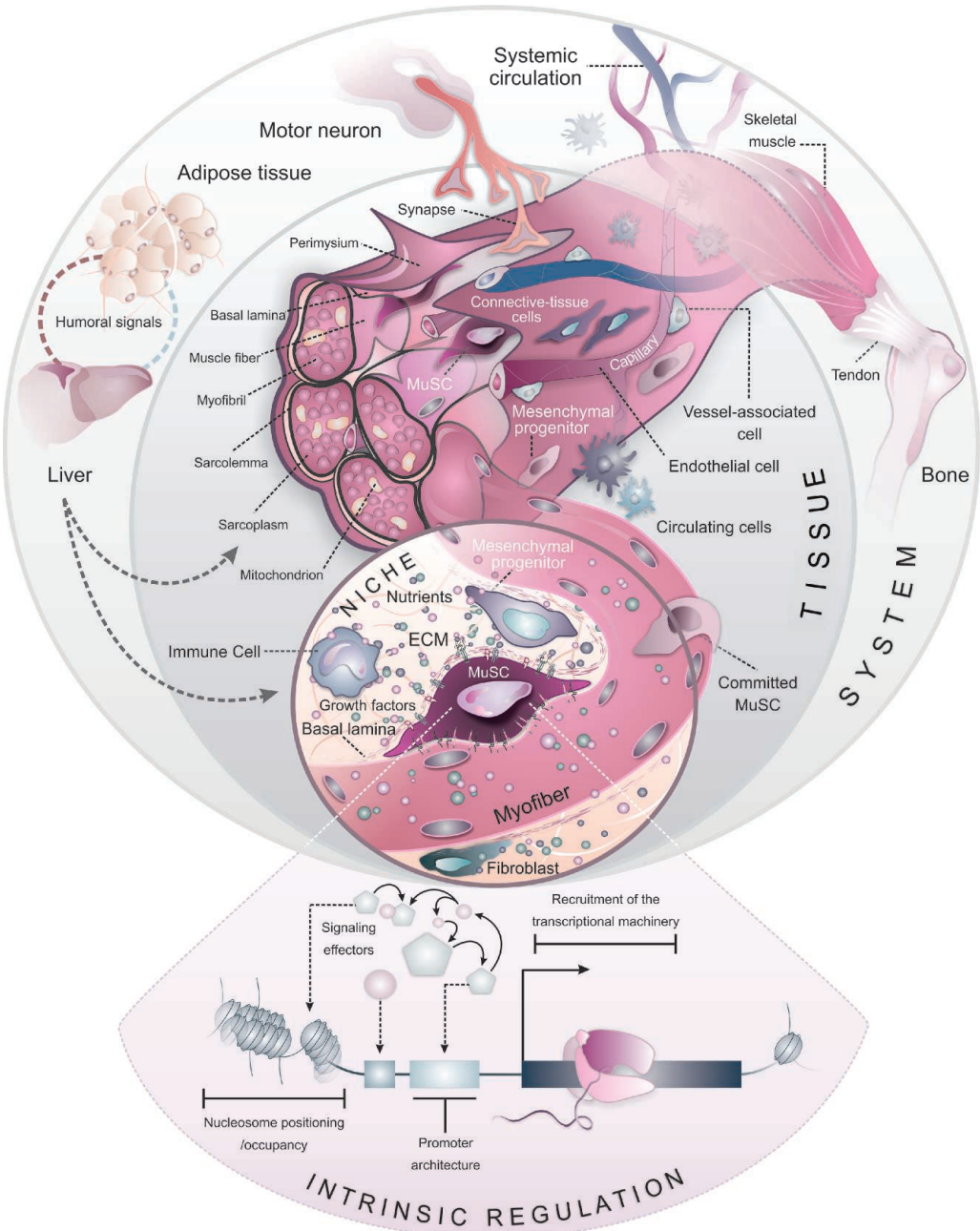

Fig. 1. The skeletal muscle stem cell niche. The niche microenvironment is composed of structural elements, locally bound and secreted signaling molecules, and cell-cell interactions. The niche that maintains MuSCs in their quiescent state in the absence of muscle injury is composed of two major compartments: the interface with the muscle fibers and the basal lamina. In the immediate phase following injury, the niche contains debris of degenerated muscle fibers and a high abundance of pro-inflammatory immune cells. Subsequently, the niche changes into a milieu that promotes MuSC proliferation and is characterized by extensive ECM synthesis by fibroblastic cells and angiogenesis. In the differentiative phase, anti-inflammatory macrophage subsets become dominant and MuSC-derived myoblasts fuse into young muscle fibers that are reinnervated as basal laminae mature. Systemic signals, including nutrients, hormones, and circulating growth factors, regulate MuSC function in quiescence and regeneration directly or influence them by mediating effects at the tissue level or by support cells. Intrinsic mechanisms, such as epigenetic adaptations, telomerase activity, and constitutively activated or repressed signaling loops, act in concert with extrinsic mechanisms to regulate MuSCs.

Our more recent work has continued to investigate the role of the Wnt7a potentiator FN for MuSC function. We discovered that aging severely perturbs the deposition of FN in the regenerative niche (*3*). Loss of FN affects a substantial number of pathways and cellular mechanisms implicated in MuSC aging. Reconstitution of FN levels in the aged niche remobilizes stem cells and restores youth-like SkM regeneration. These findings represent a previously unknown aging mechanism. Present studies aim to identify the age-affected cell type secreting FN. It has already been possible to narrow down a cell population positive for the surface markers CD45, CD31, and CD11b that includes immune cells, hematopoietic cells, and endothelial cells.

The scientific understanding of the MuSC niche in health and disease has substantially advanced. The identification of regulatory hubs in the niche interactome that can be modulated to maintain, restore, or enhance the regenerative capacity of SkM tissue represents a unique opportunity for the targeted development of therapeutics and will likely improve the outcome of cell therapy treatments for muscular dystrophy. ■

GRAPHIC: O. MASHINCHIAN *ET AL.* (*2*)

REFERENCES AND NOTES

1. C. F. Bentzinger, Y. X. Wang, N. A. Dumont, M. A. Rudnicki, *EMBO Rep.* **14**, 1062 (2013).
2. O. Mashinchian, A. Pisconti, E. Le Moal, C. F. Bentzinger, *Curr. Top. Dev. Biol.* **126**, 23 (2018).
3. L. Lukjanenko *et al.*, *Nat. Med.* **22**, 897 (2016).
4. C. F. Bentzinger, P. Barzaghi, S. Lin, M. A. Ruegg, *FASEB J.* **19**, 934 (2005).
5. C. F. Bentzinger *et al.*, *Cell Stem Cell* **12**, 75 (2013).
6. N. A. Dumont *et al.*, *Nat. Med.* **21**, 1455 (2015).
7. J. von Maltzahn, J. M. Renaud, G. Parise, M. A. Rudnicki, *Proc. Natl. Acad. Sci. U.S.A.* **109**, 20614 (2012).
8. C. F. Bentzinger *et al.*, *J. Cell Biol.* **205**, 97 (2014).
9. J. von Maltzahn, C. F. Bentzinger, M. A. Rudnicki, *Nat. Cell Biol.* **14**, 186 (2011).
10. J. von Maltzahn, R. Zinoviev, N. C. Chang, C. F. Bentzinger, M. A. Rudnicki, *Nat. Commun.* **4**, 2869 (2013).
11. Patent PCT/US2012/055396.
12. Patent PCT/US2015/022992.
13. Patent PCT/CA2010/000601.

10.1126/science.aaw3613

Best supporting actors

C. Florian Bentzinger

Science **363** (6431), 1051.
DOI: 10.1126/science.aaw3613

THE AMERICAN ASSOCIATION FOR THE ADVANCEMENT OF SCIENCE LICENSE TERMS AND CONDITIONS

Mar 08, 2019

This Agreement between Omid Mashinchian ("You") and The American Association for the Advancement of Science ("The American Association for the Advancement of Science") consists of your license details and the terms and conditions provided by The American Association for the Advancement of Science and Copyright Clearance Center.

License Number	4544101498377
License date	Mar 08, 2019
Licensed Content Publisher	The American Association for the Advancement of Science
Licensed Content Publication	Science
Licensed Content Title	Best supporting actors
Licensed Content Author	C. Florian Bentzinger
Licensed Content Date	Mar 8, 2019
Licensed Content Volume	363
Licensed Content Issue	6431
Volume number	363
Issue number	6431
Type of Use	Thesis / Dissertation
Requestor type	Scientist/individual at a research institution
Format	Print
Portion	Full Text
Order reference number	
Title of your thesis / dissertation	Generation of Uncommitted Human iPSC Derived Muscle Stem Cells for Therapeutic Applications
Expected completion date	Mar 2019
Estimated size(pages)	150
Requestor Location	Omid Mashinchian NIHS, Campus EPFL, EPFL-Innovation Park BUILDING-H Lausanne, Vaud 1015 Switzerland Attn: Omid Mashinchian
Billing Type	Invoice
Billing Address	Omid Mashinchian NIHS, Campus EPFL, EPFL-Innovation Park BUILDING-H Lausanne, Switzerland 1015 Attn: Omid Mashinchian
Total	0.00 CHF
Terms and Conditions	

American Association for the Advancement of Science TERMS AND CONDITIONS

Regarding your request, we are pleased to grant you non-exclusive, non-transferable permission, to republish the AAAS material identified above in your work identified above, subject to the terms and conditions herein. We must be contacted for permission for any uses other than those specifically identified in your request above.

The following credit line must be printed along with the AAAS material: "From [Full Reference Citation]. Reprinted with permission from AAAS."

All required credit lines and notices must be visible any time a user accesses any part of the AAAS material and must appear on any printed copies and authorized user might make.

This permission does not apply to figures / photos / artwork or any other content or materials included in your work that are credited to non-AAAS sources. If the requested material is sourced to or references non-AAAS sources, you must obtain authorization from that source as well before using that material. You agree to hold harmless and indemnify AAAS against any claims arising from your use of any content in your work that is credited to non-AAAS sources.

If the AAAS material covered by this permission was published in Science during the years 1974 - 1994, you must also obtain permission from the author, who may grant or withhold permission, and who may or may not charge a fee if permission is granted. See original article for author's address. This condition does not apply to news articles.

The AAAS material may not be modified or altered except that figures and tables may be modified with permission from the author. Author permission for any such changes must be secured prior to your use.

Whenever possible, we ask that electronic uses of the AAAS material permitted herein include a hyperlink to the original work on AAAS's website (hyperlink may be embedded in the reference citation).

AAAS material reproduced in your work identified herein must not account for more than 30% of the total contents of that work.

AAAS must publish the full paper prior to use of any text.

AAAS material must not imply any endorsement by the American Association for the Advancement of Science.

This permission is not valid for the use of the AAAS and/or Science logos.

AAAS makes no representations or warranties as to the accuracy of any information contained in the AAAS material covered by this permission, including any warranties of merchantability or fitness for a particular purpose.

If permission fees for this use are waived, please note that AAAS reserves the right to charge for reproduction of this material in the future.

Permission is not valid unless payment is received within sixty (60) days of the issuance of this permission. If payment is not received within this time period then all rights granted herein shall be revoked and this permission will be considered null and void.

In the event of breach of any of the terms and conditions herein or any of CCC's Billing and Payment terms and conditions, all rights granted herein shall be revoked and this permission will be considered null and void.

AAAS reserves the right to terminate this permission and all rights granted herein at its discretion, for any purpose, at any time. In the event that AAAS elects to terminate this permission, you will have no further right to publish, publicly perform, publicly display, distribute or otherwise use any matter in which the AAAS content had been included, and all fees paid hereunder shall be fully refunded to you. Notification of termination will be sent to the contact information as supplied by you during the request process and termination shall be immediate upon sending the notice. Neither AAAS nor CCC shall be liable for any costs, expenses, or damages you may incur as a result of the termination of this permission, beyond the refund noted above.

This Permission may not be amended except by written document signed by both parties.

The terms above are applicable to all permissions granted for the use of AAAS material. Below you will find additional conditions that apply to your particular type of use.

FOR A THESIS OR DISSERTATION

If you are using figure(s)/table(s), permission is granted for use in print and electronic versions of your dissertation or thesis. A full text article may be used in print versions only of a dissertation or thesis.

Permission covers the distribution of your dissertation or thesis on demand by ProQuest / UMI, provided the AAAS material covered by this permission remains in situ.

If you are an Original Author on the AAAS article being reproduced, please refer to your License to Publish for rules on reproducing your paper in a dissertation or thesis.

FOR JOURNALS:

Permission covers both print and electronic versions of your journal article, however the AAAS material may not be used in any manner other than within the context of your article.

FOR BOOKS/TEXTBOOKS:

If this license is to reuse figures/tables, then permission is granted for non-exclusive world rights in all languages in both print and electronic formats (electronic formats are defined below).

If this license is to reuse a text excerpt or a full text article, then permission is granted for non-exclusive world rights in English only. You have the option of securing either print or electronic rights or both, but electronic rights are not automatically granted and do garner additional fees. Permission for translations of text excerpts or full text articles into other languages must be obtained separately.

Licenses granted for use of AAAS material in electronic format books/textbooks are valid only in cases where the electronic version is equivalent to or substitutes for the print version of the book/textbook. The AAAS material reproduced as permitted herein must remain in situ and must not be exploited separately (for example, if permission covers the use of a full text article, the article may not be offered for access or for purchase as a stand-alone unit), except in the case of permitted textbook companions as noted below.

You must include the following notice in any electronic versions, either adjacent to the reprinted AAAS material or in the terms and conditions for use of your electronic products: "Readers may view, browse, and/or download material for temporary copying purposes only, provided these uses are for noncommercial personal purposes. Except as provided by law, this material may not be further reproduced, distributed, transmitted, modified, adapted, performed, displayed, published, or sold in whole or in part, without prior written permission from the publisher."

If your book is an academic textbook, permission covers the following companions to your textbook, provided such companions are distributed only in conjunction with your textbook at no additional cost to the user:

- Password-protected website
- Instructor's image CD/DVD and/or PowerPoint resource
- Student CD/DVD

All companions must contain instructions to users that the AAAS material may be used for non-commercial, classroom purposes only. Any other uses require the prior written permission from AAAS.

If your license is for the use of AAAS Figures/Tables, then the electronic rights granted herein permit use of the Licensed Material in any Custom Databases that you distribute the electronic versions of your textbook through, so long as the Licensed Material remains within the context of a chapter of the title identified in your request and cannot be downloaded by a user as an independent image file.

Rights also extend to copies/files of your Work (as described above) that you are required to provide for use by the visually and/or print disabled in compliance with state and federal laws.

This permission only covers a single edition of your work as identified in your request.

FOR NEWSLETTERS:

Permission covers print and/or electronic versions, provided the AAAS material reproduced

as permitted herein remains in situ and is not exploited separately (for example, if permission covers the use of a full text article, the article may not be offered for access or for purchase as a stand-alone unit)

FOR ANNUAL REPORTS:

Permission covers print and electronic versions provided the AAAS material reproduced as permitted herein remains in situ and is not exploited separately (for example, if permission covers the use of a full text article, the article may not be offered for access or for purchase as a stand-alone unit)

FOR PROMOTIONAL/MARKETING USES:

Permission covers the use of AAAS material in promotional or marketing pieces such as information packets, media kits, product slide kits, brochures, or flyers limited to a single print run. The AAAS Material may not be used in any manner which implies endorsement or promotion by the American Association for the Advancement of Science (AAAS) or Science of any product or service. AAAS does not permit the reproduction of its name, logo or text on promotional literature.

If permission to use a full text article is permitted, The Science article covered by this permission must not be altered in any way. No additional printing may be set onto an article copy other than the copyright credit line required above. Any alterations must be approved in advance and in writing by AAAS. This includes, but is not limited to, the placement of sponsorship identifiers, trademarks, logos, rubber stamping or self-adhesive stickers onto the article copies.

Additionally, article copies must be a freestanding part of any information package (i.e. media kit) into which they are inserted. They may not be physically attached to anything, such as an advertising insert, or have anything attached to them, such as a sample product. Article copies must be easily removable from any kits or informational packages in which they are used. The only exception is that article copies may be inserted into three-ring binders.

FOR CORPORATE INTERNAL USE:

The AAAS material covered by this permission may not be altered in any way. No additional printing may be set onto an article copy other than the required credit line. Any alterations must be approved in advance and in writing by AAAS. This includes, but is not limited to the placement of sponsorship identifiers, trademarks, logos, rubber stamping or self-adhesive stickers onto article copies.

If you are making article copies, copies are restricted to the number indicated in your request and must be distributed only to internal employees for internal use.

If you are using AAAS Material in Presentation Slides, the required credit line must be visible on the slide where the AAAS material will be reprinted

If you are using AAAS Material on a CD, DVD, Flash Drive, or the World Wide Web, you must include the following notice in any electronic versions, either adjacent to the reprinted AAAS material or in the terms and conditions for use of your electronic products: "Readers may view, browse, and/or download material for temporary copying purposes only, provided these uses are for noncommercial personal purposes. Except as provided by law, this material may not be further reproduced, distributed, transmitted, modified, adapted, performed, displayed, published, or sold in whole or in part, without prior written permission from the publisher." Access to any such CD, DVD, Flash Drive or Web page must be restricted to your organization's employees only.

FOR CME COURSE and SCIENTIFIC SOCIETY MEETINGS:

Permission is restricted to the particular Course, Seminar, Conference, or Meeting indicated in your request. If this license covers a text excerpt or a Full Text Article, access to the reprinted AAAS material must be restricted to attendees of your event only (if you have been granted electronic rights for use of a full text article on your website, your website must be password protected, or access restricted so that only attendees can access the content on your site).

If you are using AAAS Material on a CD, DVD, Flash Drive, or the World Wide Web, you must include the following notice in any electronic versions, either adjacent to the reprinted AAAS material or in the terms and conditions for use of your electronic products: "Readers may view, browse, and/or download material for temporary copying purposes only, provided these uses are for noncommercial personal purposes. Except as provided by law, this material may not be further reproduced, distributed, transmitted, modified, adapted, performed, displayed, published, or sold in whole or in part, without prior written permission from the publisher."

FOR POLICY REPORTS:

These rights are granted only to non-profit organizations and/or government agencies. Permission covers print and electronic versions of a report, provided the required credit line appears in both versions and provided the AAAS material reproduced as permitted herein remains in situ and is not exploited separately.

FOR CLASSROOM PHOTOCOPIES:

Permission covers distribution in print copy format only. Article copies must be freestanding and not part of a course pack. They may not be physically attached to anything or have anything attached to them.

FOR COURSEPACKS OR COURSE WEBSITES:

These rights cover use of the AAAS material in one class at one institution. Permission is valid only for a single semester after which the AAAS material must be removed from the Electronic Course website, unless new permission is obtained for an additional semester. If the material is to be distributed online, access must be restricted to students and instructors enrolled in that particular course by some means of password or access control.

FOR WEBSITES:

You must include the following notice in any electronic versions, either adjacent to the reprinted AAAS material or in the terms and conditions for use of your electronic products: "Readers may view, browse, and/or download material for temporary copying purposes only, provided these uses are for noncommercial personal purposes. Except as provided by law, this material may not be further reproduced, distributed, transmitted, modified, adapted, performed, displayed, published, or sold in whole or in part, without prior written permission from the publisher."

Permissions for the use of Full Text articles on third party websites are granted on a case by case basis and only in cases where access to the AAAS Material is restricted by some means of password or access control. Alternately, an E-Print may be purchased through our reprints department (brocheleau@rockwaterinc.com).

REGARDING FULL TEXT ARTICLE USE ON THE WORLD WIDE WEB IF YOU ARE AN ‘ORIGINAL AUTHOR’ OF A SCIENCE PAPER

If you chose "Original Author" as the Requestor Type, you are warranting that you are one of authors listed on the License Agreement as a "Licensed content author" or that you are acting on that author's behalf to use the Licensed content in a new work that one of the authors listed on the License Agreement as a "Licensed content author" has written.

Original Authors may post the ‘Accepted Version’ of their full text article on their personal or on their University website and not on any other website. The ‘Accepted Version’ is the version of the paper accepted for publication by AAAS including changes resulting from peer review but prior to AAAS’s copy editing and production (in other words not the AAAS published version).

FOR MOVIES / FILM / TELEVISION:

Permission is granted to use, record, film, photograph, and/or tape the AAAS material in connection with your program/film and in any medium your program/film may be shown or heard, including but not limited to broadcast and cable television, radio, print, world wide web, and videocassette.

The required credit line should run in the program/film's end credits.

FOR MUSEUM EXHIBITIONS:

Permission is granted to use the AAAS material as part of a single exhibition for the

duration of that exhibit. Permission for use of the material in promotional materials for the exhibit must be cleared separately with AAAS (please contact us at permissions@aaas.org).

FOR TRANSLATIONS:

Translation rights apply only to the language identified in your request summary above. The following disclaimer must appear with your translation, on the first page of the article, after the credit line: "This translation is not an official translation by AAAS staff, nor is it endorsed by AAAS as accurate. In crucial matters, please refer to the official English-language version originally published by AAAS."

FOR USE ON A COVER:

Permission is granted to use the AAAS material on the cover of a journal issue, newsletter issue, book, textbook, or annual report in print and electronic formats provided the AAAS material reproduced as permitted herein remains in situ and is not exploited separately

By using the AAAS Material identified in your request, you agree to abide by all the terms and conditions herein.

Questions about these terms can be directed to the AAAS Permissions department permissions@aaas.org.

Other Terms and Conditions:

v 2

SPRINGER NATURE

Title: The central role of muscle stem cells in regenerative failure with aging

Author: Helen M Blau, Benjamin D Cosgrove, Andrew T V Ho

Publication: Nature Medicine

Publisher: Springer Nature

Date: Aug 6, 2015

Order Completed

Thank you for your order.

This Agreement between Omid Mashinchian ("You") and Springer Nature ("Springer Nature") consists of your license details and the terms and conditions provided by Springer Nature and Copyright Clearance Center.

Your confirmation email will contain your order number for future reference.

printable details

License Number	4612010048482
License date	Jun 18, 2019
Licensed Content Publisher	Springer Nature
Licensed Content Publication	Nature Medicine
Licensed Content Title	The central role of muscle stem cells in regenerative failure with aging
Licensed Content Author	Helen M Blau, Benjamin D Cosgrove, Andrew T V Ho
Licensed Content Date	Aug 6, 2015
Licensed Content Volume	21
Licensed Content Issue	8
Type of Use	Thesis/Dissertation
Requestor type	academic/university or research institute
Format	electronic
Portion	figures/tables/illustrations
Number of figures/tables/illustrations	2
High-res required	no
Will you be translating?	no
Circulation/distribution	<501
Author of this Springer Nature content	no
Title	Generation of Uncommitted Human iPSC Derived Muscle Stem Cells for Therapeutic Applications
Institution name	n/a
Expected presentation date	Jul 2019
Portions	Figure 3
Requestor Location	Omid Mashinchian NIHS, Campus EPFL, EPFL-Innovation Park BUILDING-H

Lausanne, Vaud 1015
Switzerland
Attn: Omid Mashinchian

Total 0.00 CHF

ORDER MORE CLOSE WINDOW

- The system will either provide you with an immediate price quote or direct your request to the NEJM Permissions Department for further processing through the RightsLink interface.
- When prompted to continue, either sign in to your existing RightsLink account, or create a new account if you do not already have one, and follow the additional prompts to secure permission.

Confirmation of your permission and related terms and conditions will be sent to you instantly via email for most requests. Some requests may require Publisher review.

If you have questions about using the RightsLink service, please contact:

RightsLink® Customer Support
+1-877-622-5543 (toll free)
+1-978-777-9929
Email: customercare@copyright.com

For general questions about NEJM Permissions, email permissions@nejm.org.

Permission for Authors

If you are the author of an article that has been published in NEJM, see Author Permissions.

Reuse of Content Within a Thesis or Dissertation

Content (full-text or portions thereof) may be used in print and electronic versions of a dissertation or thesis without formal permission from the Massachusetts Medical Society (MMS), Publisher of the *New England Journal of Medicine*.

The following credit line must be printed along with the copyrighted material:

> Reproduced with permission from (scientific reference citation), Copyright Massachusetts Medical Society.

Third-Party Content

Grants of permissions apply only to copyrighted materials that the MMS owns and not to copyrighted texts or illustrations from other sources.

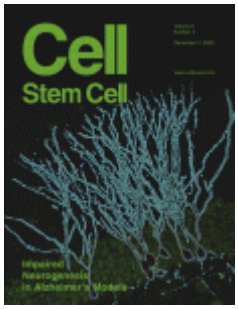

Title: Aging Disrupts Muscle Stem Cell Function by Impairing Matricellular WISP1 Secretion from Fibro-Adipogenic Progenitors

Author: Laura Lukjanenko,Sonia Karaz,Pascal Stuelsatz,Uxia Gurriaran-Rodriguez,Joris Michaud,Gabriele Dammone,Federico Sizzano,Omid Mashinchian,Sara Ancel,Eugenia Migliavacca,Sophie Liot,Guillaume Jacot,Sylviane Metairon,Frederic Raymond,Patrick Descombes et al.

Publication: Cell Stem Cell

Publisher: Elsevier

Date: 7 March 2019

**Ce document a été imprimé au Centre d'impression EPFL,
imprimerie climatiquement neutre, certifiée myClimate.**